

573

NPSEC-93-009

NAVAL POSTGRADUATE SCHOOL

Monterey, California



Predicting Radiation Characteristics from Antenna Physical Dimensions

by

Daniel S. Dietrich
//
R. Clark Robertson

December 1992

Approved for public release; distribution unlimited.

FedDocs
D208 14/2: NPS-EC-93-009

Naval Postgraduate School
Monterey, California 93943-5000

Rear Admiral T. A. Mercer
Superintendent

H. Schull
Provost

This report was prepared and funded by NAVMARINTCEN.

Reproduction of all or part of this report is authorized.

This report was prepared by:

UNCLASSIFIED

KNOX LIBRARY
NAVAL POSTGRADUATE SCHOOL
MONTEREY CA 93943-5101

SECURITY CLASSIFICATION OF THIS PAGE

REPORT DOCUMENTATION PAGE

Form Approved
OMB No. 0704-0188

1a REPORT SECURITY CLASSIFICATION Unclassified			1b RESTRICTIVE MARKINGS		
2a SECURITY CLASSIFICATION AUTHORITY			3 DISTRIBUTION/AVAILABILITY OF REPORT Approved for public release; distribution is unlimited.		
2b DECLASSIFICATION/DOWNGRADING SCHEDULE			4 PERFORMING ORGANIZATION REPORT NUMBER(S) NPSEC-009		
6a NAME OF PERFORMING ORGANIZATION Naval Postgraduate School			6b OFFICE SYMBOL (If applicable) 31		7a NAME OF MONITORING ORGANIZATION NAVMARINTCEN
6c ADDRESS (City, State, and ZIP Code) Monterey, CA 93943-5000			7b ADDRESS (City, State, and ZIP Code) DI433 4301 Suitland Washington DC 20395-5020		
8a NAME OF FUNDING / SPONSORING ORGANIZATION DI433 NAVMARINTCEN		8b OFFICE SYMBOL (If applicable)		9 PROCUREMENT INSTRUMENT IDENTIFICATION NUMBER	
8c ADDRESS (City, State, and ZIP Code) DI433 4301 Suitland Washington DC 20395-5020			10 SOURCE OF FUNDING NUMBERS		
			PROGRAM ELEMENT NO	PROJECT NO	TASK NO
			WORK UNIT ACCESSION NO		
11 TITLE (Include Security Classification) Predicting Radiation Characteristics from Antenna Physical Dimensions					
12 PERSONAL AUTHOR(S) Daniel S. Dietrich and R. Clark Robertson					
13a TYPE OF REPORT		13b TIME COVERED FROM 3/92 TO 12/92		14 DATE OF REPORT (Year, Month, Day) 1992 December 10	
				15 PAGE COUNT 287	
16 SUPPLEMENTARY NOTATION The views in this report are those of the author and do not reflect the official policy or position of the Department of Defense or the U.S. Government.					
17 COSATI CODES			18 SUBJECT TERMS (Continue on reverse if necessary and identify by block number)		
FIELD	GROUP	SUB-GROUP	Radiation pattern, average radiated power, radiation resistance, directivity, effective area/length, space wave, surface wave, surface wave attenuation factor		
19 ABSTRACT (Continue on reverse if necessary and identify by block number) This report explains the fundamental theory and equations used in writing a set of software applications which predict antenna radiation parameters. Each application predicts the radiation characteristics of a particular type of antenna over a planar surface which serves as a model of either earth or seawater. The radiation parameter predictions are based solely on an antenna's physical dimensions, the properties of the underlying surface, and electromagnetic theory. Existing electric field equations provide the basis for radiation parameter predictions, and the accuracy of the predicted radiation parameters is totally dependent upon the extent to which the electric field equations used realistically model the actual radiated electromagnetic fields of the antennas. In addition to a review of applicable electromagnetic field theory, this report is also intended to be a user's guide for the corresponding computer applications. The appendices contain computer hardcopies of sample calculations for several antenna types and remarks regarding the conformity of predicted radiation parameters to expectations. Radiation parameters computed thus far are consistent with expectations based on other computational programs and empirical measurements.					
20 DISTRIBUTION/AVAILABILITY OF ABSTRACT <input checked="" type="checkbox"/> UNCLASSIFIED/UNLIMITED <input type="checkbox"/> SAME AS RPT <input type="checkbox"/> DTIC USERS			21 ABSTRACT SECURITY CLASSIFICATION Unclassified		
22a NAME OF RESPONSIBLE INDIVIDUAL R. Clark Robertson			22b TELEPHONE (Include Area Code) (408) 656-2383		22c OFFICE SYMBOL EC/Rc

ABSTRACT

This report explains the fundamental theory and equations used in writing a set of software applications which predict antenna radiation parameters. Each application predicts the radiation characteristics of a particular type of antenna over a planar surface which serves as a model of either earth or seawater. The radiation parameter predictions are based solely on an antenna's physical dimensions, the properties of the underlying surface, and electromagnetic theory. Existing electric field equations provide the basis for radiation parameter predictions, and the accuracy of the predicted radiation parameters is totally dependent upon the extent to which the electric field equations used realistically model the actual radiated electromagnetic fields of the antennas.

In addition to a review of applicable electromagnetic field theory, this report is also intended to be a user's guide for the corresponding computer applications. The appendices contain computer hardcopies of sample calculations for several antenna types and remarks regarding the conformity of predicted radiation parameters to expectations. Radiation parameters computed thus far are consistent with expectations based on other computational programs and empirical measurements.

TABLE OF CONTENTS

I.	BACKGROUND AND PURPOSE.....	1
II.	INTRODUCTION.....	2
III.	FUNDAMENTAL ELECTROMAGNETIC THEORY.....	3
	A. MAXWELL'S EQUATIONS AND HELMHOLTZ'S EQUATIONS.....	3
	B. ELECTROMAGNETIC FIELD REGIONS.....	5
	C. RADIATION PATTERNS.....	6
	D. POWER DENSITY, POYNTING VECTOR AND RADIATION RESISTANCE.....	9
	E. DIRECTIONAL GAIN, DIRECTIVITY AND POWER GAIN.....	11
	F. HALF-POWER BEAMWIDTH.....	13
	G. POLARIZATION AND BANDWIDTH.....	14
	H. EFFECTIVE LENGTH AND EFFECTIVE AREA.....	15
IV.	THE VERTICAL DIPOLE ANTENNA.....	18
	A. THE ELEMENTAL DIPOLE.....	18
	B. THE ELECTRICALLY SHORT DIPOLE.....	22
	C. THE FINITE LENGTH DIPOLE.....	24
	D. GROUND PLANE EFFECTS ON THE RADIATED SPACE WAVE..	28
	E. THE SURFACE WAVE.....	32
V.	THE ELEVATED VERTICAL DIPOLE.....	39
VI.	THE VERTICAL MONOPOLE.....	44
VII.	THE HORIZONTAL DIPOLE.....	49
VIII.	THE ARBITRARILY ORIENTED DIPOLE.....	56
IX.	THE INVERTED L ANTENNA.....	61
X.	THE SLOPING LONG-WIRE ANTENNA.....	67
XI.	THE TERMINATED SLOPING V ANTENNA.....	72
XII.	THE SIDE-LOADED VERTICAL HALF-RHOMBIC ANTENNA.....	79
XIII.	THE TERMINATED SLOPING OR HORIZONTAL RHOMBIC ANTENNA.....	85
XIV.	THE TERMINATED SLOPING DOUBLE RHOMBOID ANTENNA.....	93
XV.	THE VERTICALLY POLARIZED LOG-PERIODIC DIPOLE ARRAY.....	103
XVI.	THE HORIZONTALLY POLARIZED LOG-PERIODIC DIPOLE ARRAY.....	122

XVII. THE HORIZONTAL YAGI-UDA ARRAY.....	137
XVIII. REMARKS AND CONCLUSION.....	150
APPENDIX A (VERTICAL DIPOLE COMPUTER OUTPUT).....	153
APPENDIX B (VERTICAL MONOPOLE COMPUTER OUTPUT).....	166
APPENDIX C (HORIZONTAL DIPOLE COMPUTER OUTPUT).....	179
APPENDIX D (VERTICAL LOG-PERIODIC DIPOLE ARRAY COMPUTER OUTPUT).....	214
APPENDIX E (HORIZONTAL LOG-PERIODIC DIPOLE ARRAY COMPUTER OUTPUT).....	235
APPENDIX F (HORIZONTAL YAGI-UDA ARRAY).....	256
REFERENCES.....	279
INITIAL DISTRIBUTION LIST.....	280

I. BACKGROUND AND PURPOSE

This report and associated computer software applications are submitted in fulfillment of the thesis requirements for the degree of Master of Science, Aeronautical Engineering from the Naval Postgraduate School in Monterey, CA. The thesis text explains the fundamental theory and equations used in writing a set of software applications which predict an antenna's radiation parameters. Each application predicts the radiation characteristics of a given type of antenna over a planar surface which serves as a model of either earth or seawater. The thesis requirement was generated by a request from the Naval Maritime Intelligence Center (NAVMARINTCEN). At the request of NAVMARINTCEN, Mathcad mathematical software, DOS version 3.1, was used to write the applications. The NAVMARINTCEN request was extensive enough to be tasked as two separate thesis topics. This thesis fulfills the first half of the NAVMARINTCEN requirements. Mathcad applications are complete for the following types of antennas:

1. Vertical Monopole Antenna
2. Elevated Vertical Dipole Antenna
3. Elevated Horizontal Dipole Antenna
4. Arbitrarily Oriented Dipole Antenna
5. Inverted L Antenna
6. Long-Wire Antenna
7. Terminated Sloping V Antenna
8. Side-Loaded Vertical Half Rhombic Antenna
9. Terminated Sloping or Horizontal Rhombic Antenna
10. Sloping Double Rhomboid Antenna
11. Vertically Polarized Log-Periodic Dipole Array
12. Horizontally Polarized Log-Periodic Dipole Array
13. Horizontal Yagi-Uda Array

II. INTRODUCTION

New American Heritage Dictionary defines *antenna* as 'an apparatus for sending and receiving electromagnetic waves'. An electromagnetic wave is a time-varying, self-propagating, interrelated combination of electric and magnetic fields. Antennas radiate electromagnetic fields as a function of their time-varying surface charge density and surface current density distributions. There are many different types of antennas, each with its own set of *radiation characteristics* or *radiation parameters*. These radiation characteristics are related to an antenna's radiated electromagnetic field distribution, and they determine the useful applications for a particular antenna design.

Current personal computers with high-speed processors can quickly and accurately predict antenna radiation parameters from electromagnetic theory. The Mathcad routines described in this report predict an antenna's radiation parameters based solely on its physical dimensions and electromagnetic theory. Accurately predicted radiation characteristics provide intelligence analysts with a reliable estimate of an antenna's capabilities, limitations, and vulnerabilities. Chapters III and IV are a review of applicable electromagnetic theory, and the remaining chapters describe the calculations of the associated Mathcad computer code, and are intended to be a user's guide for the associated Mathcad applications.

III. FUNDAMENTAL ELECTROMAGNETIC THEORY

A. MAXWELL'S EQUATIONS AND HELMHOLTZ'S EQUATIONS

Maxwell's equations are the basis for electromagnetic field calculations. Their differential form is given by [Ref 1: pp. 321-325]

$$\nabla \times \mathbf{E} = -\mu \frac{\partial \mathbf{H}}{\partial t} \quad (3.1a) \qquad \nabla \cdot \mathbf{E} = \frac{\rho}{\epsilon} \quad (3.1c)$$

$$\nabla \times \mathbf{H} = \mathbf{J} + \epsilon \frac{\partial \mathbf{E}}{\partial t} \quad (3.1b) \qquad \nabla \cdot \mathbf{H} = 0 \quad (3.1d)$$

Equation 3.1a is Faraday's Law, 3.1b is Ampere's Circuital Law, 3.1c is Gauss's Law, and 3.1d postulates the inexistence of magnetic charge.

Maxwell's equations dictate the relationship between the electric and magnetic field intensities (\mathbf{E} and \mathbf{H}) and the charge/current density source distributions (ρ and \mathbf{J}) (i.e., the antenna). Maxwell's equations are often applied in a source-free, current-free region, and an $e^{j\omega t}$ time dependence is assumed. The time-harmonic, free space Maxwell's equations are [Ref 1: p. 340]

$$\nabla \times \mathbf{E} = -j\omega\mu_0\mathbf{H} \quad (3.2a) \qquad \nabla \cdot \mathbf{E} = 0 \quad (3.2c)$$

$$\nabla \times \mathbf{H} = j\omega\epsilon_0\mathbf{E} \quad (3.2b) \qquad \nabla \cdot \mathbf{H} = 0 \quad (3.2d)$$

where

$$\epsilon_0 = \text{free space permittivity} = \frac{1}{36\pi} \cdot 10^{-9} \left(\frac{\text{Farads}}{\text{meter}} \right)$$

$$\mu_0 = \text{free space permeability} = 4\pi \cdot 10^{-7} \left(\frac{\text{Henrys}}{\text{meter}} \right)$$

Rather than solve Maxwell's equations directly, the method of vector potentials is often used where the scalar potential (V) and magnetic vector potential (\mathbf{A}) can be obtained from the *nonhomogeneous Helmholtz equations*

$$\nabla^2 V + \beta^2 V = -\frac{\rho}{\epsilon_0} \quad (3.3)$$

$$\nabla^2 \mathbf{A} + \beta^2 \mathbf{A} = -\mu_0 \mathbf{J} \quad (3.4)$$

where $\mathbf{H} = (1/\mu_0) (\nabla \times \mathbf{A})$ [Ref 1: pp. 338-340].

The solutions to Helmholtz's equations are the *retarded scalar potential* and the *retarded vector potential*. The value of V and \mathbf{A} at some distance (R) from the source depends on the source's charge/current density at an earlier time ($t-R/c$), where $c=1/\sqrt{\mu_0 \epsilon_0}$ is equal to the speed of light in free space. The delay (R/c) is the time required for electromagnetic waves to propagate through a distance, R , in free space from source to observation point. The solutions to the nonhomogeneous Helmholtz equations are [Ref 1: pp.338-340]

$$V(R) = \frac{1}{4\pi\epsilon_0} \int_{V'} \frac{\rho e^{-j\beta|\bar{\mathbf{R}}-\bar{\mathbf{R}}'|}}{|\bar{\mathbf{R}}-\bar{\mathbf{R}}'|} dV' \quad (3.5)$$

$$\mathbf{A}(R) = \frac{\mu_0}{4\pi} \int_{V'} \frac{\mathbf{J} e^{-j\beta|\bar{\mathbf{R}}-\bar{\mathbf{R}}'|}}{|\bar{\mathbf{R}}-\bar{\mathbf{R}}'|} dV' \quad (3.6)$$

where the *wavenumber* (β) is $\omega\sqrt{\mu_0 \epsilon_0}$ in free space, $\bar{\mathbf{R}}$ is the observation vector, and $\bar{\mathbf{R}}'$ is the source vector. The wavenumber is most often expressed as $\omega/c = 2\pi/\lambda$, where λ is the wavelength. The Mathcad applications use the expression $2\pi/\lambda$ to calculate β .

The Mathcad applications described herein assume that the antenna under analysis is radiating in free space above a defined ground plane. The free space Maxwell's equations and nonhomogeneous Helmholtz equations (using the free space wavenumber) provide the theoretical basis for deriving the equations for an antenna's radiated electromagnetic fields. The radiated **E** and **H** fields can be calculated directly from their source's charge and current densities using Maxwell's equations. However, as previously mentioned, it is often simpler to find the magnetic vector potential using Helmholtz's equations. Once the vector potential is determined, the electric and magnetic fields are calculated from $\mathbf{H} = (1/\mu_0) (\nabla \times \mathbf{A})$ and $\mathbf{E} = (1/j\omega\epsilon_0) (\nabla \times \mathbf{H})$ [Ref 1: pp. 338-341]. Existing theoretical equations for the radiated electric fields of many antenna types have been derived in this manner. These equations are used in the Mathcad applications to predict an antenna's radiated electric field distribution. Other radiation parameters are then calculated on the basis of the predicted electric field distribution.

B. ELECTROMAGNETIC FIELD REGIONS

The space surrounding an antenna is divided into three regions: the *reactive near-field*, *radiating near-field*, and *far-field* [Ref 2: pp. 22-24]. The reactive near-field occupies the space immediately surrounding the antenna out to a radius of about $0.62 \cdot (D^3/\lambda)^{1/2}$, where λ is the wavelength and D is the maximum dimension of the antenna. Reactive

electromagnetic fields dominate in this region. The radiating near-field occupies the space from the boundary of the reactive field out to a radius of about $2 \cdot (D^2/\lambda)$. Radiation fields dominate in this region, and radiation patterns are often a function of both radial and angular coordinates. The far-field region occupies all space outside the radiating near-field which meets two additional far-field requirements: $2\pi R/\lambda \gg 1$ and $R > 5D$. Radiation fields also dominate in the far-field, but field components are primarily transverse, and radiation patterns are normally a function of directional variables only. The Mathcad antenna applications are valid only in the far-field region of a given antenna.

C. RADIATION PATTERNS

A *radiation pattern* is a three-dimensional representation of an antenna's radiated electromagnetic field distribution or power distribution at a fixed distance from the antenna. Because it is difficult to depict three-dimensional images, the patterns are most often plotted in a defined vertical or horizontal plane. The Mathcad antenna applications plot two-dimensional radiation patterns in polar coordinates depicting the far-field electric field distribution. Patterns are plotted in the $\phi=0$ and $\phi=\pi/2$ vertical planes, and also in a horizontal plane at an elevation angle set by an index from the applicable 'Elevation Angle Index Table' (Table 3.1 or 3.2). Field magnitudes are normalized with respect to the maximum radiated electric field intensity. The magnitude to which each pattern is normalized is displayed below its plot.

TABLE 3.1
ELEVATION ANGLE INDEX TABLE FOR NON-ARRAY ANTENNAS

ELEVATION	INDEX	ELEVATION	INDEX
0.285°	630	46°	470
2°	624	48°	463
4°	617	50°	456
6°	610	52°	449
8°	603	54°	442
10°	596	56°	435
12°	589	58°	428
14°	582	60°	421
16°	575	62°	414
18°	568	64°	407
20°	561	66°	400
22°	554	68°	393
24°	547	70°	386
26°	540	72°	379
28°	533	74°	372
30°	526	76°	365
32°	519	78°	358
34°	512	80°	351
36°	505	82°	344
38°	498	84°	337
40°	491	86°	330
42°	484	88°	323
44°	477	88.857°	316

TABLE 3.2
ELEVATION ANGLE INDEX TABLE
FOR LOG-PERIODIC AND YAGI-UDA ARRAYS

ELEVATION	INDEX	ELEVATION	INDEX
0.57°	314	45.71°	235
2.28°	311	48.00°	231
4.57°	307	50.28°	227
6.86°	303	52.57°	223
9.14°	299	54.86°	219
11.43°	295	57.14°	215
13.71°	291	59.43°	211
16.00°	287	61.71°	207
18.28°	283	64.00°	203
20.57°	279	66.29°	199
22.86°	275	68.57°	195
25.14°	271	70.86°	191
27.43°	267	73.14°	187
29.71°	263	75.43°	183
32.00°	259	77.71°	179
34.29°	255	80.00°	175
36.57°	251	82.29°	171
38.86°	247	84.57°	167
41.14°	243	86.86°	163
43.43°	239	89.14°	159

The Mathcad applications plot the far-field radiation patterns for an antenna's *space wave*, *surface wave*, and total radiated electric field. The space wave is comprised of the electromagnetic waves which propagate directly from antenna to the field point and electromagnetic waves reflected from the surface below the antenna. The surface wave is composed of electromagnetic waves ducted along the surface, much like waveguide propagation. The total field is composed of the space wave and surface wave combined.

Space wave patterns typically vary with directional spherical coordinates, θ and ϕ , but they are predominately invariant with distance from the antenna. The surface wave attenuates exponentially with distance, and far-field surface wave patterns are a function of distance from the antenna. Total field patterns are still predominately invariant with distance, because the maximum surface wave intensity is usually many orders of magnitude less than the maximum space wave intensity. Even at distances which just meet far-field requirements, the surface wave contribution to the total field is barely significant for parameter values of interest.

D. POWER DENSITY, POYNTING VECTOR AND RADIATION RESISTANCE

The instantaneous real power flux density of an electromagnetic wave is called the *Poynting vector* (\mathcal{P}),

$$\begin{aligned}\mathcal{P}(x,y,z) &= \mathbf{E} \times \mathbf{H} = \Re\{\mathbf{E}(x,y,z) e^{j\omega t}\} \times \Re\{\mathbf{H}(x,y,z) e^{j\omega t}\} \quad (3.7) \\ &= \frac{1}{2} \Re\{\mathbf{E} \times \mathbf{H}^*\} + \frac{1}{2} \Re\{\mathbf{E} \times \mathbf{H} e^{2j\omega t}\}\end{aligned}$$

The time invariant term on the right hand side of equation 3.7 is the time average power flux density or average Poynting vector. Far-field \mathbf{E} and \mathbf{H} fields are related by the simple expression $|\mathbf{E}| = (1/\eta_0) \cdot |\mathbf{H}|$, where $\eta_0 = \sqrt{\mu_0/\epsilon_0} = 120\pi$ is the intrinsic impedance of free space. The average Poynting vector solely in terms of the radiated electric field intensity is given by [Ref 1: pp. 382-385].

$$\mathbf{P}_{avg}(x, y, z) = \frac{1}{2} \Re\{\mathbf{E} \times \mathbf{H}^*\} = \frac{1}{2} \Re\left\{\mathbf{E} \times \frac{\mathbf{E}^*}{\eta_0}\right\} = \frac{1}{2} \frac{|\mathbf{E}|^2}{\eta_0} \quad (3.8)$$

The total power flux density is composed of both the Poynting vector and the imaginary part of $\frac{1}{2}(\mathbf{E} \times \mathbf{H}^*)$ which represents the reactive power of the radiated electromagnetic fields. Far-field power flux density is predominately real and is approximately equal to the average Poynting vector. An antenna's total average radiated power is calculated by integrating the poynting vector over a Gaussian surface which surrounds the antenna in the far-field [Ref 1: pp. 382-386].

$$P_{rad} = P_{avg} = \oint_S \mathbf{P}_{avg} \cdot d\mathbf{s} = \frac{1}{2} \oint_S \Re\{\mathbf{E} \times \mathbf{H}^*\} \cdot d\mathbf{s} \quad (3.9)$$

The Mathcad applications use equations 3.8 and 3.9 for power calculations by integrating over the hemisphere which encloses the antenna with the ground plane as the lower boundary.

Radiation resistance relates an antenna's total average radiated power to its peak input current. If a DC current equal to the rms input current were applied to a resistance equal to the radiation resistance, the dissipated power would

equal the antenna's total average radiated power [Ref 3: pp. 47-48]. For the Mathcad antenna applications, the radiation resistance is defined in terms of the total average radiated power and input current by

$$R_{rad} = \frac{2P_{rad}}{|I_{in}|^2} \quad \text{or} \quad P_{rad} = \frac{|I_{in}|^2}{2} R_{rad} \quad (3.10)$$

A sinusoidal input current (or voltage response across the input terminals for Yagi-Uda Arrays) with a maximum of unity is assumed in the Mathcad applications.

E. DIRECTIONAL GAIN, DIRECTIVITY AND POWER GAIN

An *isotropic radiator* is a hypothetical antenna which radiates electromagnetic energy equally in all directions. Its radiation pattern in any plane passing through the source is a circle. All real antennas are *directional radiators* which radiate or receive electromagnetic energy more effectively in some directions compared to others. Some antennas radiate an *omnidirectional pattern* which is directional in elevation, but non-directional in azimuth.

Directive gain (D_g) is the ratio of an antenna's Poynting vector in a given direction, divided by the power flux density of an isotropic source with equal total average radiated power. *Directivity* (D_0) is the maximum value of the directive gain, and it is the primary measure of an antenna's directional properties. The power flux density of an isotropic radiator is equal to the total average radiated power divided by the surface area of a sphere at a given

distance from the antenna ($4\pi R^2$). The expression for directive gain is [Ref 2: pp. 29-31]

$$D_g(\theta, \phi) = \frac{\rho(\theta, \phi)}{\rho_{iso}} = \frac{4\pi R^2 \rho(\theta, \phi)}{P_{rad}} \quad (3.11)$$

The Mathcad applications calculate only directivity using

$$D_0 = \frac{\rho(\theta_{max}, \phi_{max})}{\rho_{iso}} = \frac{4\pi R^2 \rho(\theta_{max}, \phi_{max})}{P_{rad}} \quad (3.12)$$

Power gain accounts for an antenna's radiation efficiency in addition to its directional properties. Power gain (G_d) is defined as $4\pi R^2$ times the ratio of the Poynting vector magnitude in a given direction to the total input power to the antenna. Total input power includes losses due to ohmic power dissipation and impedance mismatches between transmission line and antenna. The ratio of total average radiated power to the total input power is the *radiation efficiency*, ρ_{eff} . The relationship between power gain, directive gain, and radiation efficiency is given by [Ref 2: pp. 42-45]

$$\rho_{eff} = \frac{P_{rad}}{P_{in}} \quad (3.13)$$

$$G_d(\theta, \phi) = \rho_{eff} D_g(\theta, \phi) \quad (3.14)$$

$$G_0 = G_{d_{max}}(\theta, \phi) = \rho_{eff} D_{g_{max}}(\theta, \phi) = \rho_{eff} D_0 \quad (3.15)$$

Since radiation efficiency and power gain account for ohmic losses and impedance mismatches, these parameters are difficult to predict based on antenna dimensions alone. For these reasons, the Mathcad applications do not predict power

gain and radiation efficiency. Gain calculations are limited to directivity since it depends only on total average radiated power and the radiated electromagnetic field distribution. The maximum *Effective Isotropic Radiated Power* (EIRP) is also calculated from $EIRP = P_{rad} \cdot D_0$ [Ref 3: p. 62].

F. HALF-POWER BEAMWIDTH

Radiation lobes are portions of the radiation pattern where a local maximum field intensity is bounded on either side by relative minimum intensities. The *major lobe*, or *main beam*, is the lobe in the direction of maximum radiated power flux density. Split beam antennas have more than one main beam. A *minor lobe* is any lobe except the main beam. *Beamwidth* refers to the *half-power beamwidth* of an antenna's main beam (or beams), and it can be measured in the vertical or horizontal. For antennas with a defined beamwidth, the power intensity drops off on either side of the point of maximum radiated average power density until it is one half of the maximum value. The angle between the radials which intersect the half power points is defined as the half-power beamwidth. Main beams are not necessarily symmetrical since the radial which intersects the point of maximum power density does not necessarily bisect the half-power radials.

The Mathcad applications do not calculate half-power beamwidth directly, but radiation patterns provide a good estimate. Since the radiation patterns depict the electric field distribution normalized to unity, a magnitude of

approximately 0.7 represents the half power-points of the pattern. If two radials are drawn from the origin through the half-power points, the angle subtended by the two radials is the antenna's half-power beamwidth.

G. POLARIZATION AND BANDWIDTH

Polarization describes the time varying properties of an antenna's radiated electric field at a set spatial coordinate as electromagnetic waves propagate outward from the antenna. Signals are usually transmitted with linear, elliptical, or circular polarization. Linear polarization is where the field vector at the spatial coordinate is directed along a fixed linear path. An elliptically polarized signal is one in which the tip of the electric field vector traces an ellipse around the fixed coordinate as the wave propagates outward. Circular polarization is a special case of elliptical polarization where the magnitude of the electric field remains constant as it rotates about the spatial coordinate. Clockwise rotation of the electric field vector is *right-hand polarization*, and counter-clockwise rotation is *left-hand polarization*. The Mathcad applications do not quantitatively predict the polarization at a selected spatial coordinate because of the computational intensity of such a calculation. Only the predominant type of polarization expected is addressed briefly in the introductory remarks of each application.

The *bandwidth* of an antenna is the range of frequencies over which its radiation characteristics meet or exceed a

specified acceptable performance standard. Because radiation characteristics of dissimilar antennas vary differently with frequency, there are no set rules or guidelines which define bandwidth for all antennas in general. Bandwidth standards vary depending on antenna design and intended application. Therefore, the Mathcad applications do not predict operational bandwidth. Instead, multiple frequencies can be input for a given configuration to determine the bandwidth for whatever standards are used to define acceptable performance.

H. EFFECTIVE LENGTH AND EFFECTIVE AREA

The *effective area*, or *effective aperture*, gives the power delivered to the antenna load when multiplied by the incident average power flux density. It is defined by [Ref 2: pp 59-63]

$$P_{rec} = A_{eff} \phi_{inc} \quad (3.16)$$

The maximum effective area is related to directivity for all antennas by [Ref 4: pp. 46-47]

$$A_{max} = \frac{\lambda^2 D_0}{4 \cdot \pi} \quad (3.17)$$

This is a theoretical maximum effective area since directivity does not account for radiation efficiency. Like directive gain and power gain, actual effective area and theoretical effective area are related by radiation efficiency

$$A_{eff} = \frac{\lambda^2 G_{max}}{4 \cdot \pi} = \rho_{eff} A_{max} \quad (3.18)$$

The maximum theoretical effective area is a good approximation of actual effective area for frequencies within the bandwidth of a well designed antenna with a high radiation efficiency.

Effective length is defined as the ratio of the voltage induced across the antenna terminals by the incident electric field and is given by [Ref 4: pp. 40-42]

$$l_{eff} = \frac{V_{in}}{|E_{inc}|} \quad (3.19)$$

Effective length is related to effective area by

$$l_{max} = 2 \sqrt{\frac{R_{rad} A_{max}}{\eta_0}} \quad (3.20)$$

Substituting equation 3.17 into equation 3.20, we get the maximum theoretical effective length in terms of wavelength, directivity, radiation resistance and intrinsic impedance of free space as

$$l_{max} = 2 \sqrt{\frac{R_{rad} \lambda^2 D_0}{4 \pi \eta_0}} \quad (3.21)$$

Finally, the actual effective length is related to the theoretical effective length by

$$l_{eff} = \rho_{eff} l_{max} \quad (3.22)$$

Effective area and effective length are actually a function of directional coordinates with respect to the source. The equations given here are for maximum values of effective area and effective length along the radial of

maximum directive gain (directivity). While effective area is a parameter more generally applied to all antennas, the Mathcad applications use equations 3.17 and 3.21 to calculate both a theoretical maximum effective area and effective length. If an antenna's radiation efficiency for a given frequency is known, the actual effective area and length can be calculated by multiplying the theoretical values by the radiation efficiency.

The next chapter on the dipole antenna explains in detail the derivation of the radiated electric field equations for a vertical dipole antenna. The elevated vertical dipole Mathcad application uses this equation to obtain the electric field distribution and total average radiated power (P_{rad}) based on an assumed sinusoidal current distribution on the antenna with a maximum of unity. Total average radiated power is then used to predict the radiation parameters discussed in the preceding paragraphs. In follow-on chapters, only the final electric field equations are presented because the derivation is similar for all types of antennas. They are primarily summary chapters which describe the calculations of each individual application, but any new or important concepts not presented in previous chapters will be discussed as required.

IV. THE VERTICAL DIPOLE ANTENNA

A. THE ELEMENTAL DIPOLE

The *current element*, or *elemental dipole*, is the building block for calculating antenna radiation parameters. The elemental dipole is a hypothetical differential length thin-wire antenna with a sinusoidally oscillating surface current. The antenna length (l) is many orders of magnitude smaller than the wavelength (λ), so the instantaneous current is considered uniform over the length of the dipole. Figure 4.1 depicts the elemental dipole oriented along the z axis in a rectangular coordinate system with its center at the origin.

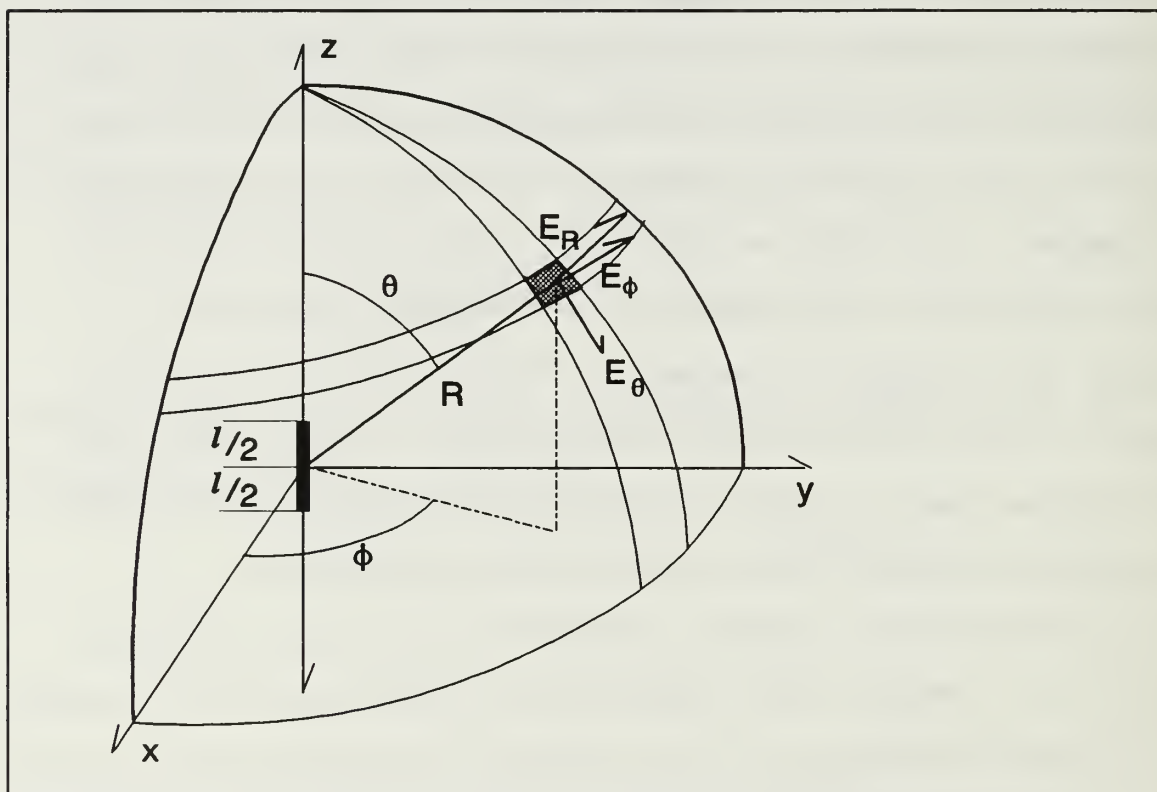


FIGURE 4.1: Elemental dipole spatial orientation.

The surface current is given by

$$i(t) = I \cos(\omega t) = \Re\{I e^{j\omega t}\} \quad (4.1)$$

and the magnetic vector potential, \mathbf{A} , is found from equation 3.6 to be

$$\mathbf{A} = \frac{\mu_0}{4\pi} \int_{c'} \frac{\mathbf{J} e^{-j\beta R}}{R} dl' = \mathbf{a}_z \frac{\mu_0 I dl}{4\pi} \left(\frac{e^{-j\beta R}}{R} \right) \quad (4.2)$$

Primed coordinates refer to source points, R is the distance from the origin to the field point, $\beta = \omega \sqrt{\mu_0 \epsilon_0}$ is the free space wavenumber, and the magnitude of the current density (\mathbf{J}) is given by I [Ref 2: pp. 100-102]. The magnetic vector potential in spherical coordinates is

$$A_R = A_z \cos(\theta) = \frac{\mu_0 I dl}{4\pi} \left(\frac{e^{-j\beta R}}{R} \right) \cos(\theta) \quad (4.3a)$$

$$A_\theta = -A_z \sin(\theta) = -\frac{\mu_0 I dl}{4\pi} \left(\frac{e^{-j\beta R}}{R} \right) \sin(\theta) \quad (4.3b)$$

$$A_\phi = 0 \quad (4.3c)$$

The magnetic field intensity, \mathbf{H} , is found from

$$\mathbf{H} = \frac{1}{\mu_0} \nabla \times \mathbf{A} = \mathbf{a}_\phi \frac{1}{\mu_0 R} \left[\frac{\partial}{\partial R} (R A_\theta) - \frac{\partial A_R}{\partial \theta} \right] \quad (4.4)$$

$$H_\phi = -\frac{I dl}{4\pi} \beta^2 \sin(\theta) \left[\frac{1}{j\beta R} + \frac{1}{(j\beta R)^2} \right] e^{-j\beta R} \quad (4.5)$$

and the electric field intensity, \mathbf{E} , is found from Ampere's Law by

$$\mathbf{E} = \frac{1}{j\omega\epsilon_0} \nabla \times \mathbf{H} = \frac{1}{j\omega\epsilon_0} \left[\mathbf{a}_r \frac{1}{R \sin(\theta)} \frac{\partial}{\partial \theta} [H_\phi \sin(\theta)] - \mathbf{a}_\theta \frac{1}{R} \frac{\partial}{\partial R} (RH_\phi) \right] \quad (4.6)$$

$$E_R = -\frac{Idl}{2\pi} \eta_0 \beta^2 \cos(\theta) \left[\frac{1}{(j\beta R)^2} + \frac{1}{(j\beta R)^3} \right] e^{-j\beta R} \quad (4.7a)$$

$$E_\theta = -\frac{Idl}{4\pi} \eta_0 \beta^2 \sin(\theta) \left[\frac{1}{(j\beta R)} + \frac{1}{(j\beta R)^2} + \frac{1}{(j\beta R)^3} \right] e^{-j\beta R} \quad (4.7b)$$

$$H_R = H_\theta = E_\phi = 0 \quad (4.7c)$$

At far-field distances, the only significant components are the first terms inside the parenthesis on the right hand side of equations 4.5 and 4.7b. The far-field \mathbf{E} and \mathbf{H} fields are functions of a single angular coordinate (θ) for a vertically orientated element [Ref 1: pp. 602-607].

Retaining only those terms that vary as $1/R$, we get the far-field electric and magnetic field intensities for the current element as

$$H_\phi = j \frac{Idl}{4\pi} \left(\frac{e^{-j\beta R}}{R} \right) \beta \sin(\theta) \quad (4.8)$$

$$E_\theta = j \frac{Idl}{4\pi} \left(\frac{e^{-j\beta R}}{R} \right) \eta_0 \beta \sin(\theta) \quad (4.9)$$

Note that the far-field relationship $|\mathbf{H}| = \eta_0 |\mathbf{E}|$ holds true for the elemental dipole's radiated fields in the far-field region.

The elemental dipole's radiated average Poynting vector (power density) is [Ref 1: 607-612]

$$\rho_{avg} = \frac{1}{2} \Re \{ \mathbf{E} \times \mathbf{H}^* \} = \mathbf{a}_r \frac{1}{2} |E_\theta| |H_\phi| = \frac{(Idl)^2}{32\pi^2 R^2} \eta_0 \beta^2 \sin^2(\theta) \quad (4.10)$$

The Poynting vector integrated over a Gaussian surface in the far-field yields the total average radiated power

$$P_{rad} = \oint_S \rho_{avg} dS = \frac{(Idl)^2}{32\pi^2} \eta_0 \beta^2 \int_0^{2\pi} \int_0^\pi [\sin^2(\theta)] \sin(\theta) d\theta d\phi \quad (4.11)$$

$$P_{rad} = 2\pi \frac{(Idl)^2}{32\pi^2} \eta_0 \beta^2 \left[\frac{\cos^3(\theta)}{3} - \cos(\theta) \right]_0^\pi = 2\pi \frac{(Idl)^2}{32\pi^2} \eta_0 \beta^2 \left(\frac{4}{3} \right)$$

$$P_{rad} = \frac{8\pi}{3} \frac{(Idl)^2}{32\pi^2} \eta_0 \beta^2 = \frac{(Idl)^2}{12\pi} \eta_0 \beta^2$$

The directive gain and directivity are found from the power density and total radiated power as

$$D_g(\theta, \phi) = \frac{4\pi R^2 \rho_{avg}}{P_{rad}} = \frac{4\pi \sin^2(\theta)}{\frac{8\pi}{3}} = \frac{3}{2} \sin^2(\theta) \quad (4.12)$$

$$D_0 = D_{g_{max}}(\theta, \phi) = D_g\left(\frac{\pi}{2}, \phi\right) = 1.5 \quad \text{or} \quad 10 \log_{10} 1.5 = 1.76 \text{ dB} \quad (4.13)$$

Radiation resistance is found directly from P_{rad} and equation 2.10 as [Ref 1: pp. 607-612].

$$P_{rad} = \frac{I^2}{2} R_{rad} = \frac{(Idl)^2}{12\pi} \eta_0 \beta^2 \quad (4.14)$$

$$P_{rad} = \frac{I^2}{2} \left[\frac{dl^2}{6\pi} 120\pi \left(\frac{2\pi}{\lambda} \right)^2 \right] = \frac{I^2}{2} \left[80\pi^2 \left(\frac{dl}{\lambda} \right)^2 \right]$$

$$R_{rad} = 80\pi^2 \left(\frac{dl}{\lambda} \right)^2 \quad (4.15)$$

B. THE ELECTRICALLY SHORT DIPOLE

The derivation of the electric field for an *electrically short dipole* is the next step in deriving the field equations for a practical finite length dipole. The electrically short dipole is a center fed thin-wire antenna oriented as in Figure 4.1 with length greater than 0.02λ , but less than 0.10λ . The current distribution is estimated as triangular where

$$\mathbf{I}(x', y', z') = \mathbf{I}(z') = \begin{cases} \mathbf{a}_z I_m \left(1 - \frac{2}{l} z'\right), & 0 \leq z' \leq \frac{l}{2} \\ \mathbf{a}_z I_m \left(1 + \frac{2}{l} z'\right), & -\frac{l}{2} \leq z' \leq 0 \end{cases} \quad (4.16)$$

where I_m is the current maximum at the center feed.

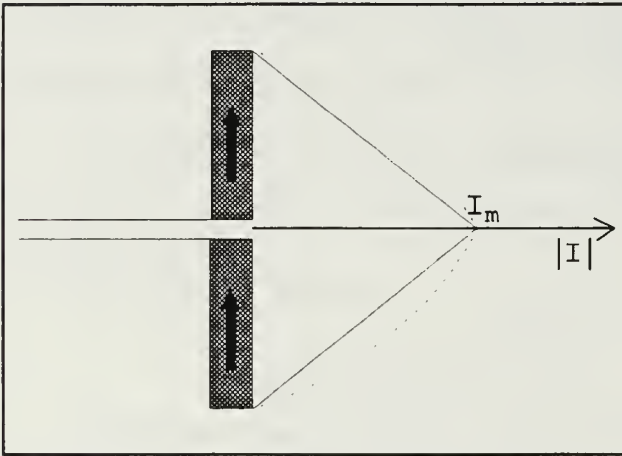


FIGURE 4.2: Current distribution for an electrically short dipole.

The dotted line in Figure 4.2 is a more exact representation of the actual current distribution, but the triangular estimate is a reasonable approximation for short dipoles.

The electrically short dipole has a magnetic vector potential given by

$$\mathbf{A}(x, y, z) = \mathbf{a}_z \frac{\mu_0 I_m}{4\pi} \left[\int_{-\frac{l}{2}}^0 \left(1 + \frac{2}{l} z'\right) \frac{e^{-j\beta R}}{R} dz' + \int_0^{\frac{l}{2}} \left(1 - \frac{2}{l} z'\right) \frac{e^{-j\beta R}}{R} dz' \right] \quad (4.17)$$

$$\mathbf{A} = \mathbf{a}_z \frac{\mu_0 I_m e^{-j\beta R}}{4\pi R} \left(\left[z' + \frac{z'^2}{l} \right]_{-\frac{l}{2}}^0 + \left[z' - \frac{z'^2}{l} \right]_0^{\frac{l}{2}} \right) = \mathbf{a}_z \frac{\mu_0 I_m l e^{-j\beta R}}{8\pi R}$$

Because dipole length is small in comparison to the far-field distance, R is considered constant throughout the integration over the length of the dipole. Note that the magnitude of the magnetic vector potential for the electrically short dipole is half that of the elemental dipole for the same current input.

The equations for the radiated electromagnetic fields are derived in the same way as for the elemental dipole, and the final expressions for the electric and magnetic field distributions of the electrically short dipole are given by

$$E_{\theta} = j\eta_0 \frac{\beta I_m l e^{-j\beta R}}{8\pi R} \sin(\theta) \quad (4.18)$$

$$H_{\phi} = j \frac{\beta I_m l e^{-j\beta R}}{8\pi R} \sin(\theta) \quad (4.19)$$

$$E_r = E_{\phi} = H_r = H_{\theta} = 0$$

Directive gain and directivity for the electrically short dipole are the same as those of the elemental dipole. The magnitudes of the radiated power density, total radiated power, and radiation resistance for the short dipole are given by [Ref 2: pp. 109-112]

$$\rho_{avg} = \frac{(Idl)^2}{128\pi^2 R^2} \eta_0 \beta^2 \sin^2(\theta) \quad (4.20)$$

$$P_{rad} = \frac{(Idl)^2}{48\pi} \eta_0 \beta^2 \quad (4.21)$$

$$R_{rad} = 20\pi^2 \left(\frac{l}{\lambda} \right)^2 \quad (4.22)$$

C. THE FINITE LENGTH DIPOLE

Finite length dipoles are center fed thin-wire antennas with negligible diameter (diameter $\ll \lambda$ and radius \ll length). Dipoles with a length greater than 0.10λ can no longer use the assumption of triangular current distribution with acceptable accuracy. The finite length dipole must account for the sinusoidal current variation along the length of the antenna. The sinusoidal surface current distribution for a finite length dipole oriented as depicted in Figure 4.1 is

$$\mathbf{I}(x', y', z') = \mathbf{I}(z') = \begin{cases} \mathbf{a}_z I_0 \sin[\beta(h-z')], & 0 \leq z' \leq \frac{l}{2} \\ \mathbf{a}_z I_0 \sin[\beta(h+z')], & -\frac{l}{2} \leq z' \leq 0 \end{cases} \quad (4.23)$$

where I_0 is the peak current input and $h = \frac{l}{2}$.

Considering the finite length dipole as an aggregate of elemental dipoles, we get the expression for the electric far-field from equation 4.7b as [Ref 2: pp. 118-120]

$$\mathbf{E}_\theta = \int_{-\frac{l}{2}}^{\frac{l}{2}} d\mathbf{E}_\theta = j \frac{\eta_0 \beta}{4\pi R} \sin(\theta) \left[\int_{-h}^h \mathbf{I}(x', y', z') e^{-j\beta r} dz' \right] \quad (4.24)$$

For purposes of the radiated electric field's phase angle, the radial field distance (R) cannot be considered constant while integrating over the length of the dipole. The variable r (which stands for $|\bar{\mathbf{R}} - \bar{\mathbf{R}}'|$) in the exponential (phase) term is approximated as $[R - z' \cos(\theta)]$, where R is the distance from the origin to the field point, and z' is the source coordinate of the vertical dipole along the z axis

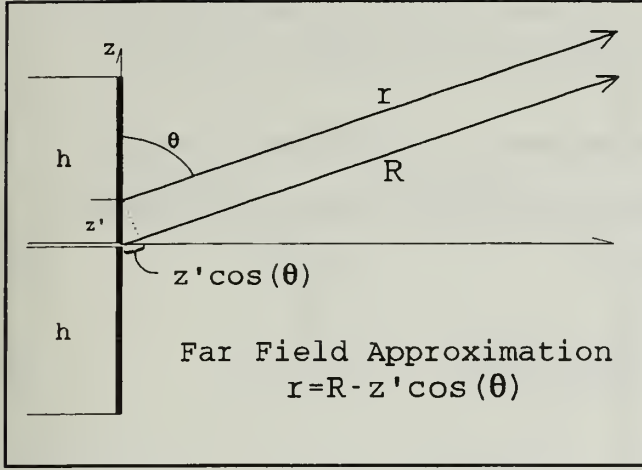


FIGURE 4.3: Phase approximation for distance variable, r .

[Ref 2: pp. 112-114]. The approximation is depicted in Figure 4.3, and is accurate in the far-field for $r > 2l^2/\lambda$. For purposes of calculating electric field magnitude, the variation of r over the length of the dipole

is negligible, and the distance from the origin to the field point (spherical coordinate R) is used in the denominator of equation 4.24. Substituting equation 4.23 for $I(x', y', z')$ into equation 4.24 and $[R - z' \cos(\theta)]$ for r in the exponential term of equation 4.24 and integrating, we get

$$\begin{aligned}
 E_\theta &= j \frac{\eta_0 \beta e^{-j\beta R}}{4\pi R} \sin(\theta) \left[\int_{-h}^0 I_0 \sin[\beta(h+z')] e^{+j\beta z' \cos(\theta)} dz' \right. \\
 &\quad \left. + \int_0^h I_0 \sin[\beta(h-z')] e^{+j\beta z' \cos(\theta)} dz' \right] \\
 &= j \frac{\eta_0 \beta e^{-j\beta R}}{4\pi R} \sin(\theta) \cdot \\
 &\quad \left[\int_{-h}^0 I_0 \sin[\beta(h+z')] [\cos[\beta z' \cos(\theta)] + j \sin[\beta z' \cos(\theta)]] dz' \right. \\
 &\quad \left. + \int_0^h I_0 \sin[\beta(h-z')] [\cos[\beta z' \cos(\theta)] + j \sin[\beta z' \cos(\theta)]] dz' \right]
 \end{aligned} \tag{4.25}$$

Since the current distribution is an even function, the odd term of $j \cdot \sin(\beta \cdot z' \cdot \cos(\theta))$ integrates to zero over the interval from $-h$ to h . Since the $\cos(\beta \cdot z' \cdot \cos(\theta))$ term is even, the integral can be written as

$$E_{\theta} = j \frac{\eta_0 \beta I_0 e^{-j\beta R}}{2\pi R} \sin(\theta) \int_0^h \sin[\beta(h-z')] \cos[\beta z' \cos(\theta)] dz' \quad (4.26)$$

After integrating, the final expressions for radiated electric and magnetic field distributions of a finite vertical dipole are given by [Ref 2: pp. 118-120]

$$E_{\theta} = j \frac{\eta_0 I_0 e^{-j\beta R}}{2\pi R} \left[\frac{\cos[\beta h \cos(\theta)] - \cos(\beta h)}{\sin(\theta)} \right] \quad (4.27)$$

$$H_{\phi} = \frac{E_{\theta}}{\eta_0} = j \frac{I_0 e^{-j\beta R}}{2\pi R} \left[\frac{\cos[\beta h \cos(\theta)] - \cos \beta h}{\sin(\theta)} \right] \quad (4.28)$$

The coefficient outside the brackets is called the *element factor*, and the expression inside the brackets is the *space factor*.

The electric field radiation pattern is a function of elevation (θ) and wavelength (λ). For a fixed wavelength, the radiation pattern for any vertical plane through the antenna axis is obtained by plotting the magnitude of equation 4.27 in polar coordinates as θ varies from zero to 2π . The pattern is normalized by multiplying the electric field magnitude by a factor such that the maximum result is one. Since electric field distribution is independent of ϕ , the pattern for $-\pi \leq \theta \leq 0$ is symmetrical with that for $0 \leq \theta \leq \pi$. Figure 4.4 depicts the normalized radiation patterns of four finite dipoles with successive lengths of $\lambda/4$, $\lambda/2$, $3\lambda/4$, and λ . These lengths simplify calculation of the electric field patterns since βh is $\pi/4$, $\pi/2$, $3\pi/4$, and π for each successive dipole. If dipole length is greater than one wave-length, the patterns

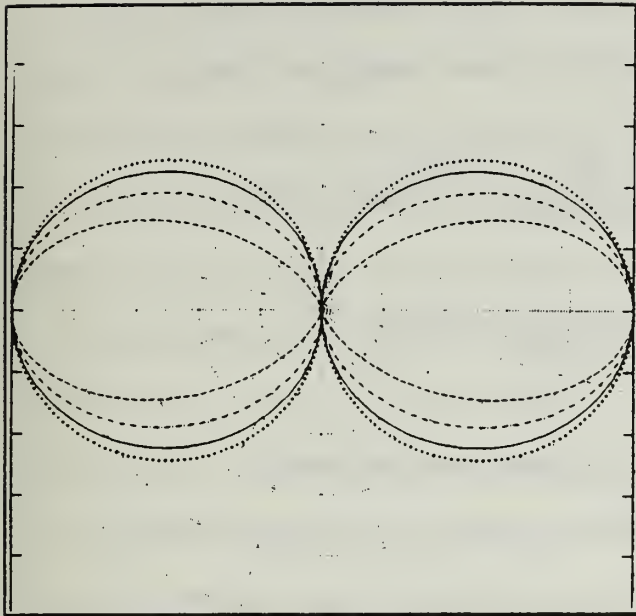


FIGURE 4.4: Vertical plane patterns for dipoles of length $l = \lambda/4$ ·····, $l = \lambda/2$ ———, $l = 3\lambda/4$ - · - · - ·, and $l = \lambda$ - - - - -.

become more complex and the number of lobes increases.

The radiated power density and total radiated power are found just as they were for the elemental dipole and the electrically short dipole. The final expressions for radiated power density and total radiated power are [Ref 2: pp. 120-124]

$$\rho_{avg} = \frac{1}{2} \Re(\mathbf{E} \times \mathbf{H}^*) = \mathbf{a}_r \frac{\eta_0 I_0^2}{8\pi^2 R^2} \left[\frac{\cos[\beta h \cos(\theta)] - \cos(\beta h)}{\sin(\theta)} \right]^2 \quad (4.29)$$

$$P_{rad} = \int_0^{2\pi} \int_0^\pi \rho_{avg} R^2 \sin(\theta) d\theta d\phi \quad (4.30)$$

$$= \frac{\eta_0 I_0^2}{4\pi} \int_0^\pi \frac{[\cos[\beta h \cos(\theta)] - \cos(\beta h)]^2}{\sin(\theta)} d\theta$$

The Mathcad applications evaluate equation 4.30 to obtain total radiated power for a sinusoidal input current with a maximum of unity. An expression for radiation resistance is also derived by Balanis [Ref 2: p. 124]. However, the Mathcad applications calculate radiation resistance from total average radiated power and equation 2.10.

When the dipole is elevated above the origin along the z axis, an additional phase shift term of $\exp[-j\beta H_0 \cos(\theta)]$ must

be included in equations 4.27 and 4.28, where H_0 is the elevation of the feed at the center of the dipole; hence,

$$E_\theta = j \frac{\eta_0 I_0 e^{-j\beta [R-H_0 \cos(\theta)]}}{2\pi R} \left[\frac{\cos[\beta h \cos(\theta)] - \cos(\beta h)}{\sin(\theta)} \right] \quad (4.31)$$

$$H_\phi = \frac{E_\theta}{\eta_0} = j \frac{I_0 e^{-j\beta [R-H_0 \cos(\theta)]}}{2\pi R} \left[\frac{\cos[\beta h \cos(\theta)] - \cos \beta h}{\sin(\theta)} \right] \quad (4.32)$$

D. GROUND PLANE EFFECTS ON THE RADIATED SPACE WAVE

The electric field equations derived in Chapters 3A-3C are free space equations which do not consider the presence of a ground plane. Since antenna orientation is described with respect to the ground plane, orientation descriptions are not really valid until a ground plane is introduced. The free space electric field distribution for a dipole oriented along the x axis or y axis is identical to the distribution for the same dipole along the z axis. The radiation pattern is displaced to correspond to the new position of the dipole, but the radiated electric field distribution relative to the antenna is unaffected.

The free space electric field equations no longer provide an accurate description of an antenna's radiated electric field distribution above a ground plane. The free space equations only provide the *direct wave component* of the space wave which propagates directly from the antenna to the field points above ground ($-\pi/2 < \theta < \pi/2$). They are not valid for $|\theta| > \pi/2$ (points below the ground plane).

A complete description of the space wave above a ground plane must include the *reflected wave component*. The reflected component consists of electromagnetic waves radiated at elevation angles corresponding to $|\theta| > \pi/2$ in the free space equations. These waves strike the ground plane and are absorbed, partially reflected, or completely reflected before reaching a field point above the ground plane. The total space wave is obtained by adding the direct wave and reflected wave components for field points defined by $-\pi/2 < \theta < \pi/2$. The distribution of the reflected waves vary relative to the antenna as its spatial orientation changes, so the electric field distribution (radiation pattern) is also affected when the antenna is repositioned with respect to the ground.

The reflected wave component is determined using *reflection coefficients* and *image theory*. Reflection coefficients determine how much of an incident electric field is reflected by a given ground plane, and they are a function of θ and the *complex index of refraction*. The complex index of refraction (n) in terms of frequency, conductivity (σ), and relative dielectric constant (ϵ_r) of the ground plane is

$$n = \frac{c}{u_p} = \frac{\sqrt{\mu_0 \epsilon_c \epsilon_0}}{\sqrt{\mu_0 \epsilon_0}} = \sqrt{\epsilon_c} = \sqrt{\epsilon_r + \frac{\sigma}{j\omega \epsilon_0}} = \sqrt{\epsilon_r - j \frac{18000\sigma}{f_{MHz}}} \quad (4.33)$$

The *vertical reflection coefficient* (Γ_v)

$$\Gamma_v = \frac{n^2 \cos(\theta_r) - \sqrt{n^2 - \sin^2(\theta_r)}}{n^2 \cos(\theta_r) + \sqrt{n^2 - \sin^2(\theta_r)}} \quad (4.34)$$

is used to find the reflected wave contribution to the θ component of the space wave. The horizontal reflection coefficient (Γ_h)

$$\Gamma_h = \frac{\cos(\theta_r) - \sqrt{n^2 - \sin^2(\theta_r)}}{\cos(\theta_r) + \sqrt{n^2 - \sin^2(\theta_r)}} \quad (4.35)$$

is used to find the reflected wave contribution to the ϕ component of the space wave [Ref 5: pp. 629-633].

Antenna image theory accounts for phase differences between the direct and reflected wave components. Phase differences are caused by the different distances travelled by the two components to a given field point. The image is a 'mirror image' located below the ground plane at a distance equal to the antenna height above ground. The distance from the image to a given field point is the distance travelled by the reflected wave to that field point. This distance is approximated by $R + H_0 \cos(\theta)$, similar in derivation to the approximation illustrated in Figure 4.4 for the direct wave distance of $R - H_0 \cos(\theta)$. The distances travelled by the two components differ by $2H_0 \cos(\theta)$, but the direct wave expression already includes the term $\exp[+j\beta H_0 \cos(\theta)]$, so the reflected wave expression includes the term $\exp[-j\beta H_0 \cos(\theta)]$ to account for any resulting phase differences.

In equations 4.34 and 4.35, the variable θ_r is the angle between the z axis and the radial from antenna image to field point. If the height of the antenna is small in comparison to the far-field distance, θ_r is approximated as θ (the angle

between the z axis and the radial from origin to field point). The Mathcad applications use this approximation to find the reflection coefficients for 632 discrete values of θ (316 for the array applications) in the interval $-\pi/2 < \theta < \pi/2$ at a specified distance (R) from the antenna.

The direct wave component of the space wave is calculated for discrete values of θ with the free space electric field equation and the phase terms derived from the antenna height. The reflected wave components are then calculated for each θ by multiplying the direct wave components by their corresponding reflection coefficients and applicable phase terms. The reflected wave components are then added to the direct wave components to obtain the total radiated space wave at each θ . The discrete results for the space wave are normalized with respect to the value with maximum magnitude, and the space wave radiation pattern is depicted by plotting the normalized field magnitudes for $-\pi/2 < \theta < \pi/2$.

The Mathcad applications plot radiation patterns assuming a planar surface below the antenna. The planar earth model provides accurate results for (1) antenna heights within several wavelengths of the surface and (2) wavelengths much smaller than the radius of the earth. The antennas addressed in this report are usually mounted well within several wavelengths of the ground, so the planar assumption is not a problem for the majority of calculations. If a configuration is encountered where the antenna is more than four or five

wavelengths above the ground, the Mathcad applications still provide a fair estimate of the radiation parameters. However, if highly accurate results are required, a computer program which accounts for the curvature of the earth should be used.

The final expression for the radiated space wave of a vertical dipole antenna is [Ref 6: p. 166]

$$\begin{aligned}
 E_{\theta} &= j \frac{\eta_0 I_0 e^{-j\beta R}}{2\pi R} \left[\frac{\cos[\beta h \cos(\theta)] - \cos(\beta h)}{\sin(\theta)} \right] \cdot \\
 &\quad \left[e^{j\beta H_0 \cos(\theta)} + \Gamma_v e^{-j\beta H_0 \cos(\theta)} \right] \\
 &= j 60 I_0 \frac{e^{-j\beta R}}{R} \left[\frac{\cos[\beta h \cos(\theta)] - \cos(\beta h)}{\sin(\theta)} \right] \cdot \\
 &\quad \left[e^{j\beta H_0 \cos(\theta)} + \Gamma_v e^{-j\beta H_0 \cos(\theta)} \right]
 \end{aligned} \tag{4.36}$$

This is the equation used in the Elevated Vertical Dipole application to calculate the space wave radiation pattern and radiated electric field distribution.

E. THE SURFACE WAVE

The radiated electric field of an antenna above a ground plane includes a *surface wave* component in addition to the space wave. The surface wave radiation pattern is a function of the distance from the antenna and the relative dielectric constant and conductivity of the ground plane. Since the surface wave attenuates exponentially with increasing range, the surface wave radiation pattern varies with distance from the antenna. While the space wave can be calculated at different distances from the antenna, its radiation pattern is predominately invariant with distance from the antenna.

Equations for the radiated electric fields of a vertical antenna above planar earth were derived by Sommerfeld in 1909 [Ref 7], but the final form of these equations is complicated and difficult to evaluate. Norton simplified these equations to a form suitable for engineering applications [Ref 8]. Norton's expression for the surface wave of an elemental vertical dipole above a ground plane is [Ref 5: p. 644]

$$j30\beta Idl(1-\Gamma_v)F\left(\frac{e^{-j\beta[R+H_0\cos(\theta)]}}{R}\right) \cdot \left[\hat{k}(1-u^2)+\hat{r}\sin(\theta)\left(1+\frac{\sin^2(\theta)}{2}\right)u\sqrt{1-u^2\sin^2(\theta)}\right] \quad (4.37)$$

Its derivation is not explained here, but references 6 and 7 give a detailed derivation. In equation 4.37, R is distance to the field point, \hat{r} and \hat{k} are unit vectors perpendicular and parallel to the antenna axis respectively, u is the inverse of the complex index of refraction (n), and F is the surface wave attenuation factor. The function F introduces a surface wave attenuation dependent upon distance, frequency, and the properties of the earth over which the wave is travelling. The attenuation factor is given by [Ref 5: pp. 644-651]

$$F_e = 1 - j\sqrt{\pi P_e} e^{-P_e} [\text{erfc}(j\sqrt{P_e})] \quad (4.38)$$

$$P_e = \frac{-j\beta Ru^2[1-u^2\sin^2(\theta)]}{2} \left[1 + \frac{\cos(\theta)}{u\sqrt{1-u^2\sin^2(\theta)}} \right]^2 \quad (4.39)$$

$$\text{or } P_e = \frac{-j\beta[R+H_0\cos(\theta)]}{2\sin^2(\theta_r)} \left[\cos(\theta_r) + \frac{\sqrt{n^2-\sin^2(\theta_r)}}{n^2} \right]^2 \quad (4.40)$$

where P_e is the complex numerical distance for vertical polarization and the erfc term is the complementary error function defined by

$$\text{erfc}(j\sqrt{P_e}) = \frac{2}{\sqrt{\pi}} \int_{j\sqrt{P_e}}^{\infty} e^{-x^2} dx \quad (4.41)$$

Mathcad is incapable of evaluating the complementary error function for complex numbers, so an asymptotic expansion and infinite series approximation [Ref 9] was written into the Mathcad code to evaluate the erfc terms.

When the magnitude of $j\sqrt{P_e}$ is less than 2.18, the Mathcad applications use

$$\text{erf}(x+jy) = \text{erf}(x) + \frac{e^{-x^2}}{2\pi X} \left[(1 - \cos(2xy)) + j \sin(2xy) \right] \quad (4.42)$$

$$+ \frac{2}{\pi} e^{-x^2} \sum_{n=1}^{\infty} \frac{e^{-\frac{1}{2}n^2}}{n^2 + 4X^2} \left[f_n(x, y) + j g_n(x, y) \right] + \epsilon(x, y) \quad \text{where}$$

$$f_n(x, y) = 2x - 2x \cosh(ny) \cos(2xy) + n \sinh(ny) \sin(2xy)$$

$$g_n(x, y) = 2x \cosh(ny) \sin(2xy) + n \sinh(ny) \cos(2xy)$$

$$|\epsilon(x, y)| \approx 10^{-16} |\text{erf}(x+jy)|$$

an infinite series approximation which evaluates $\text{erf}(j\sqrt{P_e})$, where 'erf' is the standard error function. [Ref 9 p. 299]. The solution to $\text{erfc}(j\sqrt{P_e})$ is then found by

$$\text{erfc}(x+jy) = 1 - \text{erf}(x+jy) \quad (4.43)$$

When the magnitude of $j\sqrt{P_e}$ is greater than 2.18, the Mathcad code uses

$$\sqrt{\pi}ze^{z^2}\text{erfc}(z) \approx 1 + \sum_{m=1}^{\infty} (-1)^m \frac{1 \cdot 3 \cdot 5 \cdot \dots \cdot (2m-1)}{(2z^2)^m} \quad (4.44)$$

$$\text{or } j\sqrt{\pi P_e}e^{-P_e}\text{erfc}(j\sqrt{P_e}) \approx 1 + \sum_{m=1}^{\infty} (-1)^m \frac{1 \cdot 3 \cdot 5 \cdot \dots \cdot (2m-1)}{(-2P_e)^m}$$

$$\left(z \rightarrow \infty, |\arg z| < \frac{3\pi}{4}\right)$$

an asymptotic expansion which solves for $j\sqrt{\pi P_e} \cdot \text{erfc}(j\sqrt{P_e})$ [Ref 9 p. 298]. Either of these solutions can be substituted directly into equation 4.38 to find the surface wave attenuation factor.

A magnitude of 2.18 is used as the transition point in the Mathcad applications because it provides the smoothest transition in both magnitude and phase between the series approximation and asymptotic expansion results.

For antennas which radiate an electric field with a ϕ component, the surface wave attenuation factor for horizontal polarization (F_m) must be found using

$$F_m = 1 - j\sqrt{\pi P_m}e^{-P_m}\text{erfc}(j\sqrt{P_m}) \quad (4.45)$$

$$\text{and } P_m = \frac{-j\beta(R+H_0\cos(\theta))}{2\sin^2(\theta_r)} \left[\cos(\theta_r) + \sqrt{n^2 - \sin^2(\theta_r)} \right]^2 \quad (4.46)$$

where P_m is the complex numerical distance for horizontal polarization. The variable θ_r in equations 4.40 and 4.46 for P_e and P_m , respectively is approximated as θ (just as it was for the reflection coefficients in equations 4.34 and 4.35).

The numerical distances (P_e and P_m) and the surface wave attenuation factors (F_e and F_m) are evaluated for $0^\circ \leq \theta \leq 90^\circ$ to determine surface wave radiation patterns. Their value is of most interest, however, directly at the surface ($\theta=90^\circ$) where the magnitude of F is called the *ground wave attenuation factor*. Numerical distance is proportional to distance from the antenna and the square of the frequency, while it is approximately inversely proportional to ground conductivity. When the magnitude of the numerical distance is less than about 4.5, empirical formulas show that the ground wave attenuation factor varies exponentially with numerical distance. For numerical distance magnitudes greater than 4.5, empirical formulas show that the ground wave attenuation factor is inversely proportional to the numerical distance. Numerical distance magnitudes are typically much greater than 4.5 in the far-field. This implies that the *ground wave* ($\theta=90^\circ$) field strength varies inversely with the square of the distance from the antenna since numerical distance is directly proportional to distance from the antenna and equation 4.37 shows an explicit $1/R$ dependence in addition to the attenuation factor.

The Mathcad applications determine the complex numerical distances for the same discrete values of θ described in Chapter 4.D. After determining the complementary error function for each numerical distance result, the surface wave attenuation factor is calculated for each discrete θ . The

surface wave is evaluated for each θ using the equations for the electric field distribution, and the discrete results of the surface wave are normalized with respect to the value with maximum magnitude. The surface wave pattern is depicted by plotting the normalized magnitudes for $-\pi/2 < \theta < \pi/2$. The numerical distances (P_e and P_m) at the surface ($\theta=90^\circ$) are also listed with the predicted radiation parameters.

With all of the terms defined, equation 4.37 is integrated over the length of a generic finite length vertical dipole to obtain the radiated surface wave distribution of an elevated vertical dipole [Ref 6 p.166]

$$E_\theta = j60I_0 \frac{e^{-j\beta[R+H_0\cos(\theta)]}}{R} \left[\frac{\cos[\beta h \cos(\theta)] - \cos(\beta h)}{\sin}(\theta) \right] \quad (4.47)$$

$$(1-\Gamma_v) F_e \left[\sin^2(\theta) - \frac{\sqrt{n^2 - \sin^2(\theta)}}{n^2} \cos(\theta) \right]$$

The total radiated far-field electric field distribution of an elevated vertical dipole above a planar earth can now be expressed by combining equations 4.36 and 4.37 to write

$$E_\theta = j60I_0 \frac{e^{-j\beta[R-H_0\cos(\theta)]}}{R} \left[\frac{\cos[\beta h \cos(\theta)] - \cos(\beta h)}{\sin(\theta)} \right] \quad (4.48)$$

$$\left[1 + \Gamma_v e^{-j2\beta H_0 \cos(\theta)} + (1-\Gamma_v) F_e e^{-j2\beta H_0 \cos(\theta)} \left[\sin^2(\theta) - \frac{\sqrt{n^2 - \sin^2(\theta)}}{n^2} \cos(\theta) \right] \right]$$

The first two terms inside the brackets represent the space wave and the third term represents the surface wave.

Chapter IV has defined the necessary terms and provided a detailed derivation of the total electric field distribution

for an elevated vertical dipole antenna. The result is a radiated electric field distribution with a θ component only. Most antenna types radiate an electric field with both θ and ϕ components. While a detailed derivation of an electric field ϕ component was not presented here, the necessary horizontal polarization terms associated with deriving ϕ components were discussed. When these horizontal terms are substituted for their vertical counterparts, the method used to derive the electric field equation for the ϕ component of a radiated space wave or surface wave is identical to that used in deriving the θ component for the elevated vertical dipole.

The remaining chapters of this thesis explain the antenna configuration and the calculations of each individual Mathcad application. Only the final expressions for the radiated far-field electric field distributions are provided since the derivation of each follows the same procedure as explained in this chapter. There is a lot of text repetition among the remaining chapters because each is written as a stand alone users guide for its associated Mathcad application. Any important concepts not presented in previous chapters are discussed as required.

V. THE ELEVATED VERTICAL DIPOLE

The orientation of the elevated vertical dipole is depicted in Figure 5.1, where l is the length of the dipole, H_0 is the height of the feed above ground, R is the radial coordinate, θ is the elevation coordinate, and ϕ is the azimuth coordinate.

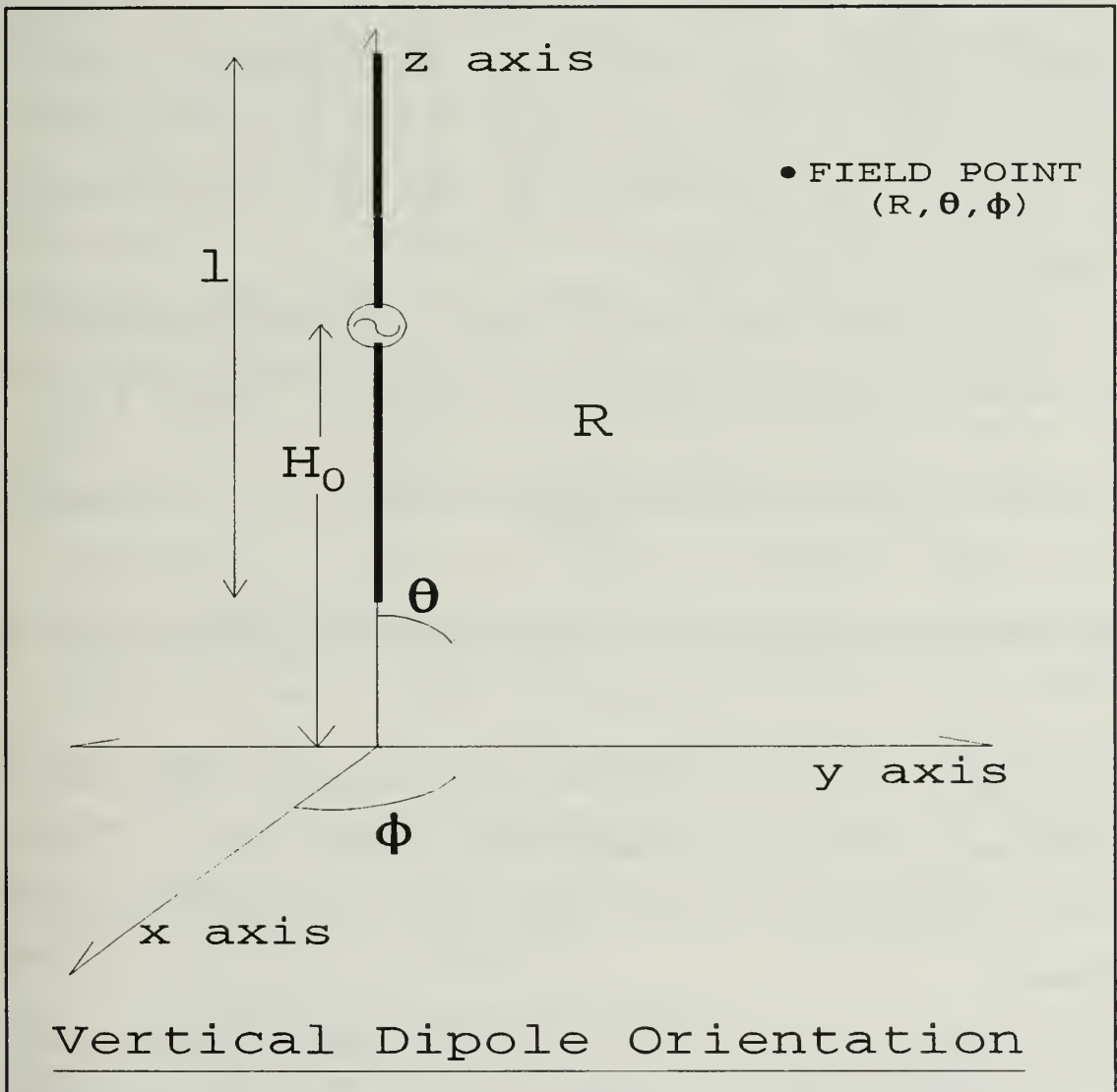


FIGURE 5.1: Spatial orientation of the elevated vertical dipole antenna for its corresponding Mathcad application.

The Mathcad application for the elevated vertical dipole requires the following inputs:

l.....length of the dipole (meters)
 f_soperational frequency (Hertz)
 H_0antenna feed height above ground plane (meters)
 Rdistance from antenna (meters)
 ϵ_rrelative dielectric constant of ground plane
 σconductivity of ground plane

The length of the dipole is used to determine the frequencies which correspond to a $\lambda/4$, $\lambda/2$, $3\lambda/4$, or λ length dipole. The user inputs the frequency and the radiation parameters discussed in Chapter 3 are calculated. Feed height (H_0) must be at least equal to the half-length of the dipole ($h=l/2$), and the distance from the antenna (R) must meet the far-field requirements of Chapter 3.C.

The equation for the radiated electric field distribution of the elevated vertical dipole was derived in Chapter 4 as

$$E_\theta = j60I_0 \frac{e^{-j\beta[R-H_0\cos(\theta)]}}{R} \left(\frac{\cos[\beta h \cos(\theta)] - \cos(\beta h)}{\sin(\theta)} \right) \quad (5.1)$$

$$\left[1 + \Gamma_v e^{-j2\beta H_0 \cos(\theta)} + (1 - \Gamma_v) F_e e^{-j2\beta H_0 \cos(\theta)} \left(\sin^2(\theta) - \frac{\sqrt{n^2 - \sin^2(\theta)}}{n^2} \cos(\theta) \right) \right]$$

The first two terms inside the brackets represent the space wave and the third term represents the surface wave. I_0 is one since a sinusoidal current input with a maximum of unity is assumed.

The requested inputs are used to calculate variables at the top of page 41 for 632 discrete values of θ which are equally incremented from $-\pi/2$ to $\pi/2$.

hhalf-length of the dipole (meters)
 λ_swavelength of the operational frequency (meters)
 βfree space wavenumber for operational frequency
 R_ddistance from antenna to field point (meters)
 R_rdistance from antenna image to field point (meters)
 nindex of refraction
 P_ecomplex numerical distance (vertical polarization)
 Γ_vvertical reflection coefficient
 F_evertical surface wave attenuation factor

The calculated variables are used to evaluate the radiated far-field space wave and surface wave for each discrete θ . The space wave and surface wave results are combined for corresponding values of θ to obtain the total radiated electric field distribution. The space wave, surface wave, and total electric field results are then normalized with respect to the maximum field intensity of each, and the normalized magnitudes are plotted for each value of θ to depict the radiation patterns. The patterns are valid for any vertical plane containing the antenna axis, because the radiated electric field does not vary with changes in ϕ .

Equations 3.8 and 3.9 are used to integrate equation 5.1 over the hemispherical Gaussian surface above the ground plane at a fixed radius (R) from the antenna to find total average radiated power (P_{rad}). With the discrete values of the electric field and total average radiated power determined, the Mathcad application predicts the following radiation characteristics from the equations in Chapter 3:

R_{rad} radiation resistance (Ohms)
 D_0 directivity
 $EIRP$effective radiated isotropic power (Watts)
 A_{max} maximum theoretical effective area (square meters)
 l_{max} maximum theoretical effective length (meters)
 P_e numerical distance (vertical polarization, $\theta=90^\circ$)
 $Angle_{max}$.elevation angle of maximum directive gain (degrees)

As an example, the Mathcad vertical dipole application was executed with the following inputs:

dipole length	3 meters
frequency	$100 \cdot 10^6$ Hertz
height of antenna feed	1.5 meters
distance from the antenna	3000 meters
relative dielectric constant	15
ground conductivity	$5 \cdot 10^{-3}$

Figures 5.2 and 5.3 depict the radiation patterns for the space wave and surface wave for this example.

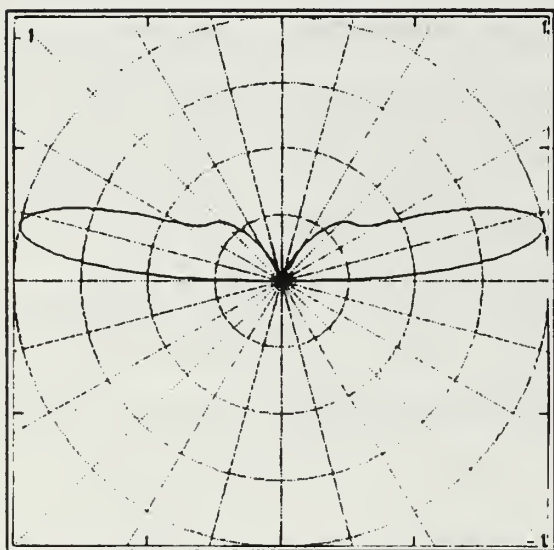


FIGURE 5.2: Vertical dipole space wave radiation pattern.

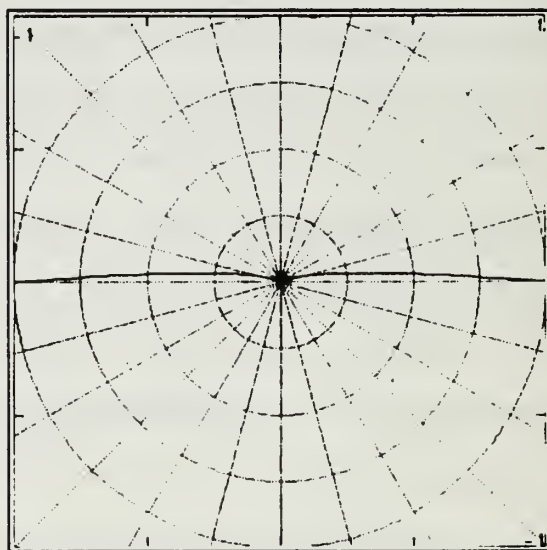


FIGURE 5.3: Vertical dipole surface wave pattern.

The following radiation parameters were predicted by the Mathcad application for a sinusoidal current input of one Amp:

Total power radiated	31.233 Watts
Radiation resistance	62.467 Ohms
Directivity	6.034
Effective isotropic radiated power	188.470 Watts
Maximum theoretical effective area	4.322 sq meters
Maximum theoretical effective length	1.692 meters
Numerical distance (vertical)	195.178
Elevation of directivity	12.266 degrees

These results are consistent with expectations for this particular configuration. Appendix A contains computer hardcopies of additional example calculations for the vertical dipole and compares predicted radiation parameters to those expected based on previous calculations.

VI. THE VERTICAL MONOPOLE

The orientation of the vertical monopole is depicted in Figure 6.1, where h is the length of the monopole, the antenna feed is at ground level, R is the radial coordinate, θ is the elevation coordinate, and ϕ is the azimuth coordinate.

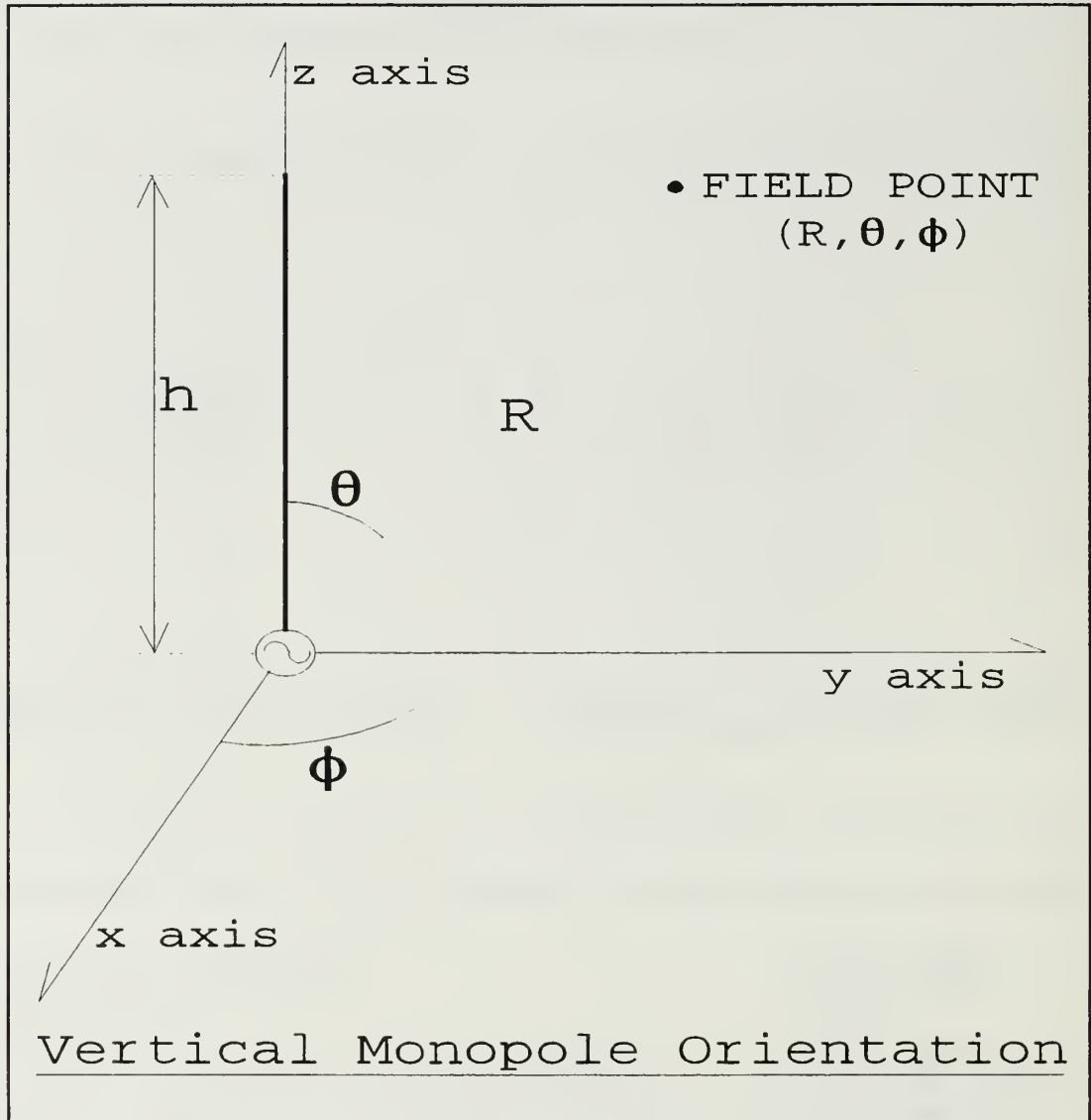


FIGURE 6.1: Spatial orientation of the vertical monopole antenna for its corresponding Mathcad application.

The Mathcad application for the vertical monopole requires the following inputs:

h.....length of the monopole (meters)
 f_s.....operational frequency (Hertz)
 R.....distance from antenna (meters)
 ε_r.....relative dielectric constant of ground plane
 σ.....conductivity of ground plane

The length of the monopole is used to determine frequencies which correspond to a λ/8, λ/4, 3λ/8, or λ/2 long monopole. The user inputs the frequency for which the radiation parameters discussed in Chapter 3 are calculated. Distance from the antenna (R) must meet the far-field requirements of Chapter 3.C.

The monopole's electric field distribution is derived in the same way as the vertical dipole equation was derived in Chapter 4 and is given by [Ref 6: p.152]

$$\begin{aligned}
 E_{\theta} = & j30I_0 \frac{e^{-j\beta R}}{R} \left[\frac{A+jB}{\sin(\theta)} + \Gamma_v \frac{A-jB}{\sin(\theta)} \right] \quad (6.1) \\
 & + (1-\Gamma_v) F_e \frac{A-jB}{\sin(\theta)} \left(\sin^2(\theta) - \frac{\sqrt{n^2 - \sin^2(\theta)}}{n^2} \cos(\theta) \right) \\
 & - j2F_e \sin(\beta h) \left(\sin^2(\theta) - \frac{\sqrt{n^2 - \sin^2(\theta)}}{n^2} \cos(\theta) \right) \frac{\sqrt{n^2 - \sin^2(\theta)}}{n^2 \sin(\theta)} \Bigg] \\
 A = & \cos[\beta h \cos(\theta)] - \cos(\beta h) \\
 B = & \sin[\beta h \cos(\theta)] - \cos(\theta) \sin(\beta h)
 \end{aligned}$$

The first two terms inside the brackets represent the space wave and the second two terms represent the surface wave. The vertical monopole's far-field electric field has a θ component only , just as the vertical dipole. I₀ is one since a sinusoidal current input with a maximum of unity is assumed.

The requested inputs are used to calculate the following variables for 632 discrete values of θ which are equally incremented from $-\pi/2$ to $\pi/2$:

λ_s wavelength of the operational frequency (meters)
 β free space wavenumber for operational frequency
 n index of refraction
 P_e complex numerical distance (vertical polarization)
 Γ_v vertical reflection coefficient
 F_e vertical surface wave attenuation factor

The calculated variables are used to evaluate the radiated far-field space wave and surface wave for each discrete θ . The space wave and surface wave results are combined for corresponding values of θ to obtain the total radiated electric field distribution. The space wave, surface wave, and total electric field results are then normalized with respect to the maximum field intensity of each, and the normalized magnitudes are plotted for each value of θ to depict the radiation patterns. The patterns are valid for any vertical plane containing the antenna axis, because the radiated electric field does not vary with changes in ϕ .

Equations 3.8 and 3.9 are used to integrate equation 6.1 over the hemispherical Gaussian surface above the ground plane at a fixed radius (R) from the antenna to find the total average radiated power (P_{rad}). With the discrete values of the electric field and total average radiated power determined, the Mathcad application predicts the radiation characteristics listed at the top of the next page from the equations in Chapter 3.

Radiation characteristics determined by the vertical monopole application are:

R_{rad} radiation resistance (Ohms)
 D_0 directivity
EIRP.....effective radiated isotropic power (Watts)
 A_{max} maximum theoretical effective area (square meters)
 l_{max} maximum theoretical effective length (meters)
 P_e numerical distance (vertical polarization, $\theta=90^\circ$)
Angle $_{max}$.elevation angle of maximum directive gain (degrees)

As an example, the Mathcad monopole application was executed with the following inputs:

monopole length	0.5 meters
frequency	$150 \cdot 10^6$ Hertz
distance from the antenna	3000 meters
relative dielectric constant	15
ground conductivity	$5 \cdot 10^{-3}$

Figures 6.2 and 6.3 depict the radiation patterns for the space wave and surface wave for this example.

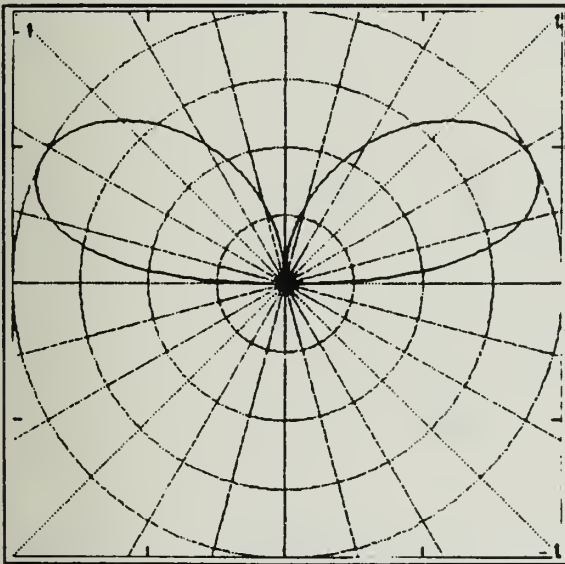


FIGURE 6.2: Monopole space wave radiation pattern.

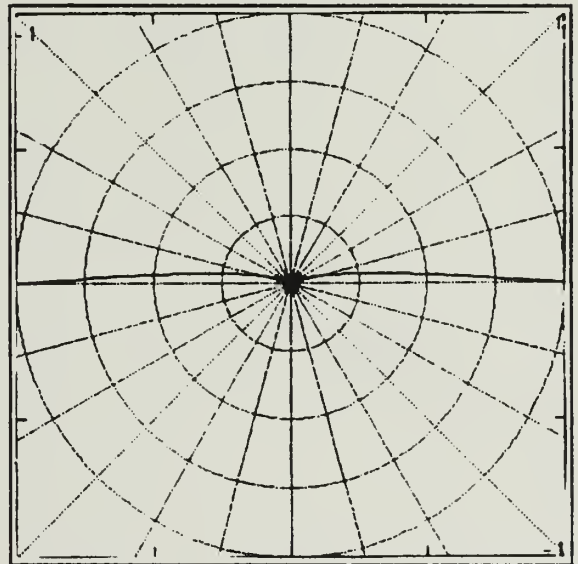


FIGURE 6.3: Monopole surface wave radiation pattern.

The following radiation parameters were predicted by the Mathcad application for a sinusoidal current input of one Amp:

Total power radiated	5.607 Watts
Radiation resistance	11.215 Ohms
Directivity	3.246
Effective isotropic radiated power	18.203 Watts
Maximum theoretical effective area	1.033 sq meters
Maximum theoretical effective length	0.351 meters
Numerical distance (vertical)	293.016
Elevation of directivity	26.815 degrees

These results are consistent with expectations for this particular configuration. Appendix B contains computer hardcopies of additional example calculations for the vertical monopole and compares predicted radiation parameters to those expected based on previous calculations.

VII. THE HORIZONTAL DIPOLE

The orientation of the horizontal dipole is depicted in Figure 7.1, where l is length of the dipole, H_0 is the height of the feed above ground, R is the radial coordinate, θ is the elevation coordinate, and ϕ is the azimuth coordinate.

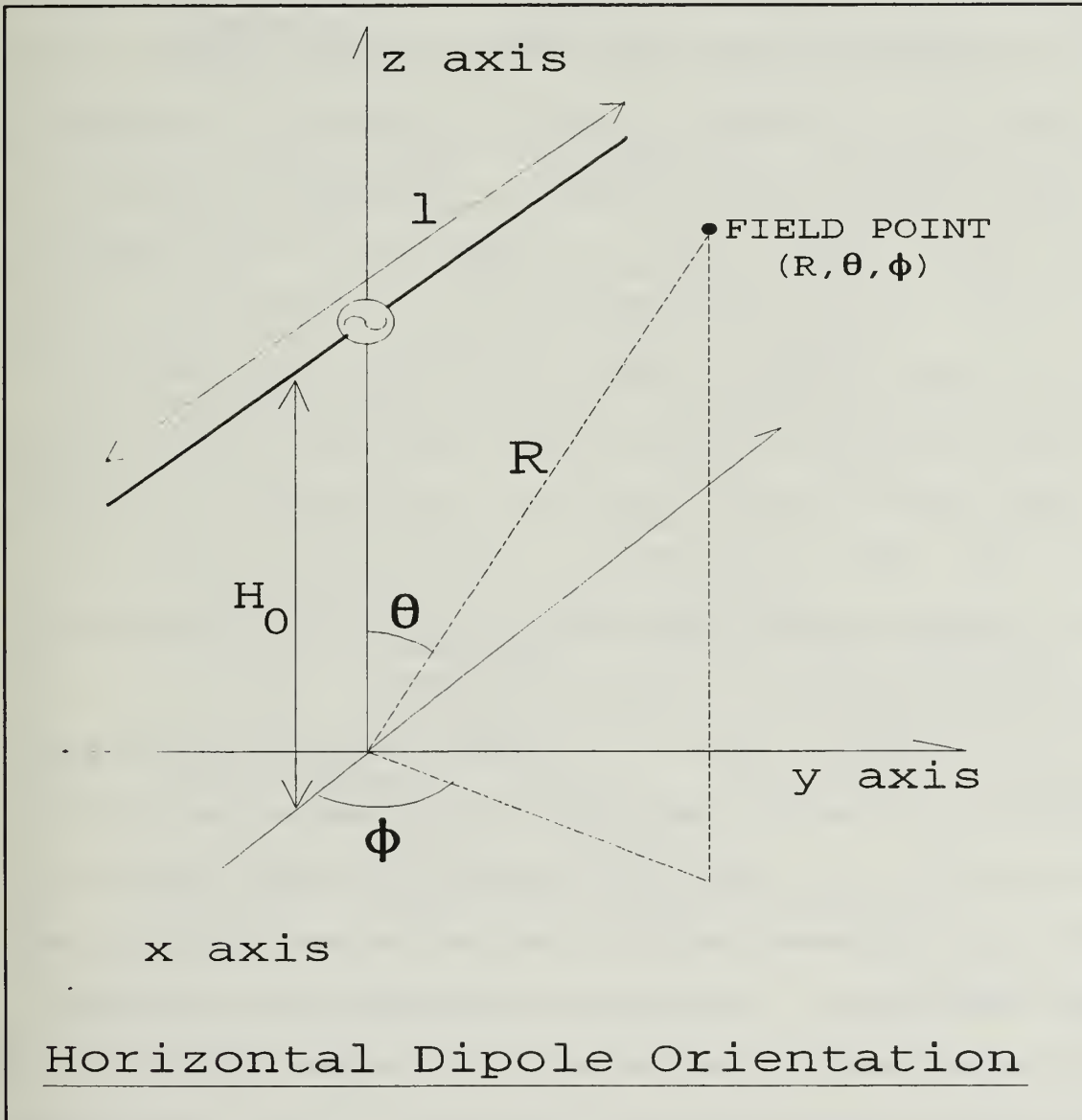


FIGURE 7.1: Spatial orientation of the horizontal dipole antenna for its corresponding Mathcad application.

The Mathcad application for the horizontal dipole requires the following inputs:

l.....length of the dipole (meters)
H₀.....antenna feed height above ground plane (meters)
f_s.....operational frequency (Hertz)
R.....distance from antenna (meters)
ε_r.....relative dielectric constant of ground plane
σ.....conductivity of ground plane
d.....elevation angle index (from Table 3.1)

The length of the dipole is used to determine frequencies which correspond to a $\lambda/4$, $\lambda/2$, $3\lambda/4$, or λ length dipole. The user inputs the frequency for which the radiation parameters discussed in Chapter 3 are computed. Feed height, H₀, must be greater than or equal to zero, and distance from the antenna (R) must meet the far-field requirements of Chapter 3.C. The elevation angle index (d) sets the elevation coordinate, θ , for which a horizontal radiation pattern is determined. Table 3.1 lists possible indices and their corresponding elevation angles from .285° to 88.857° in increments of about 2°. Indices between those listed can be used to interpolate a better approximation of a desired elevation.

The horizontal dipole's radiated electric field is a combination of $\hat{\theta}$ and $\hat{\phi}$ components. In addition, unlike the vertical dipole, its radiation pattern varies with changes in ϕ . The total radiated electric field is the vector sum of the $\hat{\theta}$ and $\hat{\phi}$ components. The electric field for the horizontal dipole is obtained in a manner analogous to that used for the vertical dipole discussed in Chapter 4. The horizontal dipole's $\hat{\theta}$ and $\hat{\phi}$ field components are given by [Ref 6: p. 144]

$$E_{\theta} = -j60I_0 \cos(\phi) \left(\frac{\cos[\beta h \sin(\theta) \cos(\phi)] - \cos(\beta h)}{1 - \sin^2(\theta) \cos^2(\phi)} \right) \quad (7.1)$$

$$\cdot \frac{e^{-j\beta[R-H_0 \cos(\theta)]}}{R} \left[\cos(\theta) (1 - \Gamma_v e^{-j2\beta H_0 \cos(\theta)}) \right. \\ \left. + (1 - \Gamma_v) F_e e^{-j2\beta H_0 \cos(\theta)} \frac{\sqrt{n^2 - \sin^2(\theta)}}{n^2} \left(\sin^2(\theta) - \frac{\sqrt{n^2 - \sin^2(\theta)}}{n^2} \cos(\theta) \right) \right]$$

$$E_{\phi} = j60I_0 \sin(\phi) \left(\frac{\cos[\beta h \sin(\theta) \cos(\phi)] - \cos(\beta h)}{1 - \sin^2(\theta) \cos^2(\phi)} \right) \quad (7.2)$$

$$\cdot \frac{e^{-j\beta[R-H_0 \cos(\theta)]}}{R} \left[1 + \Gamma_h e^{-j2\beta H_0 \cos(\theta)} + (1 - \Gamma_h) F_m e^{-j2\beta H_0 \cos(\theta)} \right]$$

The first two terms inside the brackets of each equation are the space wave components and the third terms are the surface wave components. I_0 is taken to be one, since a sinusoidal current input with a maximum of unity is assumed.

The requested inputs are used to calculate the following variables using a constant ϕ of $\phi=0$ and $\phi=\pi/2$ for 632 discrete values of θ which are equally incremented from $-\pi/2$ to $\pi/2$:

h.....half-length of the dipole (meters)
 λ_swavelength of the operational frequency (meters)
 βfree space wavenumber for operational frequency
 R_ddistance from antenna to field point (meters)
 R_rdistance from antenna image to field point (meters)
n.....index of refraction
 P_ecomplex numerical distance (vertical polarization)
 P_mcomplex numerical distance (horizontal polarization)
 Γ_vvertical reflection coefficient
 Γ_hhorizontal reflection coefficient
 F_evertical surface wave attenuation factor
 F_mhorizontal surface wave attenuation factor

The calculated variables are used to evaluate the far-field space wave and surface wave for the discrete values of θ for $\phi=0$ and $\phi=\pi/2$. The total space wave and surface wave distributions are determined from vector addition of

corresponding $\hat{\theta}$ and $\hat{\phi}$ components. The space wave and surface wave results are then combined for corresponding discrete values of θ to obtain the total radiated electric field distribution for the $\phi=0$ and $\phi=\pi/2$ vertical planes. The space wave, surface wave, and total electric field results are then normalized with respect to the maximum field intensity of each, and the normalized magnitudes are plotted for each discrete θ to depict the radiation patterns. The Mathcad horizontal dipole application computes the space wave, surface wave, and total electric field radiation patterns and radiation parameters in the $\phi=0$ and $\phi=\pi/2$ vertical planes.

The variables corresponding to the selected elevation angle index (d) are used to evaluate the radiated electric field components for the space wave and surface wave at the fixed elevation angle (θ_d) as ϕ varies from 0 to 2π in 632 equal increments. The horizontal radiation patterns are then plotted for the space wave, surface wave, and total radiated electric field just as those for the vertical planes.

To find the contributions of the $\hat{\theta}$ and $\hat{\phi}$ electric field components to the total average radiated power (P_{rad}), equations 3.8 and 3.9 are used to integrate equations 7.1 and 7.2 over the hemispherical Gaussian surface above the ground plane at a fixed radius (R) from the antenna. With the discrete values of the electric field and total average radiated power, the Mathcad application predicts the following radiation characteristics from the equations in Chapter 3:

R_{rad} radiation resistance (Ohms)
 D_0 directivity
EIRP.....effective radiated isotropic power (Watts)
 A_{max} maximum theoretical effective area (square meters)
 l_{max} maximum theoretical effective length (meters)
 P_c numerical distance (vertical polarization, $\theta=90^\circ$)
 P_m numerical distance (horizontal polarization, $\theta=90^\circ$)
 $Angle_{max}$.elevation angle of maximum directive gain (degrees)

The directivity (D_0), effective isotropic radiated power (EIRP), maximum theoretical effective area (A_{max}), maximum theoretical effective length (l_{max}), and the elevation angle of maximum directive gain ($Angle_{max}$) are all determined for both the $\phi=0$ and $\phi=\pi/2$ vertical planes.

As an example, the Mathcad horizontal dipole application was executed with the following inputs:

dipole length	1.0 meter
frequency	$150 \cdot 10^6$ Hertz
height of antenna feed	1.0 meter
distance from the antenna	3000 meters
relative dielectric constant	15
ground conductivity	10^{-2}
elevation angle index	535 ($\approx 27^\circ$)

The following radiation parameters were predicted by the Mathcad application for a sinusoidal current input of one Amp:

Total power radiated (Watts)	26.116
Radiation resistance (Ohms)	52.233
Numerical distance (vertical)	292.419
Numerical distance (horizontal)	66215.4
	<u>$\phi=0$</u> <u>$\phi=\pi/2$</u>
Directivity	1.310 7.215
EIRP (Watts)	34.221 188.435
Max eff area (sq meters)	0.417 2.297
Max eff length (meters)	0.481 1.128
$Angle_{max}$ (degrees)	45.071 28.241

Figures 7.2 through 7.7 are the space wave and surface wave radiation patterns in the $\phi=0$ and $\phi=\pi/2$ vertical planes and the designated horizontal plane for this example.

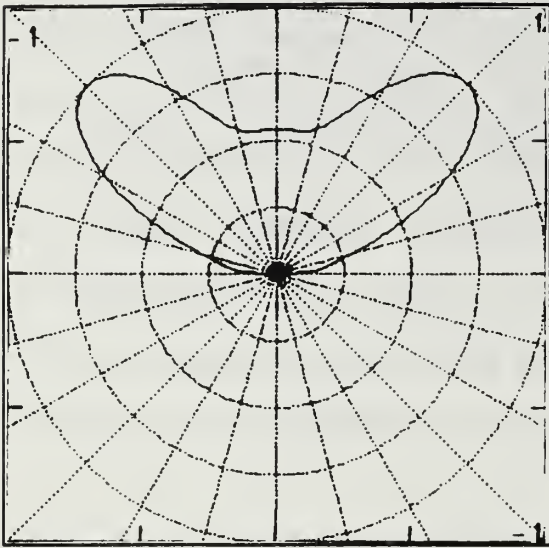


FIGURE 7.2: Horizontal dipole space wave radiation pattern for $\phi=0$ vertical plane.

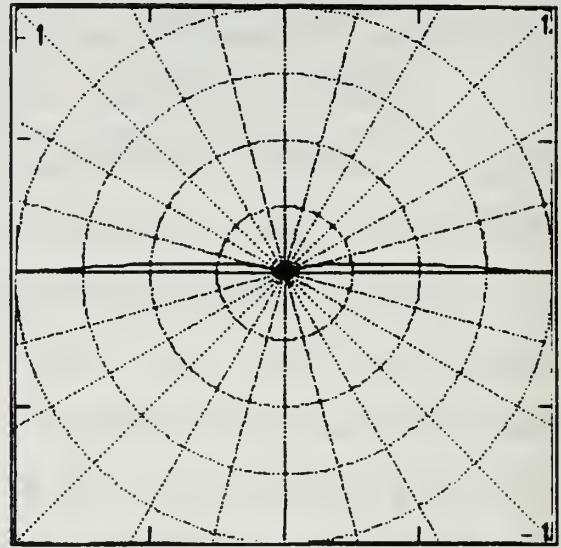


FIGURE 7.3: Horizontal dipole surface wave radiation pattern for $\phi=0$ vertical plane.

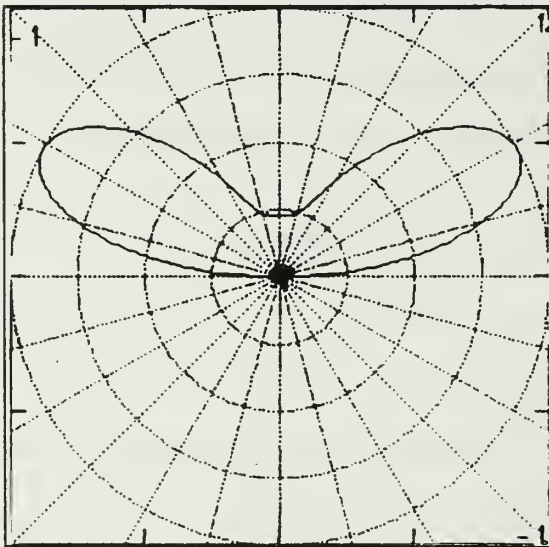


FIGURE 7.4: Horizontal dipole space wave radiation pattern for $\phi=\pi/2$ vertical plane.

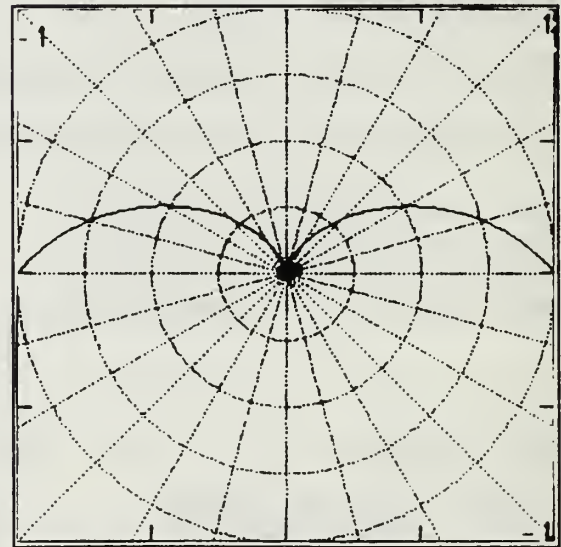


FIGURE 7.5: Horizontal dipole surface wave radiation pattern for $\phi=\pi/2$ vertical plane.

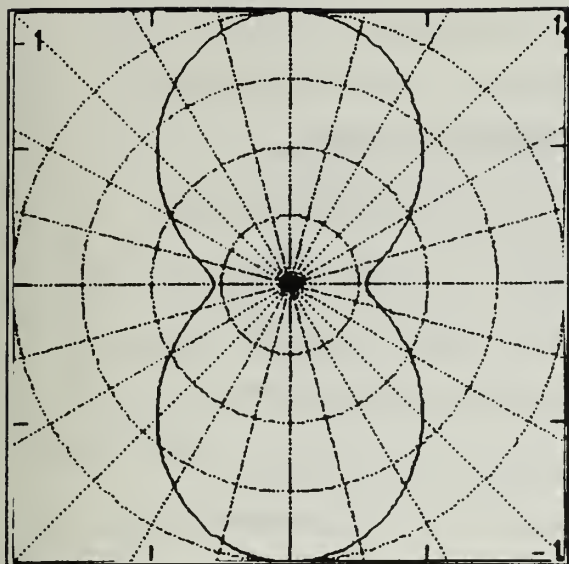


FIGURE 7.6: Horizontal dipole space wave radiation pattern for horizontal plane.

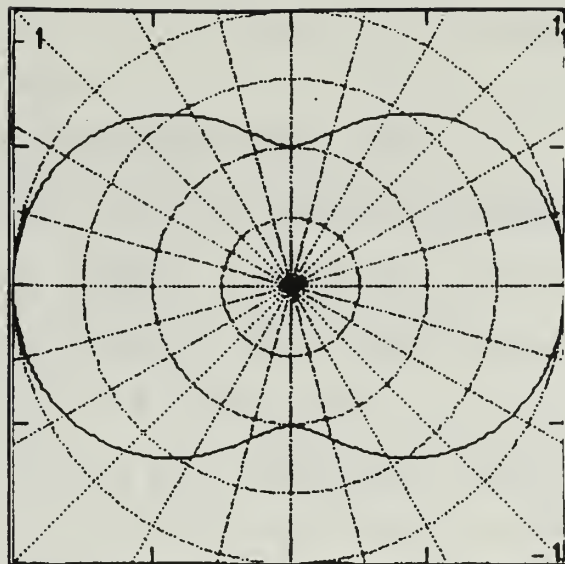


FIGURE 7.7: Horizontal dipole surface wave radiation pattern for horizontal plane.

These results are consistent with expectations for this particular configuration. Appendix C contains computer hardcopies of additional example calculations for the horizontal dipole and compares predicted radiation parameters to those expected based on previous calculations.

VIII. THE ARBITRARILY ORIENTED DIPOLE

The orientation of the arbitrarily oriented dipole is depicted in Figure 8.1, where l is length of the dipole, H_0 is the feed height above ground, α is the angle of the dipole axis with the horizontal, R is the radial coordinate, θ is the elevation coordinate, and ϕ is the azimuth coordinate.

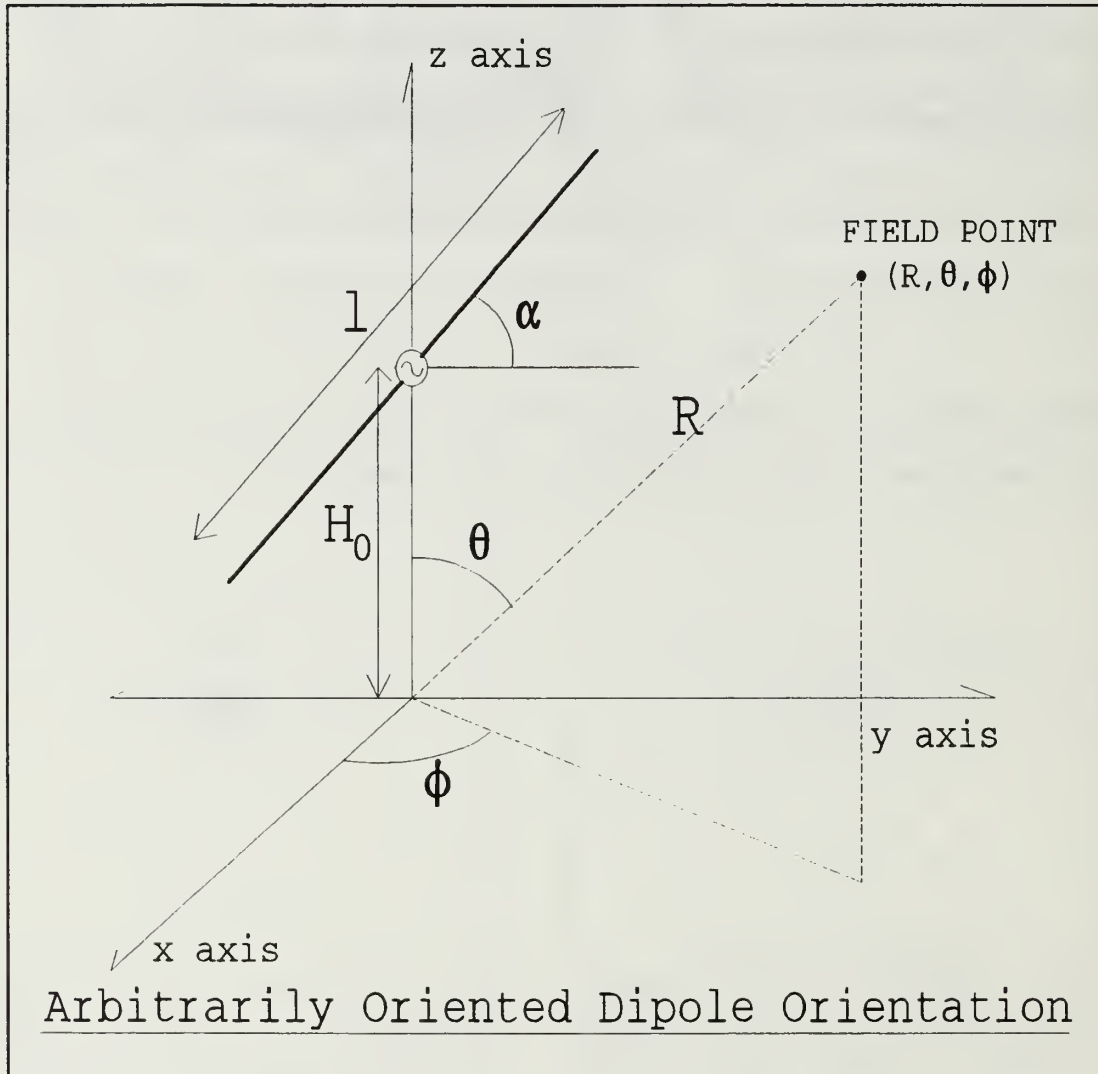


FIGURE 8.1: Spatial orientation of the arbitrarily oriented dipole antenna for its Mathcad application.

The Mathcad application for the arbitrarily oriented dipole requires the following inputs:

- l.....length of the dipole (meters)
- H_0antenna feed height above ground plane (meters)
- αangle of antenna axis with the horizontal (degrees)
- f_soperational frequency (Hertz)
- R.....distance from antenna (meters)
- ϵ_rrelative dielectric constant of ground plane
- σconductivity of ground plane
- d.....elevation angle index (from Table 3.1)

The length of the dipole is used to determine frequencies which correspond to a $\lambda/4$, $\lambda/2$, $3\lambda/4$, or λ length dipole. The user inputs the frequency for which the radiation parameters discussed in Chapter 3 are computed. Feed height, H_0 , must be greater than or equal to $(1/2) \cdot \sin(\alpha)$, and the distance from the antenna (R) must meet the far-field requirements of Chapter 3.C. The elevation angle index (d) sets the elevation coordinate, θ , for which a horizontal radiation pattern is determined. Table 3.1 lists possible indices and their corresponding elevation angles from $.285^\circ$ to 88.857° in increments of about 2° . Indices between those listed can be used to interpolate a better approximation of a desired elevation.

The radiated electric field for the arbitrarily oriented dipole is a combination of $\hat{\theta}$ and $\hat{\phi}$ components, and its radiation pattern varies with changes in ϕ . The total electric field is the vector sum of the $\hat{\theta}$ and $\hat{\phi}$ components. The arbitrarily oriented dipole's radiated electric field is obtained in a manner analogous to that used for the vertical dipole discussed in Chapter 4, and is given by

$$E_{\theta} = -j60I_0 \frac{e^{-j\beta R}}{R} e^{j\beta H_0 \cos(\theta)} \quad (8.1)$$

$$\begin{aligned} & \left\{ \frac{A_1}{1-\cos^2(\psi)} (\cos(\alpha) \sin(\phi) \cos(\theta) - \sin(\alpha) \sin(\theta)) \right. \\ & - \Gamma_v \frac{A_2}{1-\cos^2(\psi')} (\cos(\alpha) \sin(\phi) \cos(\theta) + \sin(\alpha) \sin(\theta)) e^{-j2\beta H_0 \cos(\theta)} \\ & + (1-\Gamma_v) F_e e^{-j2\beta H_0 \cos(\theta)} \frac{A_2}{1-\sin^2(\psi')} \left(\sin^2(\theta) - \frac{\sqrt{n^2 - \sin^2(\theta)}}{n^2} \cos(\theta) \right) \\ & \left. \left(\cos(\alpha) \sin(\phi) \frac{\sqrt{n^2 - \sin^2(\theta)}}{n^2} - \sin(\alpha) \sin(\theta) \right) \right\} \end{aligned}$$

$$E_{\phi} = j60I_0 \frac{e^{-j\beta R}}{R} e^{j\beta H_0 \cos(\theta)} \cos(\alpha) \cos(\phi) \quad (8.2)$$

$$\left\{ \frac{A_1}{1-\cos^2(\psi)} + \frac{A_2}{1-\cos^2(\psi')} e^{-j2\beta H_0 \cos(\theta)} (\Gamma_h + (1-\Gamma_h) F_m) \right\}$$

$$\text{where } A_1 = \cos[\beta h \cos(\psi)] - \cos(\beta h)$$

$$\cos(\psi) = \cos(\theta) \sin(\alpha) + \sin(\theta) \cos(\alpha) \sin(\phi)$$

$$A_2 = \cos[\beta h \cos(\psi')] - \cos(\beta h)$$

$$\cos(\psi') = \sin(\theta) \cos(\alpha) \sin(\phi) - \cos(\theta) \sin(\alpha)$$

Equation 8.1 is the $\hat{\theta}$ component (vertically polarized), and equation 8.2 is the $\hat{\phi}$ (horizontally polarized) component [Ref 6: p. 174-175]. The first two terms inside the brackets of each equation represent the space wave components and the third terms represent the surface wave components. I_0 is taken to be one, since a sinusoidal current input with a maximum of unity is assumed.

The requested inputs are used to calculate the following variables using a constant ϕ of $\phi=0$ and $\phi=\pi/2$ for 632 discrete values of θ which are equally incremented from $-\pi/2$ to $\pi/2$:

hhalf-length of the dipole (meters)
 λ_swavelength of the operational frequency (meters)
 βfree space wavenumber for operational frequency
 R_ddistance from antenna to field point (meters)
 R_rdistance from antenna image to field point (meters)
 nindex of refraction
 P_ecomplex numerical distance (vertical polarization)
 P_mcomplex numerical distance (horizontal polarization)
 Γ_vvertical reflection coefficient
 Γ_hhorizontal reflection coefficient
 F_evertical surface wave attenuation factor
 F_mhorizontal surface wave attenuation factor

The calculated variables are used to evaluate the far-field space wave and surface wave for the discrete values of θ for $\phi=0$ and $\phi=\pi/2$. The total space wave and surface wave distributions are determined from vector addition of corresponding $\hat{\theta}$ and $\hat{\phi}$ components. The space wave and surface wave results are then combined for corresponding discrete values of θ to obtain the total radiated electric field distribution for the $\phi=0$ and $\phi=\pi/2$ vertical planes. The space wave, surface wave, and total electric field results are then normalized with respect to the maximum field intensity of each, and the normalized magnitudes are plotted for each discrete θ to depict the radiation patterns. The arbitrarily oriented dipole Mathcad application computes the space wave, surface wave, and total electric field radiation patterns and radiation parameters in the $\phi=0$ and $\phi=\pi/2$ vertical planes.

The variables corresponding to the selected elevation angle index (d) are used to evaluate the radiated electric

field components for the space wave and surface wave at the fixed elevation angle (θ_d) as ϕ varies from 0 to 2π in 632 equal increments. The horizontal radiation patterns are then plotted for the space wave, surface wave, and total radiated electric field just as those in the vertical planes.

To find the contributions of the $\hat{\theta}$ and $\hat{\phi}$ electric field components to the total average radiated power, P_{rad} , equations 3.8 and 3.9 are used to integrate equations 8.1 and 8.2 over the hemispherical Gaussian surface above the ground plane at a fixed radius (R) from the antenna. The sum of the two integrals is the antenna's P_{rad} . With the discrete values of the electric field and total average radiated power determined, the Mathcad application predicts the following radiation characteristics from the equations in Chapter 3:

R_{rad} radiation resistance (Ohms)
 D_0 directivity
 EIRP.....effective radiated isotropic power (Watts)
 A_{max} maximum theoretical effective area (square meters)
 l_{max} maximum theoretical effective length (meters)
 P_e numerical distance (vertical polarization, $\theta=90^\circ$)
 P_m numerical distance (horizontal polarization, $\theta=90^\circ$)
 $Angle_{max}$.elevation angle of maximum directive gain (degrees)

The directivity (D_0), effective isotropic radiated power (EIRP), maximum theoretical effective area (A_{max}), maximum theoretical effective length (l_{max}), and the elevation angle of maximum directive gain ($Angle_{max}$) are all determined for both the $\phi=0$ and $\phi=\pi/2$ vertical planes.

IX. THE INVERTED L ANTENNA

The orientation of the inverted L antenna is depicted in Figure 9.1, where H is length of the vertical antenna segment, l is the length of the horizontal antenna segment, the feed is at ground level, R is the radial coordinate, θ is the elevation coordinate, and ϕ is the azimuth coordinate.

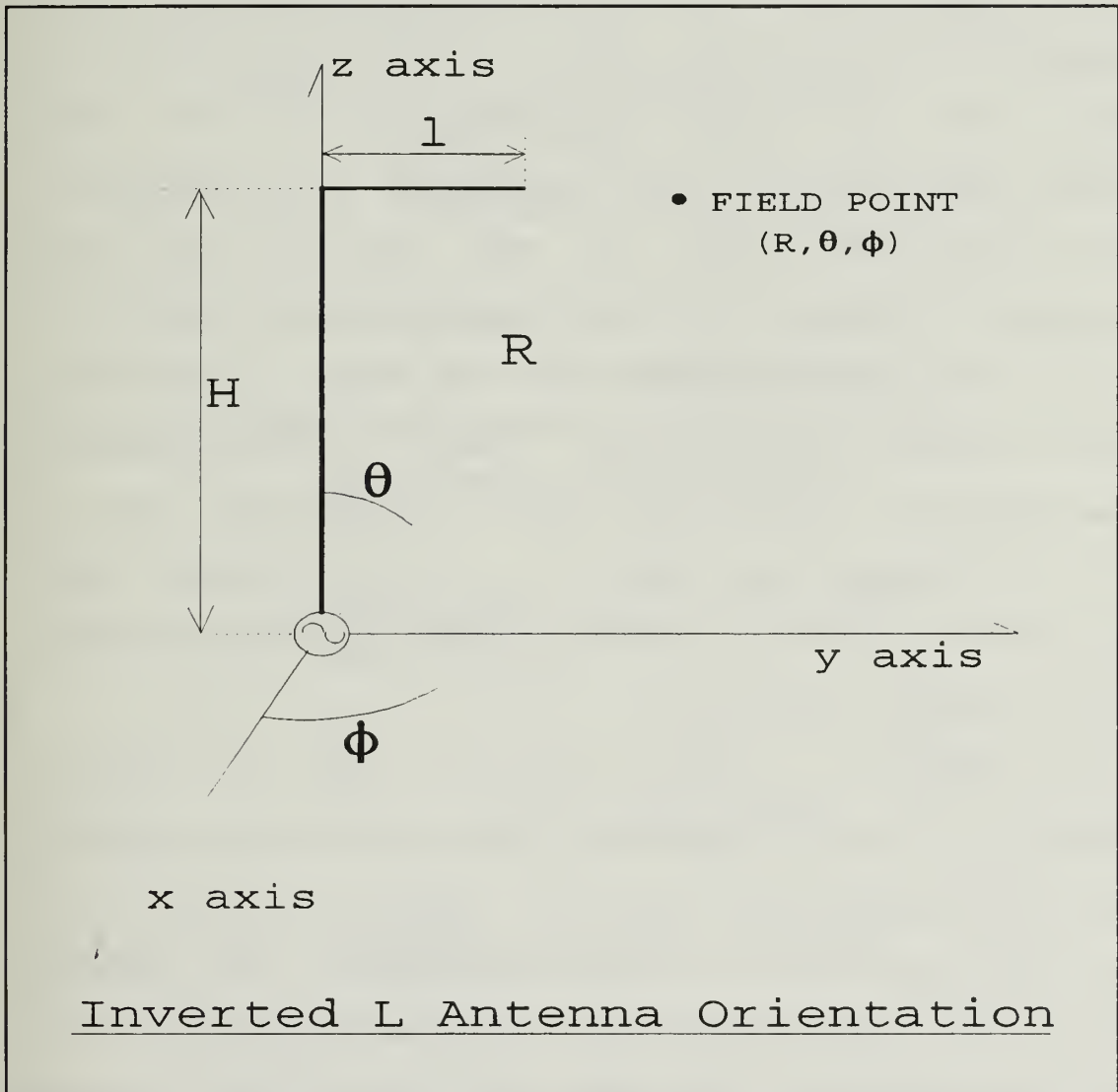


FIGURE 9.1: Spatial orientation of the inverted L antenna for its corresponding Mathcad application.

The Mathcad application for the inverted L antenna requires the following inputs:

H.....length of vertical antenna segment (meters)
l.....length of horizontal antenna segment (meters)
 f_soperational frequency (Hertz)
R.....distance from antenna (meters)
 ϵ_rrelative dielectric constant of ground plane
 σconductivity of ground plane
d.....elevation angle index (from Table 3.1)

The combined length of the vertical and horizontal antenna segments ($H+l$) is used to determine frequencies which correspond to a $\lambda/8$, $\lambda/4$, $3\lambda/8$, or $\lambda/2$ long inverted L antenna. The user inputs the frequency for which the radiation parameters discussed in Chapter 3 are computed. Distance from the antenna (R) must meet the far-field requirements of Chapter 3.C. The elevation angle index (d) sets the elevation coordinate, θ , for which a horizontal radiation pattern is determined. Table 3.1 lists possible indices and their corresponding elevation angles from $.285^\circ$ to 88.857° in increments of about 2° . Indices between those listed can be used to interpolate a better approximation of a desired elevation.

The inverted L's radiated electric field is a varying combination of $\hat{\theta}$ and $\hat{\phi}$ components, and its radiation pattern varies with changes in ϕ . The total radiated electric field is the vector sum of the $\hat{\theta}$ and $\hat{\phi}$ components. The radiated electric field for the inverted L antenna is obtained in a manner analogous to that used for the vertical dipole discussed in Chapter 4. The radiated fields of each antenna

segment are considered separately, and superposition is used to determine the total radiated electric field. The vertical segment radiates only a $\hat{\theta}$ field component, but the horizontal segment radiates both $\hat{\theta}$ and $\hat{\phi}$ components. The electric field equations for the inverted L are [Ref 6: p. 169-170]

$$E_{\theta,v} = j30I_0 \frac{e^{-j\beta R}}{R} \left[\frac{A_v + jB_v}{\sin(\theta)} + \Gamma_v \frac{A_v - jB_v}{\sin(\theta)} \right] \quad (9.1)$$

$$+ (1 - \Gamma_v) F_e \frac{A_v - jB_v}{\sin(\theta)} \left(\sin^2(\theta) - \frac{\sqrt{n^2 - \sin^2(\theta)}}{n^2} \cos(\theta) \right)$$

$$- [\sin[\beta(H+1)] - \sin(\beta l) \cos(\beta H \cos(\theta))] \\ + j \sin(\beta l) \sin[\beta H \cos(\theta)]]$$

$$\cdot j2F_e \left(\sin^2(\theta) - \frac{\sqrt{n^2 - \sin^2(\theta)}}{n^2} \cos(\theta) \right) \left(\frac{\sqrt{n^2 - \sin^2(\theta)}}{n^2 \sin(\theta)} \right)]$$

where $A_v = \cos[\beta H \cos(\theta)] \cos(\beta l) - \cos[\beta(H+1)]$
 $-\sin[\beta H \cos(\theta)] \cos(\theta) \sin(\beta l)$
 $B_v = \sin[\beta H \cos(\theta)] \cos(\beta l) - \cos(\theta) \sin[\beta(H+1)]$
 $+\cos[\beta H \cos(\theta)] \cos(\theta) \sin(\beta l)$

$$E_{\theta,h} = -j30I_0 \frac{\sin(\phi) \cos(\theta)}{1 - \sin^2(\theta) \sin^2(\phi)} \frac{e^{-j\beta R}}{R} e^{\tan^{-1} \frac{B_h}{A_h}} \sqrt{A_h^2 + B_h^2} \quad (9.2)$$

$$\left[1 - \Gamma_v e^{-j2\beta H \cos(\theta)} + \left(\sin^2(\theta) - \frac{\sqrt{n^2 - \sin^2(\theta)}}{n^2} \cos(\theta) \right) \right. \\ \left. \cdot (1 - \Gamma_v) F_e e^{-j2\beta H \cos(\theta)} \frac{\sqrt{n^2 - \sin^2(\theta)}}{n^2} \right]$$

$$E_{\phi,h} = j30I_0 \frac{\cos(\phi)}{1 - \sin^2(\theta) \sin^2(\phi)} \frac{e^{-j\beta R}}{R} e^{\tan^{-1} \frac{B_h}{A_h}} \sqrt{A_h^2 + B_h^2} \quad (9.3)$$

$$[1 + \Gamma_h e^{-j2\beta H \cos(\theta)} + (1 - \Gamma_h) F_m e^{-j2\beta H \cos(\theta)}]$$

where $A_h = \cos[\beta l \sin(\theta) \sin(\phi)] - \cos(\beta l)$
 $B_h = \sin[\beta l \sin(\theta) \sin(\phi)] - \sin(\theta) \sin(\phi) \sin(\beta l)$

Equation 9.1 is the $\hat{\theta}$ component for the vertical segment, equation 9.2 is the $\hat{\theta}$ (vertically polarized) component for the horizontal segment, and equation 9.3 is the $\hat{\phi}$ (horizontally polarized) component for the horizontal segment. The first two terms inside the brackets of each equation are the space wave components and any additional terms are the surface wave components. I_0 is taken to be one, since a sinusoidal current input with maximum of unity is assumed.

The requested inputs are used to calculate the following variables using a constant ϕ of $\phi=0$ and $\phi=\pi/2$ for 632 discrete values of θ which are equally incremented from $-\pi/2$ to $\pi/2$:

h.....half-length of the dipole (meters)
 λ_s wavelength of the operational frequency (meters)
 β free space wavenumber for operational frequency
 R_d distance from antenna to field point (meters)
 R_r distance from antenna image to field point (meters)
n.....index of refraction
 P_e complex numerical distance (vertical polarization)
 P_m complex numerical distance (horizontal polarization)
 Γ_v vertical reflection coefficient
 Γ_h horizontal reflection coefficient
 F_e vertical surface wave attenuation factor
 F_m horizontal surface wave attenuation factor

The calculated variables are used to evaluate the far-field space wave and surface wave for the discrete values of θ for $\phi=0$ and $\phi=\pi/2$. The total space wave and surface wave distributions are determined from vector addition of corresponding $\hat{\theta}$ and $\hat{\phi}$ components. The space wave and surface wave results are then combined for corresponding discrete values of θ to obtain the total radiated electric field distribution for the $\phi=0$ and $\phi=\pi/2$ vertical planes. The space wave, surface wave, and total electric field results are then

normalized with respect to the maximum field intensity of each, and the normalized magnitudes are plotted for each discrete θ to depict the radiation patterns. The inverted L Mathcad application computes the space wave, surface wave, and total electric field radiation patterns and radiation parameters in the $\phi=0$ and $\phi=\pi/2$ vertical planes.

The variables corresponding to the selected elevation angle index (d) are used to evaluate the radiated electric field components for the space wave and surface wave at the fixed elevation angle (θ_d) as ϕ varies from 0 to 2π in 632 equal increments. The horizontal radiation patterns are then plotted for the space wave, surface wave, and total radiated electric field just as those for the vertical planes.

To find the contributions of the $\hat{\theta}$ and $\hat{\phi}$ electric field components to the total average radiated power, P_{rad} , equations 3.8 and 3.9 are used to integrate equations 9.1, 9.2, and 9.3 over the hemispherical Gaussian surface above the ground plane at a fixed radius (R) from the antenna. The sum of the integrals is the antenna's P_{rad} . With the discrete values of the electric field and total average radiated power determined, the Mathcad application predicts the following radiation parameters using the equations from Chapter 3:

R_{rad} radiation resistance (Ohms)
 D_0 directivity
EIRP.....effective isotropic radiated power (Watts)
 A_{max} maximum theoretical effective area (square meters)
 l_{max} maximum theoretical effective length (meters)
 P_c numerical distance (vertical polarization, $\theta=90^\circ$)
 P_m numerical distance (horizontal polarization, $\theta=90^\circ$)
Angle_{max} .elevation angle of maximum directive gain (degrees)

The directivity (D_0), effective isotropic radiated power (EIRP), maximum theoretical effective area (A_{\max}), maximum theoretical effective length (l_{\max}), and the elevation angle of maximum directive gain (Angle_{\max}) are all determined for both the $\phi=0$ and $\phi=\pi/2$ vertical planes.

X. THE SLOPING LONG-WIRE ANTENNA

The orientation of the sloping long-wire antenna is depicted in Figure 10.1, where l is length of the antenna, the feed is at ground level, α is the angle of the antenna with the horizontal, R is the radial coordinate, θ is the elevation coordinate, and ϕ is the azimuth coordinate.

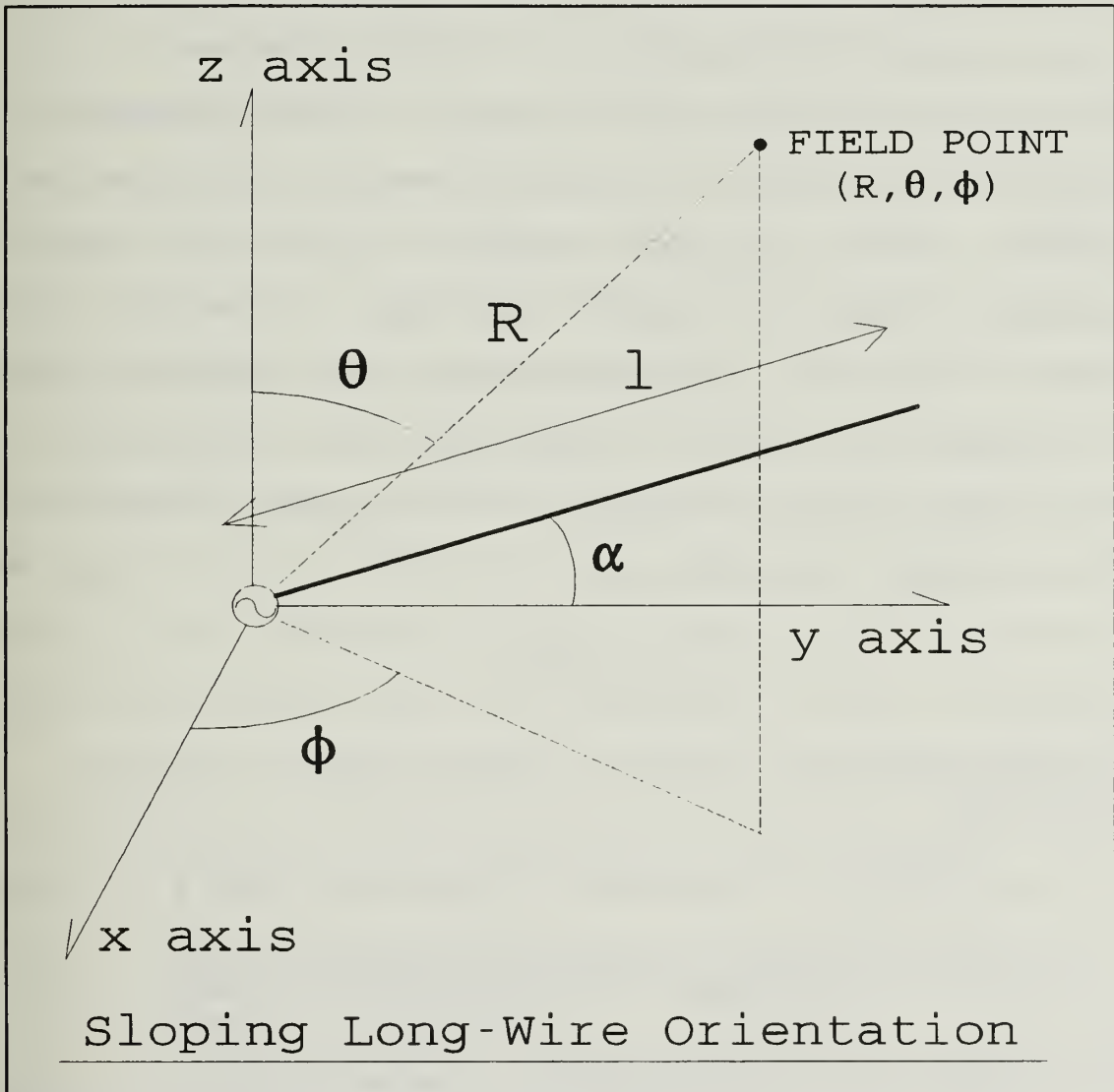


FIGURE 10.1: Spatial orientation of the sloping long-wire antenna for its corresponding Mathcad application.

The Mathcad application for the sloping long-wire antenna requires the following inputs:

l.....length of the antenna (meters)
 αangle of antenna with horizontal (degrees)
 f_soperational frequency (Hertz)
 Rdistance from antenna (meters)
 ϵ_rrelative dielectric constant of ground plane
 σconductivity of ground plane
 delevation angle index (from Table 3.1)

The user inputs the frequency (f_s) for which the radiation parameters discussed in Chapter 3 are computed. The distance from the antenna (R) must meet the far-field requirements of Chapter 3.C. The elevation angle index (d) sets the elevation coordinate, θ , for which a horizontal radiation pattern is determined. Table 3.1 lists possible indices and their corresponding elevation angles from $.285^\circ$ to 88.857° in increments of about 2° . Indices between those listed can be used to interpolate a better estimate of a desired elevation.

The electric field equations for the sloping long-wire are given by [Ref 6: p. 180-181]

$$E_\theta = -j30I_0 \frac{e^{-j\beta R}}{R}$$

$$\left\{ \frac{A_1 + jB_1}{1 - \cos^2(\psi)} [\cos(\alpha) \sin(\phi) \cos(\theta) - \sin(\alpha) \sin(\phi)] \right. \quad (10.1)$$

$$- \Gamma_v \frac{A_2 + jB_2}{1 - \cos^2(\psi')} [\cos(\alpha) \sin(\phi) \cos(\theta) + \sin(\alpha) \sin(\theta)]$$

$$+ (1 - \Gamma_v) F_e \frac{A_2 + jB_2}{1 - \cos^2(\psi')} \left(\sin^2(\theta) - \frac{\sqrt{n^2 - \sin^2(\theta)}}{n^2} \cos(\theta) \right)$$

$$\left. \left(\cos(\alpha) \sin(\phi) \frac{\sqrt{n^2 - \sin^2(\theta)}}{n^2} - \sin(\alpha) \sin(\theta) \right) \right]$$

$$E_{\phi} = j30I_0 \frac{e^{-j\beta R}}{R} \cos(\alpha) \cos(\phi) \quad (10.2)$$

$$\left[\frac{A_1 + jB_1}{1 - \cos^2(\psi)} + \Gamma_h \frac{A_2 + jB_2}{1 - \cos^2(\psi')} + (1 - \Gamma_h) F_m \frac{A_2 + jB_2}{1 - \cos^2(\psi')} \right]$$

$$\text{where } A_1 = \cos[\beta l \cos(\psi)] - \cos(\beta l)$$

$$B_1 = \sin[\beta l \cos(\psi)] - \sin(\beta l) \cos(\psi)$$

$$\cos(\psi) = \cos(\theta) \sin(\alpha) + \sin(\theta) \cos(\alpha) \sin(\phi)$$

$$A_2 = \cos[\beta l \cos(\psi')] - \cos(\beta l)$$

$$B_2 = \sin[\beta l \cos(\psi')] - \sin(\beta l) \cos(\psi')$$

$$\cos(\psi') = \sin(\theta) \cos(\alpha) \sin(\phi) - \cos(\theta) \sin(\alpha)$$

The radiated electric field for the sloping long-wire is obtained in a manner analogous to the vertical dipole equation discussed in Chapter 4. The long-wire's radiated electric field is a varying combination of $\hat{\theta}$ and $\hat{\phi}$ components, and its radiation patterns vary with changes in ϕ . The total radiated electric field is the vector sum of the $\hat{\theta}$ and $\hat{\phi}$ components. The first two terms inside the brackets of each equation are the space wave components and the additional terms are the surface wave components. I_0 is taken to be one since a sinusoidal current input with a maximum of unity is assumed.

Requested inputs are used to compute the variables on the next page using a constant ϕ of $\phi=0$ and $\phi=\pi/2$ for 632 discrete values of θ which are equally incremented from $-\pi/2$ to $\pi/2$.

λ_s wavelength of the operational frequency (meters)
 β free space wavenumber for operational frequency
 n index of refraction
 P_e complex numerical distance (vertical polarization)
 P_m complex numerical distance (horizontal polarization)
 Γ_v vertical reflection coefficient
 Γ_h horizontal reflection coefficient
 F_e vertical surface wave attenuation factor
 F_m horizontal surface wave attenuation factor

The calculated variables are used to evaluate the far-field space wave and surface wave for the discrete values of θ for $\phi=0$ and $\phi=\pi/2$. The total space wave and surface wave distributions are determined from vector addition of corresponding $\hat{\theta}$ and $\hat{\phi}$ components. The space wave and surface wave results are then combined for corresponding discrete values of θ to obtain the total radiated electric field distribution for the $\phi=0$ and $\phi=\pi/2$ vertical planes. The space wave, surface wave, and total electric field results are then normalized with respect to the maximum field intensity of each, and the normalized magnitudes are plotted for each discrete θ to depict the radiation patterns. The sloping long-wire Mathcad application computes the space wave, surface wave, and total electric field radiation patterns and radiation parameters in the $\phi=0$ and $\phi=\pi/2$ vertical planes.

The variables corresponding to the selected elevation angle index (d) are used to evaluate the radiated electric field components for the space wave and surface wave at the fixed elevation angle (θ_d) as ϕ varies from 0 to 2π in 632 equal increments. The horizontal radiation patterns are then plotted for the space wave, surface wave, and total radiated electric field just as those for the vertical planes.

To find the contributions of the $\hat{\theta}$ and $\hat{\phi}$ electric field components to the total average radiated power, P_{rad} , equations 3.8 and 3.9 are used to integrate equations 10.1 and 10.2 over the hemispherical Gaussian surface above the ground plane at

a fixed radius (R) from the antenna. The sum of the integrals is the antenna's P_{rad} . With the discrete values of the electric field and total average radiated power determined, the Mathcad application predicts the following radiation parameters using the equations from Chapter 3:

R_{rad} radiation resistance (Ohms)
 D_0 directivity
 EIRP effective isotropic radiated power (Watts)
 A_{max} maximum theoretical effective area (square meters)
 l_{max} maximum theoretical effective length (meters)
 P_e numerical distance (vertical polarization, $\theta=90^\circ$)
 P_m numerical distance (horizontal polarization, $\theta=90^\circ$)
 $\text{Angle}_{\text{max}}$.elevation angle of maximum directive gain (degrees)

The directivity (D_0), effective isotropic radiated power (EIRP), maximum theoretical effective area (A_{max}), maximum theoretical effective length (l_{max}), and the elevation angle of maximum directive gain ($\text{Angle}_{\text{max}}$) are all determined for both the $\phi=0$ and $\phi=\pi/2$ vertical planes.

XI. THE TERMINATED SLOPING V ANTENNA

The orientation of the terminated sloping V antenna is depicted on the next page in Figure 11.1, where l is length of the antenna wires (numbered 1 and 2), H_0 is the feed height above ground, H_1 is the height of the termination points above ground, γ is the angle subtended by the wires, η is the angle between the x axis and the projection of the antenna legs in the x-y plane, α is the angle between the plane which contains the antenna and the x-y plane, R is the radial coordinate, θ is the elevation coordinate, and ϕ is the azimuth coordinate.

The Mathcad application for the sloping V antenna requires the following inputs:

llength of the antenna legs(meters)
 H_0feed height above ground (meters)
 H_1height of termination points above ground (meters)
 γangle subtended by the antenna legs (degrees)
 f_soperational frequency (Hertz)
 Rdistance from antenna (meters)
 ϵ_rrelative dielectric constant of ground plane
 σconductivity of ground plane
 delevation angle index (from Table 3.1)

The user inputs the frequency (f_s) for which the radiation parameters discussed in Chapter 3 are computed. The feed height (H_0) and termination height (H_1) can be any value greater than zero. The angle α is found from H_0 , H_1 , wire length (l), and the half-angle between the wires ($\gamma/2$) by

$$\alpha = \sin^{-1} \left[\frac{H_1 - H_0}{l \cdot \cos\left(\frac{\gamma}{2}\right)} \right] \quad (11.1)$$

increments of about 2°. Indices between those listed can be used to interpolate a better estimate of a desired elevation.

The radiated electric field for the sloping V antenna is obtained in a manner analogous to that used for the vertical dipole discussed in Chapter 4. The sloping V electric field equations are given by [Ref 6: p. 185-186]

$$E_{\theta,1} = 30 I_0 \frac{e^{-j\beta R}}{R} \left\{ \cos(\alpha) \cos(\theta) \cos(\phi - \eta) \left[\frac{1 - e^{-j\beta 1U_1}}{U_1} \right. \right. \quad (11.3)$$

$$\left. - \Gamma_v \frac{1 - e^{-j\beta 1U_3}}{U_3} e^{-j2\beta H_0 \cos(\theta)} + (1 - \Gamma_v) F_e \frac{1 - e^{-j\beta 1U_3}}{U_3} e^{-j2\beta H_0 \cos(\theta)} \right.$$

$$\left. \left(\sin^2(\theta) - \frac{\sqrt{n^2 - \sin^2(\theta)}}{n^2} \cos(\theta) \right) \frac{\sqrt{n^2 - \sin^2(\theta)}}{n^2 \cos(\theta)} \right]$$

$$- \sin(\alpha) \sin(\theta) \left[\frac{1 - e^{-j\beta 1U_1}}{U_1} + \Gamma_v \frac{1 - e^{-j\beta 1U_3}}{U_3} e^{-j2\beta H_0 \cos(\theta)} \right.$$

$$\left. + (1 - \Gamma_v) F_e \frac{1 - e^{-j\beta 1U_3}}{U_3} e^{-j2\beta H_0 \cos(\theta)} \left(\sin^2(\theta) - \frac{\sqrt{n^2 - \sin^2(\theta)}}{n^2} \cos(\theta) \right) \right] \Bigg\}$$

$$E_{\phi,1} = 30 I_0 \frac{e^{-j\beta R}}{R} \cos(\alpha) \sin(\phi - \eta) \left[\frac{1 - e^{-j\beta 1U_1}}{U_1} \right. \quad (11.4)$$

$$\left. + \Gamma_h \frac{1 - e^{-j\beta 1U_3}}{U_3} e^{-j2\beta H_0 \cos(\theta)} + (1 - \Gamma_h) F_m \frac{1 - e^{-j\beta 1U_3}}{U_3} e^{-j2\beta H_0 \cos(\theta)} \right]$$

$$\text{where } U_1 = 1 - \cos(\Psi_1) \quad U_3 = 1 - \cos(\Psi_3)$$

$$\cos(\Psi_1) = \cos(\theta) \sin(\alpha) + \sin(\theta) \cos(\alpha) \cos(\phi - \eta)$$

$$\cos(\Psi_3) = \sin(\theta) \cos(\alpha) \cos(\phi - \eta) - \cos(\theta) \sin(\alpha)$$

$$\begin{aligned}
E_{\theta,2} = & 30 I_0 \frac{e^{-j\beta R}}{R} \left\{ -\cos(\alpha) \cos(\theta) \cos(\phi+\eta) \left[\frac{1-e^{-j\beta 1U_2}}{U_2} \right. \right. \\
& - \Gamma_v \frac{1-e^{-j\beta 1U_4}}{U_4} e^{-j2\beta H_0 \cos(\theta)} + (1-\Gamma_v) F_e \frac{1-e^{-j\beta 1U_4}}{U_4} e^{-j2\beta H_0 \cos(\theta)} \\
& \left. \left(\sin^2(\theta) - \frac{\sqrt{n^2 - \sin^2(\theta)}}{n^2} \cos(\theta) \right) \frac{\sqrt{n^2 - \sin^2(\theta)}}{n^2 \cos(\theta)} \right] \\
& + \sin(\alpha) \sin(\theta) \left[\frac{1-e^{-j\beta 1U_2}}{U_2} + \Gamma_v \frac{1-e^{-j\beta 1U_4}}{U_4} e^{-j2\beta H_0 \cos(\theta)} \right. \\
& \left. \left. + (1-\Gamma_v) F_e \frac{1-e^{-j\beta 1U_4}}{U_4} e^{-j2\beta H_0 \cos(\theta)} \left(\sin^2(\theta) - \frac{\sqrt{n^2 - \sin^2(\theta)}}{n^2} \cos(\theta) \right) \right] \right\}
\end{aligned} \quad (11.5)$$

$$\begin{aligned}
E_{\phi,1} = & -30 I_0 \frac{e^{-j\beta R}}{R} \cos(\alpha) \sin(\phi+\eta) \left[\frac{1-e^{-j\beta 1U_2}}{U_2} \right. \\
& \left. + \Gamma_h \frac{1-e^{-j\beta 1U_4}}{U_4} e^{-j2\beta H_0 \cos(\theta)} + (1-\Gamma_h) F_m \frac{1-e^{-j\beta 1U_4}}{U_4} e^{-j2\beta H_0 \cos(\theta)} \right]
\end{aligned} \quad (11.6)$$

$$\text{where } U_2 = 1 - \cos(\Psi_2) \quad U_4 = 1 - \cos(\Psi_4)$$

$$\cos(\Psi_2) = \cos(\theta) \sin(\alpha) + \sin(\theta) \cos(\alpha) \cos(\phi-\eta)$$

$$\cos(\Psi_4) = \sin(\theta) \cos(\alpha) \cos(\phi+\eta) - \cos(\theta) \sin(\alpha)$$

The sloping V's radiated electric field is a varying combination of $\hat{\theta}$ and $\hat{\phi}$ components, and its radiation pattern varies with changes in ϕ . The total radiated electric field is the vector sum of the $\hat{\theta}$ and $\hat{\phi}$ components. The fields of each antenna leg are considered separately, and superposition is used to determine the total electric field. Equations 11.3 and 11.4 are the radiated $\hat{\theta}$ and $\hat{\phi}$ components, respectively for

number one, and equations 11.5 and 11.6 are the $\hat{\theta}$ and $\hat{\phi}$ components, respectively for wire number two. The first two terms inside each set of brackets represent the space wave components and any additional terms represent the surface wave components. I_0 is taken to be one, since a sinusoidal current input with a maximum of unity is assumed.

The requested inputs are used to calculate the following variables using a constant ϕ of $\phi=0$ and $\phi=\pi/2$ for 632 discrete values of θ which are equally incremented from $-\pi/2$ to $\pi/2$:

λ_s wavelength of the operational frequency (meters)
 β free space wavenumber for operational frequency
 n index of refraction
 P_e complex numerical distance (vertical polarization)
 P_m complex numerical distance (horizontal polarization)
 Γ_v vertical reflection coefficient
 Γ_h horizontal reflection coefficient
 F_e vertical surface wave attenuation factor
 F_m horizontal surface wave attenuation factor

The calculated variables are used to evaluate the far-field space wave and surface wave for the discrete values of θ for $\phi=0$ and $\phi=\pi/2$. The total space wave and surface wave distributions are determined from vector addition of corresponding $\hat{\theta}$ and $\hat{\phi}$ components. The space wave and surface wave results are then combined for corresponding discrete values of θ to obtain the total radiated electric field distribution for the $\phi=0$ and $\phi=\pi/2$ vertical planes. The space wave, surface wave, and total electric field results are then normalized with respect to the maximum field intensity of each, and the normalized magnitudes are plotted for each discrete θ to depict the radiation patterns. The sloping V

Mathcad application computes the space wave, surface wave, and total electric field radiation patterns and radiation parameters in the $\phi=0$ and $\phi=\pi/2$ vertical planes.

The variables corresponding to the selected elevation angle index (d) are used to evaluate the radiated electric field components for the space wave and surface wave at the fixed elevation angle (θ_d) as ϕ varies from 0 to 2π in 632 equal increments. The horizontal radiation patterns are then plotted for the space wave, surface wave, and total radiated electric field just as those for the vertical planes.

To find the contributions of the $\hat{\theta}$ and $\hat{\phi}$ electric field components to the total average radiated power, P_{rad} , equations 3.8 and 3.9 are used to integrate equations 11.3, 11.4, 11.5, and 11.6 over the hemispherical Gaussian surface above the ground plane at a fixed radius (R) from the antenna. The sum of the integrals is the antenna's P_{rad} . With the discrete values of the electric field and total average radiated power determined, the Mathcad application predicts the following radiation parameters using the equations from Chapter 3:

R_{rad} radiation resistance (Ohms)
 D_0 directivity
EIRP.....effective isotropic radiated power (Watts)
 A_{max} maximum theoretical effective area (square meters)
 l_{max} maximum theoretical effective length (meters)
 P_e numerical distance (vertical polarization, $\theta=90^\circ$)
 P_m numerical distance (horizontal polarization, $\theta=90^\circ$)
 $\text{Angle}_{\text{max}}$.elevation angle of maximum directive gain (degrees)

The directivity (D_0), effective isotropic radiated power (EIRP), maximum theoretical effective area (A_{max}), maximum

theoretical effective length (l_{\max}), and the elevation angle of maximum directive gain (Angle_{\max}) are all determined for both the $\phi=0$ and $\phi=\pi/2$ vertical planes.

XII. THE SIDE-LOADED VERTICAL HALF RHOMBIC ANTENNA

The orientation of the side-loaded vertical half rhombic antenna is depicted in Figure 12.1, where l is length of the antenna wires (numbered 1 and 2), the feed is at ground level, α is the angle between the antenna wires and the horizontal plane, R is the radial coordinate, θ is the elevation coordinate, and ϕ is the azimuth coordinate.

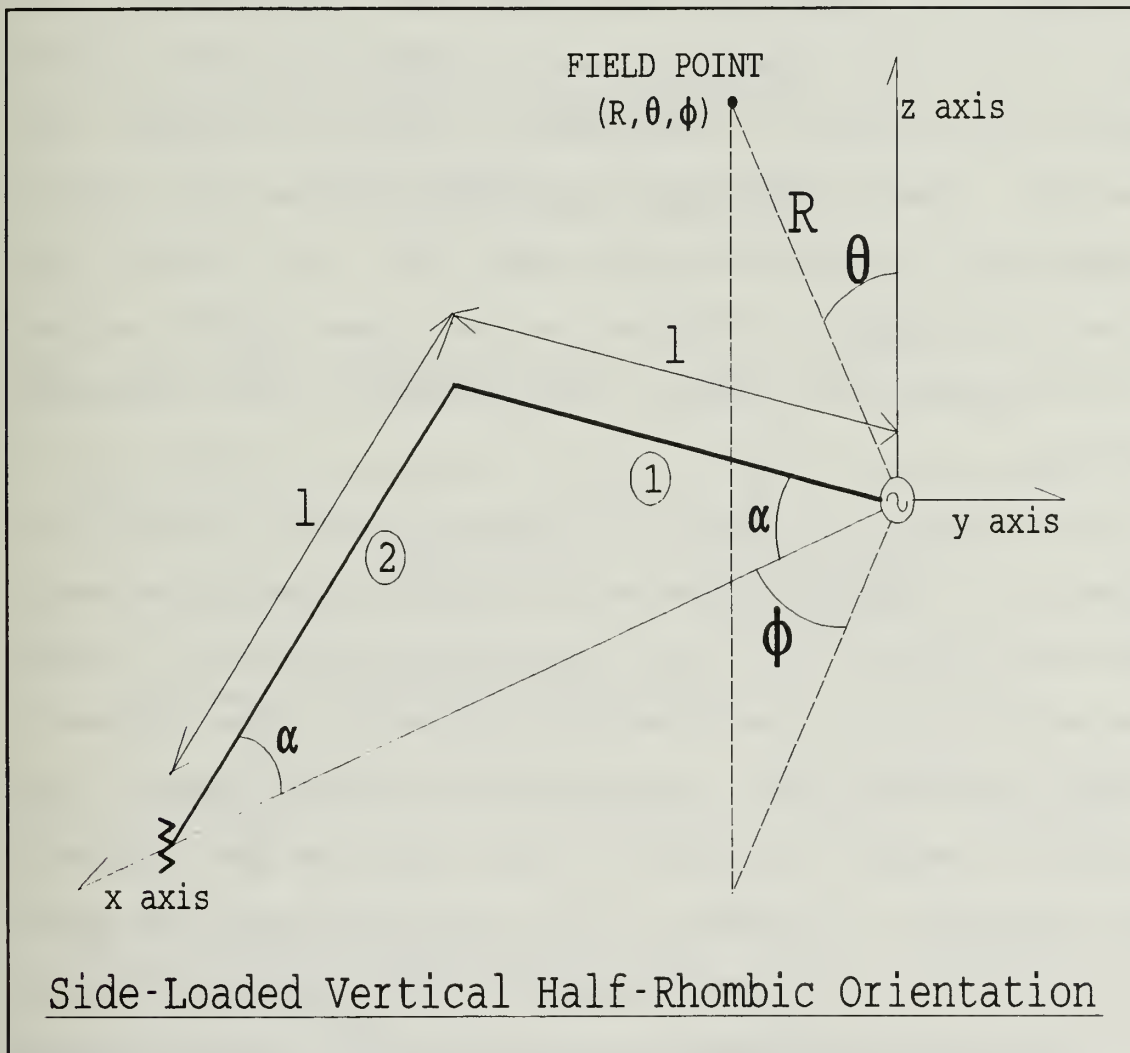


FIGURE 12.1: Spatial orientation of the side-loaded vertical half rhombic antenna for its Mathcad application.

The Mathcad application for the vertical half rhombic antenna requires the following inputs:

- l.....length of the antenna legs(meters)
- αangle of antenna wires with horizontal (degrees)
- f_soperational frequency (Hertz)
- R.....distance from antenna (meters)
- ϵ_rrelative dielectric constant of ground plane
- σconductivity of ground plane
- d.....elevation angle index (from Table 3.1)

The user inputs the frequency (f_s) for which the radiation parameters discussed in Chapter 3 are computed. Distance from the antenna (R) must meet the far-field requirements of Chapter 3.C. The elevation angle index (d) sets the θ coordinate for which a horizontal radiation pattern is determined. Table 3.1 lists possible indices and their corresponding elevation angles from $.285^\circ$ to 88.857° in increments of about 2° . Indices between those listed can be used to interpolate a better approximation of a desired elevation.

The vertical half rhombic's radiated electric field is a combination of $\hat{\theta}$ and $\hat{\phi}$ components, and its radiation pattern varies with changes in ϕ . The total radiated electric field is the vector sum of the $\hat{\theta}$ and $\hat{\phi}$ components. The radiated electric field for the vertical half rhombic antenna is obtained in a manner analogous to that used for the vertical dipole discussed in Chapter 4. The radiated fields of each antenna leg are considered separately, and superposition is used to determine the total electric field. The electric field equations for the half rhombic are [Ref 6: p. 198-200]

$$\begin{aligned}
E_{\theta,1} = 30 I_0 \frac{e^{-j\beta R}}{R} & \left\{ \cos(\alpha) \cos(\theta) \cos(\phi) \left[\frac{1-e^{-j\beta 1U_1}}{U_1} \right. \right. \\
& - \Gamma_v \frac{1-e^{-j\beta 1U_2}}{U_2} + (1-\Gamma_v) F_e \frac{1-e^{-j\beta 1U_2}}{U_2} \\
& \left. \left(\sin^2(\theta) - \frac{\sqrt{n^2 - \sin^2(\theta)}}{n^2} \cos(\theta) \right) \frac{\sqrt{n^2 - \sin^2(\theta)}}{n^2 \cos(\theta)} \right] \\
& + \sin(\alpha) \sin(\theta) \left[\frac{1-e^{-j\beta 1U_1}}{U_1} + \Gamma_v \frac{1-e^{-j\beta 1U_2}}{U_2} \right. \\
& \left. \left. + (1-\Gamma_v) F_e \frac{1-e^{-j\beta 1U_2}}{U_2} \left(\sin^2(\theta) - \frac{\sqrt{n^2 - \sin^2(\theta)}}{n^2} \cos(\theta) \right) \right] \right\} \quad (12.1)
\end{aligned}$$

$$\begin{aligned}
E_{\phi,1} = -30 I_0 \frac{e^{-j\beta R}}{R} \cos(\alpha) \sin(\phi) & \left[\frac{1-e^{-j\beta 1U_1}}{U_1} \right. \\
& \left. + \Gamma_h \frac{1-e^{-j\beta 1U_2}}{U_2} + (1-\Gamma_h) F_m \frac{1-e^{-j\beta 1U_2}}{U_2} \right] \quad (12.2)
\end{aligned}$$

$$\begin{aligned}
E_{\theta,2} = -30 I_0 \frac{e^{-j\beta R}}{R} e^{-j\beta 1U_1} & \left\{ \cos(\alpha) \cos(\theta) \cos(\phi) \left[\frac{1-e^{-j\beta 1U_2}}{U_2} \right. \right. \\
& - \Gamma_v \frac{1-e^{-j\beta 1U_1}}{U_1} e^{-j2\beta 1 \sin(\alpha) \cos(\theta)} + (1-\Gamma_v) F_e \frac{1-e^{-j\beta 1U_1}}{U_1} e^{-j2\beta 1 \sin(\alpha) \cos(\theta)} \\
& \left. \left(\sin^2(\theta) - \frac{\sqrt{n^2 - \sin^2(\theta)}}{n^2} \cos(\theta) \right) \frac{\sqrt{n^2 - \sin^2(\theta)}}{n^2 \cos(\theta)} \right] \\
& + \sin(\alpha) \sin(\theta) \left[\frac{1-e^{-j\beta 1U_2}}{U_2} + \Gamma_v \frac{1-e^{-j\beta 1U_1}}{U_1} e^{-j2\beta 1 \sin(\alpha) \cos(\theta)} \right. \\
& \left. \left. + (1-\Gamma_v) F_e \frac{1-e^{-j\beta 1U_1}}{U_1} e^{-j2\beta 1 \sin(\alpha) \cos(\theta)} \left(\sin^2(\theta) - \frac{\sqrt{n^2 - \sin^2(\theta)}}{n^2} \cos(\theta) \right) \right] \right\} \quad (12.3)
\end{aligned}$$

$$\begin{aligned}
E_{\phi,2} = -30 I_0 \frac{e^{-j\beta R}}{R} \cos(\alpha) \sin(\phi) & \left[\frac{1-e^{-j\beta 1U_2}}{U_2} e^{-j\beta 1U_1} \right. \\
& \left. + \Gamma_h \frac{1-e^{-j\beta 1U_1}}{U_1} e^{-j\beta 1U_2} + (1-\Gamma_h) F_m \frac{1-e^{-j\beta 1U_1}}{U_1} e^{-j\beta 1U_2} \right] \quad (12.4)
\end{aligned}$$

where U_1 and U_2 are given by

$$U_1 = 1 - \cos(\Psi_1) \quad U_2 = 1 - \cos(\Psi_2)$$

$$\cos(\Psi_1) = \cos(\theta) \sin(\alpha) + \sin(\theta) \cos(\alpha) \cos(\phi)$$

$$\cos(\Psi_2) = \sin(\theta) \cos(\alpha) \cos(\phi) - \cos(\theta) \sin(\alpha)$$

Equations 12.1 and 12.2 are the $\hat{\theta}$ (vertically polarized) and $\hat{\phi}$ (horizontally polarized) components, respectively for leg number one, and equations 12.3 and 12.4 are the $\hat{\theta}$ and $\hat{\phi}$ components, respectively for leg number two. The first two terms inside each set of brackets are the space wave components and any additional terms are the surface wave components. I_0 is taken to be one, since a sinusoidal current input with a maximum of unity is assumed. The requested inputs are used to calculate the following variables using a constant ϕ of $\phi=0$ and $\phi=\pi/2$ for 632 discrete values of θ which are equally incremented from $-\pi/2$ to $\pi/2$:

λ_s wavelength of the operational frequency (meters)
 β free space wavenumber for operational frequency
 n index of refraction
 P_e complex numerical distance (vertical polarization)
 P_m complex numerical distance (horizontal polarization)
 Γ_v vertical reflection coefficient
 Γ_h horizontal reflection coefficient
 F_e vertical surface wave attenuation factor
 F_m horizontal surface wave attenuation factor

The calculated variables are used to evaluate the far-field space wave and surface wave for the discrete values of θ for $\phi=0$ and $\phi=\pi/2$. The total space wave and surface wave distributions are determined from vector addition of corresponding $\hat{\theta}$ and $\hat{\phi}$ components. The space wave and surface

wave results are then combined for corresponding discrete values of θ to obtain the total radiated electric field distribution for the $\phi=0$ and $\phi=\pi/2$ vertical planes. The space wave, surface wave, and total electric field results are then normalized with respect to the maximum field intensity of each, and the normalized magnitudes are plotted for each discrete θ to depict the radiation patterns. The vertical half rhombic Mathcad application computes the space wave, surface wave, and total electric field radiation patterns and radiation parameters in the $\phi=0$ and $\phi=\pi/2$ vertical planes.

The variables corresponding to the selected elevation angle index (d) are used to evaluate the radiated electric field components for the space wave and surface wave at the fixed elevation angle (θ_d) as ϕ varies from 0 to 2π in 632 equal increments. The horizontal radiation patterns are then plotted for the space wave, surface wave, and total radiated electric field just as those for the vertical planes.

To find the contributions of the $\hat{\theta}$ and $\hat{\phi}$ electric field components to the total average radiated power, P_{rad} , equations 3.8 and 3.9 are used to integrate equations 12.1, 12.2, 12.3, and 12.4 over the hemispherical Gaussian surface above the ground plane at a fixed radius (R) from the antenna. The sum of the integrals is the antenna's P_{rad} . With the discrete values of the electric field and total average radiated power determined, the Mathcad application predicts the following radiation parameters using the equations from Chapter 3:

R_{rad} radiation resistance (Ohms)
 D_0 directivity
EIRP.....effective isotropic radiated power (Watts)
 A_{max} maximum theoretical effective area (square meters)
 l_{max} maximum theoretical effective length (meters)
 P_e numerical distance (vertical polarization, $\theta=90^\circ$)
 P_m numerical distance (horizontal polarization, $\theta=90^\circ$)
 $\text{Angle}_{\text{max}}$.elevation angle of maximum directive gain (degrees)

The directivity (D_0), effective isotropic radiated power (EIRP), maximum theoretical effective area (A_{max}), maximum theoretical effective length (l_{max}), and the elevation angle of maximum directive gain ($\text{Angle}_{\text{max}}$) are all determined for both the $\phi=0$ and $\phi=\pi/2$ vertical planes.

XIII. THE TERMINATED SLOPING OR HORIZONTAL RHOMBIC ANTENNA

The orientation of the terminated sloping or horizontal rhombic antenna is depicted on the next page in Figure 13.1, where l is the length of the antenna wires (numbered 1 to 4), H_0 is the feed height above ground, H_2 is the height of the termination point above ground, γ is the angle subtended by the feed wires (1 and 2), η is the angle between the x axis and the projection of the feed wires in the x-y plane, α is the angle between the plane which contains the antenna and the x-y plane, R is the radial coordinate, θ is the elevation coordinate, and ϕ is the azimuth coordinate.

The Mathcad application for the rhombic antenna requires the following inputs:

l.....length of the antenna legs(meters)
 H_0feed height above ground (meters)
 H_2height of termination point above ground (meters)
 γangle subtended by the antenna legs (degrees)
 f_soperational frequency (Hertz)
 Rdistance from antenna (meters)
 ϵ_rrelative dielectric constant of ground plane
 σconductivity of ground plane
d.....elevation angle index (from Table 3.1)

The feed height (H_0) and termination height (H_2) can be any value greater than zero. The angle α is found from H_0 , H_2 , wire length (l), and the half-angle between the wires ($\gamma/2$) by

$$\alpha = \sin^{-1} \left[\frac{H_2 - H_0}{2l \cdot \cos\left(\frac{\gamma}{2}\right)} \right] \quad (13.1)$$

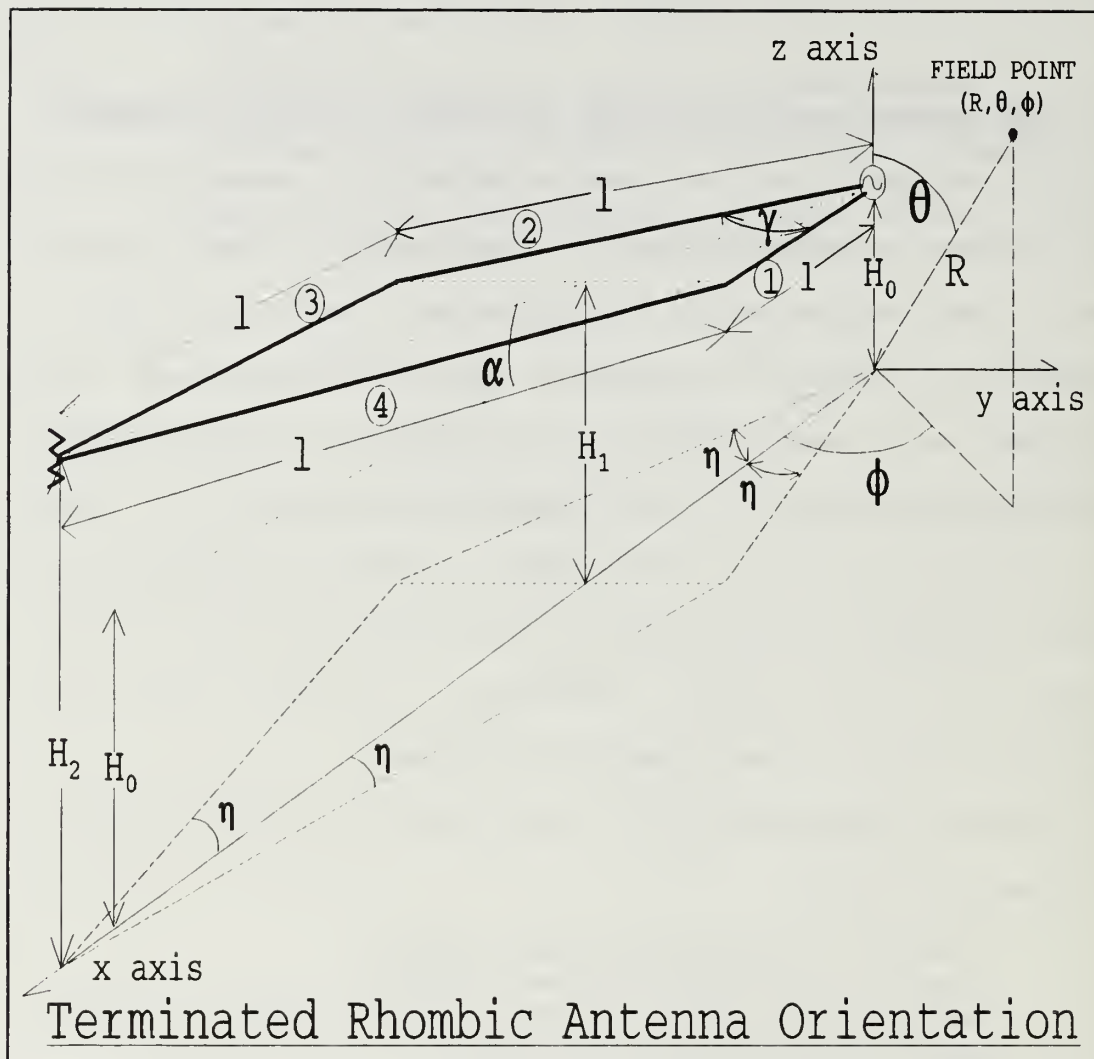


FIGURE 13.1: Spatial orientation of the terminated sloping or horizontal rhombic antenna for its Mathcad application.

The angle η is then found from α and $\gamma/2$ by

$$\eta = \tan^{-1} \left[\frac{\tan\left(\frac{\gamma}{2}\right)}{\cos(\alpha)} \right] \quad (13.2)$$

The user inputs the frequency (f_s) for which the radiation parameters discussed in Chapter 3 are computed. Distance from the antenna (R) must meet the far-field requirements of Chapter 3.C. The elevation angle index (d) sets the θ

coordinate for which a horizontal radiation pattern is determined. Table 3.1 lists possible indices and their corresponding elevation angles from .285° to 88.857° in increments of about 2°. Indices between those listed can be used to interpolate a better estimate of a desired elevation.

The radiated electric field for the rhombic antenna is obtained in a manner analogous to that for the vertical dipole discussed in Chapter 4. The radiated field of each wire is considered separately, and superposition is used to determine the total electric field. The rhombic's electric field equations are [Ref 6: p. 183-191]

$$\begin{aligned}
 E_{\theta,1} = & 30 I_0 \frac{e^{-j\beta R}}{R} \left\{ \cos(\alpha) \cos(\theta) \cos(\phi - \eta) \left[\frac{1 - e^{-j\beta 1U_1}}{U_1} \right. \right. \quad (13.3) \\
 & - \Gamma_v \frac{1 - e^{-j\beta 1U_3}}{U_3} e^{-j2\beta H_0 \cos(\theta)} + (1 - \Gamma_v) F_e \frac{1 - e^{-j\beta 1U_3}}{U_3} e^{-j2\beta H_0 \cos(\theta)} \\
 & \left. \left(\sin^2(\theta) - \frac{\sqrt{n^2 - \sin^2(\theta)}}{n^2} \cos(\theta) \right) \frac{\sqrt{n^2 - \sin^2(\theta)}}{n^2 \cos(\theta)} \right] \\
 & - \sin(\alpha) \sin(\theta) \left[\frac{1 - e^{-j\beta 1U_1}}{U_1} + \Gamma_v \frac{1 - e^{-j\beta 1U_3}}{U_3} e^{-j2\beta H_0 \cos(\theta)} \right. \\
 & \left. \left. + (1 - \Gamma_v) F_e \frac{1 - e^{-j\beta 1U_3}}{U_3} e^{-j2\beta H_0 \cos(\theta)} \left(\sin^2(\theta) - \frac{\sqrt{n^2 - \sin^2(\theta)}}{n^2} \cos(\theta) \right) \right] \right\} \\
 E_{\phi,1} = & 30 I_0 \frac{e^{-j\beta R}}{R} \cos(\alpha) \sin(\phi - \eta) \left[\frac{1 - e^{-j\beta 1U_1}}{U_1} \right. \quad (13.4) \\
 & \left. + \Gamma_h \frac{1 - e^{-j\beta 1U_3}}{U_3} e^{-j2\beta H_0 \cos(\theta)} + (1 - \Gamma_h) F_m \frac{1 - e^{-j\beta 1U_3}}{U_3} e^{-j2\beta H_0 \cos(\theta)} \right]
 \end{aligned}$$

$$\begin{aligned}
E_{\theta,2} = & 30 I_0 \frac{e^{-j\beta R}}{R} \left\{ -\cos(\alpha) \cos(\theta) \cos(\phi+\eta) \left[\frac{1-e^{-j\beta 1U_2}}{U_2} \right. \right. \\
& -\Gamma_v \frac{1-e^{-j\beta 1U_4}}{U_4} e^{-j2\beta H_0 \cos(\theta)} + (1-\Gamma_v) F_e \frac{1-e^{-j\beta 1U_4}}{U_4} e^{-j2\beta H_0 \cos(\theta)} \\
& \left. \left(\sin^2(\theta) - \frac{\sqrt{n^2 - \sin^2(\theta)}}{n^2} \cos(\theta) \right) \frac{\sqrt{n^2 - \sin^2(\theta)}}{n^2 \cos(\theta)} \right] \\
& + \sin(\alpha) \sin(\theta) \left[\frac{1-e^{-j\beta 1U_2}}{U_2} + \Gamma_v \frac{1-e^{-j\beta 1U_4}}{U_4} e^{-j2\beta H_0 \cos(\theta)} \right. \\
& \left. \left. + (1-\Gamma_v) F_e \frac{1-e^{-j\beta 1U_4}}{U_4} e^{-j2\beta H_0 \cos(\theta)} \left(\sin^2(\theta) - \frac{\sqrt{n^2 - \sin^2(\theta)}}{n^2} \cos(\theta) \right) \right] \right\} \quad (13.5)
\end{aligned}$$

$$\begin{aligned}
E_{\phi,2} = & -30 I_0 \frac{e^{-j\beta R}}{R} \cos(\alpha) \sin(\phi+\eta) \left[\frac{1-e^{-j\beta 1U_2}}{U_2} \right. \\
& \left. + \Gamma_h \frac{1-e^{-j\beta 1U_4}}{U_4} e^{-j2\beta H_0 \cos(\theta)} + (1-\Gamma_h) F_m \frac{1-e^{-j\beta 1U_4}}{U_4} e^{-j2\beta H_0 \cos(\theta)} \right] \quad (13.6)
\end{aligned}$$

$$\begin{aligned}
E_{\theta,3} = & 30 I_0 \frac{e^{-j\beta R}}{R} e^{-j\beta 1U_2} \left\{ -\cos(\alpha) \cos(\theta) \cos(\phi-\eta) \left[\frac{1-e^{-j\beta 1U_1}}{U_1} \right. \right. \\
& -\Gamma_v \frac{1-e^{-j\beta 1U_3}}{U_3} e^{-j2\beta H_1 \cos(\theta)} + (1-\Gamma_v) F_e \frac{1-e^{-j\beta 1U_3}}{U_3} e^{-j2\beta H_1 \cos(\theta)} \\
& \left. \left(\sin^2(\theta) - \frac{\sqrt{n^2 - \sin^2(\theta)}}{n^2} \cos(\theta) \right) \frac{\sqrt{n^2 - \sin^2(\theta)}}{n^2 \cos(\theta)} \right] \\
& + \sin(\alpha) \sin(\theta) \left[\frac{1-e^{-j\beta 1U_1}}{U_1} + \Gamma_v \frac{1-e^{-j\beta 1U_3}}{U_3} e^{-j2\beta H_1 \cos(\theta)} \right. \\
& \left. \left. + (1-\Gamma_v) F_e \frac{1-e^{-j\beta 1U_3}}{U_3} e^{-j2\beta H_1 \cos(\theta)} \left(\sin^2(\theta) - \frac{\sqrt{n^2 - \sin^2(\theta)}}{n^2} \cos(\theta) \right) \right] \right\} \quad (13.7)
\end{aligned}$$

$$\begin{aligned}
E_{\phi,3} = & -30 I_0 \frac{e^{-j\beta R}}{R} e^{-j\beta 1U_2} \cos(\alpha) \sin(\phi-\eta) \left[\frac{1-e^{-j\beta 1U_1}}{U_1} \right. \\
& \left. + \Gamma_h \frac{1-e^{-j\beta 1U_3}}{U_3} e^{-j2\beta H_1 \cos(\theta)} + (1-\Gamma_h) F_m \frac{1-e^{-j\beta 1U_3}}{U_3} e^{-j2\beta H_1 \cos(\theta)} \right] \quad (13.8)
\end{aligned}$$

$$\begin{aligned}
E_{\theta,4} = 30 I_0 \frac{e^{-j\beta R}}{R} e^{-j\beta 1U_1} & \left\{ \cos(\alpha) \cos(\theta) \cos(\phi+\eta) \left[\frac{1-e^{-j\beta 1U_2}}{U_2} \right. \right. \\
& - \Gamma_v \frac{1-e^{-j\beta 1U_4}}{U_4} e^{-j2\beta H_1 \cos(\theta)} + (1-\Gamma_v) F_e \frac{1-e^{-j\beta 1U_4}}{U_4} e^{-j2\beta H_1 \cos(\theta)} \\
& \left. \left(\sin^2(\theta) - \frac{\sqrt{n^2 - \sin^2(\theta)}}{n^2} \cos(\theta) \right) \frac{\sqrt{n^2 - \sin^2(\theta)}}{n^2 \cos(\theta)} \right] \\
& - \sin(\alpha) \sin(\theta) \left[\frac{1-e^{-j\beta 1U_2}}{U_2} + \Gamma_v \frac{1-e^{-j\beta 1U_4}}{U_4} e^{-j2\beta H_1 \cos(\theta)} \right. \\
& \left. \left. + (1-\Gamma_v) F_e \frac{1-e^{-j\beta 1U_4}}{U_4} e^{-j2\beta H_1 \cos(\theta)} \left(\sin^2(\theta) - \frac{\sqrt{n^2 - \sin^2(\theta)}}{n^2} \cos(\theta) \right) \right] \right\} \quad (13.9)
\end{aligned}$$

$$\begin{aligned}
E_{\phi,4} = 30 I_0 \frac{e^{-j\beta R}}{R} e^{-j\beta 1U_1} \cos(\alpha) \sin(\phi+\eta) & \left[\frac{1-e^{-j\beta 1U_2}}{U_2} \right. \\
& \left. + \Gamma_h \frac{1-e^{-j\beta 1U_4}}{U_4} e^{-j2\beta H_1 \cos(\theta)} + (1-\Gamma_h) F_m \frac{1-e^{-j\beta 1U_4}}{U_4} e^{-j2\beta H_1 \cos(\theta)} \right] \quad (13.10)
\end{aligned}$$

where U_1 , U_2 , U_3 , and U_4 are given by

$$\begin{aligned}
U_1 &= 1 - \cos(\Psi_1) & U_2 &= 1 - \cos(\Psi_2) \\
U_3 &= 1 - \cos(\Psi_3) & U_4 &= 1 - \cos(\Psi_4)
\end{aligned}$$

where

$$\begin{aligned}
\cos(\Psi_1) &= \cos(\theta) \sin(\alpha) + \sin(\theta) \cos(\alpha) \cos(\phi-\eta) \\
\cos(\Psi_2) &= \cos(\theta) \sin(\alpha) + \sin(\theta) \cos(\alpha) \cos(\phi-\eta) \\
\cos(\Psi_3) &= \sin(\theta) \cos(\alpha) \cos(\phi-\eta) - \cos(\theta) \sin(\alpha) \\
\cos(\Psi_4) &= \sin(\theta) \cos(\alpha) \cos(\phi+\eta) - \cos(\theta) \sin(\alpha)
\end{aligned}$$

The rhombic's radiated electric field is a varying combination of $\hat{\theta}$ and $\hat{\phi}$ components, and its radiation pattern varies with changes in ϕ . The total radiated electric field is the vector sum of the $\hat{\theta}$ and $\hat{\phi}$ components. Equations 13.3 and 13.4 are the $\hat{\theta}$ (vertically polarized) and $\hat{\phi}$ (horizontally polarized)

components, respectively for wire one, and equations 13.5 and 13.6 are the $\hat{\theta}$ and $\hat{\phi}$ components, respectively for wire number two. Equations 13.7 and 13.8 are the analogous equations for wire three, and 13.9 and 13.10 are those for wire four. The first two terms inside each set of brackets represent the space wave components, and any additional terms represent the surface wave components. I_0 is taken to be one, since a sinusoidal current input with a maximum of unity is assumed.

The requested inputs are used to calculate the following variables using a constant ϕ of $\phi=0$ and $\phi=\pi/2$ for 632 discrete values of θ which are equally incremented from $-\pi/2$ to $\pi/2$:

λ_s wavelength of the operational frequency (meters)
 β free space wavenumber for operational frequency
 n index of refraction
 P_e complex numerical distance (vertical polarization)
 P_m complex numerical distance (horizontal polarization)
 Γ_v vertical reflection coefficient
 Γ_h horizontal reflection coefficient
 F_e vertical surface wave attenuation factor
 F_m horizontal surface wave attenuation factor

The calculated variables are used to evaluate the far-field space wave and surface wave for the discrete values of θ for $\phi=0$ and $\phi=\pi/2$. The total space wave and surface wave distributions are determined from vector addition of corresponding $\hat{\theta}$ and $\hat{\phi}$ components. The space wave and surface wave results are then combined for corresponding discrete values of θ to obtain the total radiated electric field distribution for the $\phi=0$ and $\phi=\pi/2$ vertical planes. The space wave, surface wave, and total electric field results are then

normalized with respect to the maximum field intensity of each, and the normalized magnitudes are plotted for each discrete θ to depict the radiation patterns. The rhombic antenna Mathcad application computes the space wave, surface wave, and total electric field radiation patterns and radiation parameters in the $\phi=0$ and $\phi=\pi/2$ vertical planes.

The variables corresponding to the selected elevation angle index (d) are used to evaluate the radiated electric field components for the space wave and surface wave at the selected elevation angle (θ_d) as ϕ varies from 0 to 2π in 632 equal increments. The horizontal radiation patterns are then plotted for the space wave, surface wave, and total radiated electric field just as those for the vertical planes.

To find the contributions of the $\hat{\theta}$ and $\hat{\phi}$ electric field components to the total average radiated power, P_{rad} , equations 3.8 and 3.9 are used to integrate equations 13.3 to 13.10 over the hemispherical Gaussian surface above the ground plane at a fixed radius (R) from the antenna. The sum of the integrals is the antenna's P_{rad} . With the discrete values of the electric field and total average radiated power determined, the Mathcad application predicts the following radiation parameters using the equations from Chapter 3:

R_{rad} radiation resistance (Ohms)
 D_0 directivity
 EIRP.....effective isotropic radiated power (Watts)
 A_{max} maximum theoretical effective area (square meters)
 l_{max} maximum theoretical effective length (meters)
 P_e numerical distance (vertical polarization, $\theta=90^\circ$)
 P_m numerical distance (horizontal polarization, $\theta=90^\circ$)
 $Angle_{max}$.elevation angle of maximum directive gain (degrees)

The directivity (D_0), effective isotropic radiated power (EIRP), maximum theoretical effective area (A_{\max}), maximum theoretical effective length (l_{\max}), and the elevation angle of maximum directive gain (Angle_{\max}) are all determined for both the $\phi=0$ and $\phi=\pi/2$ vertical planes.

XIV. THE TERMINATED SLOPING DOUBLE RHOMBOID ANTENNA

The orientation of the terminated sloping double rhomboid antenna is depicted on the next page in Figure 14.1, where l_1 is the length of the four short antenna wires (A, D, E, and H), l_2 is the length of the four long antenna wires (B, C, F, and G), l_3 is the length of the radials which connect the feed to the two termination points, H_0 is the feed height above ground, H_3 is the height of the termination points above ground, γ is the angle between by the radials which connect the feed to the termination points, δ is the angle between the termination radials and the short feed wires, η is the angle between the termination radials and the long feed wires, α is the angle between the plane which contains the antenna and the x-y plane, R is the radial coordinate, θ is the elevation coordinate, and ϕ is the azimuth coordinate.

The Mathcad application for the double rhomboid antenna requires the following inputs:

- l_1 length of the short antenna wires (meters)
- l_2 length of the long antenna wires (meters)
- l_3 length of the termination radials (meters)
- H_0 feed height above ground (meters)
- H_3 height of termination points above ground (meters)
- γ angle subtended by termination radials (degrees)
- f_s operational frequency (Hertz)
- R distance from antenna (meters)
- ϵ_r relative dielectric constant of ground plane
- σ conductivity of ground plane
- d elevation angle index (from Table 3.1)

The feed height (H_0) and termination height (H_3) can be any value greater than zero. The length of the radials to the

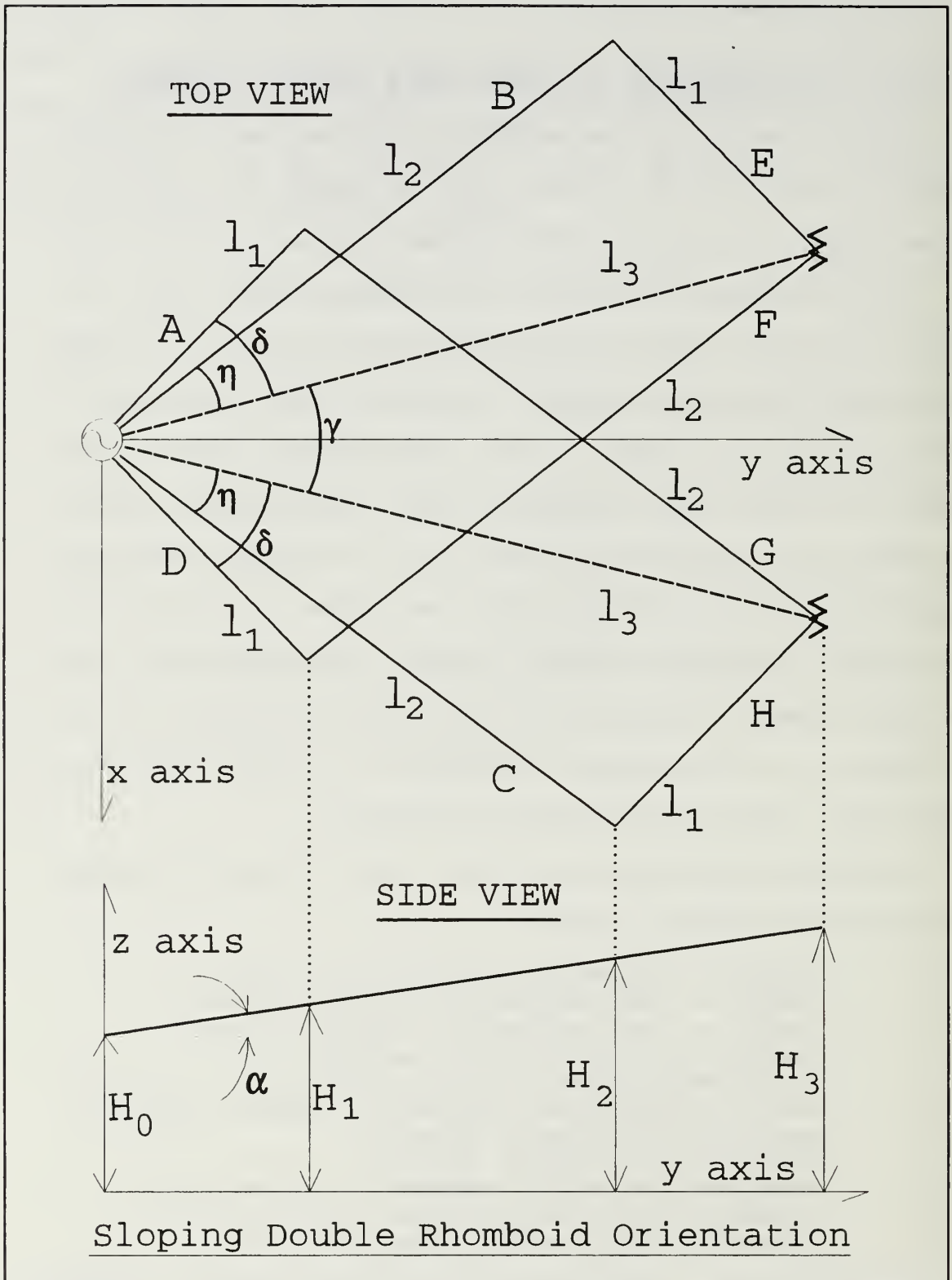


FIGURE 14.1: Spatial orientation of the terminated sloping double rhomboid antenna for its Mathcad application.

termination points must be less than the combined lengths of a long and short antenna wire ($l_3 < l_1 + l_2$). The angle η is found from the law of sines and cosines by

$$\eta = \sin^{-1} \left\{ \frac{l_1}{l_2} \sin \left[\cos^{-1} \left(\frac{(l_1)^2 + (l_3)^2 - (l_2)^2}{2l_1 l_3} \right) \right] \right\} \quad (14.1)$$

The angle δ is also found from the law of cosines by

$$\delta = \left\{ \cos^{-1} \left[\frac{(l_1)^2 + (l_3)^2 - (l_2)^2}{2l_1 l_3} \right] \right\} - \gamma \quad (14.2)$$

The angle α is then found from H_0 , H_3 , l_1 , l_2 , and the half-angle between the wires ($\gamma/2$) by

$$\alpha = \sin^{-1} \left[\frac{H_3 - H_0}{l_1 \cdot \cos\left(\frac{\gamma}{2} + \delta\right) + l_2 \cdot \cos\left(\frac{\gamma}{2} + \eta\right)} \right] \quad (14.3)$$

The user inputs the frequency (f_s) for which the radiation parameters discussed in Chapter 3 are computed. Distance from the antenna (R) must meet the far-field requirements of Chapter 3.C, and the elevation angle index (d) sets the θ coordinate for which a horizontal radiation pattern is determined. Table 3.1 lists possible indices and their corresponding elevation angles from $.285^\circ$ to 88.857° in increments of about 2° . Indices between those listed can be used to interpolate a better estimate of a desired elevation.

The radiated electric field for the double rhomboid is obtained in a manner analogous to that used for the vertical dipole discussed in Chapter 4. The electric field equations for the double rhomboid are given by [Ref 6: p. 238-244]

$$\begin{aligned}
E_{\theta,A} = & 30 I_0 \frac{e^{-j\beta R}}{R} \left\{ \cos(\alpha) \cos(\theta) \sin\left(\phi - \frac{\gamma}{2} - \delta\right) \left[\frac{1 - e^{-j\beta l_1 U_1}}{U_1} \right. \right. \\
& - \Gamma_v \frac{1 - e^{-j\beta l_1 U_5}}{U_5} e^{-j2\beta H_0 \cos(\theta)} + (1 - \Gamma_v) F_e \frac{1 - e^{-j\beta l_1 U_5}}{U_5} e^{-j2\beta H_0 \cos(\theta)} \\
& \left. \left(\sin^2(\theta) - \frac{\sqrt{n^2 - \sin^2(\theta)}}{n^2} \cos(\theta) \right) \frac{\sqrt{n^2 - \sin^2(\theta)}}{n^2 \cos(\theta)} \right] \\
& - \sin(\alpha) \sin(\theta) \left[\frac{1 - e^{-j\beta l_1 U_1}}{U_1} + \Gamma_v \frac{1 - e^{-j\beta l_1 U_5}}{U_5} e^{-j2\beta H_0 \cos(\theta)} \right. \\
& \left. \left. + (1 - \Gamma_v) F_e \frac{1 - e^{-j\beta l_1 U_5}}{U_5} e^{-j2\beta H_0 \cos(\theta)} \left(\sin^2(\theta) - \frac{\sqrt{n^2 - \sin^2(\theta)}}{n^2} \cos(\theta) \right) \right] \right\} \quad (14.4)
\end{aligned}$$

$$\begin{aligned}
E_{\phi,A} = & -30 I_0 \frac{e^{-j\beta R}}{R} \cos(\alpha) \sin\left(\phi - \frac{\gamma}{2} - \delta\right) \left[\frac{1 - e^{-j\beta l_1 U_1}}{U_1} \right. \\
& \left. + \Gamma_h \frac{1 - e^{-j\beta l_1 U_5}}{U_5} e^{-j2\beta H_0 \cos(\theta)} + (1 - \Gamma_h) F_m \frac{1 - e^{-j\beta l_1 U_5}}{U_5} e^{-j2\beta H_0 \cos(\theta)} \right] \quad (14.5)
\end{aligned}$$

$$\begin{aligned}
E_{\theta,B} = & 30 I_0 \frac{e^{-j\beta R}}{R} \left\{ \cos(\alpha) \cos(\theta) \sin\left(\phi - \frac{\gamma}{2} - \eta\right) \left[\frac{1 - e^{-j\beta l_2 U_2}}{U_2} \right. \right. \\
& - \Gamma_v \frac{1 - e^{-j\beta l_2 U_6}}{U_6} e^{-j2\beta H_0 \cos(\theta)} + (1 - \Gamma_v) F_e \frac{1 - e^{-j\beta l_2 U_6}}{U_6} e^{-j2\beta H_0 \cos(\theta)} \\
& \left. \left(\sin^2(\theta) - \frac{\sqrt{n^2 - \sin^2(\theta)}}{n^2} \cos(\theta) \right) \frac{\sqrt{n^2 - \sin^2(\theta)}}{n^2 \cos(\theta)} \right] \\
& - \sin(\alpha) \sin(\theta) \left[\frac{1 - e^{-j\beta l_2 U_2}}{U_2} + \Gamma_v \frac{1 - e^{-j\beta l_2 U_6}}{U_6} e^{-j2\beta H_0 \cos(\theta)} \right. \\
& \left. \left. + (1 - \Gamma_v) F_e \frac{1 - e^{-j\beta l_2 U_6}}{U_6} e^{-j2\beta H_0 \cos(\theta)} \left(\sin^2(\theta) - \frac{\sqrt{n^2 - \sin^2(\theta)}}{n^2} \cos(\theta) \right) \right] \right\} \quad (14.6)
\end{aligned}$$

$$\begin{aligned}
E_{\phi,B} = & -30 I_0 \frac{e^{-j\beta R}}{R} \cos(\alpha) \cos\left(\phi - \frac{\gamma}{2} - \eta\right) \left[\frac{1 - e^{-j\beta l_2 U_2}}{U_2} \right. \\
& \left. + \Gamma_h \frac{1 - e^{-j\beta l_2 U_6}}{U_6} e^{-j2\beta H_0 \cos(\theta)} + (1 - \Gamma_h) F_m \frac{1 - e^{-j\beta l_2 U_6}}{U_6} e^{-j2\beta H_0 \cos(\theta)} \right] \quad (14.7)
\end{aligned}$$

$$\begin{aligned}
E_{\theta, c} = 30 I_0 \frac{e^{-j\beta R}}{R} & \left\{ -\cos(\alpha) \cos(\theta) \sin\left(\phi + \frac{\gamma}{2} + \eta\right) \left[\frac{1 - e^{-j\beta l_2 U_3}}{U_3} \right. \right. \\
& - \Gamma_v \frac{1 - e^{-j\beta l_2 U_7}}{U_7} e^{-j2\beta H_0 \cos(\theta)} + (1 - \Gamma_v) F_e \frac{1 - e^{-j\beta l_2 U_7}}{U_7} e^{-j2\beta H_0 \cos(\theta)} \\
& \left. \left(\sin^2(\theta) - \frac{\sqrt{n^2 - \sin^2(\theta)}}{n^2} \cos(\theta) \right) \frac{\sqrt{n^2 - \sin^2(\theta)}}{n^2 \cos(\theta)} \right] \\
& + \sin(\alpha) \sin(\theta) \left[\frac{1 - e^{-j\beta l_2 U_3}}{U_3} + \Gamma_v \frac{1 - e^{-j\beta l_2 U_7}}{U_7} e^{-j2\beta H_0 \cos(\theta)} \right. \\
& \left. \left. + (1 - \Gamma_v) F_e \frac{1 - e^{-j\beta l_2 U_7}}{U_7} e^{-j2\beta H_0 \cos(\theta)} \left(\sin^2(\theta) - \frac{\sqrt{n^2 - \sin^2(\theta)}}{n^2} \cos(\theta) \right) \right] \right\} \quad (14.8)
\end{aligned}$$

$$\begin{aligned}
E_{\phi, c} = 30 I_0 \frac{e^{-j\beta R}}{R} & \cos(\alpha) \cos\left(\phi + \frac{\gamma}{2} + \eta\right) \left[\frac{1 - e^{-j\beta l_2 U_3}}{U_3} \right. \\
& \left. + \Gamma_h \frac{1 - e^{-j\beta l_2 U_7}}{U_7} e^{-j2\beta H_0 \cos(\theta)} + (1 - \Gamma_h) F_m \frac{1 - e^{-j\beta l_2 U_7}}{U_7} e^{-j2\beta H_0 \cos(\theta)} \right] \quad (14.9)
\end{aligned}$$

$$\begin{aligned}
E_{\theta, D} = 30 I_0 \frac{e^{-j\beta R}}{R} & \left\{ -\cos(\alpha) \cos(\theta) \cos\left(\phi + \frac{\gamma}{2} + \delta\right) \left[\frac{1 - e^{-j\beta l_1 U_4}}{U_4} \right. \right. \\
& - \Gamma_v \frac{1 - e^{-j\beta l_1 U_8}}{U_8} e^{-j2\beta H_0 \cos(\theta)} + (1 - \Gamma_v) F_e \frac{1 - e^{-j\beta l_1 U_8}}{U_8} e^{-j2\beta H_0 \cos(\theta)} \\
& \left. \left(\sin^2(\theta) - \frac{\sqrt{n^2 - \sin^2(\theta)}}{n^2} \cos(\theta) \right) \frac{\sqrt{n^2 - \sin^2(\theta)}}{n^2 \cos(\theta)} \right] \\
& + \sin(\alpha) \sin(\theta) \left[\frac{1 - e^{-j\beta l_1 U_4}}{U_4} + \Gamma_v \frac{1 - e^{-j\beta l_1 U_8}}{U_8} e^{-j2\beta H_0 \cos(\theta)} \right. \\
& \left. \left. + (1 - \Gamma_v) F_e \frac{1 - e^{-j\beta l_1 U_8}}{U_8} e^{-j2\beta H_0 \cos(\theta)} \left(\sin^2(\theta) - \frac{\sqrt{n^2 - \sin^2(\theta)}}{n^2} \cos(\theta) \right) \right] \right\} \quad (14.10)
\end{aligned}$$

$$\begin{aligned}
E_{\phi, D} = 30 I_0 \frac{e^{-j\beta R}}{R} & \cos(\alpha) \cos\left(\phi + \frac{\gamma}{2} + \delta\right) \left[\frac{1 - e^{-j\beta l_1 U_4}}{U_4} \right. \\
& \left. + \Gamma_h \frac{1 - e^{-j\beta l_1 U_8}}{U_8} e^{-j2\beta H_0 \cos(\theta)} + (1 - \Gamma_h) F_m \frac{1 - e^{-j\beta l_1 U_8}}{U_8} e^{-j2\beta H_0 \cos(\theta)} \right] \quad (14.11)
\end{aligned}$$

$$\begin{aligned}
E_{\theta, E} = & 30 I_0 \frac{e^{-j\beta R}}{R} e^{-j\beta l_2 U_2} \left\{ \cos(\alpha) \cos(\theta) \sin\left(\phi + \frac{\gamma}{2} + \delta\right) \right. \\
& \left[\frac{1 - e^{-j\beta l_1 U_4}}{U_4} - \Gamma_v \frac{1 - e^{-j\beta l_1 U_8}}{U_8} e^{-j2\beta H_2 \cos(\theta)} + (1 - \Gamma_v) F_e \frac{1 - e^{-j\beta l_1 U_8}}{U_8} \right. \\
& \cdot e^{-j2\beta H_2 \cos(\theta)} \left(\sin^2(\theta) - \frac{\sqrt{n^2 - \sin^2(\theta)}}{n^2} \cos(\theta) \right) \frac{\sqrt{n^2 - \sin^2(\theta)}}{n^2 \cos(\theta)} \left. \right] \\
& - \sin(\alpha) \sin(\theta) \left[\frac{1 - e^{-j\beta l_1 U_4}}{U_4} + \Gamma_v \frac{1 - e^{-j\beta l_1 U_8}}{U_8} e^{-j2\beta H_2 \cos(\theta)} \right. \\
& \left. \left. + (1 - \Gamma_v) F_e \frac{1 - e^{-j\beta l_1 U_8}}{U_8} e^{-j2\beta H_2 \cos(\theta)} \left(\sin^2(\theta) - \frac{\sqrt{n^2 - \sin^2(\theta)}}{n^2} \cos(\theta) \right) \right] \right\} \quad (14.12)
\end{aligned}$$

$$\begin{aligned}
E_{\phi, E} = & -30 I_0 \frac{e^{-j\beta R}}{R} e^{-j\beta l_2 U_2} \cos(\alpha) \cos\left(\phi + \frac{\gamma}{2} + \delta\right) \left[\frac{1 - e^{-j\beta l_1 U_4}}{U_4} \right. \\
& \left. + \Gamma_h \frac{1 - e^{-j\beta l_1 U_8}}{U_8} e^{-j2\beta H_2 \cos(\theta)} + (1 - \Gamma_h) F_m \frac{1 - e^{-j\beta l_1 U_8}}{U_8} e^{-j2\beta H_2 \cos(\theta)} \right] \quad (14.13)
\end{aligned}$$

$$\begin{aligned}
E_{\theta, F} = & 30 I_0 \frac{e^{-j\beta R}}{R} e^{-j\beta l_1 U_4} \left\{ -\cos(\alpha) \cos(\theta) \cos\left(\phi - \frac{\gamma}{2} - \eta\right) \right. \\
& \left[\frac{1 - e^{-j\beta l_2 U_2}}{U_2} - \Gamma_v \frac{1 - e^{-j\beta l_2 U_6}}{U_6} e^{-j2\beta H_1 \cos(\theta)} + (1 - \Gamma_v) F_e \frac{1 - e^{-j\beta l_2 U_6}}{U_6} \right. \\
& \cdot e^{-j2\beta H_1 \cos(\theta)} \left(\sin^2(\theta) - \frac{\sqrt{n^2 - \sin^2(\theta)}}{n^2} \cos(\theta) \right) \frac{\sqrt{n^2 - \sin^2(\theta)}}{n^2 \cos(\theta)} \left. \right] \\
& + \sin(\alpha) \sin(\theta) \left[\frac{1 - e^{-j\beta l_2 U_2}}{U_2} + \Gamma_v \frac{1 - e^{-j\beta l_2 U_6}}{U_6} e^{-j2\beta H_1 \cos(\theta)} \right. \\
& \left. \left. + (1 - \Gamma_v) F_e \frac{1 - e^{-j\beta l_2 U_6}}{U_6} e^{-j2\beta H_1 \cos(\theta)} \left(\sin^2(\theta) - \frac{\sqrt{n^2 - \sin^2(\theta)}}{n^2} \cos(\theta) \right) \right] \right\} \quad (14.14)
\end{aligned}$$

$$\begin{aligned}
E_{\phi, F} = & 30 I_0 \frac{e^{-j\beta R}}{R} e^{-j\beta l_1 U_4} \cos(\alpha) \cos\left(\phi - \frac{\gamma}{2} - \eta\right) \left[\frac{1 - e^{-j\beta l_2 U_2}}{U_2} \right. \\
& \left. + \Gamma_h \frac{1 - e^{-j\beta l_2 U_6}}{U_6} e^{-j2\beta H_1 \cos(\theta)} + (1 - \Gamma_h) F_m \frac{1 - e^{-j\beta l_2 U_6}}{U_6} e^{-j2\beta H_1 \cos(\theta)} \right] \quad (14.15)
\end{aligned}$$

$$\begin{aligned}
E_{\theta, G} = & 30 I_0 \frac{e^{-j\beta R}}{R} e^{-j\beta l_1 U_1} \left\{ \cos(\alpha) \cos(\theta) \cos\left(\phi + \frac{\gamma}{2} + \eta\right) \right. \\
& \left[\frac{1 - e^{-j\beta l_2 U_3}}{U_3} - \Gamma_v \frac{1 - e^{-j\beta l_2 U_7}}{U_7} e^{-j2\beta H_1 \cos(\theta)} + (1 - \Gamma_v) F_e \frac{1 - e^{-j\beta l_2 U_7}}{U_7} \right. \\
& \cdot e^{-j2\beta H_1 \cos(\theta)} \left(\sin^2(\theta) - \frac{\sqrt{n^2 - \sin^2(\theta)}}{n^2} \cos(\theta) \right) \frac{\sqrt{n^2 - \sin^2(\theta)}}{n^2 \cos(\theta)} \left. \right] \\
& - \sin(\alpha) \sin(\theta) \left[\frac{1 - e^{-j\beta l_2 U_3}}{U_3} + \Gamma_v \frac{1 - e^{-j\beta l_2 U_7}}{U_7} e^{-j2\beta H_1 \cos(\theta)} \right. \\
& \left. \left. + (1 - \Gamma_v) F_e \frac{1 - e^{-j\beta l_2 U_7}}{U_7} e^{-j2\beta H_1 \cos(\theta)} \left(\sin^2(\theta) - \frac{\sqrt{n^2 - \sin^2(\theta)}}{n^2} \cos(\theta) \right) \right] \right\}
\end{aligned} \quad (14.16)$$

$$\begin{aligned}
E_{\phi, G} = & -30 I_0 \frac{e^{-j\beta R}}{R} e^{-j\beta l_1 U_1} \cos(\alpha) \cos\left(\phi + \frac{\gamma}{2} + \eta\right) \left[\frac{1 - e^{-j\beta l_2 U_3}}{U_3} \right. \\
& \left. + \Gamma_h \frac{1 - e^{-j\beta l_2 U_7}}{U_7} e^{-j2\beta H_1 \cos(\theta)} + (1 - \Gamma_h) F_m \frac{1 - e^{-j\beta l_2 U_7}}{U_7} e^{-j2\beta H_1 \cos(\theta)} \right]
\end{aligned} \quad (14.17)$$

$$\begin{aligned}
E_{\theta, H} = & 30 I_0 \frac{e^{-j\beta R}}{R} e^{-j\beta l_2 U_3} \left\{ -\cos(\alpha) \cos(\theta) \sin\left(\phi - \frac{\gamma}{2} - \delta\right) \right. \\
& \left[\frac{1 - e^{-j\beta l_1 U_1}}{U_1} - \Gamma_v \frac{1 - e^{-j\beta l_1 U_5}}{U_5} e^{-j2\beta H_2 \cos(\theta)} + (1 - \Gamma_v) F_e \frac{1 - e^{-j\beta l_1 U_5}}{U_5} \right. \\
& \cdot e^{-j2\beta H_2 \cos(\theta)} \left(\sin^2(\theta) - \frac{\sqrt{n^2 - \sin^2(\theta)}}{n^2} \cos(\theta) \right) \frac{\sqrt{n^2 - \sin^2(\theta)}}{n^2 \cos(\theta)} \left. \right] \\
& + \sin(\alpha) \sin(\theta) \left[\frac{1 - e^{-j\beta l_1 U_1}}{U_1} + \Gamma_v \frac{1 - e^{-j\beta l_1 U_5}}{U_5} e^{-j2\beta H_2 \cos(\theta)} \right. \\
& \left. \left. + (1 - \Gamma_v) F_e \frac{1 - e^{-j\beta l_1 U_5}}{U_5} e^{-j2\beta H_2 \cos(\theta)} \left(\sin^2(\theta) - \frac{\sqrt{n^2 - \sin^2(\theta)}}{n^2} \cos(\theta) \right) \right] \right\}
\end{aligned} \quad (14.18)$$

$$\begin{aligned}
E_{\phi, H} = & 30 I_0 \frac{e^{-j\beta R}}{R} e^{-j\beta l_2 U_3} \cos(\alpha) \cos\left(\phi - \frac{\gamma}{2} - \delta\right) \left[\frac{1 - e^{-j\beta l_1 U_1}}{U_1} \right. \\
& \left. + \Gamma_h \frac{1 - e^{-j\beta l_1 U_5}}{U_5} e^{-j2\beta H_2 \cos(\theta)} + (1 - \Gamma_h) F_m \frac{1 - e^{-j\beta l_1 U_5}}{U_5} e^{-j2\beta H_2 \cos(\theta)} \right]
\end{aligned} \quad (14.19)$$

where $U_1, U_2, U_3, U_4, U_5, U_6, U_7$, and U_8 are given by

$$\begin{aligned} U_1 &= 1 - \cos(\Psi_1) & U_2 &= 1 - \cos(\Psi_2) \\ U_3 &= 1 - \cos(\Psi_3) & U_4 &= 1 - \cos(\Psi_4) \\ U_5 &= 1 - \cos(\Psi_5) & U_6 &= 1 - \cos(\Psi_6) \\ U_7 &= 1 - \cos(\Psi_7) & U_8 &= 1 - \cos(\Psi_8) \quad \text{where} \end{aligned}$$

$$\begin{aligned} \cos(\Psi_1) &= \cos(\theta) \sin(\alpha) + \sin(\theta) \cos(\alpha) \sin(\phi - \alpha - \delta) \\ \cos(\Psi_2) &= \cos(\theta) \sin(\alpha) + \sin(\theta) \cos(\alpha) \sin(\phi - \alpha - \eta) \\ \cos(\Psi_3) &= \cos(\theta) \sin(\alpha) + \sin(\theta) \cos(\alpha) \sin(\phi + \alpha + \eta) \\ \cos(\Psi_4) &= \cos(\theta) \sin(\alpha) + \sin(\theta) \cos(\alpha) \sin(\phi + \alpha + \delta) \\ \cos(\Psi_5) &= \sin(\theta) \cos(\alpha) \sin(\phi - \alpha - \delta) - \cos(\theta) \sin(\alpha) \\ \cos(\Psi_6) &= \sin(\theta) \cos(\alpha) \sin(\phi - \alpha - \eta) - \cos(\theta) \sin(\alpha) \\ \cos(\Psi_7) &= \sin(\theta) \cos(\alpha) \sin(\phi + \alpha + \eta) - \cos(\theta) \sin(\alpha) \\ \cos(\Psi_8) &= \sin(\theta) \cos(\alpha) \sin(\phi + \alpha + \delta) - \cos(\theta) \sin(\alpha) \end{aligned}$$

The double rhomboid's radiated electric field is a combination of $\hat{\theta}$ and $\hat{\phi}$ components, and its radiation pattern varies with changes in ϕ . The total electric field is the vector sum of the $\hat{\theta}$ and $\hat{\phi}$ components. The radiated fields of each antenna wire are considered separately, and superposition is used to determine the total electric field. Equations 14.4 and 14.5 are the $\hat{\theta}$ (vertically polarized) and $\hat{\phi}$ (horizontally polarized) components, respectively for wire A, and equations 14.6 and 14.7 are the $\hat{\theta}$ and $\hat{\phi}$ components, respectively for wire B. Equations 14.8 and 14.9 are the analogous equations for wire C, 14.10 and 14.11 those for wire D, 14.12 and 14.13 those for wire E, 14.14 and 14.15 those for wire F, 14.16 and 14.17 those for wire G, and 14.18 and 14.19 those for wire H.

The first two terms inside each set of brackets represent the space wave components and any additional terms represent the surface wave components. I_0 is taken to be one since a sinusoidal current input with a maximum of unity is assumed.

The requested inputs are used to calculate the following variables using a constant ϕ of $\phi=0$ and $\phi=\pi/2$ for 632 discrete values of θ which are equally incremented from $-\pi/2$ to $\pi/2$:

λ_s wavelength of the operational frequency (meters)
 β free space wavenumber for operational frequency
 n index of refraction
 P_e complex numerical distance (vertical polarization)
 P_m complex numerical distance (horizontal polarization)
 Γ_v vertical reflection coefficient
 Γ_h horizontal reflection coefficient
 F_e vertical surface wave attenuation factor
 F_m horizontal surface wave attenuation factor

The calculated variables are used to evaluate the far-field space wave and surface wave for the discrete values of θ with $\phi=0$ and $\phi=\pi/2$. The total space wave and surface wave distributions are determined from vector addition of corresponding $\hat{\theta}$ and $\hat{\phi}$ components. The space wave and surface wave results are then combined for corresponding discrete values of θ to obtain the total radiated electric field distribution for the $\phi=0$ and $\phi=\pi/2$ vertical planes. The space wave, surface wave, and total electric field results are then normalized with respect to the maximum field intensity of each, and the normalized magnitudes are plotted for each discrete θ to depict the radiation patterns. The Mathcad double rhomboid antenna application computes the space wave, surface wave, and total electric field radiation patterns and radiation parameters in the $\phi=0$ and $\phi=\pi/2$ vertical planes.

The variables corresponding to the selected elevation angle index (d) are used to evaluate the radiated electric field components for the space wave and surface wave at the fixed elevation angle (θ_d) as ϕ varies from 0 to 2π in 632 equal increments. The horizontal radiation patterns are then plotted for the space wave, surface wave, and total radiated electric field just as those for the vertical planes.

To find the contributions of the $\hat{\theta}$ and $\hat{\phi}$ electric field components to the total average radiated power, P_{rad} , equations 3.8 and 3.9 are used to integrate equations 14.4 to 14.19 over the hemispherical Gaussian surface above the ground plane at a fixed radius (R) from the antenna. The sum of the integrals is the antenna's P_{rad} . With the discrete values of the electric field and total average radiated power determined, the Mathcad application predicts the following radiation parameters using the equations from Chapter 3:

R_{rad} radiation resistance (Ohms)
 D_0 directivity
 EIRP.....effective isotropic radiated power (Watts)
 A_{max} maximum theoretical effective area (square meters)
 l_{max} maximum theoretical effective length (meters)
 P_e numerical distance (vertical polarization, $\theta=90^\circ$)
 P_m numerical distance (horizontal polarization, $\theta=90^\circ$)
 Angle_{max} .elevation angle of maximum directive gain (degrees)

The directivity (D_0), effective isotropic radiated power (EIRP), maximum theoretical effective area (A_{max}), maximum theoretical effective length (l_{max}), and the elevation angle of maximum directive gain (Angle_{max}) are all determined for both the $\phi=0$ and $\phi=\pi/2$ vertical planes.

XV. THE VERTICALLY POLARIZED LOG-PERIODIC DIPOLE ARRAY

The orientation of the vertically polarized log-periodic dipole array is depicted in Figure 15.1, where N is the number of dipoles, n is an index equal to $0, 1, 2, \dots, N-1$, l_n is the length of the $n^{\text{th}}+1$ dipole, d_n is the distance between the $n^{\text{th}}+1$ and $n^{\text{th}}+2$ dipole elements, H_0 is the height of the antenna feed above ground, H_n is the height of the $n^{\text{th}}+1$ dipole center, Ψ is the angle between the vertical axis and the array's center axis, α_1 is the angle between the center axis and the line which connects the upper tips of the elements, α_2 is the angle between the center axis and the line which connects the lower tips of the elements, α_3 is the angle between the horizontal and the line connecting the lower tips of the elements, R is the radial coordinate, θ is the elevation coordinate, and ϕ is the azimuth coordinate.

The Mathcad application for the vertically polarized log-periodic array requires the following inputs:

Nnumber of dipole elements
 l_0length of the shortest dipole (meters)
 l_1length of the second shortest dipole (meters)
 d_0distance between first two elements (meters)
 rad_0radius of the shortest dipole (meters)
 H_0feed height above ground plane (meters)
 Ψangle from vertical axis to array axis (degrees)
 f_soperational frequency (Hertz)
 Rdistance from array (meters)
 ϵ_rrelative dielectric constant of ground plane
 σconductivity of ground plane
 welevation angle index (from Table 3.2)
 ADMtransmission line characteristic admittance
 $TIMP$termination impedance connected to longest dipole

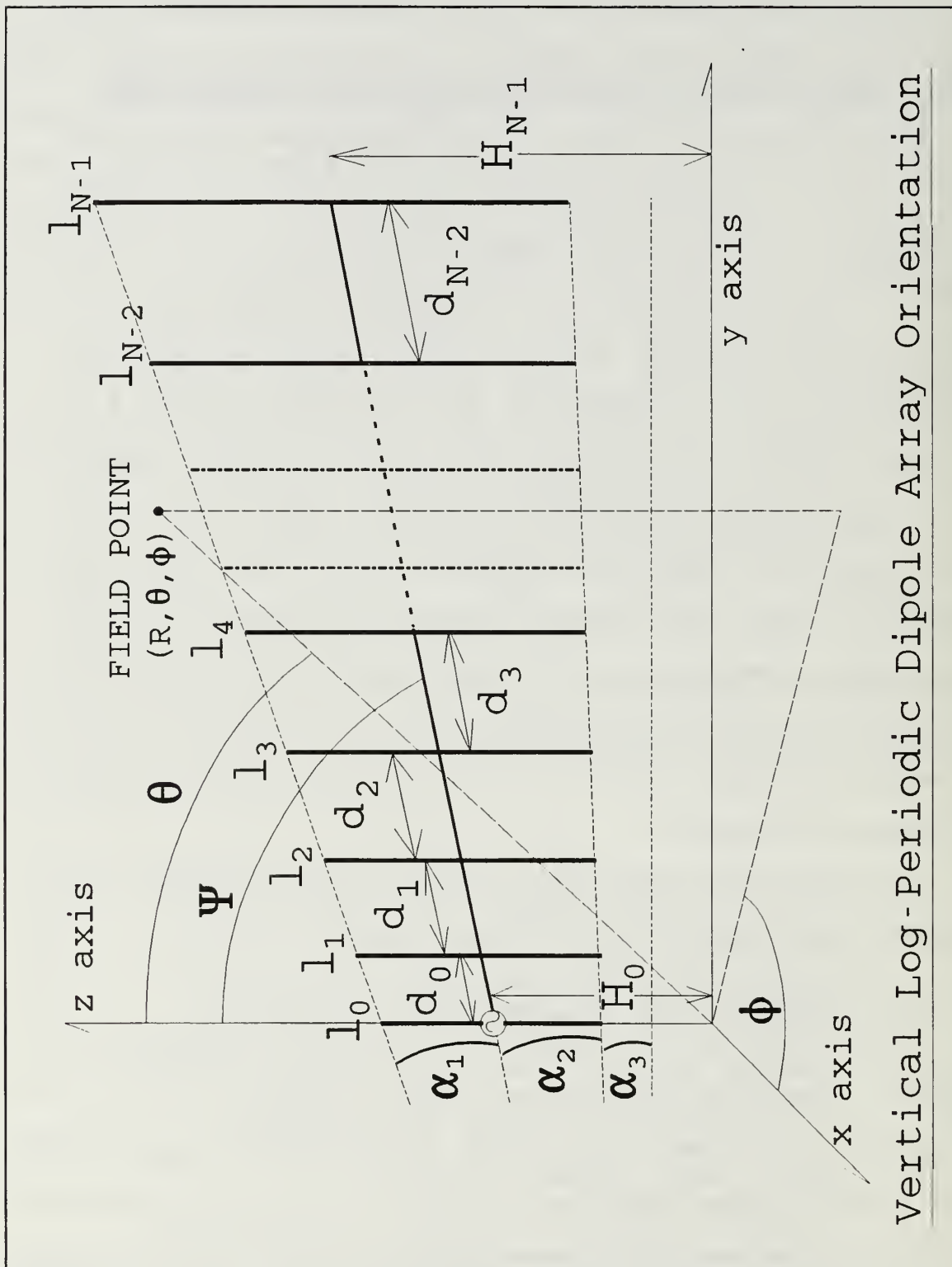


FIGURE 15.1: Spatial orientation of the vertically polarized log-periodic dipole array for its corresponding Mathcad application.

The user inputs the frequency for which the radiation parameters discussed in Chapter 3 are computed. The lengths of the first two elements (l_0 and l_1) are used to calculate the log-periodic relationship (τ) given by [Ref 10: p. 317]

$$\tau = \frac{l_n}{l_{n+1}} \quad (n=0,1,2,\dots,N-2,N-1) \quad (15.1)$$

The remaining element lengths (l_2 to l_{N-1}) are then found from

$$l_{n+1} = \frac{l_n}{\tau} \quad (15.2)$$

As noted in equation 15.1, indices start at zero instead of 1, so an index simply refers to the index-plus-one position in terms of successive values for a given parameter. This is to maintain continuity with Mathcad which also indexes from zero. The radius of the first element (rad_0) is used to find the remaining radii by substituting rad_n and rad_{n+1} for l_n and l_{n+1} in equation 15.2. The angle between the vertical axis and the array axis (Ψ) can be between 0° and 90° . The angles α_2 and α_3 are found by substituting

$$\alpha_2 + \alpha_3 = \frac{\pi}{2} - \Psi \quad (15.3)$$

into

$$\frac{d_n}{l_{n+1}} = \frac{1 - \tau}{\sin(\alpha_2 + \alpha_3) - \tan(\alpha_3) \cos(\alpha_2 + \alpha_3)} \quad (15.4)$$

which yields

$$\alpha_3 = \tan^{-1} \left[\frac{h_n + d_n \sin\left(\frac{\pi}{2} - \Psi\right) - h_{n+1}}{d_n \cos\left(\frac{\pi}{2} - \Psi\right)} \right]$$

The angle α_1 is then found from [Ref 10: pp. 351-354]

$$\frac{\sin(\alpha_1)}{\cos(\alpha_1 + \alpha_2 + \alpha_3)} = \frac{\sin(\alpha_2)}{\cos(\alpha_3)} \quad (15.5)$$

or

$$\alpha_1 = \tan^{-1} \left[\frac{\sin(\alpha_2) \cos(\alpha_2 + \alpha_3)}{\cos(\alpha_3) + \sin(\alpha_2) \sin(\alpha_2 + \alpha_3)} \right]$$

The remaining separations (d_1 to d_{N-2}) are then found from equation 15.4. The dipole half-lengths (h_n) are found from $l_n/2$, the feed height (H_0) must be at least equal to the half-length of the longest dipole (h_{N-1}), and distance from the array (R) must meet the far-field requirements of Chapter 3.C. The elevation angle index (w) sets the θ coordinate for which a horizontal radiation pattern is determined. Table 3.2 lists possible indices and their corresponding elevation angles from $.57^\circ$ to 89.1° in increments of about 2.3° . Indices between those listed can be used to interpolate a better approximation of a desired elevation. The termination impedance (TIMP) is assumed to be connected to the array's center axis opposite the feed at a distance of $h_{N-1}/2$ from the longest element. Typical termination impedances are the transmission line's matched impedance (complex conjugate) or a short circuit (zero). The characteristic admittance (ADM) is simply the inverse of the transmission line's characteristic impedance.

If computed lengths, separations and radii are not desired, they can be entered manually as described on the page two of the application. Consult a Mathcad manual to be certain the entries are made correctly.

The open circuit impedance matrices must be calculated to determine the current distribution among the dipole elements. The matrix of open circuit mutual impedances between the dipole elements is represented as

$$[Z] = \begin{bmatrix} Z_{0,0} & Z_{0,1} & Z_{0,2} & \cdot & \cdot & \cdot & \cdot & Z_{0,(N-1)} \\ Z_{1,0} & Z_{1,1} & Z_{1,2} & \cdot & \cdot & \cdot & \cdot & Z_{1,(N-1)} \\ Z_{2,0} & Z_{2,1} & Z_{2,2} & \cdot & \cdot & \cdot & \cdot & Z_{2,(N-1)} \\ \cdot & \cdot & \cdot & \cdot & \cdot & \cdot & \cdot & \cdot \\ \cdot & \cdot & \cdot & \cdot & \cdot & \cdot & \cdot & \cdot \\ Z_{(N-1),0} & Z_{(N-1),1} & Z_{(N-1),2} & \cdot & \cdot & \cdot & \cdot & Z_{(N-1),(N-1)} \end{bmatrix} \quad (15.6)$$

Each main diagonal term ($Z_{i,i}$) is the self-impedance of the $i^{\text{th}}+1$ dipole. The off-diagonal terms ($Z_{i,k}$) are the mutual impedances between the $i^{\text{th}}+1$ and $k^{\text{th}}+1$ elements. Subscripts i and k are matrix indices from $0,1,2,\dots,N-1$.

The matrix of open circuit mutual impedances between the actual dipoles and their images is represented as

$$[ZI] = \begin{bmatrix} ZI_{0,0} & ZI_{0,1} & ZI_{0,2} & \cdot & \cdot & \cdot & \cdot & ZI_{1(N-1)} \\ ZI_{1,0} & ZI_{1,1} & ZI_{1,2} & \cdot & \cdot & \cdot & \cdot & ZI_{1,(N-1)} \\ ZI_{2,0} & ZI_{2,1} & ZI_{2,2} & \cdot & \cdot & \cdot & \cdot & ZI_{2,(N-1)} \\ \cdot & \cdot & \cdot & \cdot & \cdot & \cdot & \cdot & \cdot \\ \cdot & \cdot & \cdot & \cdot & \cdot & \cdot & \cdot & \cdot \\ ZI_{(N-1),0} & ZI_{(N-1),1} & ZI_{(N-1),2} & \cdot & \cdot & \cdot & \cdot & ZI_{(N-1),(N-1)} \end{bmatrix} \quad (15.7)$$

The main diagonal terms ($ZI_{i,i}$) are the mutual impedances between the $i^{\text{th}}+1$ element and its image, and the off-diagonal terms ($ZI_{i,k}$) are the mutual impedances between the $i^{\text{th}}+1$ element and the image of the $k^{\text{th}}+1$ element.

The main diagonal self-impedance terms of equation 15.6 ($Z_{i,i}$) are found from [Ref 6: pp. 205-206]

$$Z_{i,i} = \frac{60}{1 - \cos(2\beta h_i)} \left[e^{-j2\beta h_i} [Q(U_0) - 2Q(U_1)] \right. \quad (15.8)$$

$$\left. + e^{j2\beta h_i} [Q(V_0) - 2Q(V_1)] + 2[Q(U'_0) - Q(U_1) - Q(V_1)] + 2Q(U'_0)[1 + \cos(2\beta h_i)] \right]$$

$$\text{where } Q(x) = Ci(x) - jSi(x) = \int_{-\infty}^x \frac{\cos(y)}{y} dy - j \int_0^x \frac{\sin(y)}{y} dy \quad (15.9)$$

$$U_0 = \beta \left[\sqrt{2rad_i^2 + 4h_i^2} - 2h_i \right] \quad U'_0 = \sqrt{2}\beta rad_i \quad V_0 = \beta \left[\sqrt{2rad_i^2 + 4h_i^2} + 2h_i \right]$$

$$U_1 = \beta \left[\sqrt{2rad_i^2 + h_i^2} - h_i \right] \quad V_1 = \beta \left[\sqrt{2rad_i^2 + h_i^2} + h_i \right]$$

For $\Psi = 90^\circ$, the off-diagonal mutual impedance terms of equation 15.6 ($Z_{i,i}$) are given by [Ref 11]

$$Z_{i,k} = Z_{k,i} = \frac{60}{\cos[\beta(h_i - h_k)] - \cos[\beta(h_i + h_k)]} \quad (15.10)$$

$$\left[e^{-j\beta(h_i + h_k)} [Q(U_0) - Q(U_1) - Q(U_2)] + e^{j\beta(h_i + h_k)} [Q(V_0) - Q(V_1) - Q(V_2)] \right.$$

$$\left. + e^{-j\beta(h_i - h_k)} [Q(U'_0) - Q(V_1) - Q(U_2)] + e^{j\beta(h_i - h_k)} [Q(V'_0) - Q(U_1) - Q(V_2)] \right.$$

$$\left. + 2Q(\beta D_{i,k}) (\cos[\beta(h_i - h_k)] + \cos[\beta(h_i + h_k)]) \right]$$

$$\text{where } Q(x) = Ci(x) - jSi(x) = \int_{-\infty}^x \frac{\cos(y)}{y} dy - j \int_0^x \frac{\sin(y)}{y} dy$$

$$U_0 = \beta \left[\sqrt{D_{i,k}^2 + (h_i + h_k)^2} - (h_i + h_k) \right]$$

$$V_0 = \beta \left[\sqrt{D_{i,k}^2 + (h_i + h_k)^2} + (h_i + h_k) \right]$$

$$U'_0 = \beta \left[\sqrt{D_{i,k}^2 + (h_i - h_k)^2} - (h_i - h_k) \right]$$

$$V'_0 = \beta \left[\sqrt{D_{i,k}^2 + (h_i - h_k)^2} + (h_i - h_k) \right]$$

$$U_1 = \beta \left[\sqrt{D_{i,k}^2 + h_i^2} - h_i \right]$$

$$V_1 = \beta \left[\sqrt{D_{i,k}^2 + h_i^2} + h_i \right]$$

$$U_2 = \beta \left[\sqrt{D_{i,k}^2 + h_k^2} - h_k \right]$$

$$V_2 = \beta \left[\sqrt{D_{i,k}^2 + h_k^2} + h_k \right]$$

For Ψ less than 90° , the dipoles are in echelon. The expression for the mutual impedance terms of equation 15.6 ($Z_{i,k}$) for an echelon configuration is given by [Ref 12]

$$\begin{aligned}
 Z_{i,j} = & 15 \left\{ e^{-j\beta(h_i - SD_{i,k})} [Q(U_0) - Q(U_1)] + e^{j\beta(h_i - SD_{i,k})} [Q(V_0) - Q(V_1)] \right. \\
 & + e^{-j\beta(h_i + SD_{i,k})} [Q(U'_0) - Q(U_2)] + e^{j\beta(h_i + SD_{i,k})} [Q(V'_0) - Q(V_2)] \\
 & + e^{-j\beta(h_i - 2h_k - SD_{i,k})} [Q(U_3) - Q(U_1)] + e^{j\beta(h_i - 2h_k - SD_{i,k})} [Q(V_3) - Q(V_1)] \\
 & + e^{-j\beta(h_i + 2h_k + SD_{i,k})} [Q(U_4) - Q(U_2)] + e^{j\beta(h_i + 2h_k + SD_{i,k})} [Q(V_4) - Q(V_2)] \\
 & + 2\cos(\beta h_i) e^{-j\beta SD_{i,k}} [Q(W_2) - Q(W_1)] + 2\cos(\beta h_i) e^{j\beta SD_{i,k}} [Q(Y_2) - Q(Y_1)] \\
 & \left. + 2\cos(\beta h_i) [e^{-j\beta(2h_k + SD_{i,k})} [Q(W_2) - Q(W_3)] + e^{j\beta(2h_k + SD_{i,k})} [Q(Y_2) - Q(Y_3)]] \right\}
 \end{aligned}
 \tag{15.11}$$

where $Q(x) = Ci(x) - j \cdot Si(x) = \int_{\infty}^x \frac{\cos(y)}{y} dy - j \cdot \int_0^x \frac{\sin(y)}{y} dy$

$$\begin{aligned}
 U_0 &= \beta \left[\sqrt{D_{i,k}^2 + (SD_{i,k} - h_i)^2} + (SD_{i,k} - h_i) \right] \\
 V_0 &= \beta \left[\sqrt{D_{i,k}^2 + (SD_{i,k} - h_i)^2} - (SD_{i,k} - h_i) \right] \\
 U'_0 &= \beta \left[\sqrt{D_{i,k}^2 + (SD_{i,k} + h_i)^2} - (SD_{i,k} + h_i) \right] \\
 V'_0 &= \beta \left[\sqrt{D_{i,k}^2 + (SD_{i,k} + h_i)^2} + (SD_{i,k} + h_i) \right] \\
 U_1 &= \beta \left[\sqrt{D_{i,k}^2 + (SD_{i,k} - h_i + h_k)^2} + (SD_{i,k} - h_i + h_k) \right] \\
 V_1 &= \beta \left[\sqrt{D_{i,k}^2 + (SD_{i,k} - h_i + h_k)^2} - (SD_{i,k} - h_i + h_k) \right] \\
 U_2 &= \beta \left[\sqrt{D_{i,k}^2 + (SD_{i,k} + h_i + h_k)^2} - (SD_{i,k} + h_i + h_k) \right] \\
 V_2 &= \beta \left[\sqrt{D_{i,k}^2 + (SD_{i,k} + h_i + h_k)^2} + (SD_{i,k} + h_i + h_k) \right] \\
 U_3 &= \beta \left[\sqrt{D_{i,k}^2 + (SD_{i,k} - h_i + 2h_k)^2} + (SD_{i,k} - h_i + 2h_k) \right] \\
 V_3 &= \beta \left[\sqrt{D_{i,k}^2 + (SD_{i,k} - h_i + 2h_k)^2} - (SD_{i,k} - h_i + 2h_k) \right] \\
 U_4 &= \beta \left[\sqrt{D_{i,k}^2 + (SD_{i,k} + h_i + 2h_k)^2} - (SD_{i,k} + h_i + 2h_k) \right]
 \end{aligned}$$

$$\begin{aligned}
V_4 &= \beta \left[\sqrt{D_{i,k}^2 + (SD_{i,k} + h_i + 2h_k)^2} + (SD_{i,k} + h_i + 2h_k) \right] \\
W_1 &= \beta \left[\sqrt{D_{i,k}^2 + SD_{i,k}^2} - SD_{i,k} \right] \\
Y_1 &= \beta \left[\sqrt{D_{i,k}^2 + SD_{i,k}^2} + SD_{i,k} \right] \\
W_2 &= \beta \left[\sqrt{D_{i,k}^2 + (SD_{i,k} + h_k)^2} - (SD_{i,k} + h_k) \right] \\
Y_2 &= \beta \left[\sqrt{D_{i,k}^2 + (SD_{i,k} + h_k)^2} + (SD_{i,k} + h_k) \right] \\
W_3 &= \beta \left[\sqrt{D_{i,k}^2 + (SD_{i,k} + 2h_k)^2} - (SD_{i,k} + 2h_k) \right] \\
Y_3 &= \beta \left[\sqrt{D_{i,k}^2 + (SD_{i,k} + 2h_k)^2} + (SD_{i,k} + 2h_k) \right]
\end{aligned}$$

The $D_{i,k}$ terms in equations 15.10 and 15.11 are the perpendicular distances between the $i^{\text{th}}+1$ and $k^{\text{th}}+1$ elements given by

$$D_{i,k} = D_{k,i} = \sum_{n=i}^{k-1} d_n \cdot \sin(\Psi) \quad (15.12)$$

The $SD_{i,k}$ terms for equation 15.11 are the vertical distance from the center of the $i^{\text{th}}+1$ dipole to the z coordinate of the nearest end of the $k^{\text{th}}+1$ dipole and are given by

$$SD_{i,k} = SD_{k,i} = \sum_{n=i}^{k-1} d_n \cdot \cos(\Psi) - h_j \quad (15.13)$$

For ground planes with high conductivities relative to the operating frequency, it is necessary to compute equation 15.7, $[ZI]$, for the mutual impedances between the elements and their images. The main diagonal terms $(ZI_{i,i})$ are the mutual impedances between the $i^{\text{th}}+1$ dipole and its own image. These $Z_{i,i}$ terms are calculated from the mutual impedance equation for a collinear configuration given by [Ref 12]

$$\begin{aligned}
ZI_{i,i} = & 15 \left\{ e^{-j\beta(h_i - hi_{i,i})} [Q(U_0) - Q(U_1)] + e^{j\beta(h_i - hi_{i,i})} \ln \left[\frac{hi_{i,i}}{hi_{i,i} - h_i} \right] \right. \\
& + e^{j\beta(h_i + hi_{i,i})} [Q(V'_0) - Q(V_2)] + e^{-j\beta(h_i + hi_{i,i})} \ln \left[\frac{hi_{i,i} + 2h_i}{hi_{i,i} + h_i} \right] \\
& + e^{j\beta(h_i + hi_{i,i})} [Q(U_3) - Q(U_1)] + e^{-j\beta(h_i + hi_{i,i})} \ln \left[\frac{hi_{i,i}}{hi_{i,i} + h_i} \right] \\
& + e^{j\beta(3h_i + hi_{i,i})} [Q(V_4) - Q(V_2)] + e^{-j\beta(3h_i + hi_{i,i})} \ln \left[\frac{hi_{i,i} + 2h_i}{hi_{i,i} + 3h_i} \right] \\
& + 2\cos(\beta h_i) e^{j\beta hi_{i,i}} [Q(Y_2) - Q(Y_1)] + 2\cos(\beta h_i) e^{-j\beta hi_{i,i}} \ln \left[\frac{hi_{i,i}}{hi_{i,i} + h_i} \right] \\
& + 2\cos(\beta h_i) e^{j\beta(2h_i + hi_{i,i})} [Q(Y_2) - Q(Y_3)] \\
& \left. + 2\cos(\beta h_i) e^{-j\beta(2h_i + hi_{i,i})} \ln \left[\frac{hi_{i,i} + 2h_i}{hi_{i,i} + h_i} \right] \right\}
\end{aligned} \quad (15.14)$$

where $Q(x) = Ci(x) - j \cdot Si(x) = \int_{\infty}^x \frac{\cos(y)}{y} dy - j \int_0^x \frac{\sin(y)}{y} dy$

$$U_0 = \beta \left[\sqrt{D_{i,k}^2 + (hi_{i,k} - h_i)^2} + (hi_{i,k} - h_i) \right]$$

$$V_0 = \beta \left[\sqrt{D_{i,k}^2 + (hi_{i,k} - h_i)^2} - (hi_{i,k} - h_i) \right]$$

$$U'_0 = \beta \left[\sqrt{D_{i,k}^2 + (hi_{i,k} + h_i)^2} - (hi_{i,k} + h_i) \right]$$

$$V'_0 = \beta \left[\sqrt{D_{i,k}^2 + (hi_{i,k} + h_i)^2} + (hi_{i,k} + h_i) \right]$$

$$U_1 = \beta \left[\sqrt{D_{i,k}^2 + (hi_{i,k} - h_i + h_k)^2} + (hi_{i,k} - h_i + h_k) \right]$$

$$V_1 = \beta \left[\sqrt{D_{i,k}^2 + (hi_{i,k} - h_i + h_k)^2} - (hi_{i,k} - h_i + h_k) \right]$$

$$U_2 = \beta \left[\sqrt{D_{i,k}^2 + (hi_{i,k} + h_i + h_k)^2} - (hi_{i,k} + h_i + h_k) \right]$$

$$V_2 = \beta \left[\sqrt{D_{i,k}^2 + (hi_{i,k} + h_i + h_k)^2} + (hi_{i,k} + h_i + h_k) \right]$$

$$U_3 = \beta \left[\sqrt{D_{i,k}^2 + (hi_{i,k} - h_i + 2h_k)^2} + (hi_{i,k} - h_i + 2h_k) \right]$$

$$V_3 = \beta \left[\sqrt{D_{i,k}^2 + (hi_{i,k} - h_i + 2h_k)^2} - (hi_{i,k} - h_i + 2h_k) \right]$$

$$\begin{aligned}
U_4 &= \beta \left[\sqrt{D_{i,k}^2 + (hi_{i,k} + h_i + 2h_k)^2} - (hi_{i,k} + h_i + 2h_k) \right] \\
V_4 &= \beta \left[\sqrt{D_{i,k}^2 + (hi_{i,k} + h_i + 2h_k)^2} + (hi_{i,k} + h_i + 2h_k) \right] \\
W_1 &= \beta \left[\sqrt{D_{i,k}^2 + hi_{i,k}^2} - hi_{i,k} \right] & Y_1 &= \beta \left[\sqrt{D_{i,k}^2 + hi_{i,k}^2} + hi_{i,k} \right] \\
W_2 &= \beta \left[\sqrt{D_{i,k}^2 + (hi_{i,k} + h_k)^2} - (hi_{i,k} + h_k) \right] \\
Y_2 &= \beta \left[\sqrt{D_{i,k}^2 + (hi_{i,k} + h_k)^2} + (hi_{i,k} + h_k) \right] \\
W_3 &= \beta \left[\sqrt{D_{i,k}^2 + (hi_{i,k} + 2h_k)^2} - (hi_{i,k} + 2h_k) \right] \\
Y_3 &= \beta \left[\sqrt{D_{i,k}^2 + (hi_{i,k} + 2h_k)^2} + (hi_{i,k} + 2h_k) \right]
\end{aligned}$$

The symbol $hi_{i,i}$ in equation 15.14 is the height of the $i^{th}+1$ dipole above the nearest end of its own image, and with $i=k$ is obtained from

$$hi_{i,k} = H_i + H_k - h_k \quad (15.15)$$

The off-diagonal mutual impedances between the dipoles and the images ($ZI_{i,k}$) are found using equation 15.13, except the $Q(x)$ arguments are those given for equation 15.14, but with $SD_{i,k}$ replaced by $hi_{i,k}$ from equation 15.15.

The function $Q(x)$ given by equation 15.9 is defined in terms of sine [$Si(x)$] and cosine [$Ci(x)$] integrals. Mathcad is incapable of evaluating $Si(x)$ and $Ci(x)$ directly, so a series expansion and polynomial approximation are written into the Mathcad code for both the sine and cosine integrals to evaluate the functions $Q(x)$. The arguments for $Q(x)$ are always real, so it is unnecessary to find $Si(x)$ and $Ci(x)$ expressions valid for complex numbers. For arguments less than one, $Si(x)$ and $Ci(x)$ are evaluated by series expansions given by [Ref 9: p. 232]

$$Si(x) = \sum_{n=0}^{\infty} \frac{(-1)^n x^{2n+1}}{(2n+1)(2n+1)!} \quad (15.16)$$

$$Ci(x) = \gamma + \ln(x) + \sum_{n=1}^{\infty} \frac{(-1)^n x^{2n}}{(2n)(2n)!} \quad (15.17)$$

where $\gamma = 0.5772156649$

For arguments greater than one, $Si(x)$ and $Ci(x)$ are defined in terms of two auxiliary functions, $f(x)$ and $g(x)$ given by [Ref 9: p. 233]

$$f(x) = \frac{1}{x} \left(\frac{x^8 + a_1 x^6 + a_2 x^4 + a_3 x^2 + a_4}{x^8 + b_1 x^6 + b_2 x^4 + b_3 x^2 + b_4} \right) + \epsilon(x) \quad (15.18)$$

where $|\epsilon(x)| < 5 \cdot 10^{-7}$

$a_1 = 38.027264$	$b_1 = 40.021433$
$a_2 = 265.187033$	$b_2 = 322.624911$
$a_3 = 335.677320$	$b_3 = 570.236280$
$a_4 = 38.102495$	$b_4 = 157.105423$

$$g(x) = \frac{1}{x^2} \left(\frac{x^8 + a_1 x^6 + a_2 x^4 + a_3 x^2 + a_4}{x^8 + b_1 x^6 + b_2 x^4 + b_3 x^2 + b_4} \right) + \epsilon(x) \quad (15.19)$$

where $|\epsilon(x)| < 3 \cdot 10^{-7}$

$a_1 = 42.242855$	$b_1 = 48.196927$
$a_2 = 302.757865$	$b_2 = 482.485984$
$a_3 = 352.018498$	$b_3 = 1114.978885$
$a_4 = 21.821899$	$b_4 = 449.690326$

The sine and cosine integral functions are then defined in terms of these auxiliary functions by [Ref 9: p. 232]

$$Si(x) = \frac{\pi}{2} - f(x) \cos(x) - g(x) \sin(x) \quad (15.20)$$

$$Ci(x) = f(x) \sin(x) - g(x) \cos(x) \quad (15.21)$$

In addition to the mutual impedance matrices, it is necessary to calculate the short circuit admittance matrix to determine the elemental current distribution. The short circuit admittance matrix is given by [Ref 10: p. 321]

$$[Y] = \begin{bmatrix} Y_{0,0} & Y_{0,1} & 0 & 0 & 0 & . & . & 0 \\ Y_{1,0} & Y_{1,1} & Y_{1,2} & 0 & 0 & . & . & 0 \\ 0 & Y_{2,1} & Y_{2,2} & Y_{2,3} & 0 & . & . & . \\ 0 & 0 & Y_{3,2} & Y_{3,3} & Y_{3,4} & . & . & . \\ . & . & . & . & . & . & . & . \\ 0 & 0 & 0 & . & . & Y_{(N-2),(N-3)} & Y_{(N-2),(N-2)} & Y_{(N-2),(N-1)} \\ 0 & 0 & 0 & . & . & 0 & Y_{(N-1),(N-2)} & Y_{(N-1),(N-1)} \end{bmatrix} \quad (15.22)$$

where the diagonal terms are given by

$$Y_{0,0} = -jY_0 \cot(\beta d_0) \quad \text{and} \quad Y_{(N-1),(N-1)} = Y'_T - jY_0 \cot(\beta d_{N-1})$$

and for $0 < n < N-1$:

$$Y_{n,n} \dots Y_{(N-2),(N-2)} = -jY_0 (\cot(\beta d_{n-1}) + \csc(\beta d_n))$$

and the off diagonal terms are given by

$$Y_{(n-1),n} = Y_{n,(n-1)} = -jY_0 \csc(\beta d_{n-1})$$

The term Y_0 is the characteristic admittance of the transmission line given by the input (ADM), and Y'_T is given by

$$Y'_T = Y_0 \frac{\cos\left(\beta \frac{h_{N-1}}{2}\right) + jY_0 Z_T \sin\left(\beta \frac{h_{N-1}}{2}\right)}{Y_0 Z_T \cos\left(\beta \frac{h_{N-1}}{2}\right) + j \sin\left(\beta \frac{h_{N-1}}{2}\right)} \quad (15.23)$$

where Z_T is the termination impedance input (TIMP).

The ground conductivity relative to the operating frequency (σ_{rel}) is then computed by [Ref 6: p. 640]

$$\sigma_{rel} = \frac{\sigma}{\omega \epsilon_r \epsilon_0} = \frac{18000 \sigma}{f_{Mhz} \epsilon_r} \quad (15.24)$$

to determine which equation to use for the array's current distribution. A surface with a relative conductivity greater than 20 is considered to be highly conductive relative to the transmitted frequency and the current distribution is given by [Ref 10: p. 342]

$$[IB] = \{[U] + [Y][Z] + [Y][ZI]\}^{-1} [IREF] \quad (15.25)$$

where [U] is the N X N identity matrix. The entries of the [IB] matrix are the base currents of the dipole elements. The matrix [IREF] represents the input current to which the [IB] distribution is referenced. Since the current input is only to the feed at the center of the first element, and since the input current is sinusoidal with a maximum of unity, [IREF] is a 1 X N matrix with a one as the first entry and N-1 zeroes in the remaining positions.

For surfaces with a relative conductivity of less than 20, the mutual impedances due to the images are neglected and the current distribution is given by

$$[IB] = \{[U] + [Y][Z]\}^{-1} [IREF] \quad (15.26)$$

The electric field equations are referenced to the current maxima values for the dipole elements, [I], which are obtained from the [IB] matrix using [Ref 6: p. 209]

$$I_i = \frac{IB_i}{\sin(\beta h_i)} \quad (15.27)$$

The mutual impedance calculations are not valid when any element length is an exact integer multiple of the wavelength. When this occurs, there is a singularity error in the mutual impedance calculations, and it is necessary to vary the frequency such that no element is an exact integer multiple of the wavelength. The change required is only one or two percent, and the predicted radiation parameters are still a good estimate of those for the original frequency.

The electric field for the vertical log-periodic array is obtained for each individual dipole in a manner analogous to that used for the vertical dipole discussed in Chapter 4. The equations for the individual elements are combined into a single expression for the array's total electric field by the *array factor*. The array factor for the vertical log-periodic array is [Ref 6 p. 222]

$$A + jB = \sum_{i=0}^{N-1} I_i e^{j\beta H_i \cos(\theta)} [\cos[\beta h_i \cos(\theta)] - \cos(\beta h_i)] \cdot \quad (15.28)$$

$$\left[1 + e^{-j2\beta H_i \cos(\theta)} \left(\Gamma_v + (1 - \Gamma_v) F_e \left(\sin^2(\theta) - \frac{\sqrt{n^2 - \sin^2(\theta)}}{n^2} \cos(\theta) \right) \right) \right]$$

$$e^{j\beta Y_i \sec(\alpha_2 + \alpha_3) [\cos(\theta) \sin(\alpha_2 + \alpha_3) + \sin(\theta) \cos(\alpha_2 + \alpha_3) \sin(\phi)]}$$

where Y_i is the y coordinate of the $i_{th}+1$ dipole given by

$$Y_i = \left(\sum_{n=0}^{i-1} d_n \right) \sin(\Psi) \quad (15.29)$$

The first two terms inside the brackets of equation 15.28 represent the space wave, the third term represents the surface wave, and I_i is the current term for each element based on a sinusoidal current input with a maximum of unity. The array factor is combined with the element factor to find the expression for the total radiated electric field given by

$$E_{\theta} = \frac{j60e^{-j\beta R}}{R} \frac{A+jB}{\sin(\theta)} \quad (15.30)$$

The requested inputs are used to calculate the following variables using a constant ϕ of $\phi=0$ and $\phi=\pi/2$ for 312 discrete values of θ which are equally incremented from $-\pi/2$ to $\pi/2$:

h_i half-length of the $i^{th}+1$ dipole (meters)
 H_i height of the $i^{th}+1$ dipole (meters)
 Y_i y coordinate of the $i^{th}+1$ dipole
 I_i current for the $i^{th}+1$ dipole
 λ_s wavelength of the operational frequency (meters)
 β free space wavenumber for operational frequency
 n index of refraction
 P_e complex numerical distance for vertical polarization
 Γ_v vertical reflection coefficient
 F_e vertical surface wave attenuation factor

The calculated variables are used to evaluate the far-field space wave and surface wave for the discrete values of θ with $\phi=0$ and $\phi=\pi/2$. The space wave and surface wave results are combined for corresponding values of θ to obtain the total radiated electric field distribution for the $\phi=0$ and $\phi=\pi/2$ vertical planes. The space wave, surface wave, and total electric field results are then normalized with respect to the maximum field intensity of each, and the normalized magnitudes are plotted for each discrete θ to depict the radiation patterns. The Mathcad vertical log-periodic dipole array

application computes the space wave, surface wave, and total electric field radiation patterns and radiation parameters in the $\phi=0$ and $\phi=\pi/2$ vertical planes.

The variables corresponding to the selected elevation angle index (w) are used to evaluate the radiated electric field components for the space wave and surface wave at the fixed elevation angle (θ_w) as ϕ varies from 0 to 2π in 312 equal increments. The horizontal radiation patterns are then plotted for the space wave, surface wave, and total radiated electric field just as those for the vertical planes.

Equations 3.8 and 3.9 are used to integrate equation 15.30 over the hemispherical Gaussian surface above the ground plane at a fixed radius (R) from the array to find total average radiated power (P_{rad}). With the discrete values of the electric field and total average radiated power determined, the Mathcad application predicts the following radiation characteristics from the equations in Chapter 3.

R_{rad} radiation resistance (Ohms)
 D_0 directivity
 EIRP.....effective radiated isotropic power (Watts)
 A_{max} maximum theoretical effective area (square meters)
 l_{max} maximum theoretical effective length (meters)
 P_e numerical distance (vertical polarization, $\theta=90^\circ$)
 P_m numerical distance (horizontal polarization, $\theta=90^\circ$)
 Angle_{max} .elevation angle of maximum directive gain (degrees)

The directivity (D_0), effective isotropic radiated power (EIRP), maximum theoretical effective area (A_{max}), maximum theoretical effective length (l_{max}), and the elevation angle of maximum directive gain (Angle_{max}) are all determined for both the $\phi=0$ and $\phi=\pi/2$ vertical planes.

As an example, the Mathcad vertical log-periodic array application was executed with the following inputs:

number of elements	12
length of first dipole	3.246 meters
length of second dipole	3.732 meters
first separation distance	1.096 meters
radius of first element	0.00325 meters
height of antenna feed	8.0 meters
frequency	$10 \cdot 10^6$ Hertz
distance from the antenna	3000 meters
relative dielectric constant	4
ground conductivity	$1 \cdot 10^{-3}$
characteristic admittance	1/450 Mhos
termination impedance	0 Ohms
angle from vertical to array axis	90°
elevation angle index	285 ($\approx 17^\circ$)

Figures 15.2 through 15.7 are the space wave and surface wave radiation patterns in the $\phi=0$ and $\phi=\pi/2$ vertical planes, and the designated horizontal plane for this example.

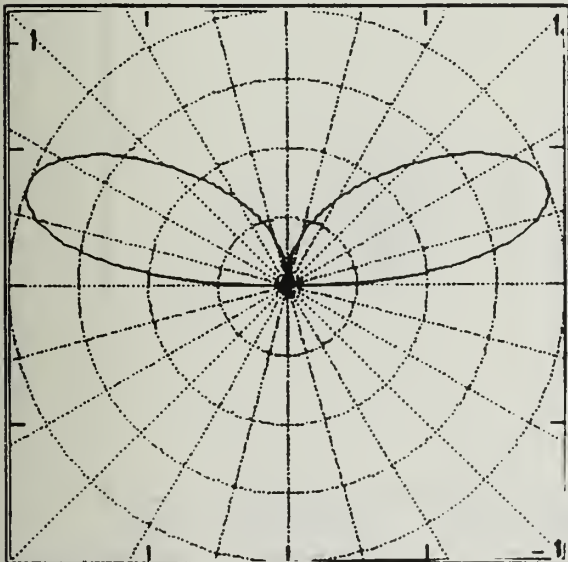


FIGURE 15.2: Vertical log-periodic space wave radiation pattern for $\phi=0$ vertical plane.

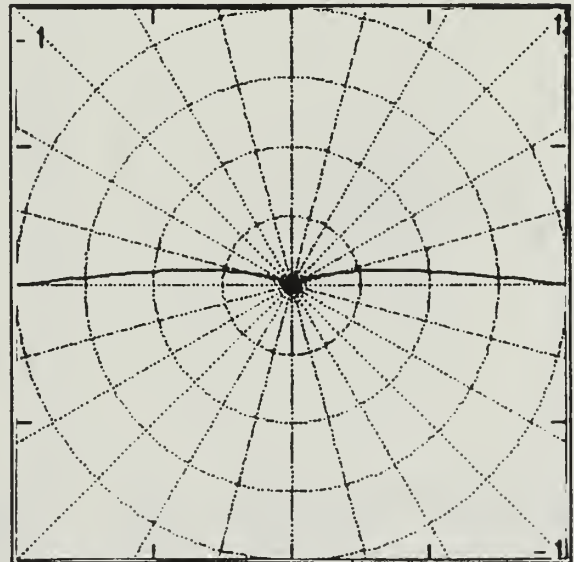


FIGURE 15.3: Vertical log-periodic surface wave radiation pattern for $\phi=0$ vertical plane.

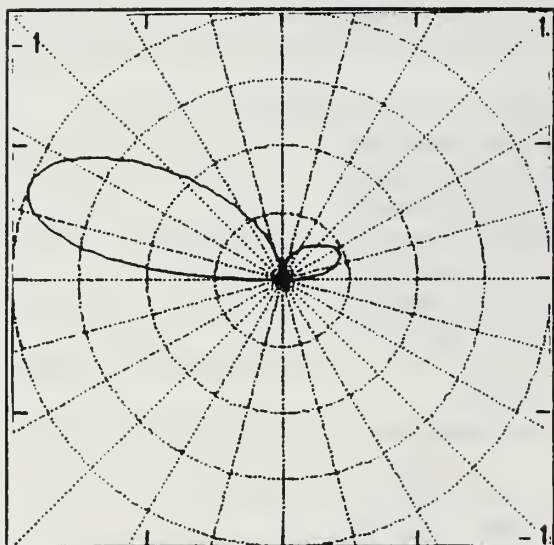


FIGURE 15.4: Vertical log-periodic space wave radiation pattern for $\phi=\pi/2$ vertical plane.

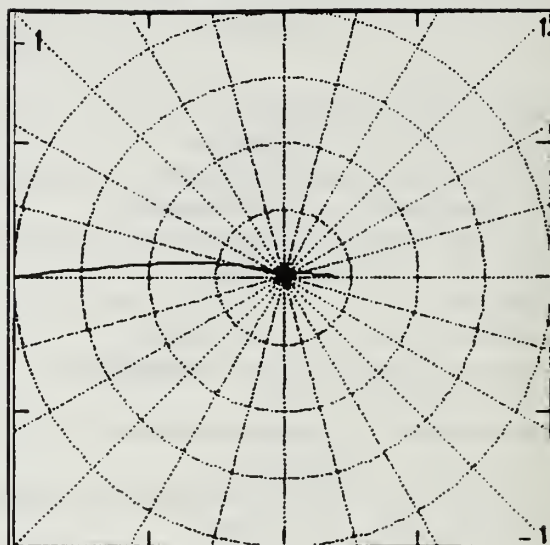


FIGURE 15.5: Vertical log-periodic surface wave radiation pattern for $\phi=\pi/2$ vertical plane.

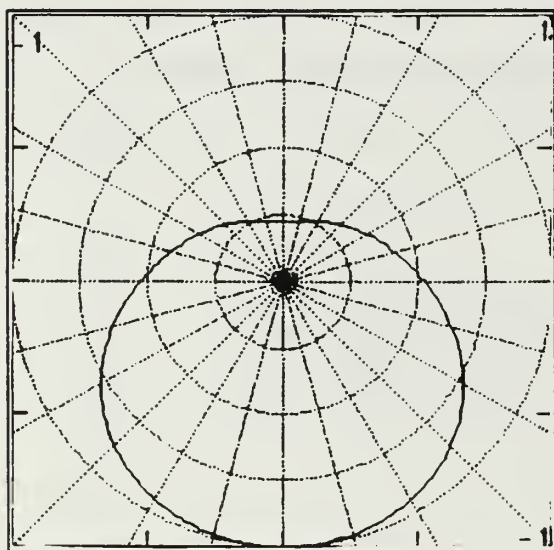


FIGURE 15.6: Vertical log-periodic space wave radiation pattern for horizontal plane.

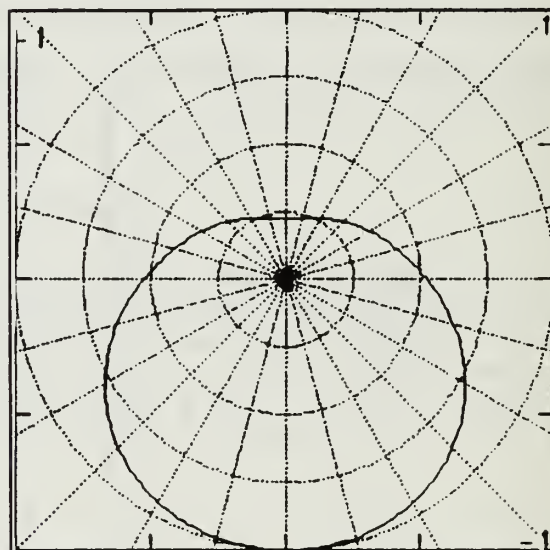


FIGURE 15.7: Vertical log-periodic surface wave radiation pattern for horizontal plane.

The following radiation parameters were predicted by the Mathcad application for a sinusoidal current input of one Amp.

Total power radiated (Watts)	37.967
Radiation resistance (Ohms)	75.934
Numerical distance (vertical)	57.126

	<u>$\phi=0$</u>	<u>$\phi=\pi/2$</u>
Directivity	3.415	12.176
EIRP (Watts)	129.656	462.272
Max eff area (sq meters)	244.578	872.012
Max eff length (meters)	14.038	26.506
Angle _{max} (degrees)	21.71	21.14

These results are consistent with expectations for this particular configuration. Appendix D contains computer hardcopies of additional example calculations for the vertical log-periodic dipole array and compares predicted radiation parameters to those expected based on previous calculations.

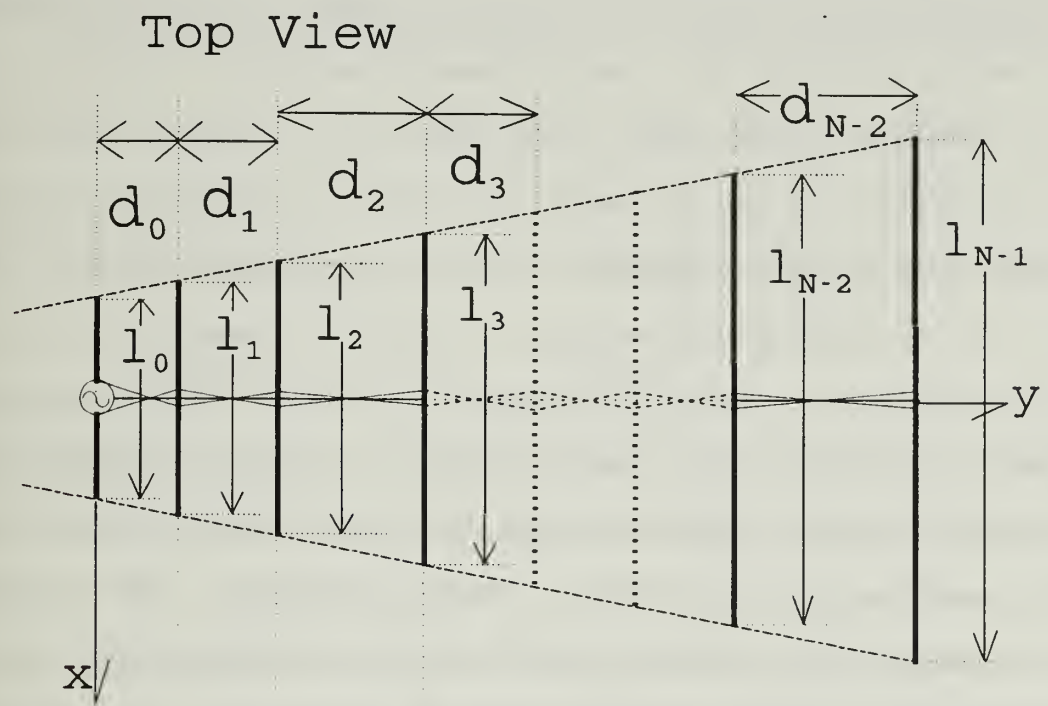
XVI. THE HORIZONTALLY POLARIZED LOG-PERIODIC DIPOLE ARRAY

The orientation of the horizontally polarized log-periodic dipole array is depicted in Figure 16.1, where N is the number of dipoles, n is an index equal to $0, 1, 2, \dots, N-1$, l_n is the length of the $n^{\text{th}}+1$ dipole, d_n is the distance between the $n^{\text{th}}+1$ and $n^{\text{th}}+2$ dipole elements, H_0 is the height of the antenna feed above ground, H_n is the height of the $n^{\text{th}}+1$ dipole, Ψ is the angle between the vertical axis and the array's center axis, α is the angle between the array's center axis and the lines which connect the tips of the elements, R is the radial coordinate, θ is the elevation coordinate, and ϕ is the azimuth coordinate.

The Mathcad application for the horizontally polarized log-periodic array requires the following inputs:

Nnumber of dipole elements
 l_0length of the shortest dipole (meters)
 l_1length of the second shortest dipole (meters)
 d_0distance between first two elements (meters)
 rad_0radius of the shortest dipole (meters)
 H_0feed height above ground plane (meters)
 Ψangle from vertical axis to array axis (degrees)
 f_soperational frequency (Hertz)
 Rdistance from array (meters)
 ϵ_rrelative dielectric constant of ground plane
 σconductivity of ground plane
 welevation angle index (from Table 3.2)
 ADMtransmission line characteristic admittance
 TIMPtermination impedance connected to longest dipole

The user inputs the frequency for which the radiation parameters discussed in Chapter 3 are computed. The lengths



Horizontal Log-Periodic Orientation

FIGURE 16.1: Spatial orientation of the horizontally polarized log-periodic dipole array for its corresponding Mathcad application.

of the first two elements (l_0 and l_1) are used to calculate the log-periodic relationship (τ) given by [Ref 10: p. 317]

$$\tau = \frac{l_n}{l_{n+1}} \quad (n=0, 1, 2, \dots, N-2, N-1) \quad (16.1)$$

The remaining element lengths (l_2 to l_{N-1}) are then found from

$$l_{n+1} = \frac{l_n}{\tau} \quad (16.2)$$

As noted in equation 16.1, indices start at zero instead of 1, so the index simply refers to the index-plus-one position in terms of successive values for a given parameter. This is to maintain continuity with Mathcad which also indexes from zero. The dipole half-lengths (h_n) are found from $l_n/2$. The radius of the first element (rad_0) is used to find remaining radii by substituting rad_n and rad_{n+1} for l_n and l_{n+1} into equation 16.2. The angle between the vertical axis and array axis (Ψ) can be between 0° and 90° , and α is found from [Ref 10: p. 319]

$$\frac{d_n}{h_{n+1}} = (1-\tau) \cot(\alpha) \quad (16.3)$$

which can be written as

$$\alpha = \tan^{-1} \left[\frac{(1-\tau) h_{n+1}}{d_n} \right] \quad (16.4)$$

The remaining separations (d_1 to d_{N-2}) are found from equation 16.3. Feed height (H_0) can be greater than or equal to zero. Distance from the array (R) must meet the far-field requirements of Chapter 3.C. The elevation angle index (w) sets the θ coordinate for which a horizontal radiation pattern is

determined. Table 3.2 lists possible indices and their corresponding elevation angles from $.57^\circ$ to 89.1° in increments of about 2.3° . Indices between those listed can be used to interpolate a better estimate of a desired elevation. The termination impedance (TIMP) is assumed to be connected to the array's center axis opposite the feed at a distance of $h_{N-1}/2$ from the last element. Typical termination impedances are the transmission line's matched impedance (complex conjugate) or a short circuit (zero). The characteristic admittance (ADM) is just the inverse of the transmission line's characteristic impedance. If computed lengths, separations and radii are not desired, they can be entered manually on page two of the application. Consult a Mathcad manual to be certain the entries are made correctly.

The open circuit impedance matrices are calculated to determine the current distribution among the dipole elements. The matrix of mutual impedances between dipole elements is represented as

$$[Z] = \begin{bmatrix} Z_{0,0} & Z_{0,1} & Z_{0,2} & \cdot & \cdot & \cdot & \cdot & Z_{0,(N-1)} \\ Z_{1,0} & Z_{1,1} & Z_{1,2} & \cdot & \cdot & \cdot & \cdot & Z_{1,(N-1)} \\ \cdot & \cdot & \cdot & \cdot & \cdot & \cdot & \cdot & \cdot \\ \cdot & \cdot & \cdot & \cdot & \cdot & \cdot & \cdot & \cdot \\ Z_{(N-1),0} & Z_{(N-1),1} & Z_{(N-1),2} & \cdot & \cdot & \cdot & \cdot & Z_{(N-1),(N-1)} \end{bmatrix} \quad (16.5)$$

Each main diagonal term ($Z_{i,i}$) is the self-impedance of the $i^{\text{th}}+1$ dipole. The off-diagonal terms ($Z_{i,k}$) are the mutual impedances between the $i^{\text{th}}+1$ and $k^{\text{th}}+1$ elements. Subscripts i and k are matrix indices ($0,1,2,\dots,N-1$).

The matrix of open circuit mutual impedances between the actual dipoles and their images is represented as

$$[ZI] = \begin{bmatrix} ZI_{0,0} & ZI_{0,1} & ZI_{0,2} & \dots & ZI_{0,(N-1)} \\ ZI_{1,0} & ZI_{1,1} & ZI_{1,2} & \dots & ZI_{1,(N-1)} \\ \cdot & \cdot & \cdot & \dots & \cdot \\ \cdot & \cdot & \cdot & \dots & \cdot \\ ZI_{(N-1),0} & ZI_{(N-1),1} & ZI_{(N-1),2} & \dots & ZI_{(N-1),(N-1)} \end{bmatrix} \quad (16.6)$$

The main diagonal terms ($ZI_{i,i}$) are the mutual impedances between the i^{th} element and its image, and the off-diagonal terms ($ZI_{i,k}$) are the mutual impedances between the i^{th} element and the image of the k^{th} element.

The main diagonal self-impedance terms of equation 16.5 are found from [Ref 6: pp. 205-206]

$$Z_{i,i} = \frac{60}{1 - \cos(2\beta h_i)} \left[e^{-j2\beta h_i} [Q(U_0) - 2Q(U_1)] \right] \quad (16.7)$$

$$+ e^{j2\beta h_i} [Q(V_0) - 2Q(V_1)] + 2[Q(U'_0) - Q(U_1) - Q(V_1)] + 2Q(U'_0)[1 + \cos(2\beta h_i)] \quad]$$

$$\text{where } Q(x) = Ci(x) - j \cdot Si(x) = \int_{\infty}^x \frac{\cos(y)}{y} dy - j \int_0^x \frac{\sin(y)}{y} dy \quad (16.8)$$

$$U_0 = \beta \left[\sqrt{2rad_i^2 + 4h_i^2} - 2h_i \right] \quad U'_0 = \sqrt{2}\beta rad_i \quad V_0 = \beta \left[\sqrt{2rad_i^2 + 4h_i^2} + 2h_i \right]$$

$$U_1 = \beta \left[\sqrt{2rad_i^2 + h_i^2} - h_i \right] \quad V_1 = \beta \left[\sqrt{2rad_i^2 + h_i^2} + h_i \right]$$

The off-diagonal mutual impedance terms of equation 16.5 are given by [Ref 11]

$$Z_{i,k} = Z_{k,i} = \frac{60}{\cos[\beta(h_i - h_k)] - \cos[\beta(h_i + h_k)]} \cdot \quad (16.9)$$

$$\begin{aligned} & \left[e^{-j\beta(h_i + h_k)} [Q(U_0) - Q(U_1) - Q(U_2)] + e^{j\beta(h_i + h_k)} [Q(V_0) - Q(V_1) - Q(V_2)] \right. \\ & + e^{-j\beta(h_i - h_k)} [Q(U'_0) - Q(V_1) - Q(U_2)] + e^{j\beta(h_i - h_k)} [Q(V'_0) - Q(U_1) - Q(V_2)] \\ & \left. + 2Q(\beta D_{i,k}) (\cos[\beta(h_i - h_k)] + \cos[\beta(h_i + h_k)]) \right] \end{aligned}$$

where $Q(x) = Ci(x) - j \cdot Si(x) = \int_{-\infty}^x \frac{\cos(y)}{y} dy - j \cdot \int_0^x \frac{\sin(y)}{y} dy$

$$\begin{aligned} U_0 &= \beta \left[\sqrt{D_{i,k}^2 + (h_i + h_k)^2} - (h_i + h_k) \right] & V_0 &= \beta \left[\sqrt{D_{i,k}^2 + (h_i + h_k)^2} + (h_i + h_k) \right] \\ U'_0 &= \beta \left[\sqrt{D_{i,k}^2 + (h_i - h_k)^2} - (h_i - h_k) \right] & V'_0 &= \beta \left[\sqrt{D_{i,k}^2 + (h_i - h_k)^2} + (h_i - h_k) \right] \\ U_1 &= \beta \left[\sqrt{D_{i,k}^2 + h_i^2} - h_i \right] & V_1 &= \beta \left[\sqrt{D_{i,k}^2 + h_i^2} + h_i \right] \\ U_2 &= \beta \left[\sqrt{D_{i,k}^2 + h_k^2} - h_k \right] & V_2 &= \beta \left[\sqrt{D_{i,k}^2 + h_k^2} + h_k \right] \end{aligned}$$

The $D_{i,k}$ terms are the distances between the $i^{th}+1$ and $k^{th}+1$ dipole elements and are given by

$$D_{i,k} = D_{k,i} = \sum_{n=i}^{k-1} d_n \quad (16.10)$$

For ground planes with high conductivities relative to the operating frequency, it is necessary to compute equation 16.6, [ZI], for the mutual impedances between the elements and their images. The mutual impedance terms ($ZI_{i,k}$) are given by equation 16.9 with the $Q(x)$ arguments

$$\begin{aligned} U_0 &= \beta \left[\sqrt{di_{i,k}^2 + (h_i + h_k)^2} - (h_i + h_k) \right] & V_0 &= \beta \left[\sqrt{di_{i,k}^2 + (h_i + h_k)^2} + (h_i + h_k) \right] \\ U'_0 &= \beta \left[\sqrt{di_{i,k}^2 + (h_i - h_k)^2} - (h_i - h_k) \right] & V'_0 &= \beta \left[\sqrt{di_{i,k}^2 + (h_i - h_k)^2} + (h_i - h_k) \right] \\ U_1 &= \beta \left[\sqrt{di_{i,k}^2 + h_i^2} - h_i \right] & V_1 &= \beta \left[\sqrt{di_{i,k}^2 + h_i^2} + h_i \right] \\ U_2 &= \beta \left[\sqrt{di_{i,k}^2 + h_k^2} - h_k \right] & V_2 &= \beta \left[\sqrt{di_{i,k}^2 + h_k^2} + h_k \right] \end{aligned}$$

The $di_{i,k}$ entries are the distance from the $i^{th}+1$ dipole to the image of the $k^{th}+1$ dipole and are given by

$$di_{i,k} = \sqrt{(H_i + H_k)^2 + (D_{i,k} \sin(\Psi))^2} \quad (16.11)$$

The function $Q(x)$ given by equation 16.8 is defined in terms of sine $[Si(x)]$ and cosine $[Ci(x)]$ integrals. Mathcad is incapable of evaluating $Si(x)$ and $Ci(x)$ directly, so a series expansion and polynomial approximation are written into the Mathcad code for both the sine and cosine integrals to evaluate the functions $Q(x)$. The arguments for $Q(x)$ are always real, so it is unnecessary to find $Si(x)$ and $Ci(x)$ expressions valid for complex numbers.

For arguments greater than one, two auxiliary functions, $f(x)$ and $g(x)$ are determined by [Ref 9: p. 233]

$$f(x) = \frac{1}{x} \left(\frac{x^8 + a_1 x^6 + a_2 x^4 + a_3 x^2 + a_4}{x^8 + b_1 x^6 + b_2 x^4 + b_3 x^2 + b_4} \right) + \epsilon(x) \quad (16.12)$$

$$\text{where} \quad |\epsilon(x)| < 5 \cdot 10^{-7}$$

$a_1 = 38.027264$	$b_1 = 40.021433$
$a_2 = 265.187033$	$b_2 = 322.624911$
$a_3 = 335.677320$	$b_3 = 570.236280$
$a_4 = 38.102495$	$b_4 = 157.105423$

$$g(x) = \frac{1}{x^2} \left(\frac{x^8 + a_1 x^6 + a_2 x^4 + a_3 x^2 + a_4}{x^8 + b_1 x^6 + b_2 x^4 + b_3 x^2 + b_4} \right) + \epsilon(x) \quad (16.13)$$

$$\text{where} \quad |\epsilon(x)| < 3 \cdot 10^{-7}$$

$a_1 = 42.242855$	$b_1 = 48.196927$
$a_2 = 302.757865$	$b_2 = 482.485984$
$a_3 = 352.018498$	$b_3 = 1114.978885$
$a_4 = 21.821899$	$b_4 = 449.690326$

and $Si(x)$ and $Ci(x)$ are defined in terms of these auxiliary functions by [Ref 9: p. 232]

$$Si(x) = \frac{\pi}{2} - f(x) \cos(x) - g(x) \sin(x) \quad (16.14)$$

$$Ci(x) = f(x) \sin(x) - g(x) \cos(x) \quad (16.15)$$

For arguments less than one, $Si(x)$ and $Ci(x)$ are evaluated by series expansions given by [Ref 9: p. 232]

$$Si(x) = \sum_{n=0}^{\infty} \frac{(-1)^n x^{2n+1}}{(2n+1)(2n+1)!} \quad (16.16)$$

$$Ci(x) = \gamma + \ln(x) + \sum_{n=1}^{\infty} \frac{(-1)^n x^{2n}}{(2n)(2n)!} \quad (16.17)$$

where $\gamma = 0.5772156649$

It is also necessary to calculate the short circuit admittance matrix to find the elemental current distribution.

The admittance matrix is given by [Ref 10: p. 321]

$$[Y] = \begin{bmatrix} Y_{0,0} & Y_{0,1} & 0 & 0 & 0 & . & . & 0 \\ Y_{1,0} & Y_{1,1} & Y_{1,2} & 0 & 0 & . & . & 0 \\ 0 & Y_{2,1} & Y_{2,2} & Y_{2,3} & 0 & . & . & . \\ 0 & 0 & Y_{3,2} & Y_{3,3} & Y_{3,4} & . & . & . \\ . & . & . & . & . & . & . & . \\ 0 & 0 & 0 & . & . & Y_{(N-2),(N-3)} & Y_{(N-2),(N-2)} & Y_{(N-2),(N-1)} \\ 0 & 0 & 0 & . & . & 0 & Y_{(N-1),(N-2)} & Y_{(N-1),(N-1)} \end{bmatrix} \quad (16.18)$$

where the diagonal terms are given by

$$Y_{0,0} = -jY_0 \cot(\beta d_0) \quad \text{and} \quad Y_{(N-1),(N-1)} = Y'_T - jY_0 \cot(\beta d_{N-1})$$

and for $0 < n < N-1$:

$$Y_{n,n} \dots Y_{(N-2),(N-2)} = -jY_0 (\cot(\beta d_{n-1}) + \cos(\beta d_n))$$

and the off diagonal terms are given by

$$Y_{(n-1),n} = Y_{n,(n-1)} = -jY_0 \csc(\beta d_{n-1})$$

The term Y_0 is the transmission line's characteristic admittance obtained from the input (ADM), and Y'_T is given by

$$Y'_T = Y_0 \frac{\cos\left(\beta \frac{h_{N-1}}{2}\right) + jY_0 Z_T \sin\left(\beta \frac{h_{N-1}}{2}\right)}{Y_0 Z_T \cos\left(\beta \frac{h_{N-1}}{2}\right) + j \sin\left(\beta \frac{h_{N-1}}{2}\right)} \quad (16.19)$$

The ground conductivity relative to the operating frequency (σ_{rel}) is then computed by [Ref 6: p. 640]

$$\sigma_{rel} = \frac{\sigma}{\omega \epsilon_r \epsilon_0} = \frac{18000 \sigma}{f_{Mhz} \epsilon_r} \quad (16.20)$$

A surface with a relative conductivity greater than 20 is considered to be highly conductive relative to the frequency and the current distribution is given by [Ref 10: p. 342]

$$[IB] = \{ [U] + [Y] [Z] + [Y] [ZI] \}^{-1} [IREF] \quad (16.21)$$

where $[U]$ is the $N \times N$ identity matrix. The entries of the $[IB]$ matrix are the base currents of the dipole elements. The matrix $[IREF]$ represents the input current to which the $[IB]$ distribution is referenced. Since the current is input only to the feed at the center of the first element, and since the input current is sinusoidal with a maximum of unity, $[IREF]$ is a $1 \times N$ matrix with a one as the first entry and $N-1$ zeroes in the remaining positions.

For surfaces with a relative conductivity of less than 20, the mutual impedances due to the image elements are neglected and the current distribution is given by

$$[IB] = \{ [U] + [Y] [Z] \}^{-1} [IREF] \quad (16.22)$$

The electric field equations are referenced to the current maxima values for the dipole elements, [I], which are obtained from the [IB] matrix using [Ref 6 p.209]

$$I_i = \frac{IB_i}{\sin(\beta h_i)} \quad (16.23)$$

The mutual impedance calculations are not valid when any element length is an exact integer multiple of the wavelength. When this occurs, there is a singularity error in the mutual impedance calculations, and it is necessary to vary the frequency such that no element is exactly an integer multiple of the wavelength. The change required is only a percent or two, and the predicted radiation parameters are still a good estimate of those for the original frequency.

The electric field for the horizontal log-periodic array is obtained for each individual dipole in a manner analogous to that for the vertical dipole discussed in Chapter 4. The equations for the individual elements are combined into a single expression for the array's total electric field by the array factors. The array factors for the horizontal log-periodic array are [Ref 6: p. 214]

$$S_\theta = \sum_{i=0}^{N-1} I_i [\cos[\beta h_i (\cos(\theta) \cos(\Psi) + \sin(\theta) \sin(\Psi) \sin(\phi))] - \cos(\beta h_i)]$$

$$\left[1 + \Gamma_v e^{-j2\beta H_i \cos(\theta)} + (1 - \Gamma_v) F_e e^{-j2\beta H_i \cos(\theta)} \frac{\sqrt{n^2 - \sin^2(\theta)}}{n^2 \cos(\theta)} \right] \quad (16.24)$$

$$\left(\sin^2(\theta) - \frac{\sqrt{n^2 - \sin^2(\theta)}}{n^2} \cos(\theta) \right) \left] e^{j\beta Y_i \csc(\Psi) [\cos(\theta) \cos(\Psi) + \sin(\theta) \sin(\Psi) \sin(\phi)]} \right.$$

$$S_{\phi} = \sum_{i=0}^{N-1} I_i [\cos[\beta h_i (\cos(\theta) \cos(\Psi) + \sin(\theta) \sin(\Psi) \sin(\phi))] - \cos(\beta h_i)]$$

$$\left[1 + \Gamma_h e^{-j2\beta H_i \cos(\theta)} + (1 - \Gamma_h) F_m e^{-j2\beta H_i \cos(\theta)} \right] \cdot \quad (16.25)$$

$$e^{j\beta Y_i \csc(\Psi) [\cos(\theta) \cos(\Psi) + \sin(\theta) \sin(\Psi) \sin(\phi)]}$$

where Y_i is the y coordinate of the $i_{th}+1$ dipole given by

$$Y_i = \left(\sum_{n=0}^{i-1} d_n \right) \sin(\Psi) \quad (16.26)$$

The first two terms inside the brackets of equations 16.24 and 16.25 represent the space wave, the third term represents the surface wave, and I_i is the current term for each element based on a sinusoidal current input with a maximum of unity. The array factors are combined with the element factors to find the total radiated electric field equation, and the expression for the radiated electric field distribution of the horizontal log-periodic dipole array is given by [Ref 6: p. 213]

$$E_{\theta} = \frac{-j60e^{-j\beta R}}{R} \frac{\cos(\phi) \cos(\theta)}{1 - \sin^2(\theta) \cos^2(\phi)} S_{\theta} \quad (16.27)$$

$$E_{\phi} = \frac{j60e^{-j\beta R}}{R} \frac{\sin(\phi)}{1 - \sin^2(\theta) \cos^2(\theta)} S_{\phi} \quad (16.28)$$

The requested inputs are used to calculate the following variables using a constant ϕ of $\phi=0$ and $\phi=\pi/2$ for 312 discrete values of θ which are equally incremented from $-\pi/2$ to $\pi/2$:

h_i half-length of the $i^{th}+1$ dipole (meters)
 H_i height of the $i^{th}+1$ dipole (meters)
 Y_i y coordinate of the $i^{th}+1$ dipole
 I_i current for the $i^{th}+1$ dipole
 λ_s wavelength of the operational frequency (meters)
 β free space wavenumber for operational frequency
 n index of refraction
 P_e complex numerical distance (vertical polarization)
 P_m complex numerical distance (horizontal polarization)
 Γ_v vertical reflection coefficient
 Γ_h horizontal reflection coefficient
 F_e vertical surface wave attenuation factor
 F_m horizontal surface wave attenuation factor

The calculated variables are used to evaluate the radiated far-field space wave and surface wave for the discrete values of θ with $\phi=0$ and $\phi=\pi/2$. The space wave and surface wave results are combined for corresponding values of θ to obtain the total radiated electric field distribution for the $\phi=0$ and $\phi=\pi/2$ vertical planes. The space wave, surface wave, and total electric field results are then normalized with respect to the maximum field intensity of each, and the normalized magnitudes are plotted for each discrete θ to depict the radiation patterns. The Mathcad horizontal log-periodic dipole array application computes the space wave, surface wave, and total electric field radiation patterns and radiation parameters in the $\phi=0$ and $\phi=\pi/2$ vertical planes.

The variables corresponding to the selected elevation angle index (w) are used to evaluate the radiated electric field components for the space wave and surface wave at the fixed elevation angle (θ_w) as ϕ varies from 0 to 2π in 312 equal increments. The horizontal radiation patterns are then plotted for the space wave, surface wave, and total radiated electric field just as those for the vertical planes.

Equations 3.8 and 3.9 are used to integrate equations 16.27 and 16.28 over the hemispherical Gaussian surface above the ground plane at a fixed radius (R) from the array to find total average radiated power (P_{rad}). With the discrete values of the electric field and total average radiated power determined, the Mathcad application predicts the following radiation characteristics from the equations in Chapter 3:

R_{rad} radiation resistance (Ohms)
 D_0 directivity
EIRP.....effective radiated isotropic power (Watts)
 A_{max} maximum theoretical effective area (square meters)
 l_{max} maximum theoretical effective length (meters)
 P_e numerical distance (vertical polarization, $\theta=90^\circ$)
 P_m numerical distance (horizontal polarization, $\theta=90^\circ$)
 $Angle_{max}$.elevation angle of maximum directive gain (degrees)

The directivity (D_0), effective isotropic radiated power (EIRP), maximum theoretical effective area (A_{max}), maximum theoretical effective length (l_{max}), and elevation angle of the directivity ($Angle_{max}$) are determined for both vertical planes.

As an example, the Mathcad horizontal log-periodic array application was executed with the following inputs:

number of elements	12
length of first dipole	3.246 meters
length of second dipole	3.732 meters
first separation distance	1.096 meters
radius of first element	0.00325 meters
height of antenna feed	8.0 meters
frequency	$20 \cdot 10^6$ Hertz
distance from the antenna	3000 meters
relative dielectric constant	4
ground conductivity	$5 \cdot 10^{-3}$
characteristic admittance	1/450
termination impedance	0 Ohms
angle from vertical to array axis	90°
elevation angle index	285 ($\approx 17^\circ$)

Figures 16.2 through 16.7 are the space wave and surface wave radiation patterns in the $\phi=0$ and $\phi=\pi/2$ vertical planes, and the designated horizontal plane for this example.

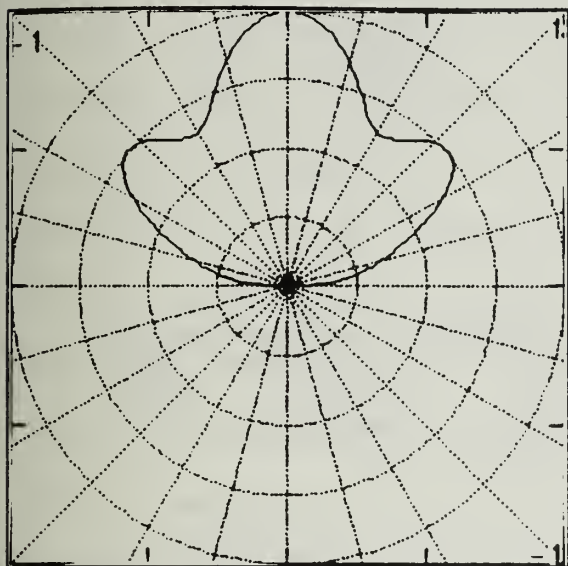


FIGURE 16.2: Horizontal log-periodic space wave radiation pattern for $\phi=0$ vertical plane.

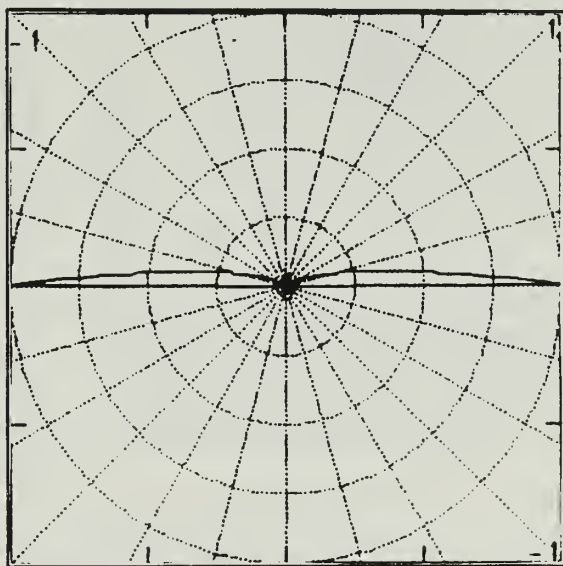


FIGURE 16.3: Horizontal log-periodic surface wave radiation pattern for $\phi=0$ vertical plane.

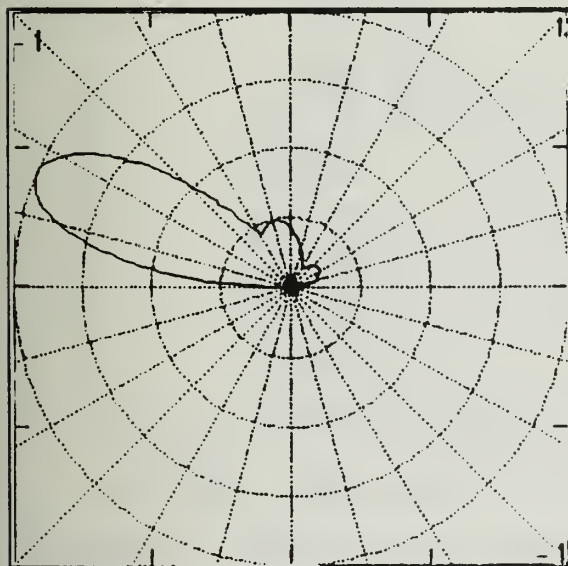


FIGURE 16.4: Horizontal log-periodic space wave radiation pattern for $\phi=\pi/2$ vertical plane.

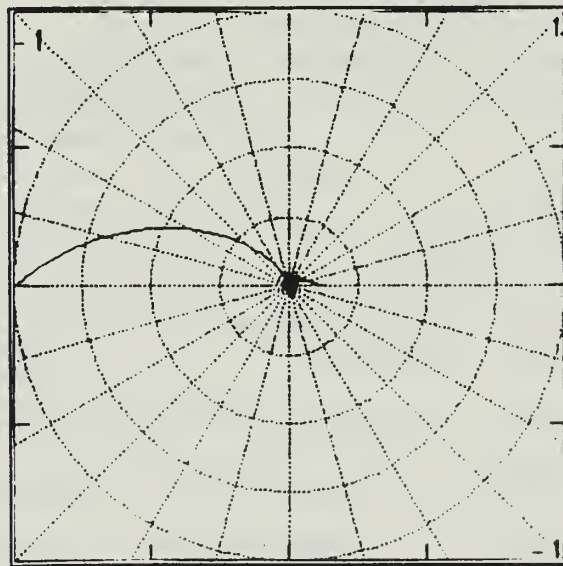


FIGURE 16.5: Horizontal log-periodic surface wave radiation pattern for $\phi=\pi/2$ vertical plane.

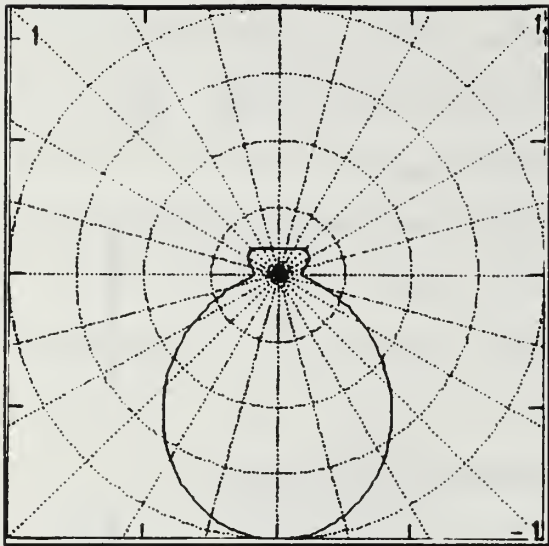


FIGURE 16.6: Horizontal log-periodic space wave radiation pattern for horizontal plane.

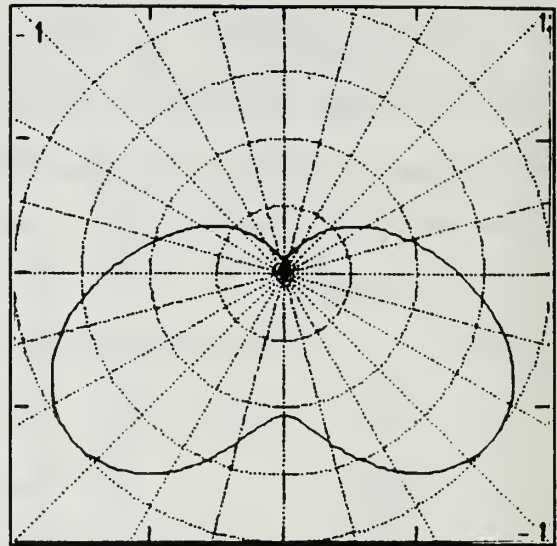


FIGURE 16.7: Horizontal log-periodic surface wave radiation pattern for horizontal plane.

The following radiation parameters were predicted by the Mathcad application for a sinusoidal current input of one Amp. The predicted radiation parameters are:

Total power radiated (Watts)	75.546
Radiation resistance (Ohms)	151.092
Numerical distance (vertical)	93.742
Numerical distance (horizontal)	3398.15

	$\phi=0$	$\phi=\pi/2$
Directivity	0.838	18.384
EIRP (Watts)	63.301	1388.82
Max eff area (sq meters)	15.003	329.159
Max eff length (meters)	4.904	22.971
Angle _{max} (degrees)	89.7	24.0

These results are consistent with expectations for this particular configuration. Appendix E contains computer hardcopies of additional example calculations for the horizontal log-periodic dipole array and compares predicted radiation parameters to those expected based on previous calculations.

XVII. THE HORIZONTAL YAGI-UDA ARRAY

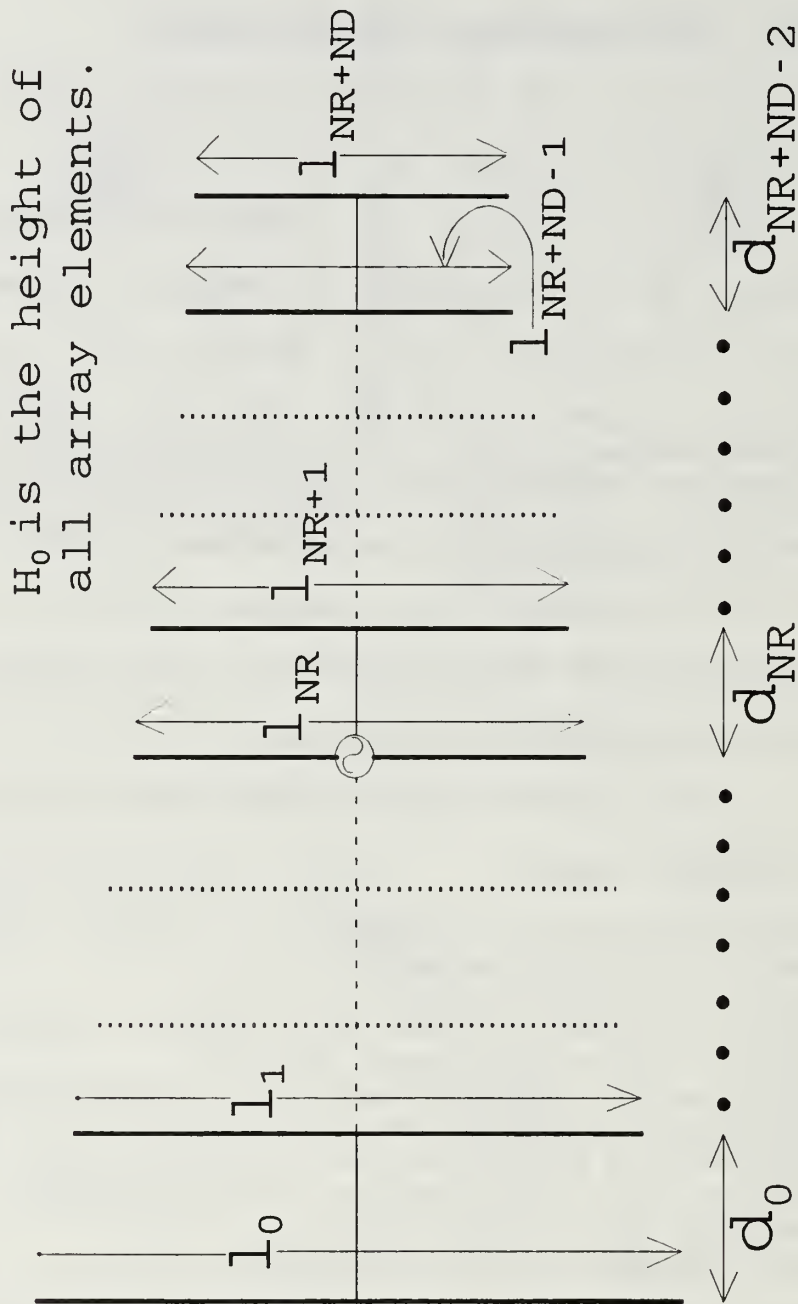
The orientation of the horizontal Yagi-Uda array is depicted in Figure 17.1, where l_{NR} is the length of the current driven element, NR is the number of parasitic reflector elements, ND is the number of parasitic director elements, n is an index equal to $0, 1, 2, \dots, NR+ND$, and l_n is the length of the $n^{th}+1$ element starting with the outermost reflector and counting consecutively toward the opposite end. The d_n terms are the separation distances between the $n^{th}+1$ and $n^{th}+2$ elements, H_0 is the height of all antenna elements above ground, R is the radial coordinate, θ is the elevation coordinate, and ϕ is the azimuth coordinate.

The Mathcad application for the horizontal Yagi-Uda array requires the following inputs:

NR.....number of reflector elements
ND.....number of director elements
 l_nlength of the $n^{th}+1$ element (meters)
 d_ndistance between $n^{th}+1$ and $n^{th}+2$ elements (meters)
 rad_nradius of the $n^{th}+1$ element (meters)
 H_0antenna height above ground plane (meters)
 f_soperational frequency (Hertz)
 Rdistance from array (meters)
 ϵ_rrelative dielectric constant of ground plane
 σconductivity of ground plane
 welevation angle index (from Table 3.2)

Unlike the log-periodic applications, all element lengths, radii, and separation distances must be input manually on page two of the application. Consult a Mathcad manual to be certain the entries are made correctly. The user

OVERHEAD VIEW



H_0 is the height of all array elements.

Horizontal Yagi-Uda Array Orientation

FIGURE 17.1: Spatial orientation of the horizontal Yagi-Uda array for its corresponding Mathcad application.

inputs the frequency for which the radiation parameters discussed in Chapter 3 are calculated. As noted in the first paragraph, indices start at zero instead of 1, so the index simply refers to the index-plus-one position in terms of successive values for a given parameter. This is to maintain continuity with Mathcad which also indexes from zero. The dipole half-lengths (h_n) are found from $l_n/2$. Antenna height (H_0) can be any value greater than or equal to zero, and the distance from the array (R) must meet the far-field requirements of Chapter 3.C. The elevation angle index (w) sets the θ coordinate for which a horizontal radiation pattern is determined. Table 3.2 lists possible indices and their corresponding elevation angles from $.57^\circ$ to 89.1° in increments of about 2.3° . Indices between those listed can be used to interpolate a better approximation of a desired elevation.

The open circuit impedance matrices are calculated to determine the current distribution among the dipole elements. The matrix of mutual impedances between the dipole elements is represented as

$$[Z] = \begin{bmatrix} Z_{0,0} & Z_{0,1} & Z_{0,2} & \cdot & \cdot & \cdot & \cdot & Z_{0,(N-1)} \\ Z_{1,0} & Z_{1,1} & Z_{1,2} & \cdot & \cdot & \cdot & \cdot & Z_{1,(N-1)} \\ Z_{2,0} & Z_{2,1} & Z_{2,2} & \cdot & \cdot & \cdot & \cdot & Z_{2,(N-1)} \\ \cdot & \cdot & \cdot & \cdot & \cdot & \cdot & \cdot & \cdot \\ \cdot & \cdot & \cdot & \cdot & \cdot & \cdot & \cdot & \cdot \\ \cdot & \cdot & \cdot & \cdot & \cdot & \cdot & \cdot & \cdot \\ Z_{(N-1),0} & Z_{(N-1),1} & Z_{(N-1),2} & \cdot & \cdot & \cdot & \cdot & Z_{(N-1),(N-1)} \end{bmatrix} \quad (17.1)$$

Each main diagonal term ($Z_{i,i}$) is the self impedance of the $i^{\text{th}}+1$ element. The off-diagonal terms ($Z_{i,k}$) are the mutual impedances between the $i^{\text{th}}+1$ and $k^{\text{th}}+1$ elements. Subscripts i and k are matrix indices ($0,1,2,\dots,NR+ND$).

The matrix of open circuit mutual impedances between the actual elements and their images is represented as

$$[ZI] = \begin{bmatrix} ZI_{0,0} & ZI_{0,1} & ZI_{0,2} & \dots & ZI_{0,(N-1)} \\ ZI_{1,0} & ZI_{1,1} & ZI_{1,2} & \dots & ZI_{1,(N-1)} \\ ZI_{2,0} & ZI_{2,1} & ZI_{2,2} & \dots & ZI_{2,(N-1)} \\ \vdots & \vdots & \vdots & \ddots & \vdots \\ ZI_{(N-1),0} & ZI_{(N-1),1} & ZI_{(N-1),2} & \dots & ZI_{(N-1),(N-1)} \end{bmatrix} \quad (17.2)$$

The main diagonal terms ($ZI_{i,i}$) are the mutual impedances between the $i^{\text{th}}+1$ element and its image, and the off-diagonal terms ($ZI_{i,k}$) are the mutual impedances between the $i^{\text{th}}+1$ element and the image of the $k^{\text{th}}+1$ element.

The main diagonal self-impedance terms of equation 17.1 are found from [Ref 6: pp. 205-206]

$$Z_{i,i} = \frac{60}{1 - \cos(2\beta h_i)} \left[e^{-j2\beta h_i} [Q(U_0) - 2Q(U_1)] \right] \quad (17.3)$$

$$+ e^{j2\beta h_i} [Q(V_0) - 2Q(V_1)] + 2[Q(U'_0) - Q(U_1) - Q(V_1)] + 2Q(U'_0)[1 + \cos(2\beta h_i)]]$$

$$\text{where } Q(x) = Ci(x) - j \cdot Si(x) = \int_{\infty}^x \frac{\cos(y)}{y} dy - j \cdot \int_0^x \frac{\sin(y)}{y} dy \quad (17.4)$$

$$U_0 = \beta \left[\sqrt{2rad_i^2 + 4h_i^2} - 2h_i \right] \quad U'_0 = \sqrt{2}\beta rad_i \quad V_0 = \beta \left[\sqrt{2rad_i^2 + 4h_i^2} + 2h_i \right]$$

$$U_1 = \beta \left[\sqrt{2rad_i^2 + h_i^2} - h_i \right] \quad V_1 = \beta \left[\sqrt{2rad_i^2 + h_i^2} + h_i \right]$$

The off-diagonal mutual impedance terms of equation 17.1 are given by [Ref 11]

$$Z_{i,k} = Z_{k,i} = \frac{60}{\cos [\beta (h_i - h_k)] - \cos [\beta (h_i + h_k)]} \quad (17.5)$$

$$\begin{aligned} & [e^{-j\beta (h_i + h_k)} [Q(U_0) - Q(U_1) - Q(U_2)] + e^{j\beta (h_i + h_k)} [Q(V_0) - Q(V_1) - Q(V_2)] \\ & + e^{-j\beta (h_i - h_k)} [Q(U'_0) - Q(V_1) - Q(U_2)] + e^{j\beta (h_i - h_k)} [Q(V'_0) - Q(U_1) - Q(V_2)] \\ & + 2Q(\beta D_{i,k}) (\cos [\beta (h_i - h_k)] + \cos [\beta (h_i + h_k)])] \end{aligned}$$

where $Q(x) = Ci(x) - j \cdot Si(x) = \int_{\infty}^x \frac{\cos(y)}{y} dy - j \int_0^x \frac{\sin(y)}{y} dy$

$$U_0 = \beta \left[\sqrt{D_{i,k}^2 + (h_i + h_k)^2} - (h_i + h_k) \right] \quad V_0 = \beta \left[\sqrt{D_{i,k}^2 + (h_i + h_k)^2} + (h_i + h_k) \right]$$

$$U'_0 = \beta \left[\sqrt{D_{i,k}^2 + (h_i - h_k)^2} - (h_i - h_k) \right] \quad V'_0 = \beta \left[\sqrt{D_{i,k}^2 + (h_i - h_k)^2} + (h_i - h_k) \right]$$

$$U_1 = \beta \left[\sqrt{D_{i,k}^2 + h_i^2} - h_i \right] \quad V_1 = \beta \left[\sqrt{D_{i,k}^2 + h_i^2} + h_i \right]$$

$$U_2 = \beta \left[\sqrt{D_{i,k}^2 + h_k^2} - h_k \right] \quad V_2 = \beta \left[\sqrt{D_{i,k}^2 + h_k^2} + h_k \right]$$

The $D_{i,k}$ terms are the distances between the $i_{th}+1$ and $k_{th}+1$ dipole elements and are given by

$$D_{i,k} = D_{k,i} = \sum_{n=i}^{k-1} d_n \quad (17.6)$$

The mutual impedances between the actual elements and their images must also be computed to determine the elemental current distribution. The mutual impedance terms of equation 17.2 ($ZI_{i,k}$) are given by equation 17.5, except the $D_{i,k}$ terms in

the $Q(x)$ arguments are replaced by $di_{i,k}$ terms which represent the distance from the $i^{th}+1$ element to the image of the $k^{th}+1$ element and are given by [Ref 6: pp. 205-208]

$$di_{i,k} = \sqrt{H_0^2 + D_{i,k}^2} \quad (17.7)$$

The function $Q(x)$ given by equations 17.4 is defined in terms of sine $[Si(x)]$ and cosine $[Ci(x)]$ integrals. Mathcad is incapable of evaluating $Si(x)$ and $Ci(x)$ directly, so a series expansion and polynomial approximation are written into the Mathcad code for both the sine and cosine integrals to evaluate the functions $Q(x)$. The arguments for $Q(x)$ are always real, so it is unnecessary to find $Si(x)$ and $Ci(x)$ expressions valid for complex numbers.

For arguments less than one, $Si(x)$ and $Ci(x)$ are evaluated by series expansions given by [Ref 9: p. 232]

$$Si(x) = \sum_{n=0}^{\infty} \frac{(-1)^n x^{2n+1}}{(2n+1)(2n+1)!} \quad (17.8)$$

$$Ci(x) = \gamma + \ln(x) + \sum_{n=1}^{\infty} \frac{(-1)^n x^{2n}}{(2n)(2n)!} \quad (17.9)$$

$$\text{where } \gamma = 0.5772156649$$

For arguments greater than one, $Si(x)$ and $Ci(x)$ are expressed in terms of auxiliary functions, $f(x)$ and $g(x)$, given by Ref 9: p.232]

$$Si(x) = \frac{\pi}{2} - f(x) \cos(x) - g(x) \sin(x) \quad (17.10)$$

$$Ci(x) = f(x) \sin(x) - g(x) \cos(x) \quad (17.11)$$

The auxiliary functions $f(x)$ and $g(x)$ are evaluated by the polynomial approximations [Ref 9: p. 233]

$$f(x) = \frac{1}{x} \left(\frac{x^8 + a_1 x^6 + a_2 x^4 + a_3 x^2 + a_4}{x^8 + b_1 x^6 + b_2 x^4 + b_3 x^2 + b_4} \right) + \epsilon(x) \quad (17.12)$$

$$\text{where} \quad |\epsilon(x)| < 5 \cdot 10^{-7}$$

$$\begin{aligned} a_1 &= 38.027264 & b_1 &= 40.021433 \\ a_2 &= 265.187033 & b_2 &= 322.624911 \\ a_3 &= 335.677320 & b_3 &= 570.236280 \\ a_4 &= 38.102495 & b_4 &= 157.105423 \end{aligned}$$

$$g(x) = \frac{1}{x^2} \left(\frac{x^8 + a_1 x^6 + a_2 x^4 + a_3 x^2 + a_4}{x^8 + b_1 x^6 + b_2 x^4 + b_3 x^2 + b_4} \right) + \epsilon(x) \quad (17.13)$$

$$\text{where} \quad |\epsilon(x)| < 3 \cdot 10^{-7}$$

$$\begin{aligned} a_1 &= 42.242855 & b_1 &= 48.196927 \\ a_2 &= 302.757865 & b_2 &= 482.485984 \\ a_3 &= 352.018498 & b_3 &= 1114.978885 \\ a_4 &= 21.821899 & b_4 &= 449.690326 \end{aligned}$$

When the mutual impedances are found, the array's base current distribution is computed from [Ref 10 p. 258-259]

$$[IB] = \{ [Z] + \Gamma_{h,0} [ZI] \}^{-1} [VREF] \quad (17.14)$$

where

$$\Gamma_{h,0} = \Gamma_h \mid_{\theta=0} = \frac{1-n}{1+n}$$

and n is the complex index of refraction. The entries of the $[IB]$ matrix are the base currents of the dipole elements, and $[VREF]$ is the voltage matrix to which the $[IB]$ distribution is referenced. Since the Yagi-Uda has only one driven element (corresponding to the NR^{th} index), and since a sinusoidal voltage response with a maximum of unity is assumed across the

input terminals, [VREF] is a 1 X NR+ND matrix with a 1 as the NRth entry and NR+ND-1 zeroes in the remaining positions. The electric field equations are referenced to the current maxima values for the dipole elements, [I], which are determined from the [IB] matrix using [Ref 6 p. 209]

$$I_i = \frac{IB_i}{\sin(\beta h_i)} \quad (17.15)$$

The mutual impedance calculations are not valid when any element length is an exact integer multiple of the wavelength. When this occurs, there is a singularity error in the mutual impedance calculations, and it is necessary to vary the frequency such that no element is exactly an integer multiple of the wavelength. The change required is only a percent or two, and the predicted radiation parameters are still a good estimate of those for the original frequency.

The electric field for the horizontal Yagi-Uda array is obtained for each element in a manner analogous to that used for the vertical dipole in Chapter 4. The equations for the individual elements are simplified into two expressions for the array's electric field components by the array factor. The Yagi-Uda's array factor is given by [Ref 6: p. 204]

$$S = \sum_{i=0}^{NR+ND-1} I_i [\cos[\beta h_i (\sin(\theta) \sin(\phi))] - \cos(\beta h_i)] e^{j\beta Y_i \sin(\theta) \sin(\phi)} \quad (17.16)$$

where Y_i is the y coordinate for the $i^{th}+1$ element given by

$$Y_i = \sum_{n=0}^{i-1} d_n \quad (17.17)$$

The array factor is multiplied by the element factors to find the equations for the total radiated electric field distribution of the horizontal Yagi-Uda array,

$$E_{\theta} = -j60 \frac{e^{-j\beta R}}{R} \frac{\cos(\phi)}{1 - \sin^2(\theta) \cos^2(\phi)} e^{j\beta H_0 \cos(\theta)} (S) \cdot \quad (17.18)$$

$$\left[\cos(\theta) (1 - \Gamma_v e^{-j2\beta H_0 \cos(\theta)}) + (1 - \Gamma_v) F_e e^{-j2\beta H_0 \cos(\theta)} \right]$$

$$\frac{\sqrt{n^2 - \sin^2(\theta)}}{n^2} \left(\sin^2(\theta) - \frac{\sqrt{n^2 - \sin^2(\theta)}}{n^2} \cos(\theta) \right) \Bigg]$$

$$E_{\phi} = j60 \frac{e^{-j\beta R}}{R} \frac{\sin(\phi)}{1 - \sin^2(\theta) \cos^2(\theta)} e^{j\beta H_0 \cos(\theta)} (S) \cdot \quad (17.19)$$

$$\left[1 + \Gamma_h e^{-j2\beta H_0 \cos(\theta)} + (1 - \Gamma_h) F_m e^{-j2\beta H_0 \cos(\theta)} \right]$$

The first two terms inside the brackets of each equation are the space wave, the third terms are the surface wave, and I_i is the current term for each element based on a sinusoidal voltage across the input terminals with a maximum of unity.

The requested inputs are used to calculate the following variables using a constant ϕ of $\phi=0$ and $\phi=\pi/2$ for 312 discrete values of θ which are equally incremented from $-\pi/2$ to $\pi/2$:

- h_i half-length of the $i^{th}+1$ element (meters)
- Y_i y coordinate of the $i^{th}+1$ element
- I_i current for the $i^{th}+1$ element
- λ_s wavelength of the operational frequency (meters)
- β free space wavenumber for operational frequency
- n index of refraction
- P_e complex numerical distance (vertical polarization)
- P_m complex numerical distance (horizontal polarization)
- Γ_v vertical reflection coefficient
- Γ_h horizontal reflection coefficient
- F_e vertical surface wave attenuation factor
- F_m horizontal surface wave attenuation factor

The calculated variables are used to evaluate the far-field space wave and surface wave for the discrete values of θ with $\phi=0$ and $\phi=\pi/2$. The space wave and surface wave results are combined for corresponding values of θ to obtain the total radiated electric field distribution for the $\phi=0$ and $\phi=\pi/2$ vertical planes. The space wave, surface wave, and total electric field results are then normalized with respect to the maximum field intensity of each, and the normalized magnitudes are plotted for each discrete θ to depict the radiation patterns. The Mathcad horizontal Yagi-Uda array application computes the space wave, surface wave, and total electric field radiation patterns and radiation parameters in the $\phi=0$ and $\phi=\pi/2$ vertical planes.

The variables corresponding to the selected elevation angle index (w) are used to evaluate the radiated electric field components for the space wave and surface wave at the fixed elevation angle (θ_w) as ϕ varies from 0 to 2π in 312 equal increments. The horizontal radiation patterns are then plotted for the space wave, surface wave, and total radiated electric field just as those for the vertical planes.

Equations 3.8 and 3.9 are used to integrate equations 17.18 and 17.19 over the hemispherical Gaussian surface above the ground plane at a fixed radius (R) from the array to find total average radiated power (P_{rad}). Since the Yagi-Uda current distribution is referenced to a sinusoidal voltage input with a maximum of unity, the radiation resistance can not be

calculated from equation 3.10 as in previous applications. Instead, radiation resistance must be found with respect to the unity voltage input using

$$P_{rad} = \frac{|V|^2}{2R_{rad}} \quad \text{or} \quad R_{rad} = \frac{|V|^2}{2P_{rad}} \quad (17.20)$$

With the discrete values of the electric field and total average radiated power, the Mathcad application predicts the following radiation characteristics from Chapter 3:

R_{rad} radiation resistance (Ohms)
 D_0 directivity
 EIRP.....effective radiated isotropic power (Watts)
 A_{max} maximum theoretical effective area (square meters)
 l_{max} maximum theoretical effective length (meters)
 P_e numerical distance (vertical polarization, $\theta=90^\circ$)
 P_m numerical distance (horizontal polarization, $\theta=90^\circ$)
 $Angle_{max}$.elevation angle of maximum directive gain (degrees)

The directivity (D_0), effective isotropic radiated power (EIRP), maximum theoretical effective area (A_{max}), maximum theoretical effective length (l_{max}), and elevation angle of the directivity ($Angle_{max}$) are determined for both vertical planes.

As an example, the Mathcad horizontal Yagi-Uda array application was executed with the following inputs:

number of reflectors	1
number of directors	1
element lengths	15.6, 15, and 14 meters
element separations	7.5 and 6.5 meters
element radii	0.001, 0.001, and 0.001 meters
height of antenna	8.0 meters
frequency	$10 \cdot 10^6$ Hertz
distance from the antenna	3000 meters
relative dielectric constant	72
ground conductivity	4
elevation angle index	285 ($\approx 17^\circ$)

Figures 17.2 through 17.7 are the space wave and surface wave radiation patterns in the $\phi=0$ and $\phi=\pi/2$ vertical planes, and the designated horizontal plane for this example.

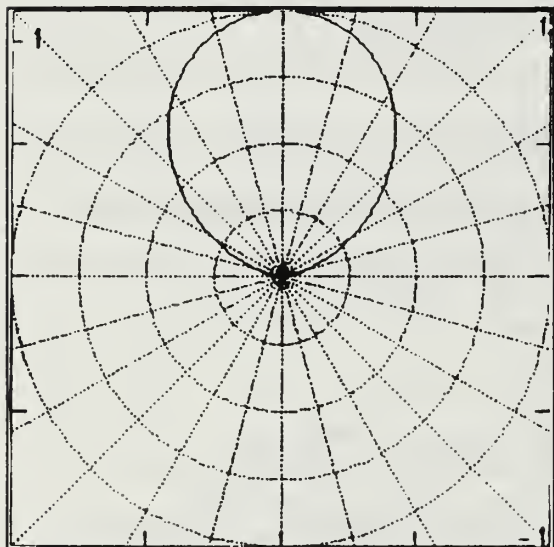


FIGURE 17.2: Horizontal Yagi-Uda space wave radiation pattern for $\phi=0$ vertical plane.

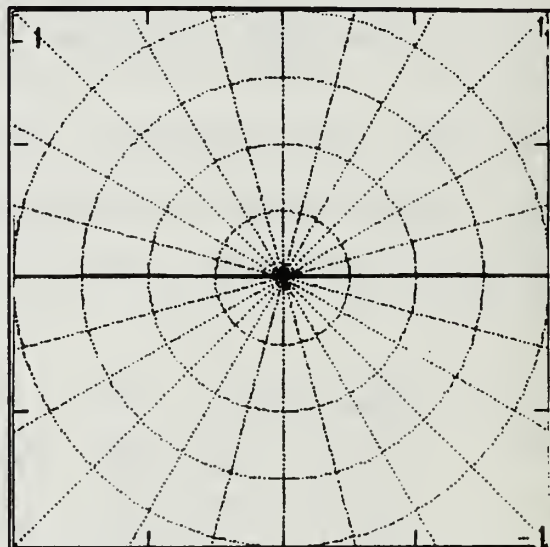


FIGURE 17.3: Horizontal Yagi-Uda surface wave radiation pattern for $\phi=0$ vertical plane.

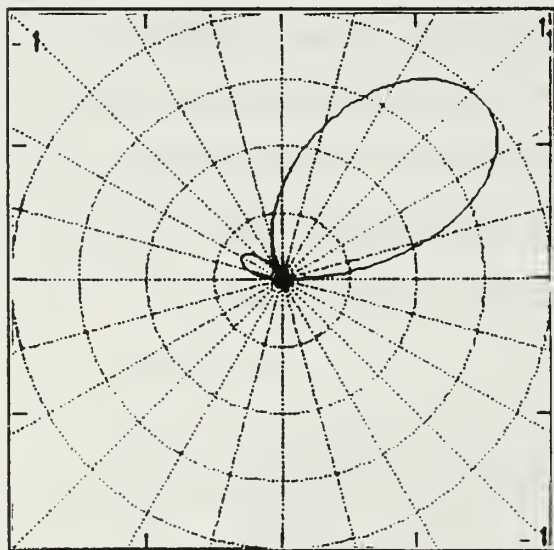


FIGURE 17.4: Horizontal Yagi-Uda space wave radiation pattern for $\phi=\pi/2$ vertical plane.

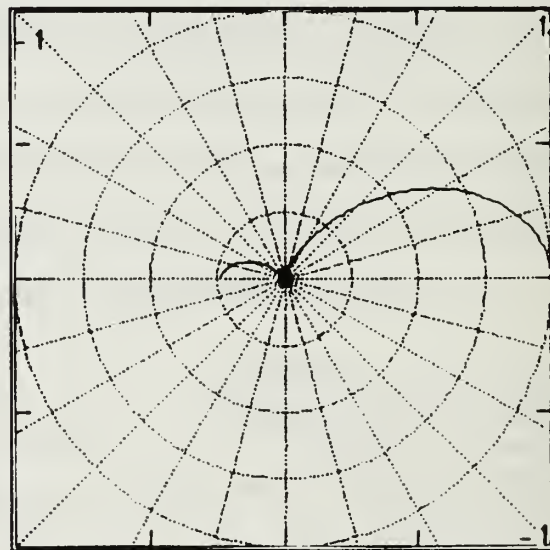


FIGURE 17.5: Horizontal Yagi-Uda surface wave radiation pattern for $\phi=\pi/2$ vertical plane.

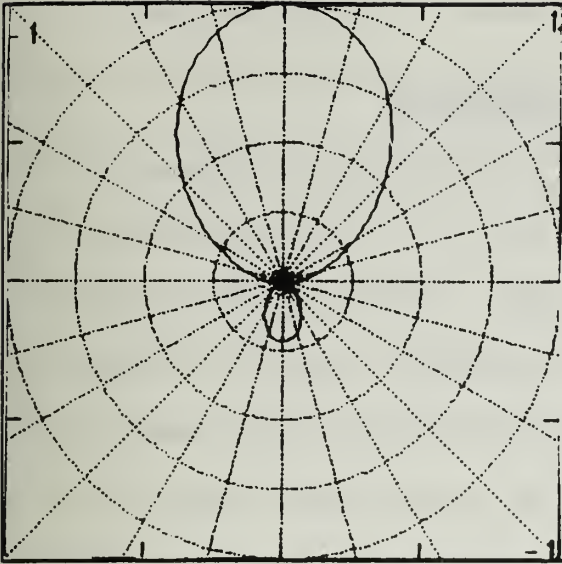


FIGURE 17.6: Horizontal Yagi-Uda space wave radiation pattern for horizontal plane.

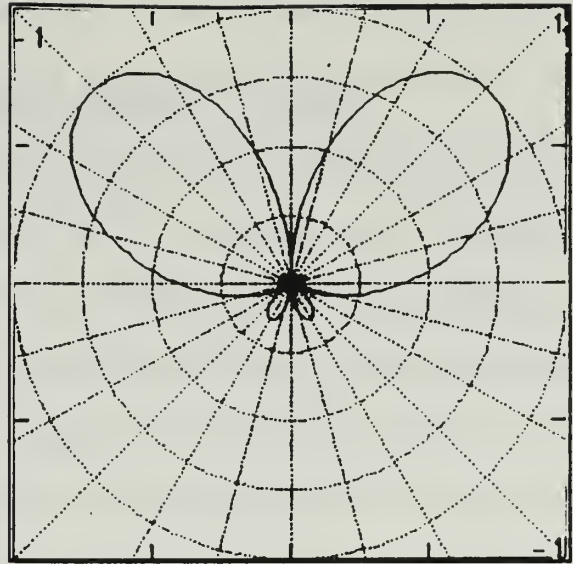


FIGURE 17.7: Horizontal Yagi-Uda surface wave radiation pattern for horizontal plane.

The predicted radiation parameters based on a one volt response across the input terminals are:

Total power radiated (Watts)	0.00482
Radiation resistance (Ohms)	103.760
Numerical distance (vertical)	0.04363
Numerical distance (horizontal)	$2.26 \cdot 10^6$

	$\phi=0$	$\phi=\pi/2$
Directivity	1.679	14.631
EIRP (Watts)	0.0081	0.0705
Max eff area (sq meters)	120.26	1047.9
Max eff length (meters)	11.506	33.966
Angle _{max} (degrees)	89.7	41.714

These results are consistent with expectations for this particular configuration. Appendix F contains computer hardcopies of additional example calculations for the horizontal Yagi-Uda array and compares predicted radiation parameters to those expected based on previous calculations.

XVIII. REMARKS AND CONCLUSION

This thesis is the culmination of nine months of research and computer programming. No new electric field equations were derived exclusively for this project. It was directed by NAVMARINTCEN prior to commencing that existing electric field equations would provide the basis for the radiation parameter predictions. The expressions used in this thesis are all previously derived by pioneers in antenna radiation theory such as Sommerfeld, Norton, Cox, King, Ma, and Walters. The equations are compiled here solely for the purpose of crediting the source references and to describe how the Mathcad code was assembled.

The accuracy of the predicted radiation characteristics is totally dependent upon the extent to which the equations used realistically model the actual radiated electric fields of the antennas. It is near impossible to obtain analytic results which accurately model an antenna's radiation characteristics in all cases. There are too many operational and environmental variables to obtain one general, all-purpose expression. Even if all possible variables could be accounted for in a single expression, computer processing times would be unacceptably long. The equations used herein are simple enough to be evaluated by Mathcad in a reasonable length of time, but the radiation parameter predictions are accurate enough to be useful for antenna analysis.

As addressed in appendices A-F, the equations presented in previous chapters and evaluated by the Mathcad applications provide radiation parameters consistent with expectations for the inputs which have been executed to date. All antenna configurations which have been computed exhibit radiation characteristics consistent with other computational programs and empirically obtained patterns and parameters. There is no way to test the accuracy of the Mathcad predictions other than empirical measurements for each antenna configuration, clearly a task beyond the scope and purpose of this report. However, adequate analysis of the Mathcad results has been provided to demonstrate that the applications provide very good estimates of antenna radiation parameters as a base level analysis tool.

Most of the applications have computations times under ten minutes. However, even with the simplified equations used by Mathcad, some of the applications can take upwards of two hours to compute on a 33 MHz 80386 PC. The applications for the rhombic, double rhomboid, and array (with more than four to five elements) antennas can take an exorbitantly long time for power calculations. For this reason, the applications should be run on the fastest PC available; a 50 MHz 80486 is preferable. Computation times can also be reduced by computing only the radiation patterns until it is determined which frequencies are of greatest interest. Then the average power calculations for those frequencies can be executed.

The Mathcad applications were written for NAVMARINTCEN to provide antenna analysts with the capability to predict radiation parameters based solely on antenna physical dimensions and ground properties. The Mathcad results computed thus far are consistent with expectations and are most likely providing accurate predictions of actual antenna radiation characteristics. Only extended use of the applications and empirical confirmation of results will prove out the accuracy of the Mathcad code. Results obtained thus far certainly justify continued use of the Mathcad code as an antenna analysis tool.

APPENDIX A:
VERTICAL DIPOLE ARRAY COMPUTER OUTPUT

This appendix contains computer hardcopies from the Mathcad vertical dipole application which show the input values and predicted radiation characteristics for two sample calculations. The configuration is a half-wave dipole at one quarter wavelength above soil ($\epsilon_r=10$ and $\sigma=10^{-2}$) for the first example and the same configuration above seawater ($\epsilon_r=72$ and $\sigma=4$) for the second. Reference 6 [p. 91] provides the radiation patterns and gain predictions from several sources for the configuration in the first example.

The elevation of maximum directive gain is slightly higher for the Mathcad output than for those given in reference 6, but the overall radiation patterns are very similar. The 4.17 (6.2 dB) value of directivity for Mathcad is quite a bit higher than the maximum gain values of about zero dB in reference 6. However, since a half-wave dipole has a free-space directivity of 1.64 (2.1 dB), one would expect the actual directivity to be closer to the Mathcad prediction because of the effect of the reflected wave (constructive and destructive interference) on the space wave, and the lower total average radiated power resulting from ground plane losses. The seawater example yields results consistent with expectations. With respect to the soil example, the seawater example's directivity is slightly higher due to a stronger reflected wave, and the surface wave is stronger at grazing angles ($\theta \approx 90^\circ$) due to higher conductivity.

VERTICAL DIPOLE

This application calculates far field radiation patterns and parameters associated with vertical thin-wire dipole antennas (diameter \ll wavelength). The antenna is mounted vertically along the z-axis in a rectangular coordinate system with the feed at the antenna's center at a set height above the surface. Required inputs are the antenna length, feed height above the surface, transmitted frequency, distance from the antenna, the conductivity and dielectric constant of the surface below the antenna. The planar earth model is assumed in predicting radiation patterns. Predicted operating frequencies assume that the antenna is a quarter-wavelength, half-wavelength, three-quarter-wavelength, or full-wavelength dipole. A sinusoidal current input with a maximum of unity is assumed. All radiation patterns are normalized with respect to the maximum electric field intensity transmitted by the antenna. Plotted radiation patterns are valid for any vertical plane passing through the antenna axis. The electric field magnitudes to which the Radiation Patterns are normalized are displayed below their respective plots. Polarization is vertical for all vertical dipoles.

Input the Dipole length in meters $l := 5$ $h := \frac{1}{2}$

Wavelengths and Frequencies

$$\lambda_1 := 4 \cdot l \quad \lambda_2 := 2 \cdot l \quad \lambda_3 := \frac{4 \cdot l}{3} \quad \lambda_4 := l$$

$$f_1 := \frac{c}{\lambda_1} \quad f_2 := \frac{c}{\lambda_2} \quad f_3 := \frac{c}{\lambda_3} \quad f_4 := \frac{c}{\lambda_4}$$

Possible Operating Frequencies (Hertz)

$$\frac{\lambda}{4} \text{ Dipole: } f_1 = 1.5 \cdot 10^7 \quad \frac{\lambda}{2} \text{ Dipole: } f_2 = 3 \cdot 10^7$$

$$\frac{3 \cdot \lambda}{4} \text{ Dipole: } f_3 = 4.5 \cdot 10^7 \quad \lambda \text{ Dipole: } f_4 = 6 \cdot 10^7$$

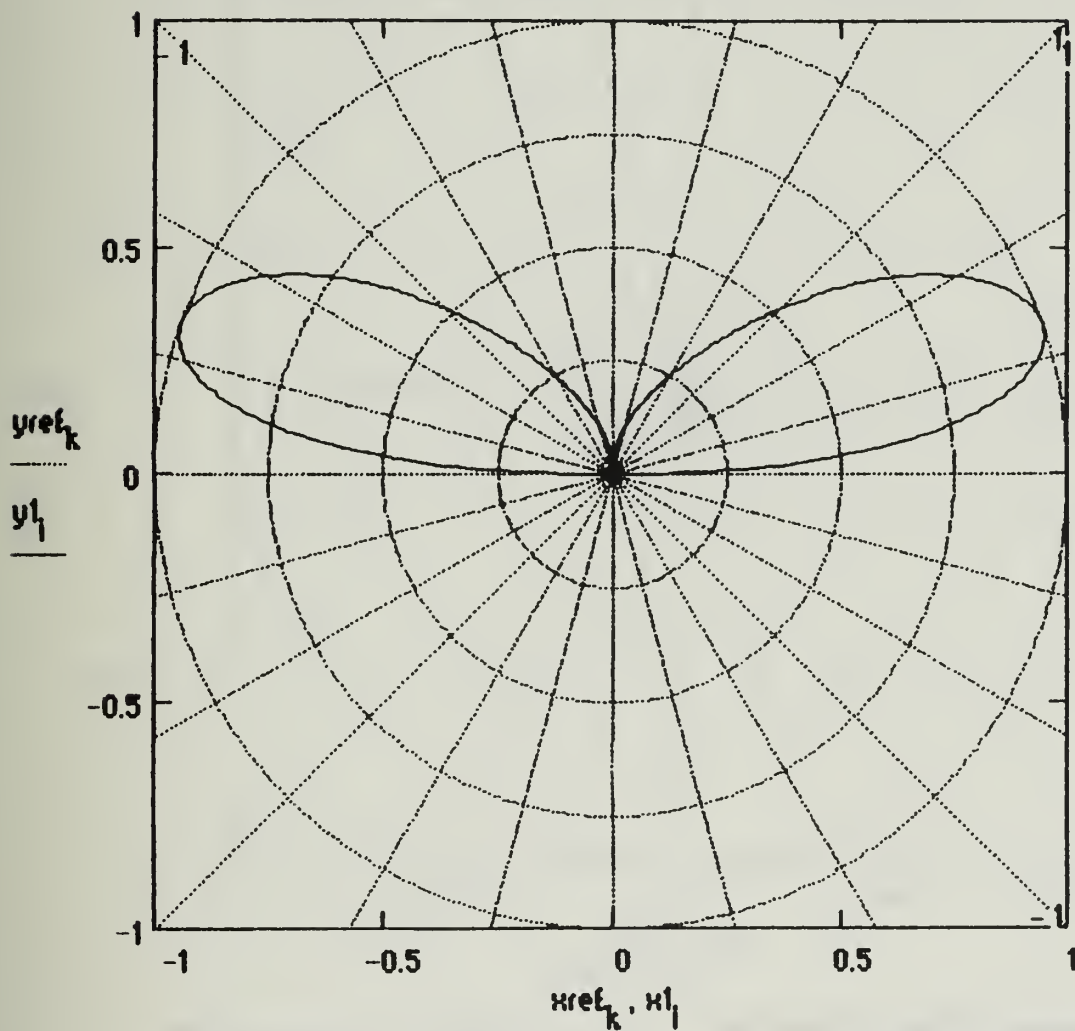
Input the operating Frequency (Hertz) $f_5 := 30 \cdot 10^6$ Input the Distance from the Antenna (meters) $R := 3000$

Input the ground Dielectric Constant $\epsilon_r := 10$ Input the ground Conductivity $\sigma := 10^{-2}$

Input the Height of the Antenna Feed (meters) $H_0 := 2.5$

Radiation Patterns valid for any Vertical Plane passing through the Antenna

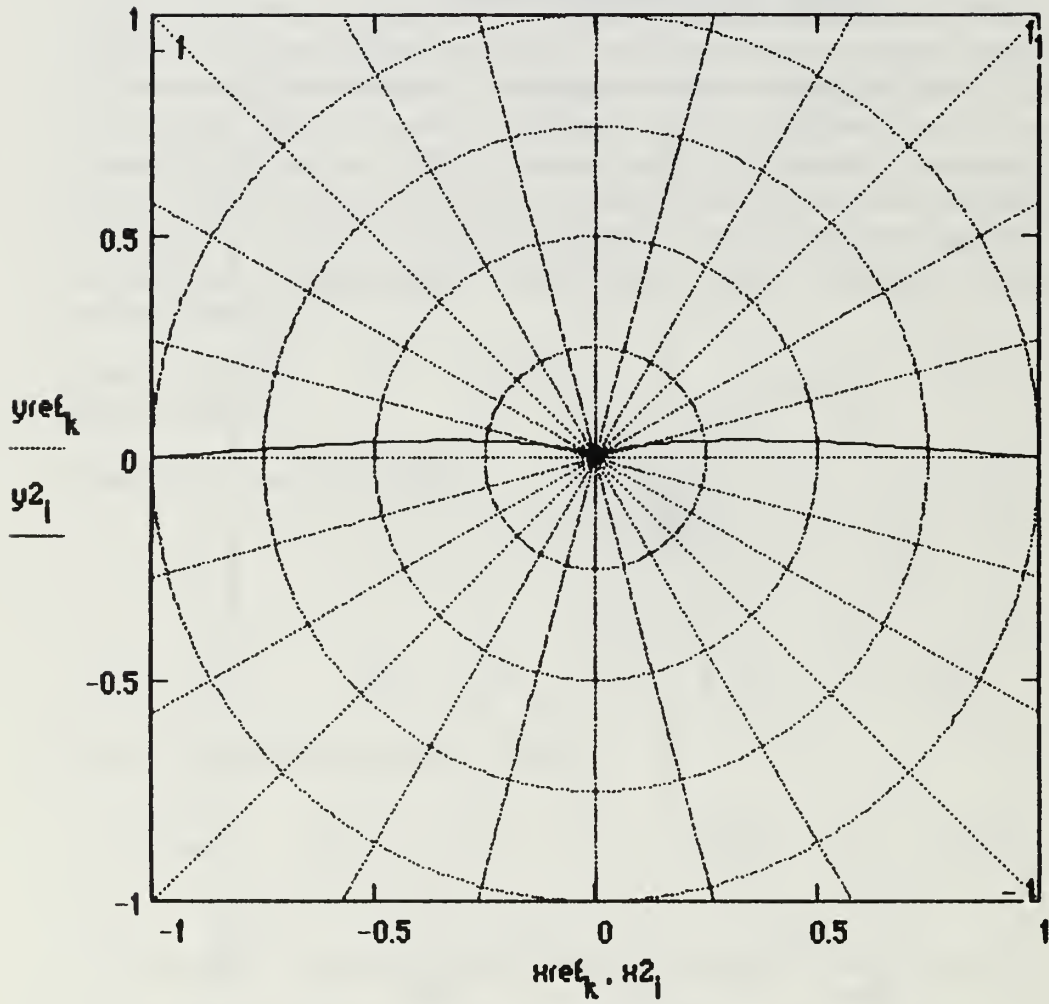
Space Wave Radiation Pattern



Maximum Space Wave Electric Field
Intensity (Volts per meter)

$$\max(\text{MagE1}) = 0.01733$$

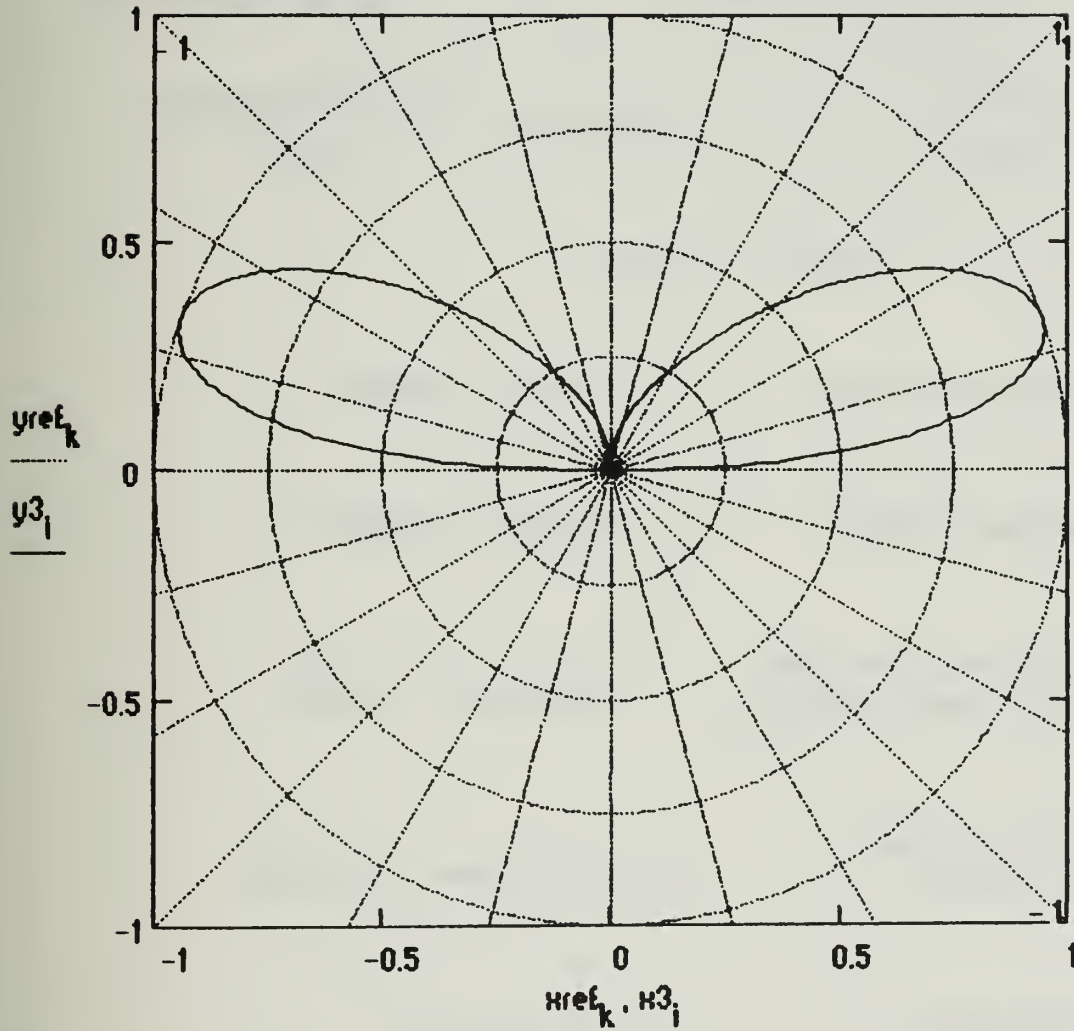
Surface Wave Radiation Pattern



Maximum Surface Wave Electric Field
Intensity (Volts per meter)

$$\max(\text{MagE2}) = 2.69275 \cdot 10^{-4}$$

Combined Space and Surface Wave Radiation Pattern



Maximum Radiated Electric Field
Intensity (Volts per meter)

$$\max(\text{MagE3}) = 0.01732$$

$$\text{power} := 30 \cdot \int_0^{\frac{\pi}{2}} \left| \frac{\cos(\beta \cdot h \cdot \cos(\zeta)) - \cos(\beta \cdot h)}{\sin(\zeta)} \cdot \left[\frac{e^{-j \cdot \beta \cdot (R - H_0 \cdot \cos(\zeta))}}{R - H_0 \cdot \cos(\zeta)} + \frac{e^{-j \cdot \beta \cdot (R + H_0 \cdot \cos(\zeta))}}{R + H_0 \cdot \cos(\zeta)} \right] \right|^2 d\zeta$$

$$\text{sqE3}_1 := \frac{(|E3_1|)^2}{2 \cdot (120 \cdot \pi)}$$

$$\text{Directivity} := \frac{4 \cdot \pi \cdot R^2 \cdot \max(\text{sqE3})}{\text{power}}$$

$$\text{Radres} := 2 \cdot \text{power}$$

Total Power Radiated (Watts)

$$\text{power} = 10.79029$$

Radiation Resistance (Ohms)

$$\text{Radres} = 21.58059$$

Directivity (maximum Power Gain
assuming 100% Antenna efficiency)

$$\text{Directivity} = 4.16784$$

Effective Isotropic Radiated
Power (EIRP) (Watts)

$$\text{Directivity} \cdot \text{power} = 44.97225$$

Maximum Effective Area
(Along Radial of Directivity)
(square meters)

$$\frac{(\lambda_5)^2 \cdot \text{Directivity}}{4 \cdot \pi} = 33.16664$$

Maximum Effective Length
(Along Radial of Directivity)
(meters)

$$2 \cdot \sqrt{\frac{\text{Radres} \cdot (\lambda_5)^2 \cdot \text{Directivity}}{480 \cdot \pi^2}} = 2.75579$$

**Numerical Distance for
Vertical Polarization**

$$|Pe_0| = 74.95924$$

**Elevation Angle of Maximum
Power Gain (Degrees)**

$$\text{Angle3} = \begin{pmatrix} 19.39778 \\ 19.39778 \end{pmatrix}$$

VERTICAL DIPOLE

This application calculates far field radiation patterns and parameters associated with vertical thin-wire dipole antennas (diameter \ll wavelength). The antenna is mounted vertically along the z-axis in a rectangular coordinate system with the feed at the antenna's center at a set height above the surface. Required inputs are the antenna length, feed height above the surface, transmitted frequency, distance from the antenna, the conductivity and dielectric constant of the surface below the antenna. The planar earth model is assumed in predicting radiation patterns. Predicted operating frequencies assume that the antenna is a quarter-wavelength, half-wavelength, three-quarter-wavelength, or full-wavelength dipole. A sinusoidal current input with a maximum of unity is assumed. All radiation patterns are normalized with respect to the maximum electric field intensity transmitted by the antenna. Plotted radiation patterns are valid for any vertical plane passing through the antenna axis. The electric field magnitudes to which the Radiation Patterns are normalized are displayed below their respective plots. Polarization is vertical for all vertical dipoles.

Input the Dipole length in meters $l := 5$ $h := \frac{1}{2}$

Wavelengths and Frequencies

$$\begin{array}{llll} \lambda_1 := 4 \cdot l & \lambda_2 := 2 \cdot l & \lambda_3 := \frac{4 \cdot l}{3} & \lambda_4 := l \\ f_1 := \frac{c}{\lambda_1} & f_2 := \frac{c}{\lambda_2} & f_3 := \frac{c}{\lambda_3} & f_4 := \frac{c}{\lambda_4} \end{array}$$

Possible Operating Frequencies (Hertz)

$$\begin{array}{llll} \frac{\lambda}{4} \text{ Dipole: } f_1 = 1.5 \cdot 10^7 & \frac{\lambda}{2} \text{ Dipole: } f_2 = 3 \cdot 10^7 \\ \frac{3 \cdot \lambda}{4} \text{ Dipole: } f_3 = 4.5 \cdot 10^7 & \lambda \text{ Dipole: } f_4 = 6 \cdot 10^7 \end{array}$$

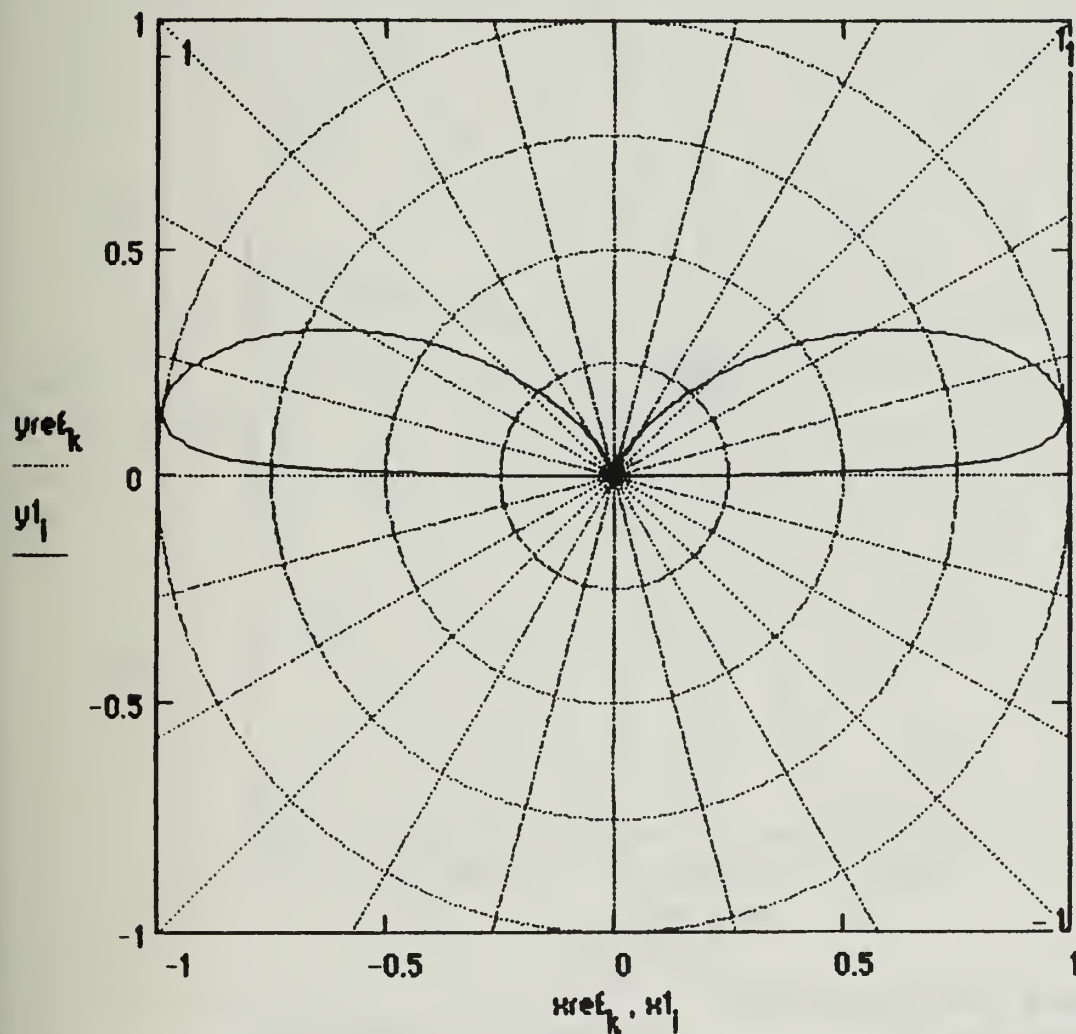
Input the operating Frequency (Hertz) $f_5 := 30 \cdot 10^6$ Input the Distance from the Antenna (meters) $R := 3000$

Input the ground Dielectric Constant $\epsilon_r := 72$ Input the ground Conductivity $\sigma := 4$

Input the Height of the Antenna Feed (meters) $H_0 := 2.5$

Radiation Patterns valid for any Vertical Plane passing through the Antenna

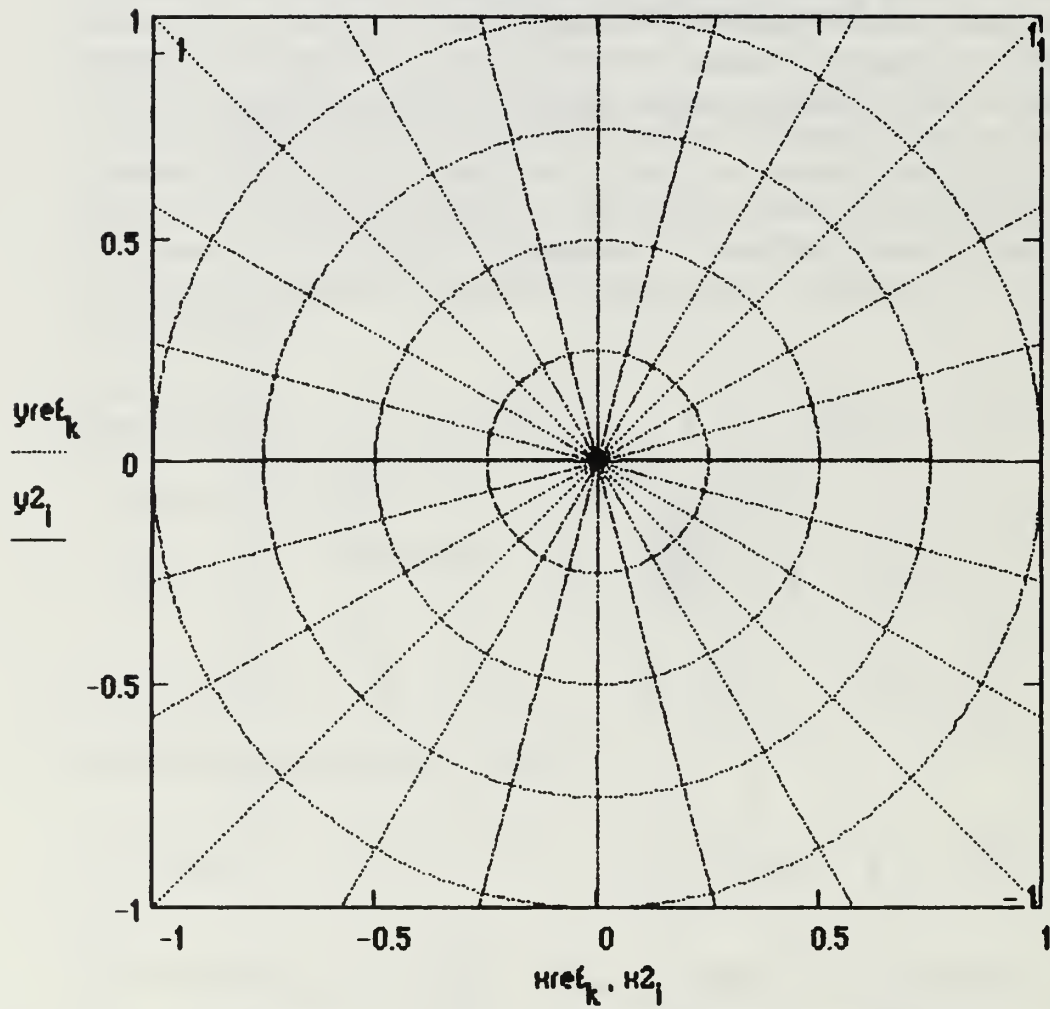
Space Wave Radiation Pattern



**Maximum Space Wave Electric Field
Intensity (Volts per meter)**

$$\max(\text{MagE1}) = 0.03394$$

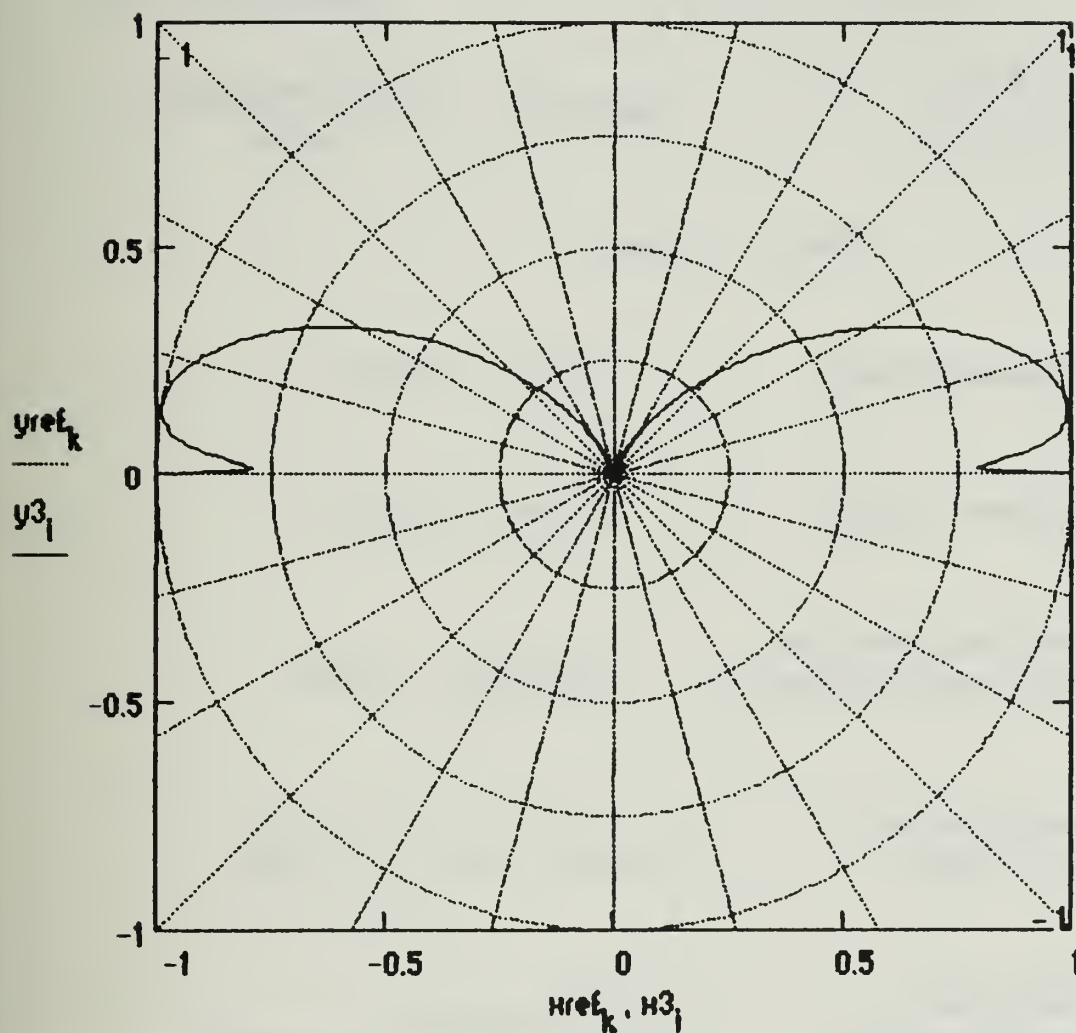
Surface Wave Radiation Pattern



Maximum Surface Wave Electric Field
Intensity (Volts per meter)

$$\max(\text{MagE2}) = 0.03331$$

Combined Space and Surface Wave Radiation Pattern



Maximum Radiated Electric Field
Intensity (Volts per meter)

$$\max(\text{MagE3}) = 0.03398$$

$$\text{power} := 30 \cdot \int_0^{\frac{\pi}{2}} \left| \frac{\cos(\beta \cdot h \cdot \cos(\xi)) - \cos(\beta \cdot h)}{\sin(\xi)} \cdot \left[\frac{e^{-j \cdot \beta \cdot (R - H_0 \cdot \cos(\xi))}}{R - H_0 \cdot \cos(\xi)} + \frac{e^{-j \cdot \beta \cdot (R + H_0 \cdot \cos(\xi))}}{R + H_0 \cdot \cos(\xi)} \right] \right|^2 d\xi$$

$$\text{sqE3}_1 := \frac{(|E3_1|)^2}{2 \cdot (120 \cdot \pi)}$$

$$\text{Directivity} := \frac{4 \cdot \pi \cdot R^2 \cdot \max(\text{sqE3})}{\text{power}}$$

$$\text{Radres} := 2 \cdot \text{power}$$

Total Power Radiated (Watts)

$$\text{power} = 37.64371$$

Radiation Resistance (Ohms)

$$\text{Radres} = 75.28741$$

Directivity (maximum Power Gain
assuming 100% Antenna efficiency)

$$\text{Directivity} = 4.59967$$

Effective Isotropic Radiated
Power (EIRP) (Watts)

$$\text{Directivity} \cdot \text{power} = 173.14876$$

Maximum Effective Area
(Along Radial of Directivity)
(square meters)

$$\frac{(\lambda_5)^2 \cdot \text{Directivity}}{4 \cdot \pi} = 36.60304$$

Maximum Effective Length
(Along Radial of Directivity)
(meters)

$$2 \cdot \sqrt{\frac{\text{Radres} \cdot (\lambda_5)^2 \cdot \text{Directivity}}{480 \cdot \pi^2}} = 5.40735$$

**Numerical Distance for
Vertical Polarization**

$$|Pe_0| = 0.39252$$

**Elevation Angle of Maximum
Power Gain (Degrees)**

$$\text{Angle3} = \begin{pmatrix} 8.55784 \\ 8.55784 \end{pmatrix}$$

APPENDIX B:
VERTICAL MONOPOLE ARRAY COMPUTER OUTPUT

This appendix contains computer hardcopies from the Mathcad vertical monopole application which show the input values and predicted radiation characteristics for two sample calculations. The configuration is a quarter-wave monopole above soil ($\epsilon_r=10$ and $\sigma=10^{-2}$) for the first example and the same configuration above seawater ($\epsilon_r=72$ and $\sigma=4$) for the second. Reference 6 [p. 89] provides the radiation patterns and gain predictions from several sources for the configuration in the first example.

The elevation of maximum directive gain is slightly higher for the Mathcad output than for those given in reference 6, but the overall radiation patterns are very similar. The 3.24 (5.1 dB) value of directivity for Mathcad is quite a bit higher than the maximum gain values of about zero dB in reference 6. However, since a half-wave dipole has a free-space directivity of 1.64 (2.1 dB), the actual directivity of a quarter-wave monopole above a ground plane should be closer to the Mathcad prediction because of the effect of the reflected wave (constructive and destructive interference) on the space wave and the lower total average radiated power resulting from ground plane losses. The seawater example yields results consistent with expectations. With respect to the soil example, the seawater example's directivity is slightly higher due to a stronger reflected wave, and the surface wave is stronger at grazing angles ($\theta \approx 90^\circ$) due to higher conductivity.

VERTICAL MONOPOLE

This application calculates far field radiation patterns and parameters associated with vertical thin-wire monopole antennas (diameter \ll wavelength). The antenna is mounted vertically along the z-axis in a rectangular coordinate system with the feed at the origin. Required inputs are the antenna length, transmitted frequency, distance from the antenna, the conductivity and dielectric constant of the surface below the antenna. The planar earth model is assumed in predicting radiation patterns. Predicted operating frequencies assume that the antenna is an eighth-wavelength, quarter-wavelength, three-eighths-wavelength, or half-wavelength monopole. A sinusoidal current input with a maximum of unity is assumed. All radiation patterns are normalized with respect to the maximum electric field intensity transmitted by the antenna. The electric field magnitudes to which the patterns are normalized are displayed below their respective plots. Radiation patterns are valid for any vertical plane passing through the z-axis, because the radiation pattern is symmetrical with respect to ϕ . Polarization is vertical for all vertical monopoles.

Input the Monopole
length in meters

$$h := 7.5$$

$$l := 2 \cdot h$$

Wavelengths and Frequencies

$$\lambda_1 := 4 \cdot l$$

$$\lambda_2 := 2 \cdot l$$

$$\lambda_3 := \frac{4 \cdot l}{3}$$

$$\lambda_4 := l$$

$$f_1 := \frac{c}{\lambda_1}$$

$$f_2 := \frac{c}{\lambda_2}$$

$$f_3 := \frac{c}{\lambda_3}$$

$$f_4 := \frac{c}{\lambda_4}$$

Possible Operating Frequencies (Hertz)

$$\frac{\lambda}{8} \quad \text{Monopole: } f_1 = 5 \cdot 10^6$$

$$\frac{\lambda}{4} \quad \text{Monopole: } f_2 = 1 \cdot 10^7$$

$$\frac{3 \cdot \lambda}{8} \quad \text{Monopole: } f_3 = 1.5 \cdot 10^7$$

$$\frac{\lambda}{2} \quad \text{Monopole: } f_4 = 2 \cdot 10^7$$

Input the operating
Frequency (Hertz)

$$f_5 := 10 \cdot 10^6$$

Input the Distance from
the Antenna (meters)

$$R := 3000$$

Input the ground
Dielectric Constant

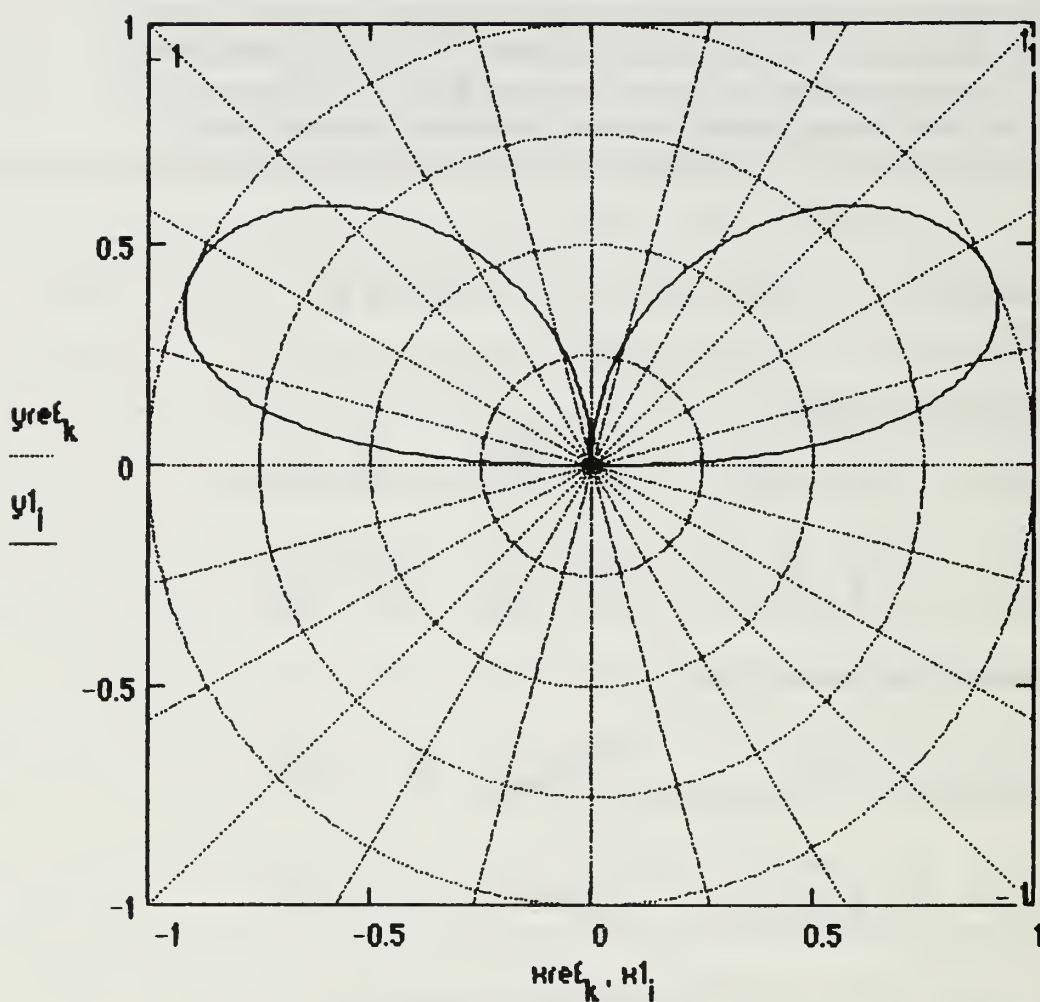
$$\epsilon_r := 10$$

Input the ground
Conductivity:

$$\sigma := 10^{-2}$$

Radiation Patterns valid for any Vertical Plane passing through the Antenna

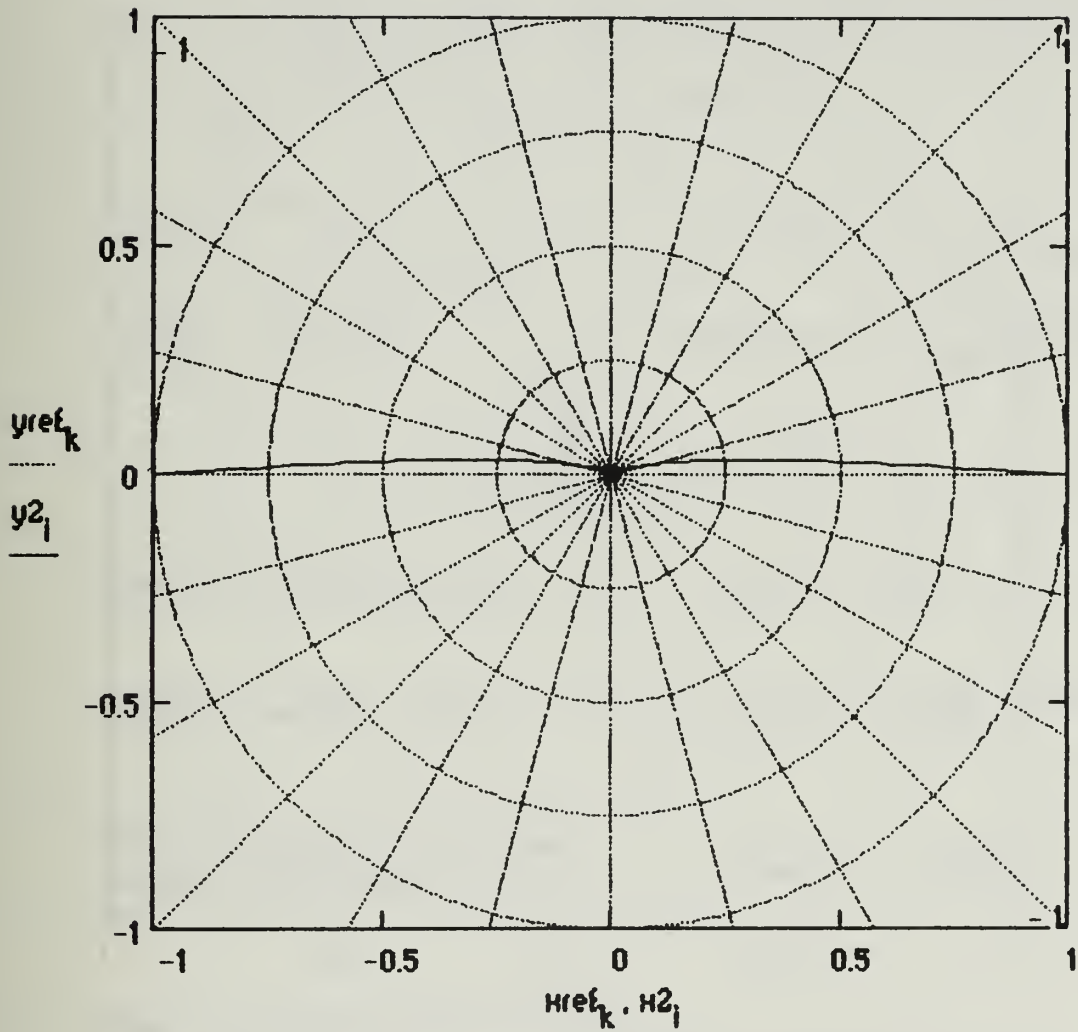
Space Wave Radiation Pattern



Maximum Space Wave Electric Field
Intensity (Volts per meter)

$$\max(\text{MagE1}) = 0.01115$$

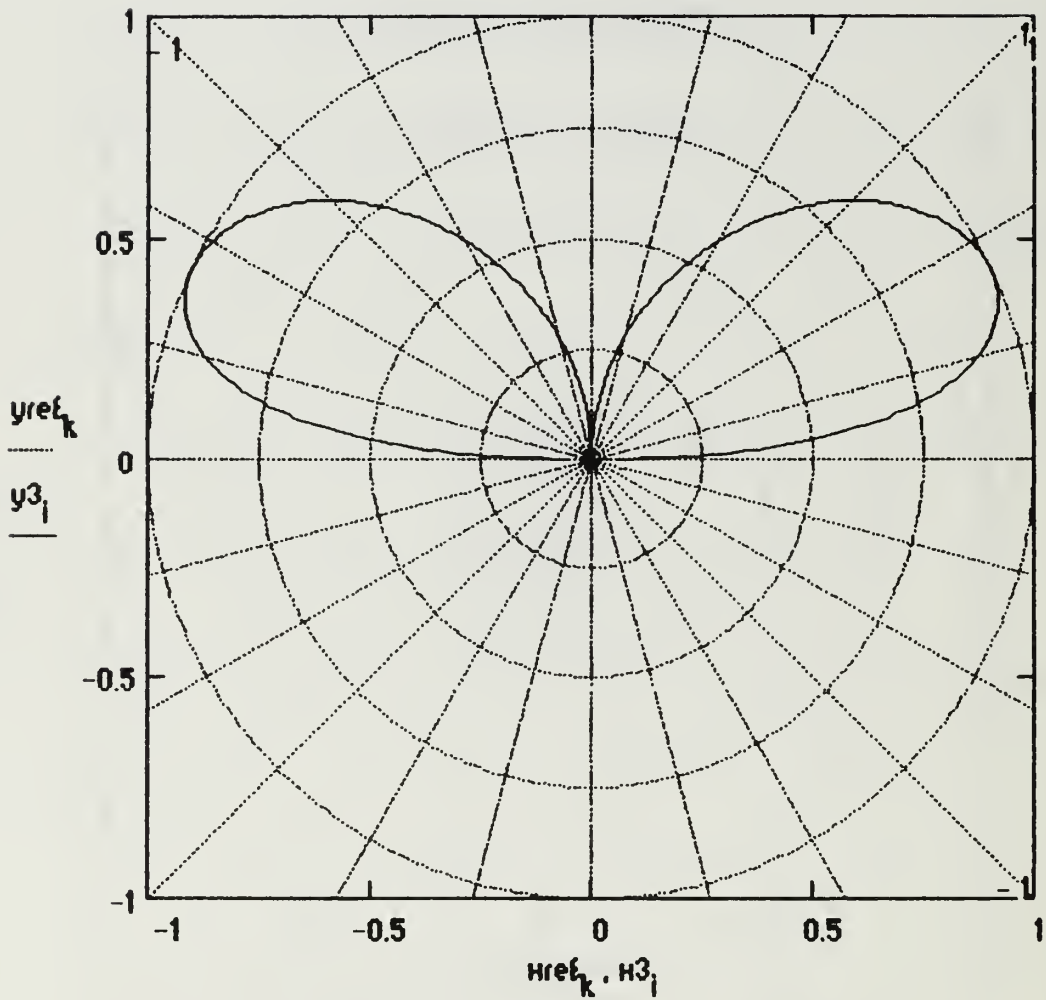
Surface Wave Pattern



Maximum Surface Wave Field Intensity
(Volts per meter)

$$\max(\text{MagE2}) = 8.23677 \cdot 10^{-4}$$

Combined Space and Surface Wave Pattern



Maximum Radiated Electric Field
Intensity (Volts per meter)

$$\max(\text{MagE3}) = 0.01114$$

$$\text{power} := \frac{7.5}{R^2} \cdot \int_0^{\frac{\pi}{2}} \left[\left| \frac{\left[\begin{array}{l} \cos(\beta \cdot h \cdot \cos(\xi)) - \cos(\beta \cdot h) \dots \\ + j \cdot \left[\begin{array}{l} \sin(\beta \cdot h \cdot \cos(\xi)) \dots \\ + (- (\cos(\xi) \cdot \sin(\beta \cdot h))) \end{array} \right] \end{array} \right]}{\sin(\xi)} \dots \right. \right. \\ \left. \left. + \frac{\left[\begin{array}{l} n^2 \cdot \cos(\xi) - \sqrt{n^2 - \sin(\xi)^2} \end{array} \right] \left[\begin{array}{l} \cos(\beta \cdot h \cdot \cos(\xi)) - \cos(\beta \cdot h) \dots \\ + \left[-j \cdot \left[\begin{array}{l} \sin(\beta \cdot h \cdot \cos(\xi)) \dots \\ + (- (\cos(\xi) \cdot \sin(\beta \cdot h))) \end{array} \right] \end{array} \right] \end{array} \right]}{\sin(\xi)} \right] \right] \cdot \frac{n^2 \cdot \cos(\xi) + \sqrt{n^2 - \sin(\xi)^2}}{n^2 \cdot \cos(\xi) - \sqrt{n^2 - \sin(\xi)^2}} \right] d\xi$$

$$\text{sqE3}_i := \frac{(|E3_i|)^2}{2 \cdot (120 \cdot \pi)}$$

$$\text{Directivity} := \frac{4 \cdot \pi \cdot R^2 \cdot \max(\text{sqE3})}{\text{power}}$$

$$\text{Radres} := 2 \cdot \text{power}$$

Total Power Radiated (Watts)

$$\text{power} = 5.74454$$

Radiation Resistance (Ohms)

$$\text{Radres} = 11.48908$$

Directivity (maximum Power Gain
assuming 100% Antenna Efficiency)

$$\text{Directivity} = 3.23898$$

Effective Isotropic Radiated
Power (EIRP) (Watts)

$$\text{Directivity} \cdot \text{power} = 18.60648$$

Maximum Effective Area
(Along Radial of Directivity)
(square meters)

$$\frac{(\lambda_5)^2 \cdot \text{Directivity}}{4 \cdot \pi} = 231.97519$$

**Maximum Effective Length
(Along Radial of Directivity)
(meters)**

$$2 \cdot \sqrt{\frac{\text{Radres} \cdot (\lambda_5)^2 \cdot \text{Directivity}}{480 \cdot \pi^2}} = 5.31775$$

**Numerical Distance for
Vertical Polarization**

$$|Pe_0| = 14.91116$$

**Elevation Angle of Maximum
Power Gain (Degrees)**

$$\text{Angle3} = \begin{pmatrix} 25.67353 \\ 25.67353 \end{pmatrix}$$

VERTICAL MONOPOLE

This application calculates far field radiation patterns and parameters associated with vertical thin-wire monopole antennas (diameter \ll wavelength). The antenna is mounted vertically along the z-axis in a rectangular coordinate system with the feed at the origin. Required inputs are the antenna length, transmitted frequency, distance from the antenna, the conductivity and dielectric constant of the surface below the antenna. The planar earth model is assumed in predicting radiation patterns. Predicted operating frequencies assume that the antenna is an eighth-wavelength, quarter-wavelength, three-eighths-wavelength, or half-wavelength monopole. A sinusoidal current input with a maximum of unity is assumed. All radiation patterns are normalized with respect to the maximum electric field intensity transmitted by the antenna. The electric field magnitudes to which the patterns are normalized are displayed below their respective plots. Radiation patterns are valid for any vertical plane passing through the z-axis, because the radiation pattern is symmetrical with respect to ϕ . Polarization is vertical for all vertical monopoles.

Input the Monopole
length in meters

$$h := 7.5$$

$$l := 2 \cdot h$$

Wavelengths and Frequencies

$$\lambda_1 := 4 \cdot l$$

$$\lambda_2 := 2 \cdot l$$

$$\lambda_3 := \frac{4 \cdot l}{3}$$

$$\lambda_4 := l$$

$$f_1 := \frac{c}{\lambda_1}$$

$$f_2 := \frac{c}{\lambda_2}$$

$$f_3 := \frac{c}{\lambda_3}$$

$$f_4 := \frac{c}{\lambda_4}$$

Possible Operating Frequencies (Hertz)

$$\frac{\lambda}{8} \quad \text{Monopole: } f_1 = 5 \cdot 10^6$$

$$\frac{\lambda}{4} \quad \text{Monopole: } f_2 = 1 \cdot 10^7$$

$$\frac{3 \cdot \lambda}{8} \quad \text{Monopole: } f_3 = 1.5 \cdot 10^7$$

$$\frac{\lambda}{2} \quad \text{Monopole: } f_4 = 2 \cdot 10^7$$

Input the operating
Frequency (Hertz) $f_5 := 10 \cdot 10^6$

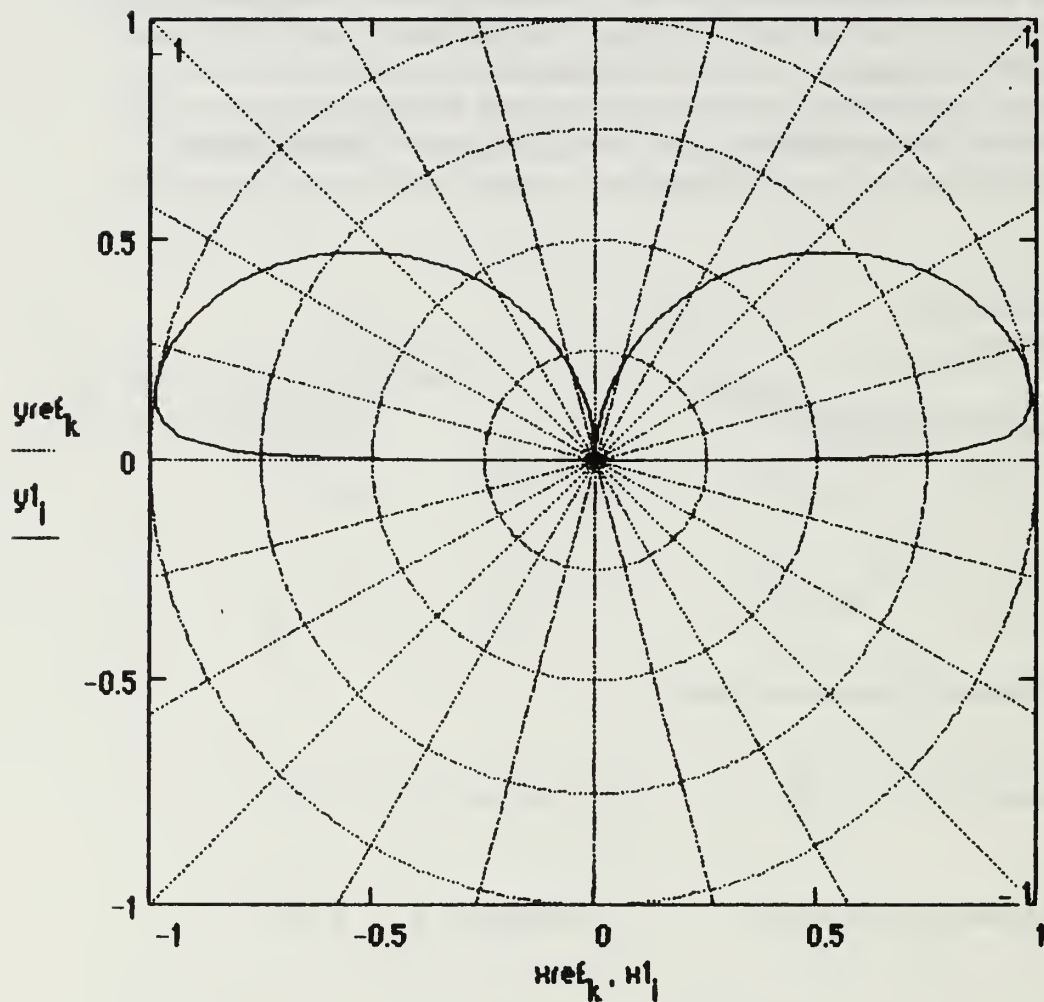
Input the Distance from
the Antenna (meters) $R := 3000$

Input the ground
Dielectric Constant $\epsilon_r := 72$

Input the ground
Conductivity: $\sigma := 4$

Radiation Patterns valid for any Vertical Plane passing through the Antenna

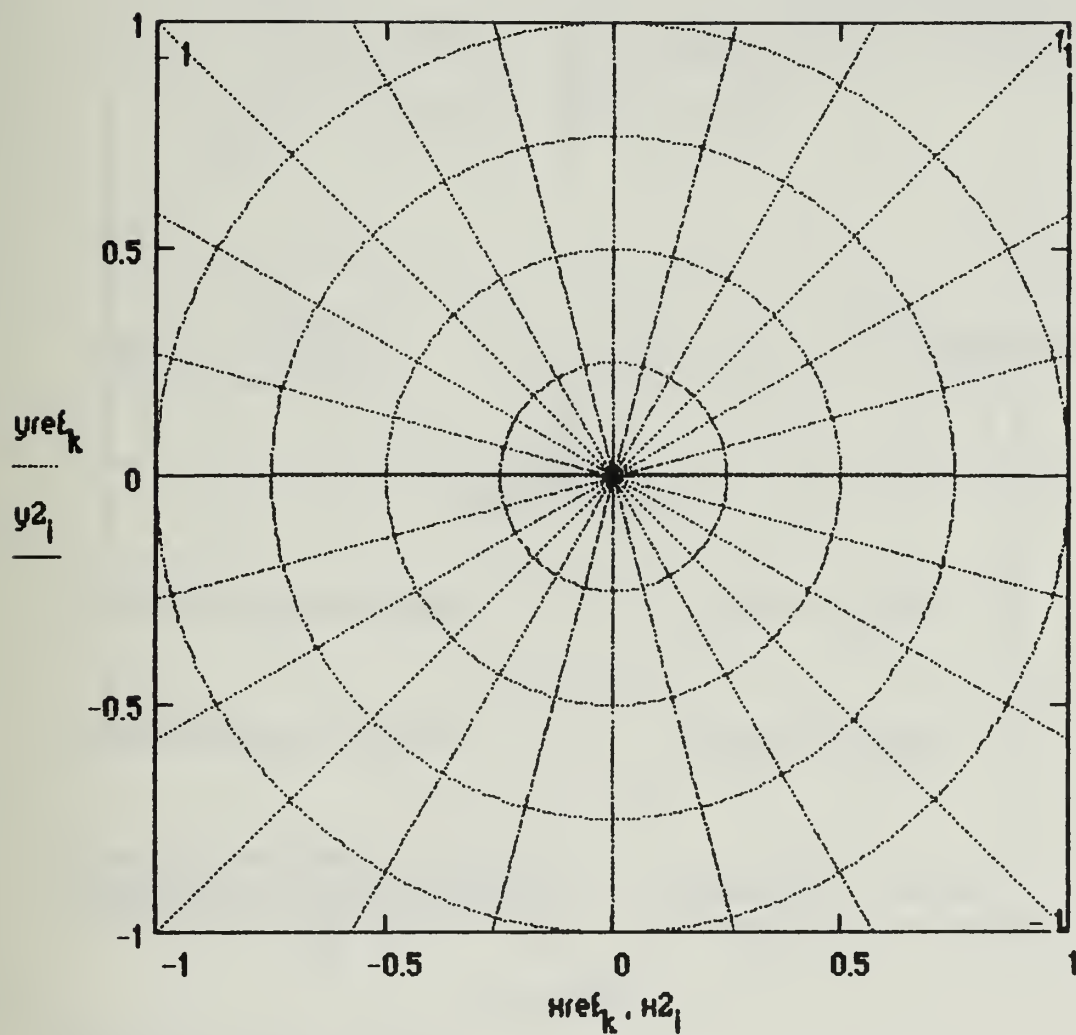
Space Wave Radiation Pattern



Maximum Space Wave Electric Field
Intensity (Volts per meter)

$$\max(\text{MagE1}) = 0.01855$$

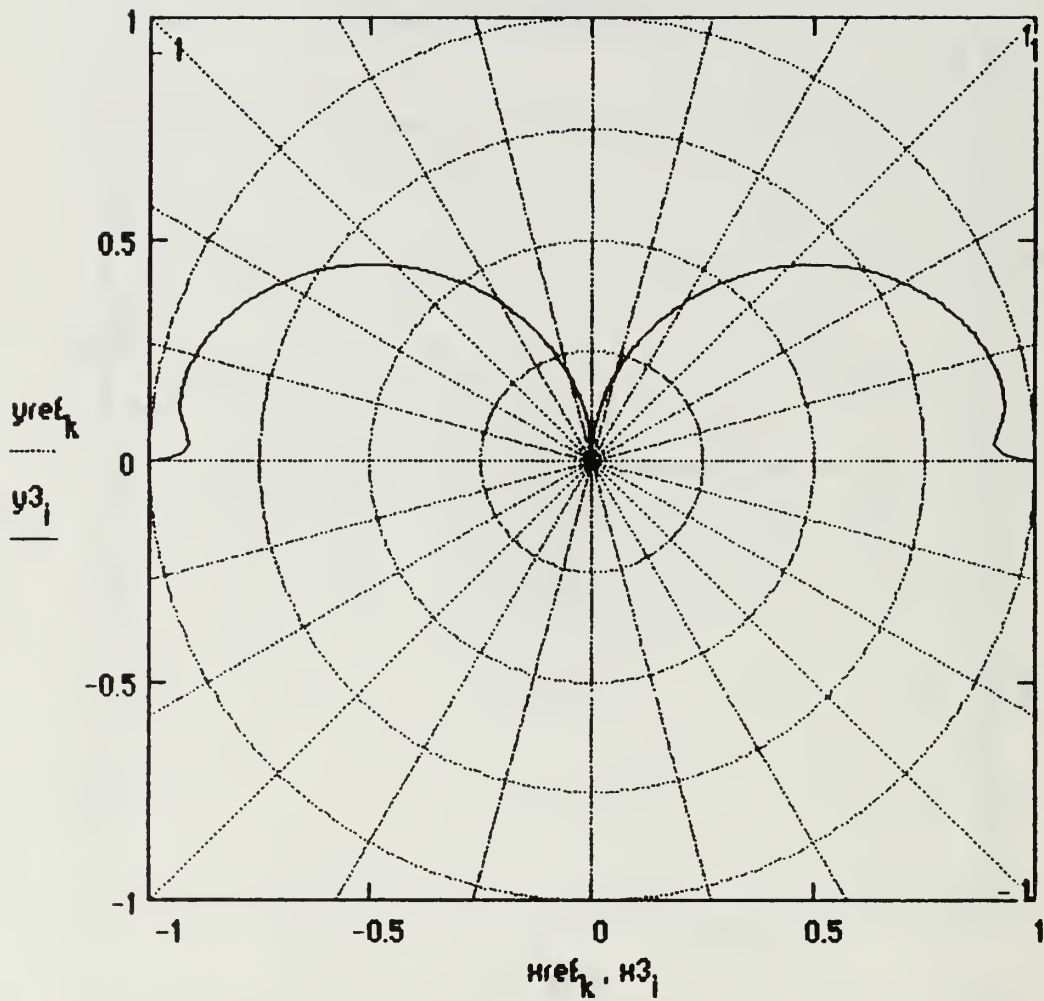
Surface Wave Pattern



Maximum Surface Wave Field Intensity
(Volts per meter)

$$\max(\text{MagE2}) = 0.01976$$

Combined Space and Surface Wave Pattern



Maximum Radiated Electric Field
Intensity (Volts per meter)

$$\max(\text{MagE3}) = 0.01976$$

$$\text{power} := \frac{7.5}{R^2} \int_0^{\frac{\pi}{2}} \left[\left| \frac{\left[\begin{array}{l} \cos(\beta \cdot h \cdot \cos(\xi)) - \cos(\beta \cdot h) \dots \\ + j \cdot \left[\begin{array}{l} \sin(\beta \cdot h \cdot \cos(\xi)) \dots \\ + (- (\cos(\xi) \cdot \sin(\beta \cdot h))) \end{array} \right] \end{array} \right]}{\sin(\xi)} \dots \right. \right. \\ \left. \left. + \frac{n^2 \cdot \cos(\xi) - \sqrt{n^2 - \sin(\xi)^2}}{n^2 \cdot \cos(\xi) + \sqrt{n^2 - \sin(\xi)^2}} \cdot \frac{\left[\begin{array}{l} \cos(\beta \cdot h \cdot \cos(\xi)) - \cos(\beta \cdot h) \dots \\ + \left[-j \cdot \left[\begin{array}{l} \sin(\beta \cdot h \cdot \cos(\xi)) \dots \\ + (- (\cos(\xi) \cdot \sin(\beta \cdot h))) \end{array} \right] \end{array} \right]}{\sin(\xi)} \right]} \right| \right] d\xi$$

$$\text{sqE3}_1 := \frac{(|E3_1|)^2}{2 \cdot (120 \cdot \pi)}$$

$$\text{Directivity} := \frac{4 \cdot \pi \cdot R^2 \cdot \max(\text{sqE3})}{\text{power}}$$

$$\text{Radres} := 2 \cdot \text{power}$$

Total Power Radiated (Watts)

$$\text{power} = 16.19454$$

Radiation Resistance (Ohms)

$$\text{Radres} = 32.38909$$

Directivity (maximum Power Gain
assuming 100% Antenna Efficiency)

$$\text{Directivity} = 3.61503$$

Effective Isotropic Radiated
Power (EIRP) (Watts)

$$\text{Directivity} \cdot \text{power} = 58.54372$$

Maximum Effective Area
(Along Radial of Directivity)
(square meters)

$$\frac{(\lambda_5)^2 \cdot \text{Directivity}}{4 \cdot \pi} = 258.9073$$

**Maximum Effective Length
(Along Radial of Directivity)
(meters)**

$$2 \cdot \sqrt{\frac{\text{Radres} \cdot (\lambda_5)^2 \cdot \text{Directivity}}{480 \cdot \pi^2}} = 9.4327$$

**Numerical Distance for
Vertical Polarization**

$$|Pe_0| = 0.04363$$

**Elevation Angle of Maximum
Power Gain (Degrees)**

$$\text{Angle3} = \begin{pmatrix} 0 \\ 0 \end{pmatrix}$$

APPENDIX C:
HORIZONTAL DIPOLE ARRAY COMPUTER OUTPUT

This appendix contains computer hardcopies from the Mathcad horizontal dipole application which show the input values and predicted radiation characteristics for four sample calculations. The configuration is a half-wave dipole at one-quarter, one-half, and three-quarters wavelengths above soil ($\epsilon_r=10$ and $\sigma=10^{-2}$) for the first three examples, respectively, and a half-wave dipole at one-quarter wavelength above seawater ($\epsilon_r=72$ and $\sigma=4$) for the fourth. Reference 6 [pp. 86-88] provides the radiation patterns and gain predictions from several sources for the configurations in the first three examples.

The radiation patterns and maximum directive gain computed by the first three Mathcad examples are almost identical to the those given in reference 6. The directivity predictions are slightly higher for Mathcad, but the overall similarity between the predicted radiation characteristics is noteworthy. The seawater example also yields results consistent with expectations. With respect to the soil example, the seawater example's directivity is slightly higher due to a stronger reflected wave, and the surface wave is slightly stronger at grazing angles ($\theta \approx 90^\circ$) due to higher conductivity. For horizontal polarization, the higher conductivity surface below the antenna does not result in a greatly enhanced surface wave and increased directivity as it does for vertical polarization.

HORIZONTAL DIPOLE

This application calculates far field radiation patterns and parameters associated with horizontal thin-wire dipole antennas (diameter \ll wavelength). The antenna is mounted above and parallel to the x-axis in a rectangular coordinate system. The feed is at the center of the antenna at a set height directly above the origin. Required inputs are the antenna length, feed height above the surface, transmitted frequency, distance from the antenna, the conductivity and dielectric constant of the surface below the antenna. The planar earth model is assumed in predicting radiation patterns. Predicted operating frequencies assume that the antenna is a quarter-wavelength, half-wavelength, three-quarter-wavelength, or full wave-length dipole. A sinusoidal current input with a maximum of unity is assumed. All radiation patterns are normalized with respect to the maximum electric field intensity transmitted by the antenna in the plane of interest. The electric field magnitudes to which the patterns are normalized are displayed below their respective plots. The radiation patterns are plotted for the $\phi=0$ and $\phi=\pi/2$ vertical planes parallel and perpendicular to the x-axis respectively. A horizontal radiation pattern is plotted at an elevation selected by the index from the elevation angle index table. Polarization is a combination of vertical and horizontal depending upon spatial orientation relative to the dipole.

Input the dipole length in meters $l := 15$ $h := \frac{1}{2}$

Input the index of the elevation angle for which to calculate the horizontal radiation pattern (from the angle index table) $d := 535$

Wavelengths and Frequencies

$$\begin{array}{llll} \lambda_1 := 4 \cdot l & \lambda_2 := 2 \cdot l & \lambda_3 := \frac{4 \cdot l}{3} & \lambda_4 := l \\ f_1 := \frac{c}{\lambda_1} & f_2 := \frac{c}{\lambda_2} & f_3 := \frac{c}{\lambda_3} & f_4 := \frac{c}{\lambda_4} \end{array}$$

Possible Operating Frequencies (Hertz)

$$\begin{array}{llll} \frac{\lambda}{4} \text{ Dipole: } & f_1 = 5 \cdot 10^6 & \frac{\lambda}{2} \text{ Dipole: } & f_2 = 1 \cdot 10^7 \\ \frac{3 \cdot \lambda}{4} \text{ Dipole: } & f_3 = 1.5 \cdot 10^7 & \lambda \text{ Dipole: } & f_4 = 2 \cdot 10^7 \end{array}$$

Input the operating
Frequency (Hertz)

$$f_5 := 10 \cdot 10^6$$

$$\lambda_5 := \frac{c}{f_5}$$

$$\beta := \frac{2 \cdot \pi}{\lambda_5}$$

Input the Height of
Antenna Feed (meters)

$$H_0 := 7.6$$

Input the ground
Dielectric Constant

$$\epsilon_r := 30$$

Input the Distance
from Antenna (meters)

$$R := 3000$$

Input the ground
Conductivity:

$$\sigma := 3 \cdot 10^{-2}$$

Index of Refraction

$$Rd_i := R - H_0 \cdot \cos(\theta_i)$$

$$Rr_i := R + H_0 \cdot \cos(\theta_i)$$

$$n := \sqrt{\epsilon_r - j \cdot \frac{18000 \cdot \sigma}{(f_5 \cdot 10^{-6})}}$$

Complex Numerical Distance
for Vertical Polarization

$$Pe_i := \frac{-j \cdot \beta \cdot Rr_i}{2 \cdot \sin(\theta_i)^2} \cdot \left(\cos(\theta_i) + \frac{\sqrt{n^2 - \sin(\theta_i)^2}}{n^2} \right)^2$$

Complex Numerical Distance
for Horizontal Polarization

$$Pm_i := \frac{-j \cdot \beta \cdot Rr_i}{2 \cdot \sin(\theta_i)^2} \cdot \left[\cos(\theta_i) + \sqrt{n^2 - (\sin(\theta_i)^2)} \right]^2$$

Vertical Reflection Coefficient

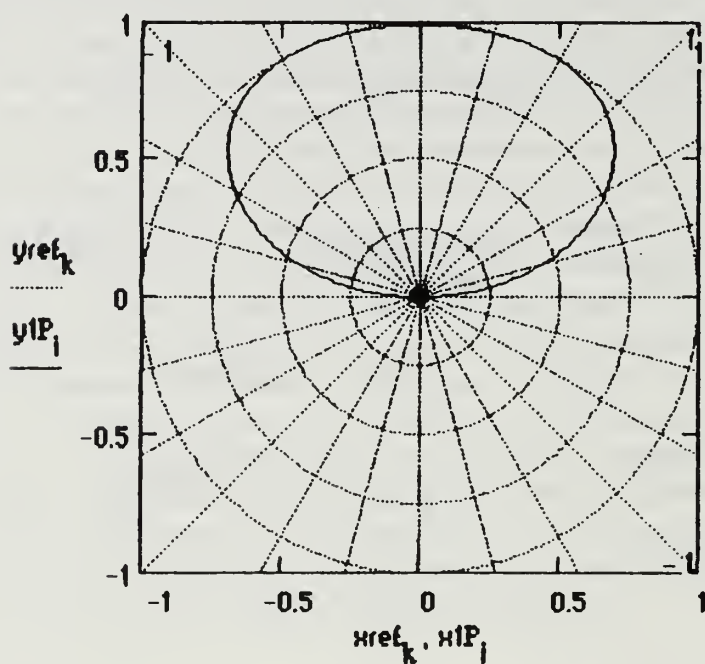
$$\Gamma_{V_i} := \frac{\left(n^2 \cdot \cos(\theta_i) \right) - \left(\sqrt{n^2 - \sin(\theta_i)^2} \right)}{\left(n^2 \cdot \cos(\theta_i) \right) + \left(\sqrt{n^2 - \sin(\theta_i)^2} \right)}$$

Horizontal Reflection Coefficient

$$\Gamma_{H_i} := \frac{\cos(\theta_i) - \left(\sqrt{n^2 - \sin(\theta_i)^2} \right)}{\cos(\theta_i) + \left(\sqrt{n^2 - \sin(\theta_i)^2} \right)}$$

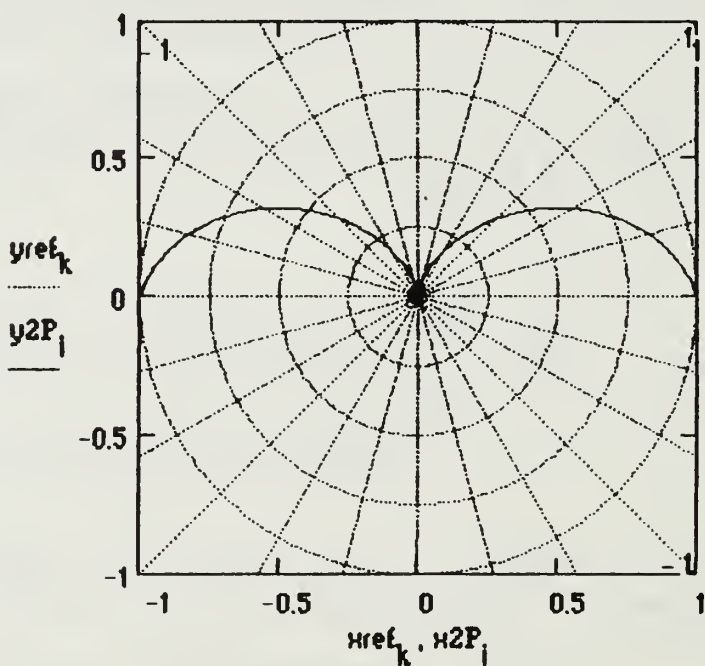
Radiation Patterns in $\Phi=\pi/2$ Plane (Perpendicular to Dipole)

Space Wave Radiation Pattern ($\Phi=\pi/2$)



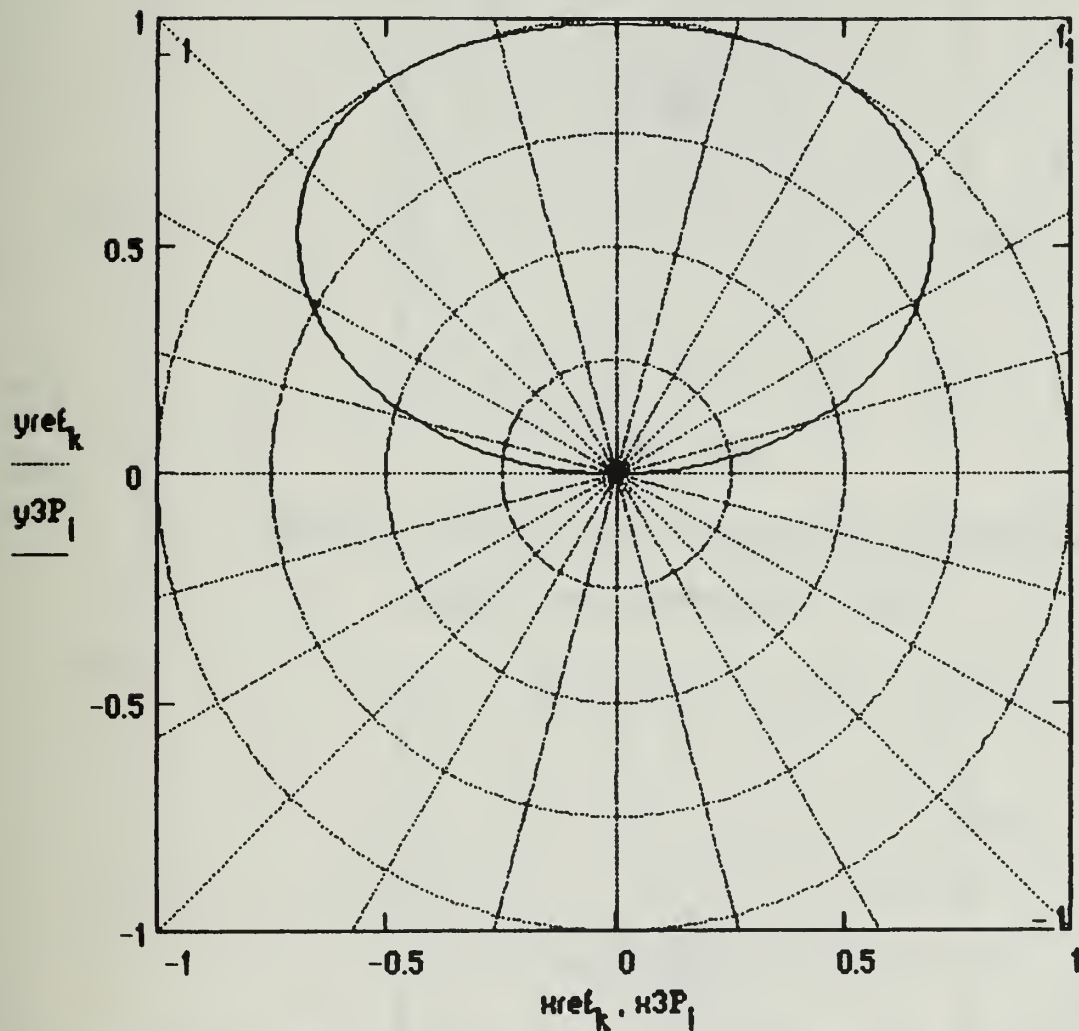
Max E-Field Intensity (Volts per meter) $\max(\text{MagE1P}) = 0.03632$

Surface Wave Radiation Pattern ($\Phi=\pi/2$)



Max E-Field Intensity (Volts per meter) $\max(\text{MagE2P}) = 1.03856 \cdot 10^{-6}$

Combined Space and Surface Wave Radiation Pattern ($\Phi = \pi/2$)

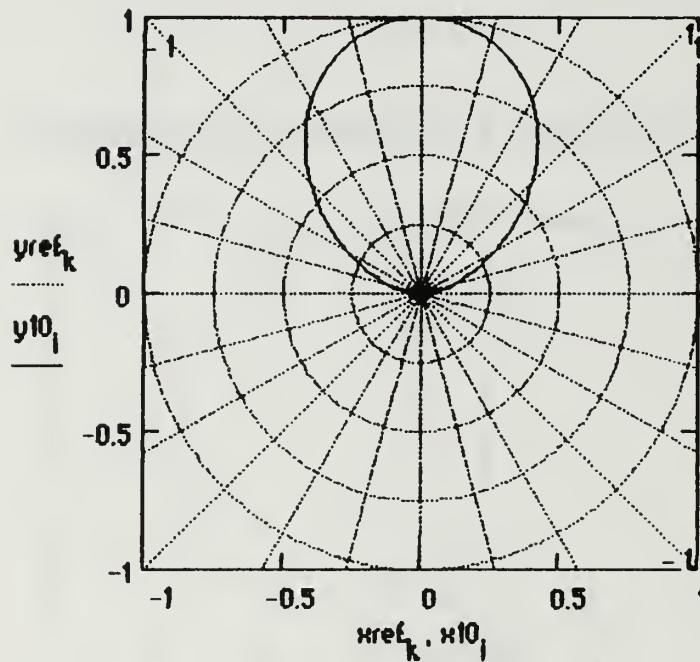


Max E-Field Intensity (Volts per meter)

$$\max(\text{MagE3P}) = 0.03632$$

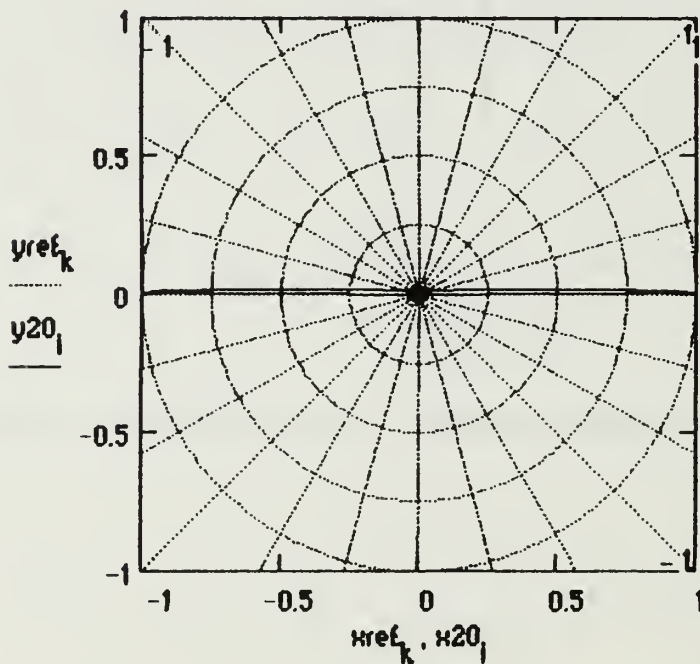
Radiation Patterns in $\Phi=0$ Plane (Parallel to Dipole)

Space Wave Radiation Pattern ($\Phi=0$)



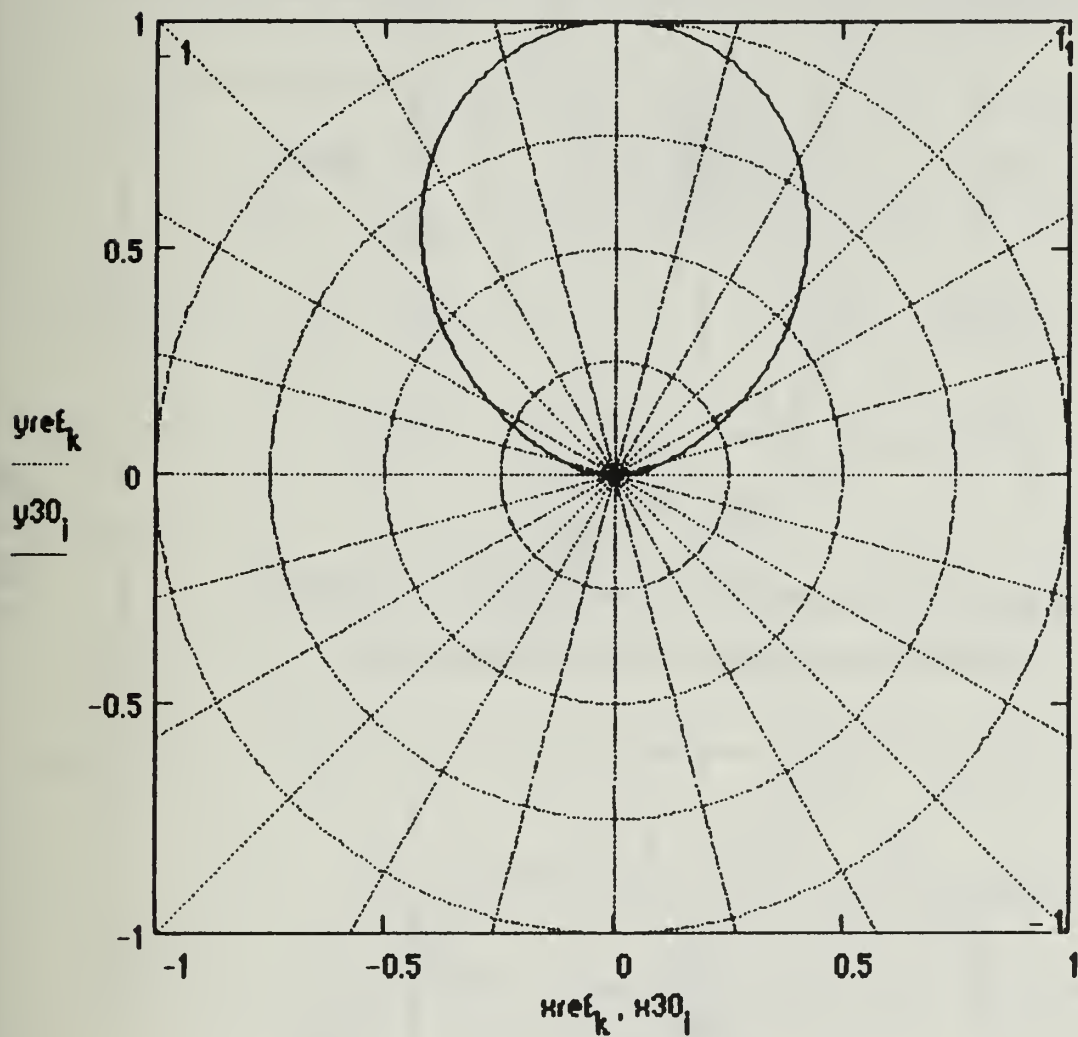
Max E-Field Intensity (Volts per meter) $\max(\text{MagE10}) = 0.03594$

Surface Wave Radiation Pattern ($\Phi=0$)



Max E-Field Intensity (Volts per meter) $\max(\text{MagE20}) = 3.84453 \cdot 10^{-4}$

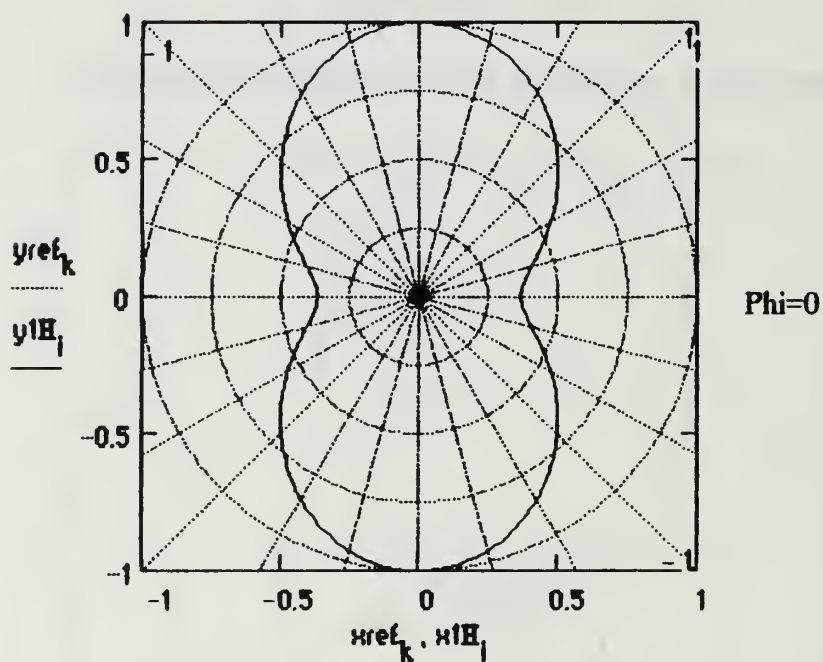
Combined Space and Surface Wave Radiation Pattern ($\Phi=0$)



Max E-Field Intensity (Volts per meter) $\max(\text{MagE30}) = 0.03594$

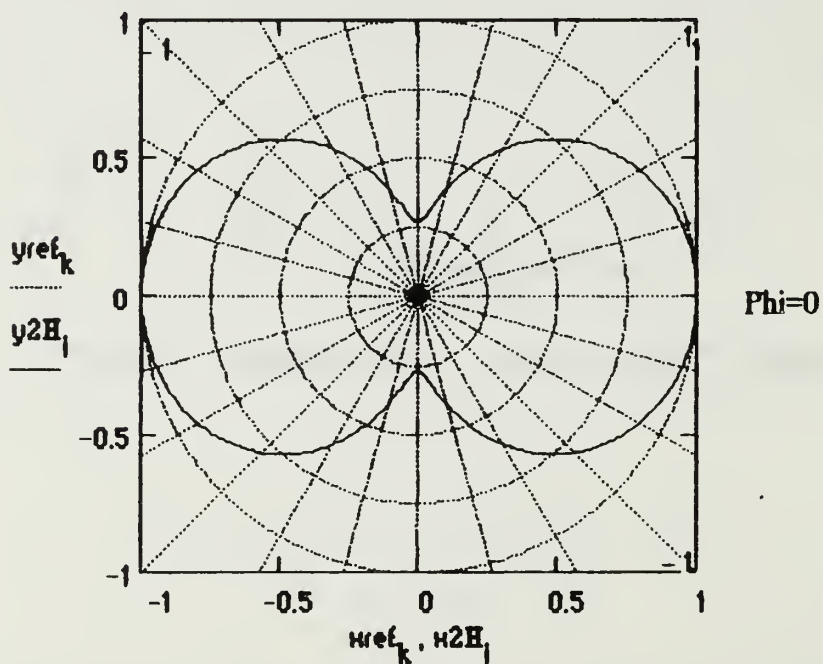
Radiation Patterns in Horizontal Plane

Space Wave Radiation Pattern



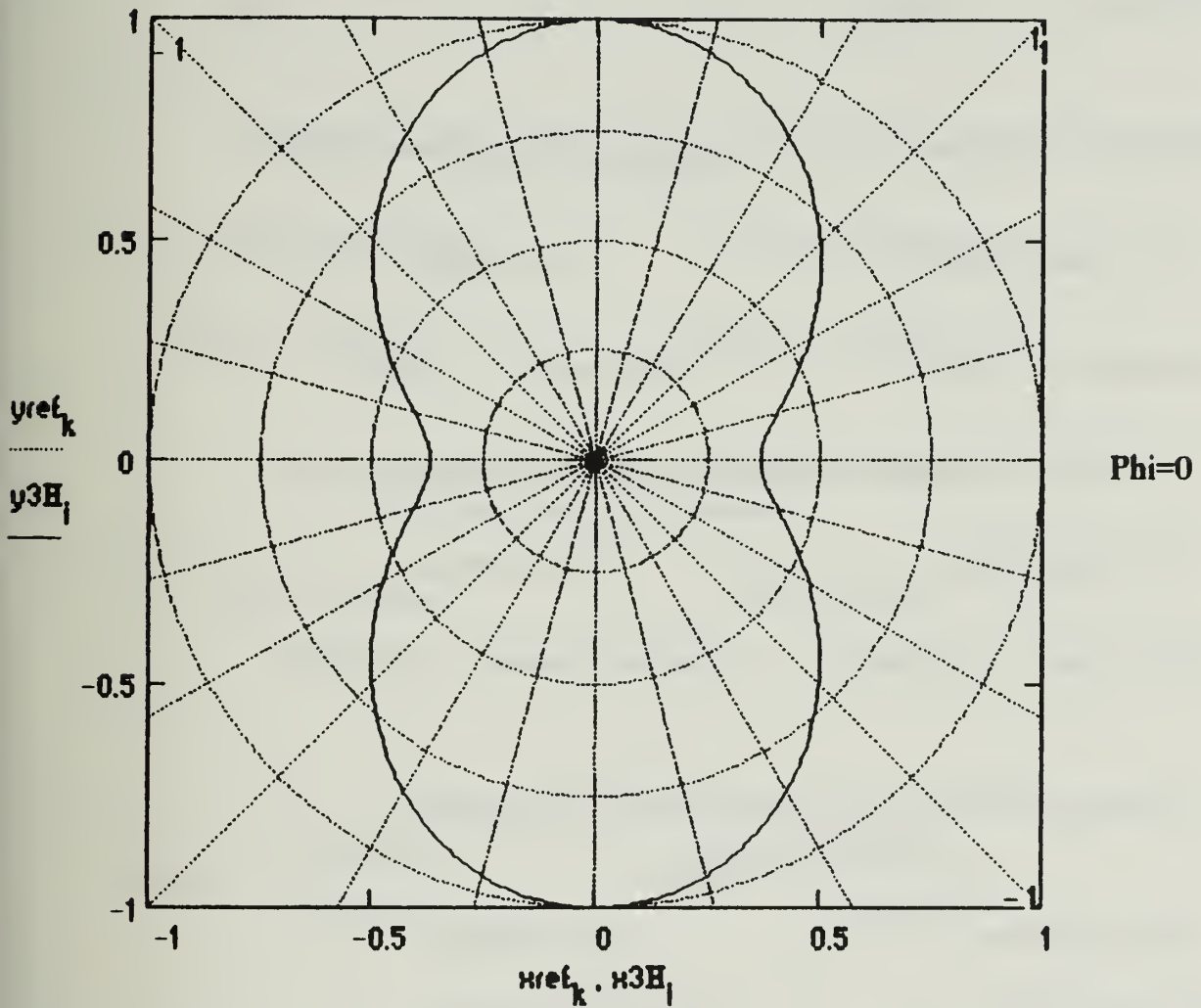
Max E-Field Intensity (Volts per meter) $\max(\text{MagE1H}) = 0.02634$

Surface Wave Radiation Pattern (Horizontal Plane)



Max E-Field Intensity (Volts per meter) $\max(\text{MagE2H}) = 2.62147 \cdot 10^{-6}$

Combined Space and Surface Wave Radiation Pattern (Horizontal Plane)



Max E-Field Intensity (Volts per meter) $\max(\text{MagE3H}) = 0.02634$

Total Power Radiated (Watts)

$$\text{power} = 37.80286$$

**Radiation Resistance (versus
Maximum Antenna Current)
(Ohms)**

$$\text{Radres} = 75.60572$$

Directivity (or Maximum Power Gain assuming 100% Antenna Efficiency)

Phi = pi/2 Plane

Phi = 0 Plane

$$\text{DirectivityP} = 5.23417$$

$$\text{Directivity0} = 5.12535$$

Effective Isotropic Radiated Power (EIRP) (Watts)

Phi = pi/2 Plane

Phi = 0 Plane

$$\text{DirectivityP} \cdot \text{power} = 197.86674$$

$$\text{Directivity0} \cdot \text{power} = 193.75275$$

**Maximum Effective Area (Along Radial of Directivity)
(square meters)**

Phi = pi/2 Plane

Phi = 0 Plane

$$\frac{(\lambda_5)^2 \cdot \text{DirectivityP}}{4 \cdot \pi} = 374.87006$$

$$\frac{(\lambda_5)^2 \cdot \text{Directivity0}}{4 \cdot \pi} = 367.07586$$

**Maximum Effective Length (Along Radial of Directivity)
(meters)**

Phi = pi/2 Plane

Phi = 0 Plane

$$2 \cdot \sqrt{\frac{\text{Radres} \cdot (\lambda_5)^2 \cdot \text{DirectivityP}}{480 \cdot \pi^2}} = 17.34132 \quad 2 \cdot \sqrt{\frac{\text{Radres} \cdot (\lambda_5)^2 \cdot \text{Directivity0}}{480 \cdot \pi^2}} = 17.1601$$

Numerical Distances

Vertical Polarization

Horizontal Polarization

$$|P_{e0}| = 5.04617$$

$$|P_{m0}| = 1.92562 \cdot 10^4$$

**Elevation Angle of Directivity (Maximum Gain)
above the Horizon (Degrees)**

Phi = pi/2 Plane

Phi = 0 Plane

$$\text{AngleP} = \begin{pmatrix} 65.8954 \\ 65.8954 \end{pmatrix}$$

$$\text{Angle0} = \begin{pmatrix} 89.85737 \\ 89.85737 \end{pmatrix}$$

HORIZONTAL DIPOLE

This application calculates far field radiation patterns and parameters associated with horizontal thin-wire dipole antennas (diameter \ll wavelength). The antenna is mounted above and parallel to the x-axis in a rectangular coordinate system. The feed is at the center of the antenna at a set height directly above the origin. Required inputs are the antenna length, feed height above the surface, transmitted frequency, distance from the antenna, the conductivity and dielectric constant of the surface below the antenna. The planar earth model is assumed in predicting radiation patterns. Predicted operating frequencies assume that the antenna is a quarter-wavelength, half-wavelength, three-quarter-wavelength, or full wavelength dipole. A sinusoidal current input with a maximum of unity is assumed. All radiation patterns are normalized with respect to the maximum electric field intensity transmitted by the antenna in the plane of interest. The electric field magnitudes to which the patterns are normalized are displayed below their respective plots. The radiation patterns are plotted for the $\phi=0$ and $\phi=\pi/2$ vertical planes parallel and perpendicular to the x-axis respectively. A horizontal radiation pattern is plotted at an elevation selected by the index from the elevation angle index table. Polarization is a combination of vertical and horizontal depending upon spatial orientation relative to the dipole.

Input the dipole length in meters $l := 7.5$ $h := \frac{1}{2}$

Input the index of the elevation angle for which to calculate the horizontal radiation pattern (from the angle index table) $d := 535$

Wavelengths and Frequencies

$$\lambda_1 := 4 \cdot l \quad \lambda_2 := 2 \cdot l \quad \lambda_3 := \frac{4 \cdot l}{3} \quad \lambda_4 := l$$

$$f_1 := \frac{c}{\lambda_1} \quad f_2 := \frac{c}{\lambda_2} \quad f_3 := \frac{c}{\lambda_3} \quad f_4 := \frac{c}{\lambda_4}$$

Possible Operating Frequencies (Hertz)

$$\frac{\lambda}{4} \text{ Dipole: } f_1 = 1 \cdot 10^7 \quad \frac{\lambda}{2} \text{ Dipole: } f_2 = 2 \cdot 10^7$$

$$\frac{3 \cdot \lambda}{4} \text{ Dipole: } f_3 = 3 \cdot 10^7 \quad \lambda \text{ Dipole: } f_4 = 4 \cdot 10^7$$

Input the operating
Frequency (Hertz)

$$f_5 := 20 \cdot 10^6$$

$$\lambda_5 := \frac{c}{f_5}$$

$$\beta := \frac{2 \cdot \pi}{\lambda_5}$$

Input the Height of
Antenna Feed (meters)

$$H_0 := 7.6$$

Input the ground
Dielectric Constant

$$\epsilon_r := 30$$

Input the Distance
from Antenna (meters)

$$R := 3000$$

Input the ground
Conductivity:

$$\sigma := 3 \cdot 10^{-2}$$

Index of Refraction

$$Rd_i := R - H_0 \cdot \cos(\theta_i)$$

$$Rr_i := R + H_0 \cdot \cos(\theta_i)$$

$$n := \sqrt{\epsilon_r - j \cdot \frac{18000 \cdot \sigma}{(f_5 \cdot 10^{-6})^2}}$$

Complex Numerical Distance
for Vertical Polarization

$$Pe_i := \frac{-j \cdot \beta \cdot Rr_i}{2 \cdot \sin(\theta_i)^2} \cdot \left(\cos(\theta_i) + \frac{\sqrt{n^2 - \sin(\theta_i)^2}}{n^2} \right)^2$$

Complex Numerical Distance
for Horizontal Polarization

$$Pm_i := \frac{-j \cdot \beta \cdot Rr_i}{2 \cdot \sin(\theta_i)^2} \cdot \left[\cos(\theta_i) + \sqrt{n^2 - (\sin(\theta_i)^2)} \right]^2$$

Vertical Reflection Coefficient

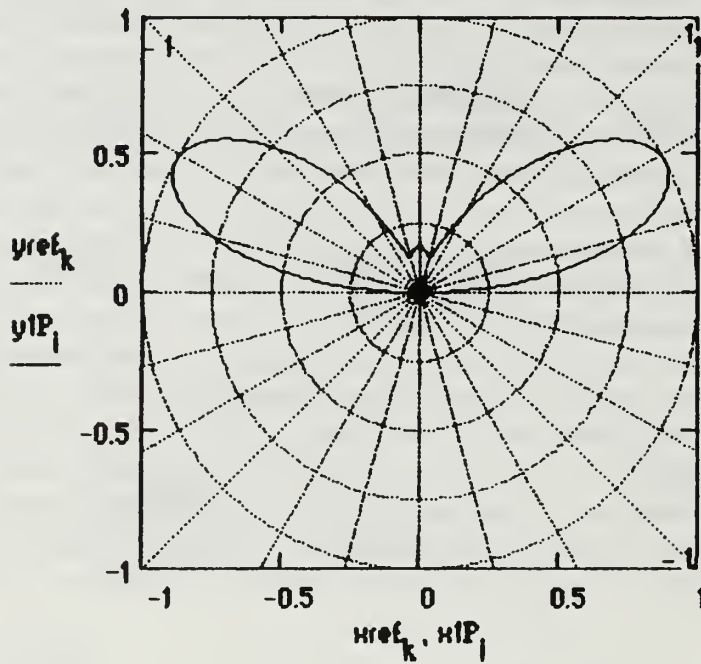
$$\Gamma_{v_i} := \frac{\left(n^2 \cdot \cos(\theta_i) \right) - \left(\sqrt{n^2 - \sin(\theta_i)^2} \right)}{\left(n^2 \cdot \cos(\theta_i) \right) + \left(\sqrt{n^2 - \sin(\theta_i)^2} \right)}$$

Horizontal Reflection Coefficient

$$\Gamma_{h_i} := \frac{\cos(\theta_i) - \left(\sqrt{n^2 - \sin(\theta_i)^2} \right)}{\cos(\theta_i) + \left(\sqrt{n^2 - \sin(\theta_i)^2} \right)}$$

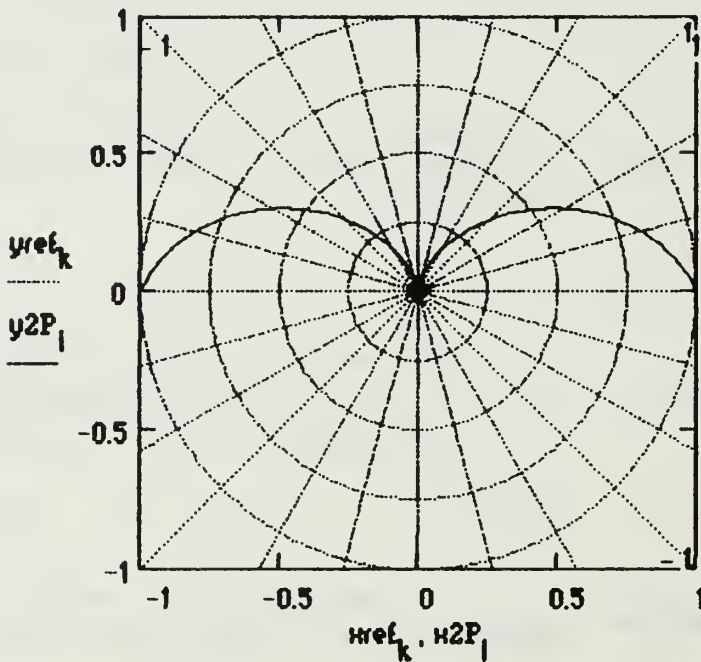
Radiation Patterns in $\Phi=\pi/2$ Plane (Perpendicular to Dipole)

Space Wave Radiation Pattern ($\Phi=\pi/2$)



Max E-Field Intensity (Volts per meter) $\max(\text{MagE1P}) = 0.03737$

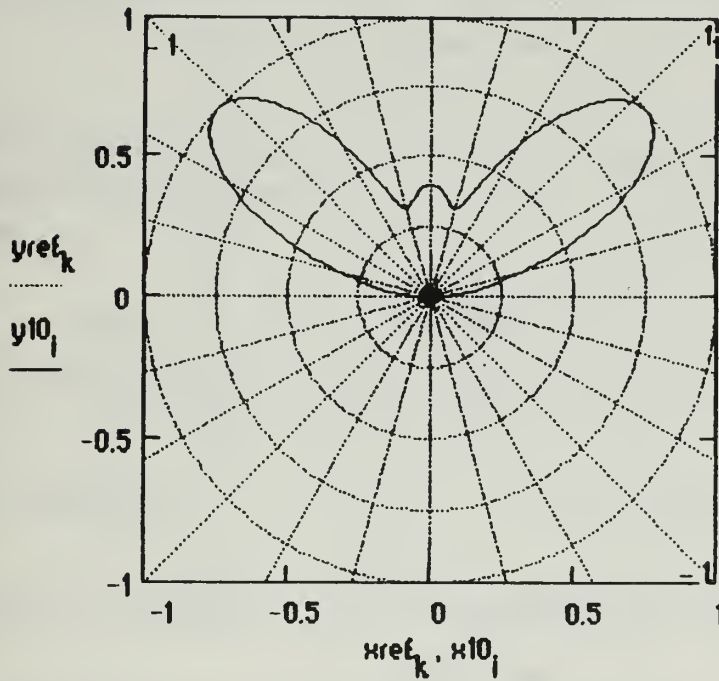
Surface Wave Radiation Pattern ($\Phi=\pi/2$)



Max E-Field Intensity (Volts per meter) $\max(\text{MagE2P}) = 8.03309 \cdot 10^{-7}$

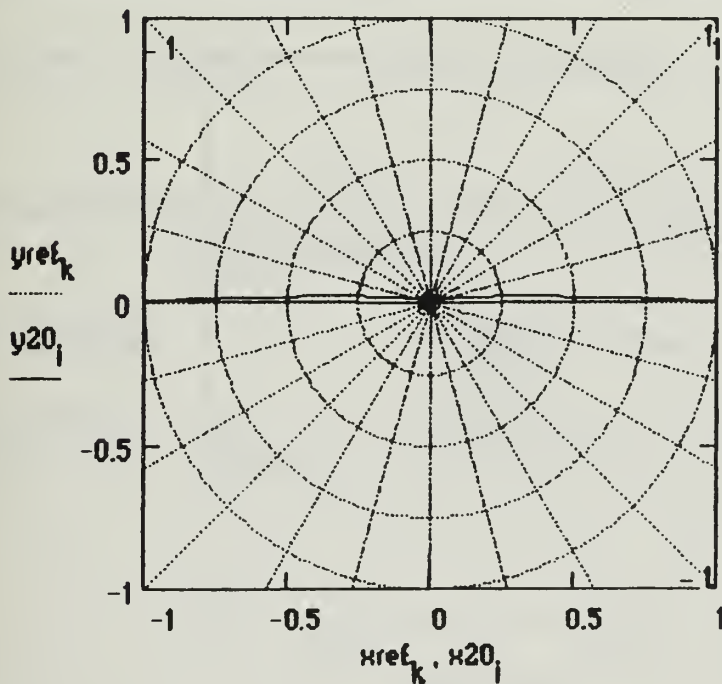
Radiation Patterns in $\Phi=0$ Plane (Parallel to Dipole)

Space Wave Radiation Pattern ($\Phi=0$)



Max E-Field Intensity (Volts per meter) $\max(\text{MagE10}) = 0.01561$

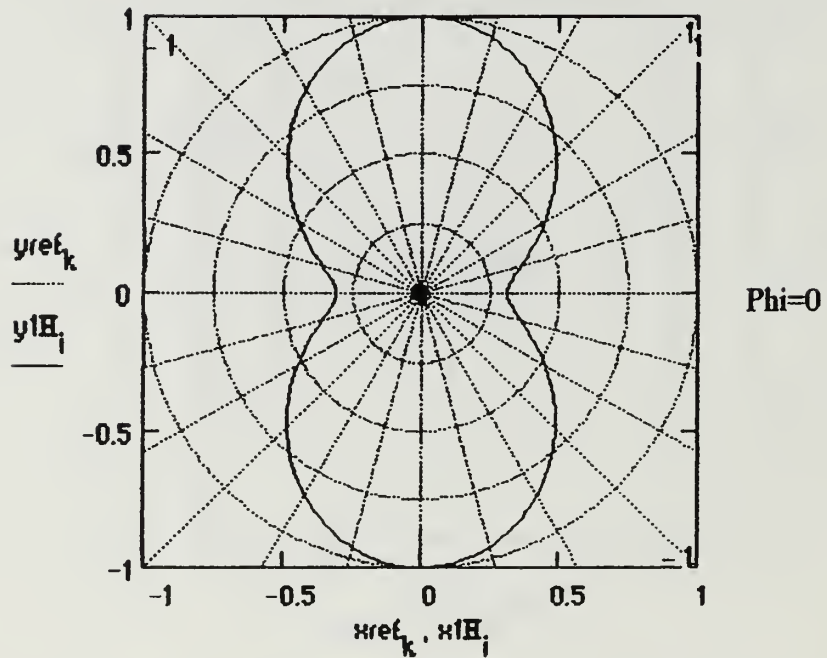
Surface Wave Radiation Pattern ($\Phi=0$)



Max E-Field Intensity (Volts per meter) $\max(\text{MagE20}) = 1.54902 \cdot 10^{-4}$

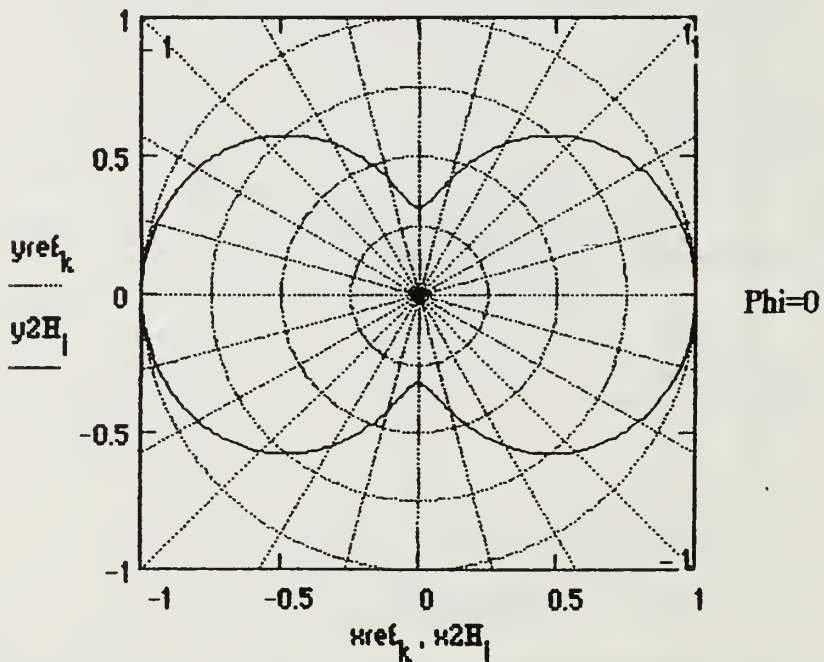
Radiation Patterns in Horizontal Plane

Space Wave Radiation Pattern



Max E-Field Intensity (Volts per meter) $\max(\text{MagE1H}) = 0.03734$

Surface Wave Radiation Pattern (Horizontal Plane)



Max E-Field Intensity (Volts per meter) $\max(\text{MagE2H}) = 1.62046 \cdot 10^{-6}$

Total Power Radiated (Watts)

$$\text{power} = 27.68975$$

**Radiation Resistance (versus
Maximum Antenna Current)
(Ohms)**

$$\text{Radres} = 55.3795$$

Directivity (or Maximum Power Gain assuming 100% Antenna Efficiency)

Phi = pi/2 Plane

Phi = 0 Plane

$$\text{DirectivityP} = 7.56408$$

$$\text{Directivity0} = 1.32021$$

Effective Isotropic Radiated Power (EIRP) (Watts)

Phi = pi/2 Plane

Phi = 0 Plane

$$\text{DirectivityP} \cdot \text{power} = 209.44744$$

$$\text{Directivity0} \cdot \text{power} = 36.55637$$

**Maximum Effective Area (Along Radial of Directivity)
(square meters)**

Phi = pi/2 Plane

Phi = 0 Plane

$$\frac{(\lambda_5)^2 \cdot \text{DirectivityP}}{4 \cdot \pi} = 135.43431$$

$$\frac{(\lambda_5)^2 \cdot \text{Directivity0}}{4 \cdot \pi} = 23.63833$$

**Maximum Effective Length (Along Radial of Directivity)
(meters)**

Phi = pi/2 Plane

Phi = 0 Plane

$$2 \cdot \sqrt{\frac{\text{Radres} \cdot (\lambda_5)^2 \cdot \text{DirectivityP}}{480 \cdot \pi^2}} = 8.92079 \quad 2 \cdot \sqrt{\frac{\text{Radres} \cdot (\lambda_5)^2 \cdot \text{Directivity0}}{480 \cdot \pi^2}} = 3.7269$$

Numerical Distances

Vertical Polarization

Horizontal Polarization

$$|P_{e0}| = 15.283$$

$$|P_{m0}| = 2.4896 \cdot 10^4$$

**Elevation Angle of Directivity (Maximum Gain)
above the Horizon (Degrees)**

Phi = pi/2 Plane

Phi = 0 Plane

$$\text{AngleP} = \begin{pmatrix} 28.24089 \\ 28.24089 \end{pmatrix}$$

$$\text{Angle0} = \begin{pmatrix} 41.64818 \\ 41.64818 \end{pmatrix}$$

HORIZONTAL DIPOLE

This application calculates far field radiation patterns and parameters associated with horizontal thin-wire dipole antennas (diameter \ll wavelength). The antenna is mounted above and parallel to the x-axis in a rectangular coordinate system. The feed is at the center of the antenna at a set height directly above the origin.

Required inputs are the antenna length, feed height above the surface, transmitted frequency, distance from the antenna, the conductivity and dielectric constant of the surface below the antenna. The planar earth model is assumed in predicting radiation patterns. Predicted operating frequencies assume that the antenna is a quarter-wavelength, half-wavelength, three-quarter-wavelength, or full wavelength dipole. A sinusoidal current input with a maximum of unity is assumed. All radiation patterns are normalized with respect to the maximum electric field intensity transmitted by the antenna in the plane of interest. The electric field magnitudes to which the patterns are normalized are displayed below their respective plots. The radiation patterns are plotted for the $\phi=0$ and $\phi=\pi/2$ vertical planes parallel and perpendicular to the x-axis respectively. A horizontal radiation pattern is plotted at an elevation selected by the index from the elevation angle index table. Polarization is a combination of vertical and horizontal depending upon spatial orientation relative to the dipole.

Input the dipole
length in meters

$$l := 5$$

$$h := \frac{1}{2}$$

Input the index of the elevation angle for
which to calculate the horizontal radiation
pattern (from the angle index table)

$$d := 535$$

Wavelengths and Frequencies

$$\lambda_1 := 4 \cdot l \qquad \lambda_2 := 2 \cdot l \qquad \lambda_3 := \frac{4 \cdot l}{3} \qquad \lambda_4 := l$$

$$f_1 := \frac{c}{\lambda_1} \qquad f_2 := \frac{c}{\lambda_2} \qquad f_3 := \frac{c}{\lambda_3} \qquad f_4 := \frac{c}{\lambda_4}$$

Possible Operating Frequencies (Hertz)

$$\frac{\lambda}{4} \text{ Dipole: } f_1 = 1.5 \cdot 10^7 \qquad \frac{\lambda}{2} \text{ Dipole: } f_2 = 3 \cdot 10^7$$

$$\frac{3 \cdot \lambda}{4} \text{ Dipole: } f_3 = 4.5 \cdot 10^7 \qquad \lambda \text{ Dipole: } f_4 = 6 \cdot 10^7$$

$$\text{Input the operating Frequency (Hertz)} \quad f_5 := 30 \cdot 10^6 \quad \lambda_5 := \frac{c}{f_5} \quad \beta := \frac{2 \cdot \pi}{\lambda_5}$$

$$\text{Input the Height of Antenna Feed (meters)} \quad H_0 := 7.6 \quad \text{Input the ground Dielectric Constant} \quad \epsilon_r := 30$$

$$\text{Input the Distance from Antenna (meters)} \quad R := 3000 \quad \text{Input the ground Conductivity:} \quad \sigma := 3 \cdot 10^{-2}$$

Index of Refraction

$$Rd_l := R - H_0 \cdot \cos(\theta_l)$$

$$Rr_l := R + H_0 \cdot \cos(\theta_l)$$

$$n := \sqrt{\epsilon_r - j \cdot \frac{18000 \cdot \sigma}{(f_5 \cdot 10^{-6})}}$$

$$\text{Complex Numerical Distance for Vertical Polarization} \quad Pe_l := \frac{-j \cdot \beta \cdot Rr_l}{2 \cdot \sin(\theta_l)^2} \cdot \left(\cos(\theta_l) + \frac{\sqrt{n^2 - \sin(\theta_l)^2}}{n^2} \right)^2$$

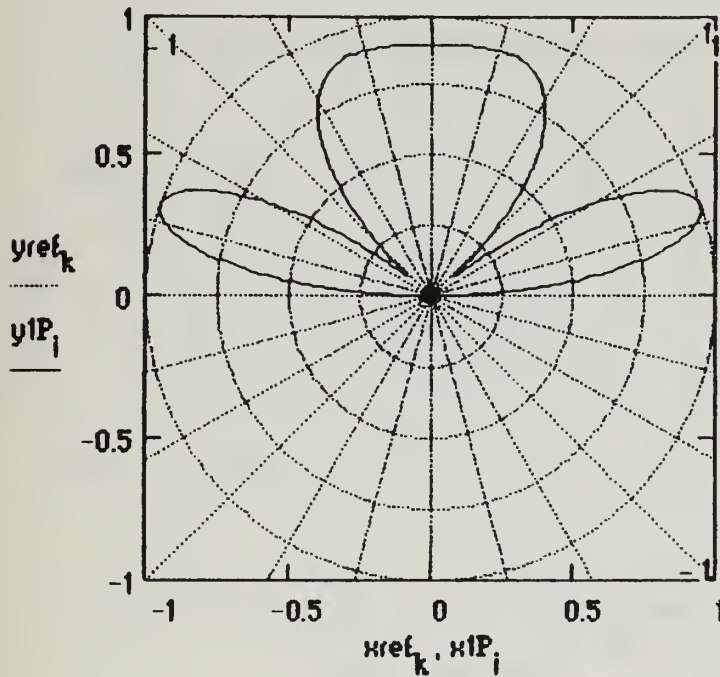
$$\text{Complex Numerical Distance for Horizontal Polarization} \quad Pm_l := \frac{-j \cdot \beta \cdot Rr_l}{2 \cdot \sin(\theta_l)^2} \cdot \left[\cos(\theta_l) + \sqrt{n^2 - (\sin(\theta_l)^2)} \right]^2$$

$$\text{Vertical Reflection Coefficient} \quad \Gamma_{v_l} := \frac{\left(n^2 \cdot \cos(\theta_l) \right) - \left(\sqrt{n^2 - \sin(\theta_l)^2} \right)}{\left(n^2 \cdot \cos(\theta_l) \right) + \left(\sqrt{n^2 - \sin(\theta_l)^2} \right)}$$

$$\text{Horizontal Reflection Coefficient} \quad \Gamma_{h_l} := \frac{\cos(\theta_l) - \left(\sqrt{n^2 - \sin(\theta_l)^2} \right)}{\cos(\theta_l) + \left(\sqrt{n^2 - \sin(\theta_l)^2} \right)}$$

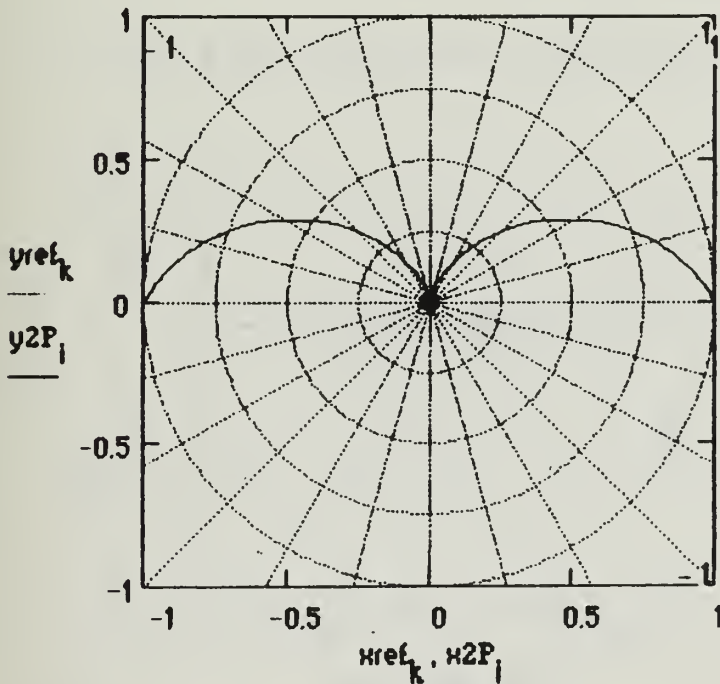
Radiation Patterns in $\Phi=\pi/2$ Plane (Perpendicular to Dipole)

Space Wave Radiation Pattern ($\Phi=\pi/2$)



Max E-Field Intensity (Volts per meter) $\max(\text{MagE1P}) = 0.03799$

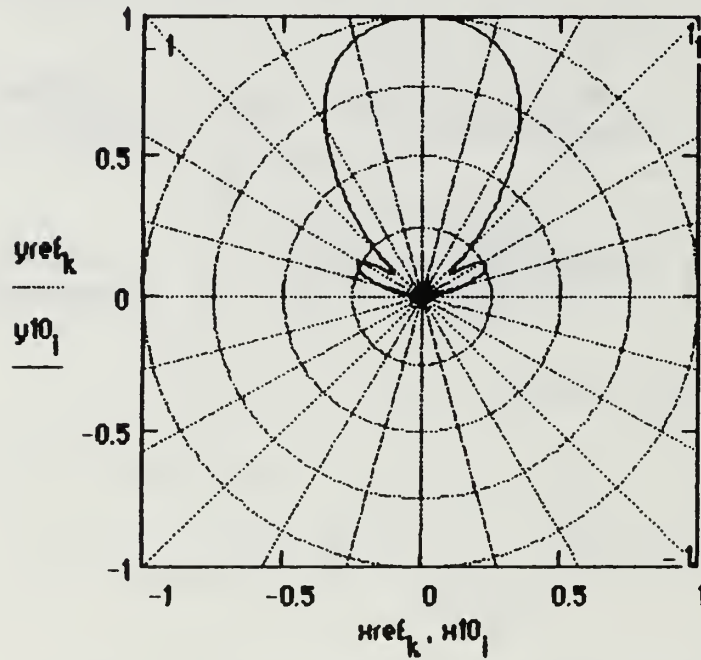
Surface Wave Radiation Pattern ($\Phi=\pi/2$)



Max E-Field Intensity (Volts per meter) $\max(\text{MagE2P}) = 6.21706 \cdot 10^{-7}$

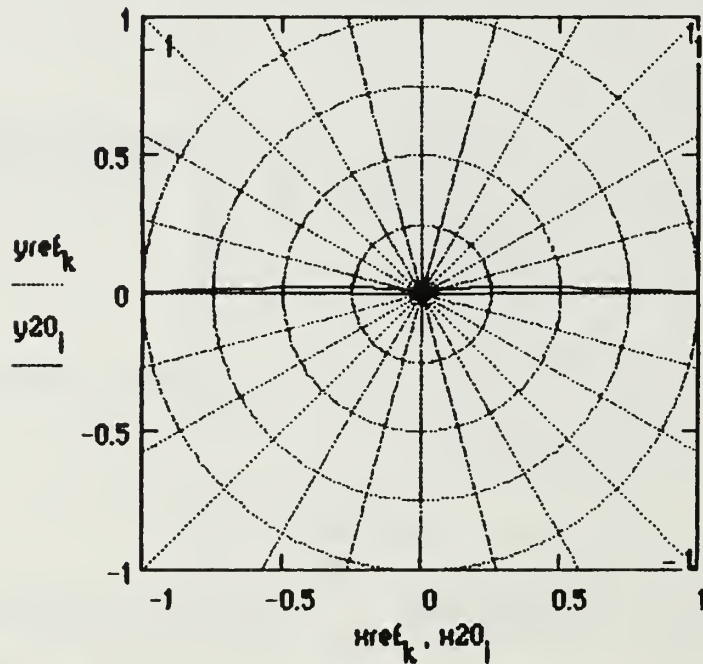
Radiation Patterns in $\Phi=0$ Plane (Parallel to Dipole)

Space Wave Radiation Pattern ($\Phi=0$)



Max E-Field Intensity (Volts per meter) $\max(\text{MagE10}) = 0.03422$

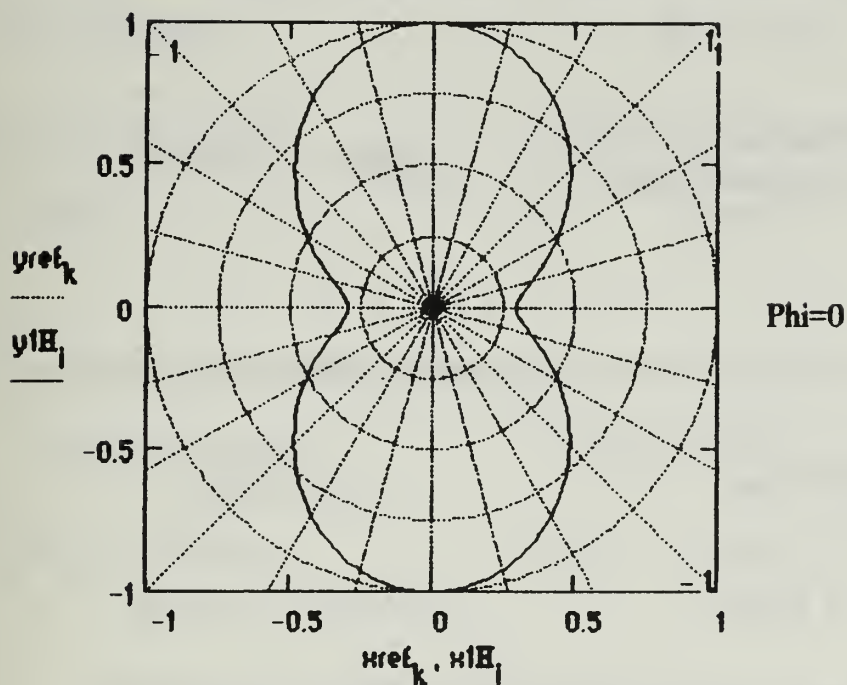
Surface Wave Radiation Pattern ($\Phi=0$)



Max E-Field Intensity (Volts per meter) $\max(\text{MagE20}) = 9.38091 \cdot 10^{-5}$

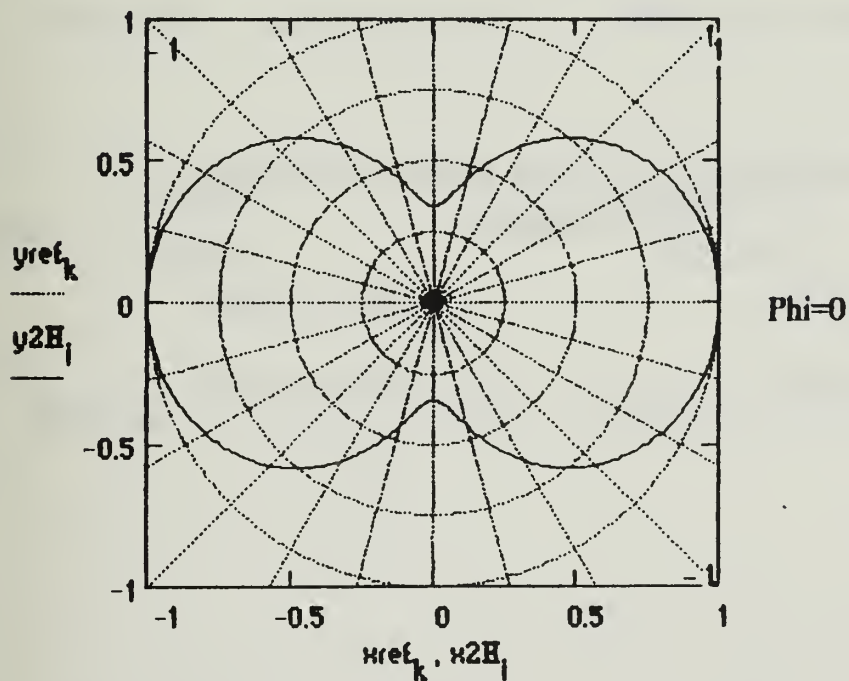
Radiation Patterns in Horizontal Plane

Space Wave Radiation Pattern



Max E-Field Intensity (Volts per meter) $\max(\text{MagE1H}) = 0.02972$

Surface Wave Radiation Pattern (Horizontal Plane)



Max E-Field Intensity (Volts per meter) $\max(\text{MagE2H}) = 1.14409 \cdot 10^{-6}$

Total Power Radiated (Watts)

$$\text{power} = 31.69054$$

**Radiation Resistance (versus
Maximum Antenna Current)
(Ohms)**

$$\text{Radres} = 63.38107$$

Directivity (or Maximum Power Gain assuming 100% Antenna Efficiency)

Phi = pi/2 Plane

Phi = 0 Plane

$$\text{DirectivityP} = 6.8304$$

$$\text{Directivity0} = 5.54301$$

Effective Isotropic Radiated Power (EIRP) (Watts)

Phi = pi/2 Plane

Phi = 0 Plane

$$\text{DirectivityP} \cdot \text{power} = 216.45893$$

$$\text{Directivity0} \cdot \text{power} = 175.66087$$

**Maximum Effective Area (Along Radial of Directivity)
(square meters)**

Phi = pi/2 Plane

Phi = 0 Plane

$$\frac{(\lambda_5)^2 \cdot \text{DirectivityP}}{4 \cdot \pi} = 54.35457$$

$$\frac{(\lambda_5)^2 \cdot \text{Directivity0}}{4 \cdot \pi} = 44.10985$$

**Maximum Effective Length (Along Radial of Directivity)
(meters)**

Phi = pi/2 Plane

Phi = 0 Plane

$$\sqrt{\frac{\text{Radres} \cdot (\lambda_5)^2 \cdot \text{DirectivityP}}{480 \cdot \pi^2}} = 6.04592 \quad 2 \cdot \sqrt{\frac{\text{Radres} \cdot (\lambda_5)^2 \cdot \text{Directivity0}}{480 \cdot \pi^2}} = 5.44643$$

Numerical Distances

Vertical Polarization

Horizontal Polarization

$$|P_{e0}| = 26.28165$$

$$|P_{m0}| = 3.21687 \cdot 10^4$$

**Elevation Angle of Directivity (Maximum Gain)
above the Horizon (Degrees)**

Phi = pi/2 Plane

Phi = 0 Plane

$$\text{AngleP} = \begin{pmatrix} 18.542 \\ 18.542 \end{pmatrix}$$

$$\text{Angle0} = \begin{pmatrix} 89.85737 \\ 89.85737 \end{pmatrix}$$

HORIZONTAL DIPOLE

This application calculates far field radiation patterns and parameters associated with horizontal thin-wire dipole antennas (diameter \ll wavelength). The antenna is mounted above and parallel to the x-axis in a rectangular coordinate system. The feed is at the center of the antenna at a set height directly above the origin. Required inputs are the antenna length, feed height above the surface, transmitted frequency, distance from the antenna, the conductivity and dielectric constant of the surface below the antenna. The planar earth model is assumed in predicting radiation patterns. Predicted operating frequencies assume that the antenna is a quarter-wavelength, half-wavelength, three-quarter-wavelength, or full wavelength dipole. A sinusoidal current input with a maximum of unity is assumed. All radiation patterns are normalized with respect to the maximum electric field intensity transmitted by the antenna in the plane of interest. The electric field magnitudes to which the patterns are normalized are displayed below their respective plots. The radiation patterns are plotted for the $\phi=0$ and $\phi=\pi/2$ vertical planes parallel and perpendicular to the x-axis respectively. A horizontal radiation pattern is plotted at an elevation selected by the index from the elevation angle index table. Polarization is a combination of vertical and horizontal depending upon spatial orientation relative to the dipole.

Input the dipole length in meters $l := 3$ $h := \frac{1}{2}$

Input the index of the elevation angle for which to calculate the horizontal radiation pattern (from the angle index table) $d := 535$

Wavelengths and Frequencies

$$\lambda_1 := 4 \cdot l \qquad \lambda_2 := 2 \cdot l \qquad \lambda_3 := \frac{4 \cdot l}{3} \qquad \lambda_4 := l$$

$$f_1 := \frac{c}{\lambda_1} \qquad f_2 := \frac{c}{\lambda_2} \qquad f_3 := \frac{c}{\lambda_3} \qquad f_4 := \frac{c}{\lambda_4}$$

Possible Operating Frequencies (Hertz)

$$\begin{array}{ll} \frac{\lambda}{4} \text{ Dipole: } f_1 = 2.5 \cdot 10^7 & \frac{\lambda}{2} \text{ Dipole: } f_2 = 5 \cdot 10^7 \\ \frac{3 \cdot \lambda}{4} \text{ Dipole: } f_3 = 7.5 \cdot 10^7 & \lambda \text{ Dipole: } f_4 = 1 \cdot 10^8 \end{array}$$

Input the operating
Frequency (Hertz)

$$f_5 := 50 \cdot 10^6$$

$$\lambda_5 := \frac{c}{f_5}$$

$$\beta := \frac{2 \cdot \pi}{\lambda_5}$$

Input the Height of
Antenna Feed (meters)

$$H_0 := 1.5$$

Input the ground
Dielectric Constant

$$\epsilon_r := 72$$

Input the Distance
from Antenna (meters)

$$R := 3000$$

Input the ground
Conductivity:

$$\sigma := 4$$

Index of Refraction

$$Rd_1 := R - H_0 \cdot \cos(\theta_1)$$

$$Rr_1 := R + H_0 \cdot \cos(\theta_1)$$

$$n := \sqrt{\epsilon_r - j \cdot \frac{18000 \cdot \sigma}{(f_5 \cdot 10^{-6})^2}}$$

Complex Numerical Distance
for Vertical Polarization

$$Pe_1 := \frac{-j \cdot \beta \cdot Rr_1}{2 \cdot \sin(\theta_1)^2} \cdot \left(\cos(\theta_1) + \frac{\sqrt{n^2 - \sin(\theta_1)^2}}{n^2} \right)^2$$

Complex Numerical Distance
for Horizontal Polarization

$$Pm_1 := \frac{-j \cdot \beta \cdot Rr_1}{2 \cdot \sin(\theta_1)^2} \cdot \left[\cos(\theta_1) + \sqrt{n^2 - (\sin(\theta_1)^2)} \right]^2$$

Vertical Reflection Coefficient

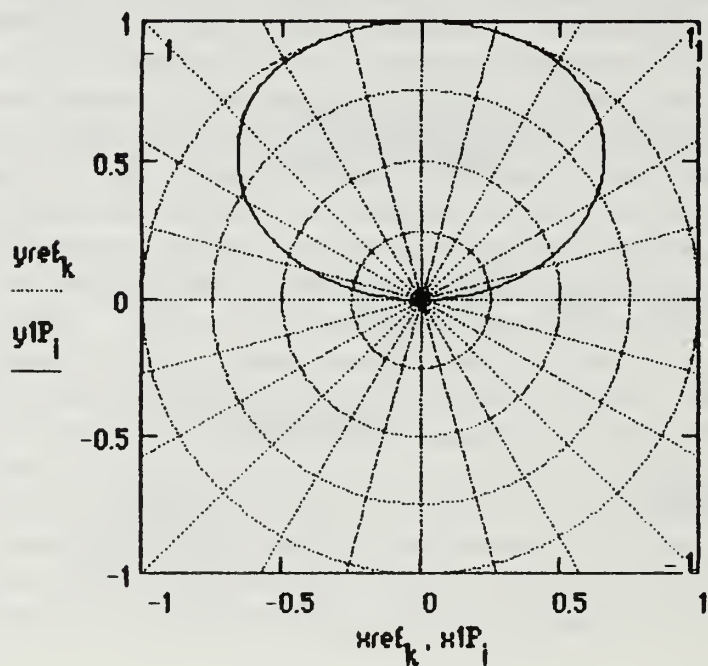
$$\Gamma_{v1} := \frac{(n^2 \cdot \cos(\theta_1)) - \left(\sqrt{n^2 - \sin(\theta_1)^2} \right)}{(n^2 \cdot \cos(\theta_1)) + \left(\sqrt{n^2 - \sin(\theta_1)^2} \right)}$$

Horizontal Reflection Coefficient

$$\Gamma_{h1} := \frac{\cos(\theta_1) - \left(\sqrt{n^2 - \sin(\theta_1)^2} \right)}{\cos(\theta_1) + \left(\sqrt{n^2 - \sin(\theta_1)^2} \right)}$$

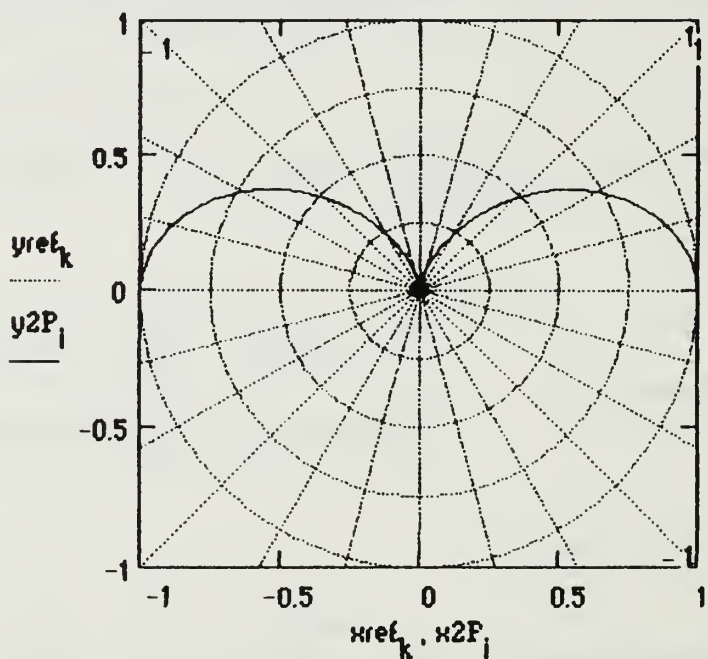
Radiation Patterns in $\Phi=\pi/2$ Plane (Perpendicular to Dipole)

Space Wave Radiation Pattern ($\Phi=\pi/2$)



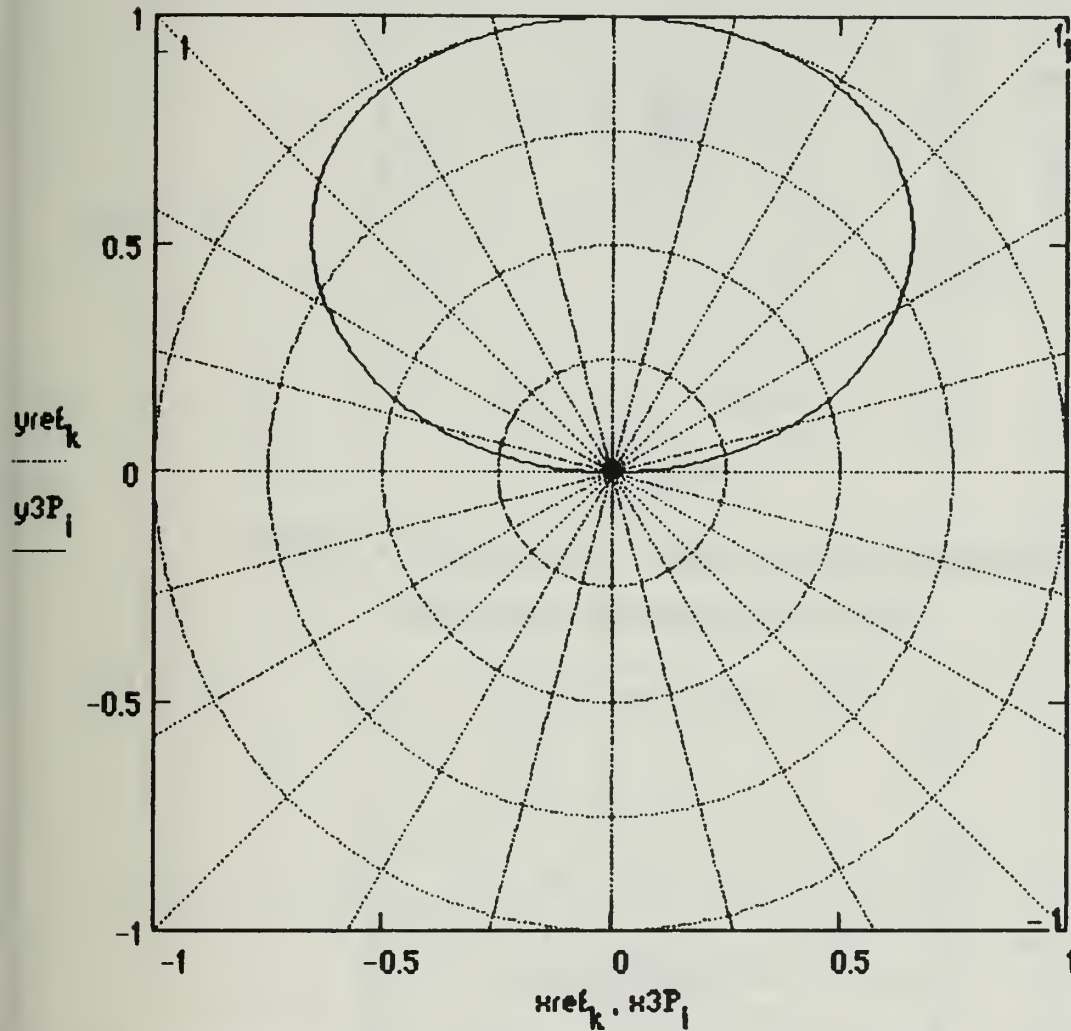
Max E-Field Intensity (Volts per meter) $\max(\text{MagE1P}) = 0.03926$

Surface Wave Radiation Pattern ($\Phi=\pi/2$)



Max E-Field Intensity (Volts per meter) $\max(\text{MagE2P}) = 8.83121 \cdot 10^{-9}$

Combined Space and Surface Wave Radiation Pattern ($\Phi = \pi/2$)

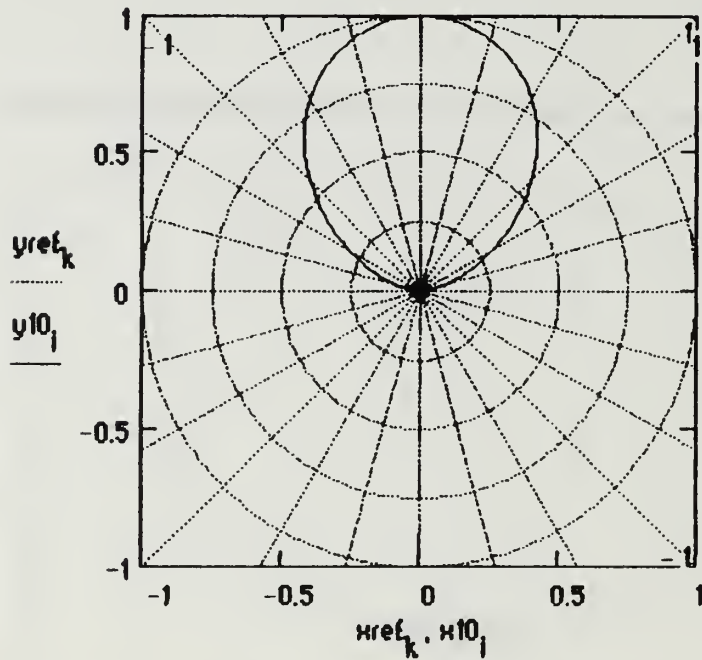


Max E-Field Intensity (Volts per meter)

$\max(\text{MagE3P}) = 0.03926$

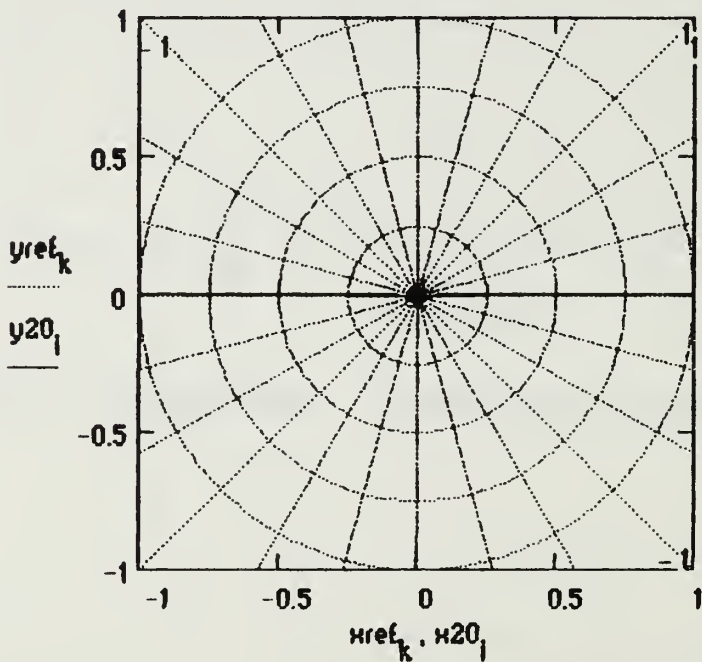
Radiation Patterns in $\Phi=0$ Plane (Parallel to Dipole)

Space Wave Radiation Pattern ($\Phi=0$)



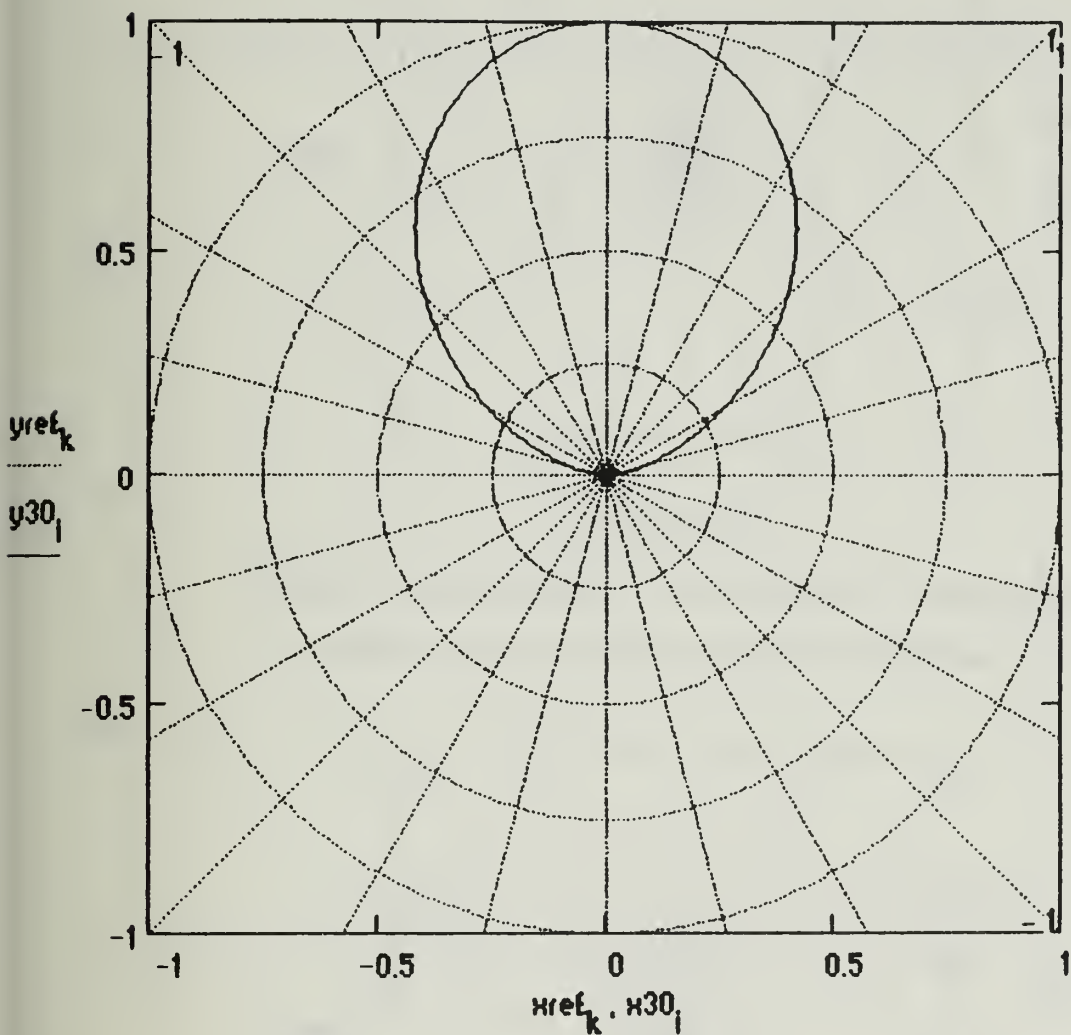
Max E-Field Intensity (Volts per meter) $\max(\text{MagE10}) = 0.03925$

Surface Wave Radiation Pattern ($\Phi=0$)



Max E-Field Intensity (Volts per meter) $\max(\text{MagE20}) = 3.2224 \cdot 10^{-4}$

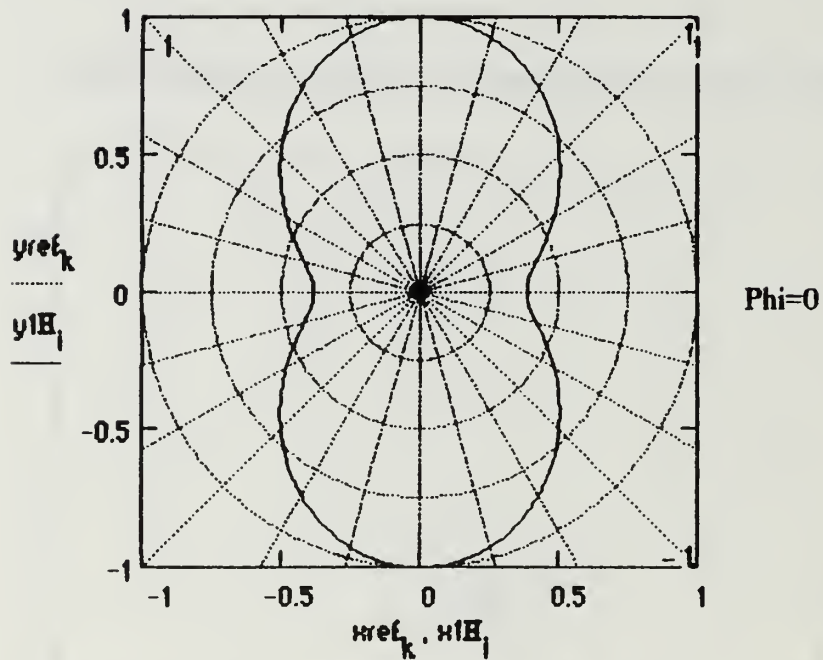
Combined Space and Surface Wave Radiation Pattern ($\Phi=0$)



Max E-Field Intensity (Volts per meter) $\max(\text{MagE30}) = 0.03925$

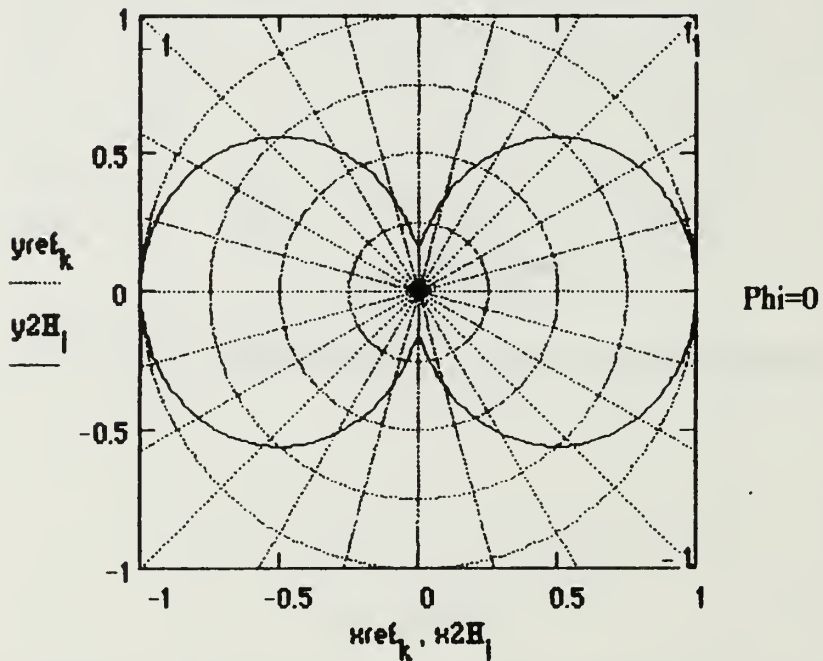
Radiation Patterns in Horizontal Plane

Space Wave Radiation Pattern



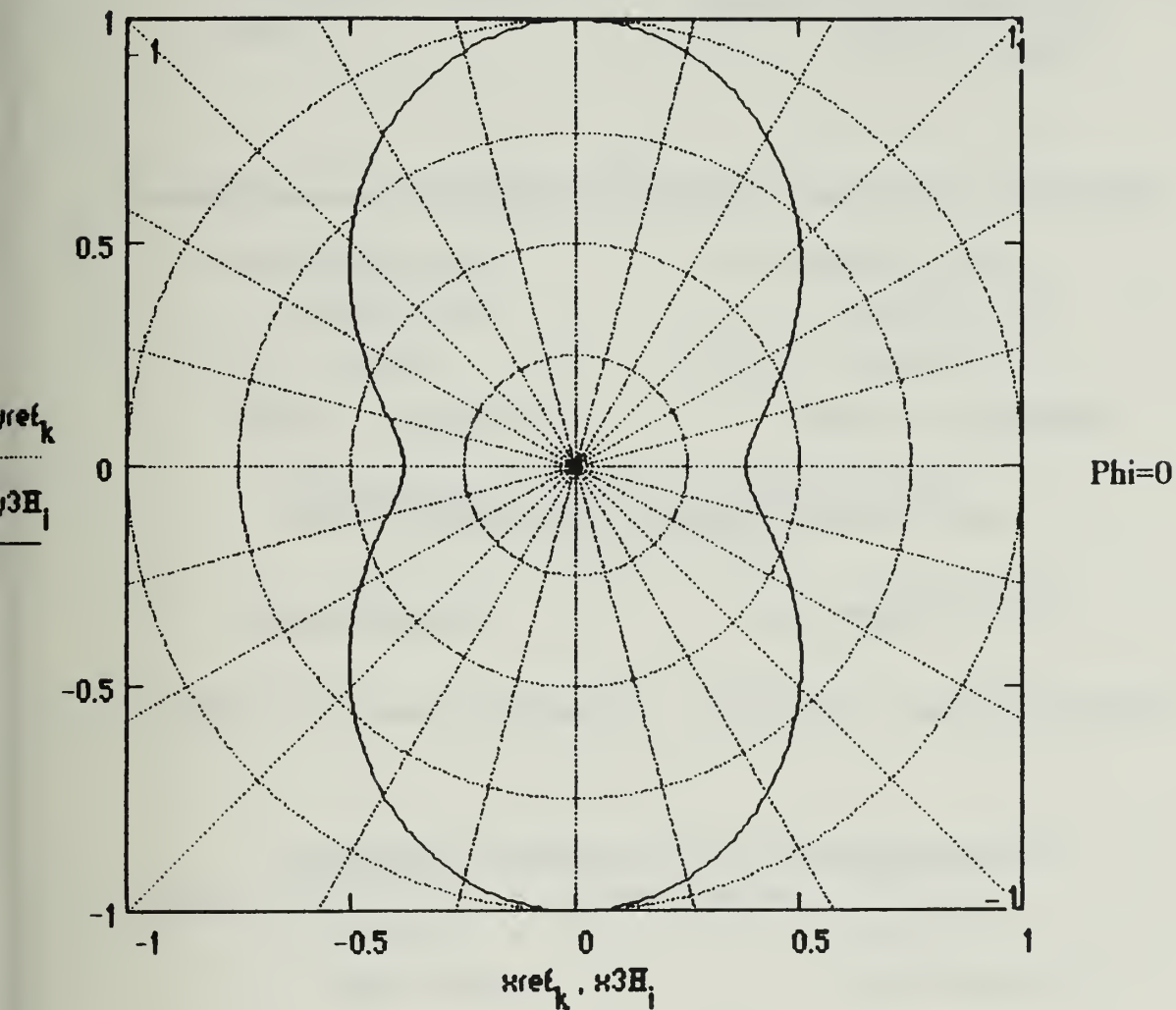
Max E-Field Intensity (Volts per meter) $\max(\text{MagE1H}) = 0.02647$

Surface Wave Radiation Pattern (Horizontal Plane)



Max E-Field Intensity (Volts per meter) $\max(\text{MagE2H}) = 4.07737 \cdot 10^{-8}$

Combined Space and Surface Wave Radiation Pattern (Horizontal Plane)



Max E-Field Intensity (Volts per meter) $\max(\text{MagE3H}) = 0.02647$

Total Power Radiated (Watts)

$$\text{power} = 41.98012$$

**Radiation Resistance (versus
Maximum Antenna Current)
(Ohms)**

$$\text{Radres} = 83.96025$$

Directivity (or Maximum Power Gain assuming 100% Antenna Efficiency)

$\Phi = \pi/2$ Plane

$\Phi = 0$ Plane

$$\text{DirectivityP} = 5.50819$$

$$\text{Directivity0} = 5.50321$$

Effective Isotropic Radiated Power (EIRP) (Watts)

$\Phi = \pi/2$ Plane

$\Phi = 0$ Plane

$$\text{DirectivityP} \cdot \text{power} = 231.23457$$

$$\text{Directivity0} \cdot \text{power} = 231.02563$$

**Maximum Effective Area (Along Radial of Directivity)
(square meters)**

$\Phi = \pi/2$ Plane

$\Phi = 0$ Plane

$$\frac{(\lambda_5)^2 \cdot \text{DirectivityP}}{4 \cdot \pi} = 15.77981$$

$$\frac{(\lambda_5)^2 \cdot \text{Directivity0}}{4 \cdot \pi} = 15.76555$$

**Maximum Effective Length (Along Radial of Directivity)
(meters)**

Phi = pi/2 Plane

Phi = 0 Plane

$$2 \cdot \sqrt{\frac{\text{Radres} \cdot (\lambda_5)^2 \cdot \text{DirectivityP}}{480 \cdot \pi^2}} = 3.74932 \quad 2 \cdot \sqrt{\frac{\text{Radres} \cdot (\lambda_5)^2 \cdot \text{Directivity0}}{480 \cdot \pi^2}} = 3.74762$$

Numerical Distances

Vertical Polarization

Horizontal Polarization

$$|P_{e0}| = 1.08943$$

$$|P_{m0}| = 2.26469 \cdot 10^6$$

**Elevation Angle of Directivity (Maximum Gain)
above the Horizon (Degrees)**

Phi = pi/2 Plane

Phi = 0 Plane

$$\text{AngleP} = \begin{pmatrix} 78.73217 \\ 78.73217 \end{pmatrix}$$

$$\text{Angle0} = \begin{pmatrix} 89.85737 \\ 89.85737 \end{pmatrix}$$

APPENDIX D:
VERTICAL LOG-PERIODIC DIPOLE ARRAY COMPUTER OUTPUT

This appendix contains computer hardcopies from the Mathcad vertical log-periodic dipole array application which show the input values and predicted radiation characteristics for two sample calculations. The configuration is a given by the inputs on the first two pages of each printout. The first antenna is mounted above soil ($\epsilon_r=10$ and $\sigma=10^{-3}$) and the second above seawater ($\epsilon_r=72$ and $\sigma=4$). Reference 6 [p. 114] provides the radiation patterns and gain predictions from several sources for the configuration in the first example.

The radiation patterns and maximum directive gain computed by the first Mathcad example are almost identical to the those given in reference 6. The directivity prediction is slightly higher for Mathcad, and the elevation of the maximum directive gain is also slightly higher, but the overall similarity between the predicted radiation characteristics is still quite good. The seawater example also yields results consistent with expectations. With respect to the soil example, the seawater example's directivity is higher due to a stronger reflected wave, and the surface wave is stronger at grazing angles ($\theta \approx 90^\circ$) due to higher conductivity.

VERTICAL LOG PERIODIC DIPOLE ARRAY

This application calculates far field radiation patterns and parameters associated with vertical log periodic dipole arrays. The antenna is oriented such that the projection of its center axis lies on the positive y-axis of a rectangular coordinate system. The antenna axis can be oriented with respect to the vertical at any angle between zero and ninety degrees. The feed is at the center of the shortest element directly above the origin. The dipole elements are bisected by the antenna axis and are parallel to the z-axis. Required inputs are the number of dipole elements, shortest and second shortest element lengths, separation between the shortest and second shortest elements, radius of the shortest element, height of the feed above the surface, angle of the antenna axis with the vertical, characteristic admittance of the line feeding the antenna, termination impedance of the antenna, transmitted frequency, distance from the antenna, the conductivity and dielectric constant of the surface below the antenna. The planar earth model is assumed in predicting radiation patterns. A sinusoidal current input with a maximum of unity is assumed. All radiation patterns are normalized with respect to the maximum electric field intensity transmitted by the antenna in the plane of interest. The electric field magnitudes to which the patterns are normalized are displayed below their respective plots. Radiation patterns are plotted for the $\phi=0$ and $\phi=\pi/2$ vertical planes perpendicular and parallel to the y-axis respectively. A horizontal radiation pattern is plotted at an elevation selected by the index from the elevation angle index table. Polarization is vertical for all vertical log-periodic antennas.

Input the number of elements	$N := 12$	Input the shortest element's Radius (meters)	$rad_0 := .00918$
Input the length of the shortest element (meters)	$l_0 := 3.673$	Input the length of the second shortest element (meters)	$l_1 := 4.373$
Input the distance from shortest to second shortest element (meters)	$d_0 := 1.0766$	Input the height of the shortest element above the surface (meters)	$H_0 := 6.87$
Input the operating Frequency (Hertz)	$f_5 := 18 \cdot 10^6$	Input the Distance from the Antenna (meters)	$R := 3000$
Input the ground Conductivity	$\sigma := 1 \cdot 10^{-3}$	Input the ground Dielectric Constant	$\epsilon_r := 10$
Input the Characteristic Admittance of the Line Feeding the Antenna (Ohms)	$ADM := \frac{1}{450}$	Input the Termination Impedance connected to longest element (Ohms)	$TIMP := 450$

Input the angle between
the vertical (z axis) and $\psi = 78$
the antenna axis (degrees)

Input the elevation index
for which to calculate the $w = 285$
horizontal radiation pattern
(from angle index table)

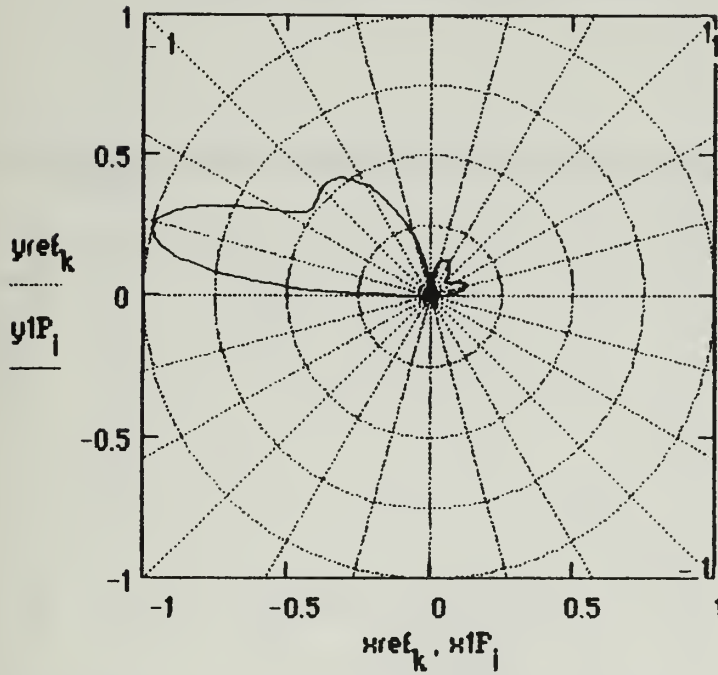
NOTE: The Vertical Log-Periodic Dipole mutual impedance calculations are not valid if there is an antenna element whose length is an exact integer multiple of the wavelength. If this occurs, there will be a singularity error in the mutual impedance calculations. If this problem arises, it will be necessary to vary the operating frequency such that no element is exactly an integer multiple of the wavelength.

If the log-periodic calculations of element length and spacing do not represent the desired antenna configuration, you can enter the values directly by selecting the variables l and d, using the define key (shift, colon), and entering the lengths and spacings by separating each successive entry by a comma.

Calculated length of elements from shortest to longest	Calculated distance between successive elements-shortest to longest	Calculated radii of elements from shortest to longest
l γ	d v	rad γ
3.673	1.0766	0.00918
4.373	1.28178	0.01093
5.20641	1.52606	0.01301
6.19864	1.8169	0.01549
7.37998	2.16316	0.01844
8.78645	2.57541	0.02196
10.46098	3.06624	0.02615
12.45463	3.6506	0.03113
14.82823	4.34633	0.03706
17.65419	5.17465	0.04412
21.01873	6.16084	0.05253
25.02447		0.06254

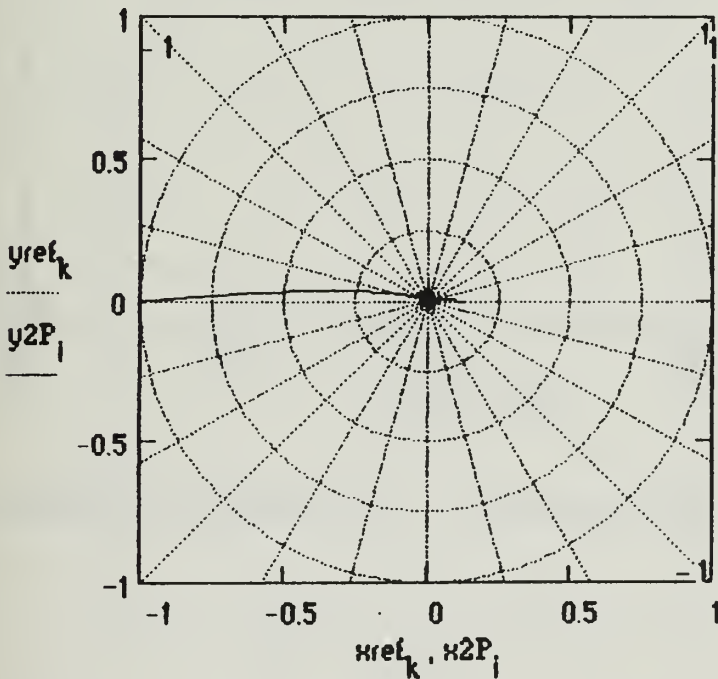
**Radiation Patterns in $\Phi=\pi/2$ Plane
(Perpendicular to X -Axis)**

Space Wave Radiation Pattern ($\Phi=\pi/2$)



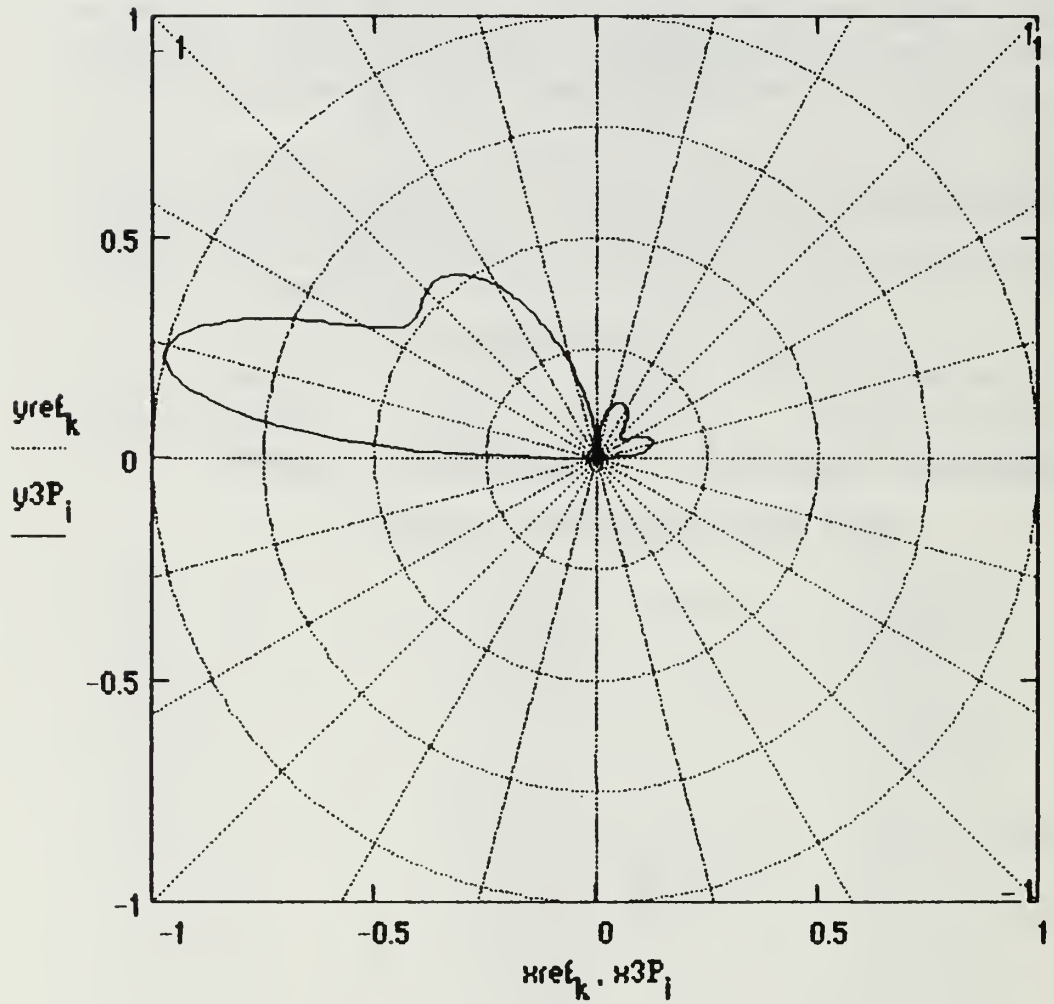
Max E-Field Intensity (Volts per meter) $\max(\text{MagE1P}) = 0.05599$

Surface Wave Radiation Pattern ($\Phi=\pi/2$)



Max E-Field Intensity (Volts per meter) $\max(\text{MagE2P}) = 0.00124$

Combined Space and Surface Wave Radiation Pattern ($\Phi = \pi/2$)

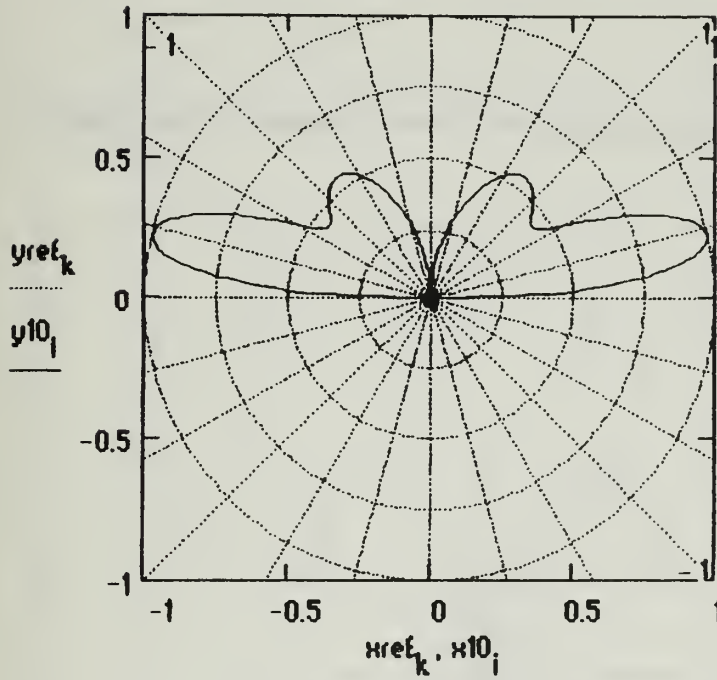


Max E-Field Intensity (Volts per meter)

$$\max(\text{MagE3P}) = 0.05583$$

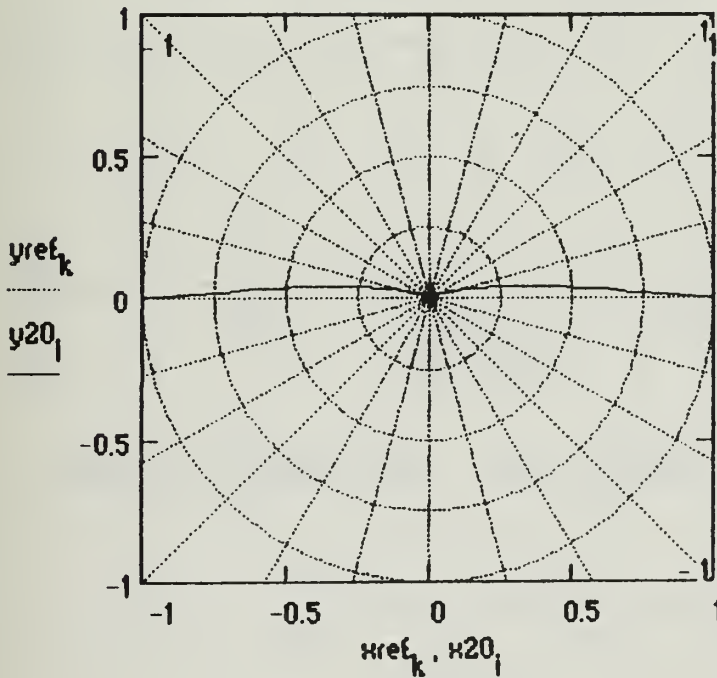
Radiation Patterns in $\Phi=0$ Plane
(Perpendicular to $\Phi=\pi/2$ Plane)

Space Wave Radiation Pattern ($\Phi=0$)



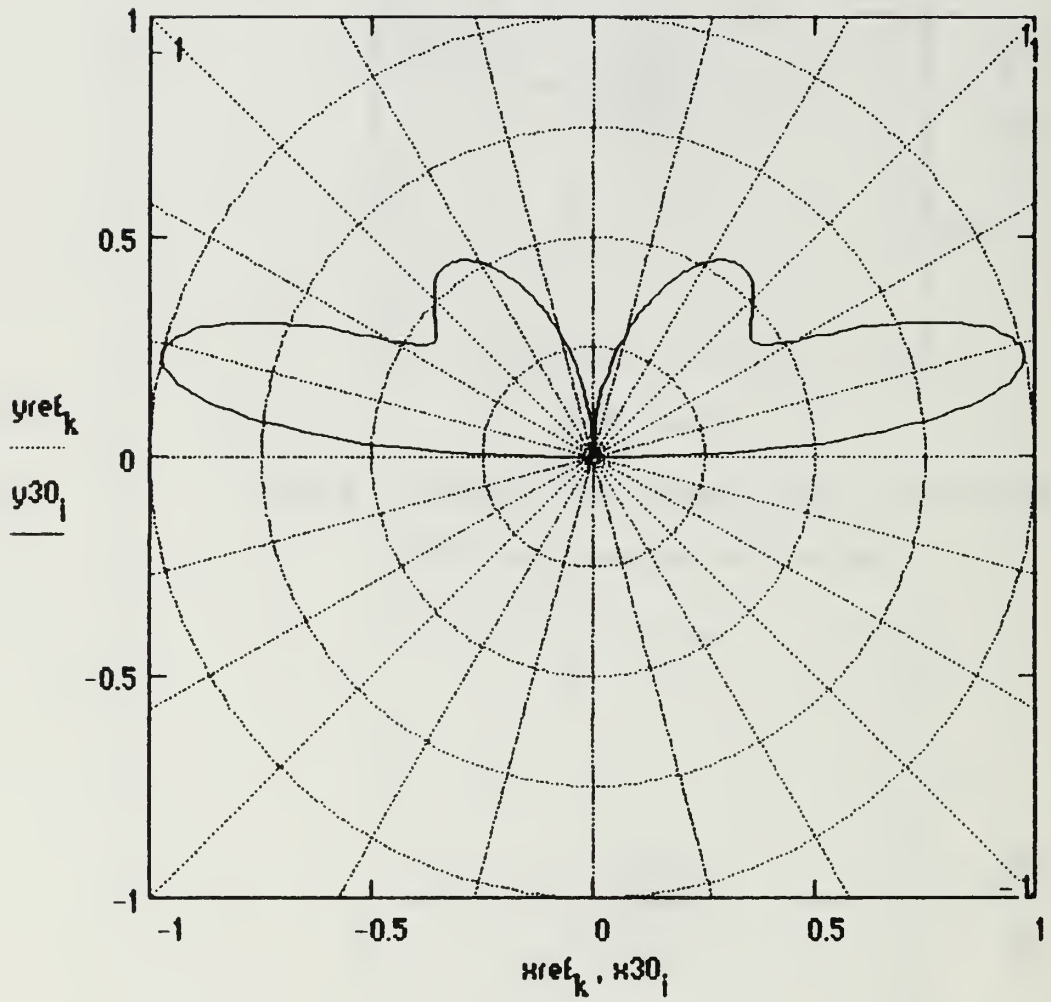
Max E-Field Intensity (Volts per meter) $\max(\text{MagE10}) = 0.03221$

Surface Wave Radiation Pattern ($\Phi=0$)



Max E-Field Intensity (Volts per meter) $\max(\text{MagE20}) = 7.64667 \cdot 10^{-4}$

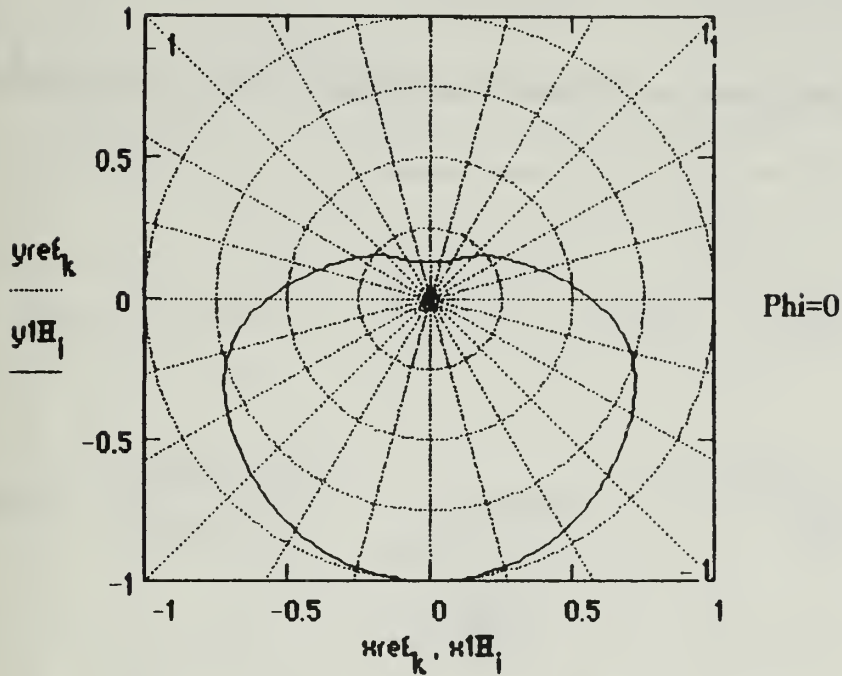
Combined Space and Surface Wave Radiation Pattern (Phi=0)



Max E-Field Intensity (Volts per meter) $\max(\text{MagE30}) = 0.0321$

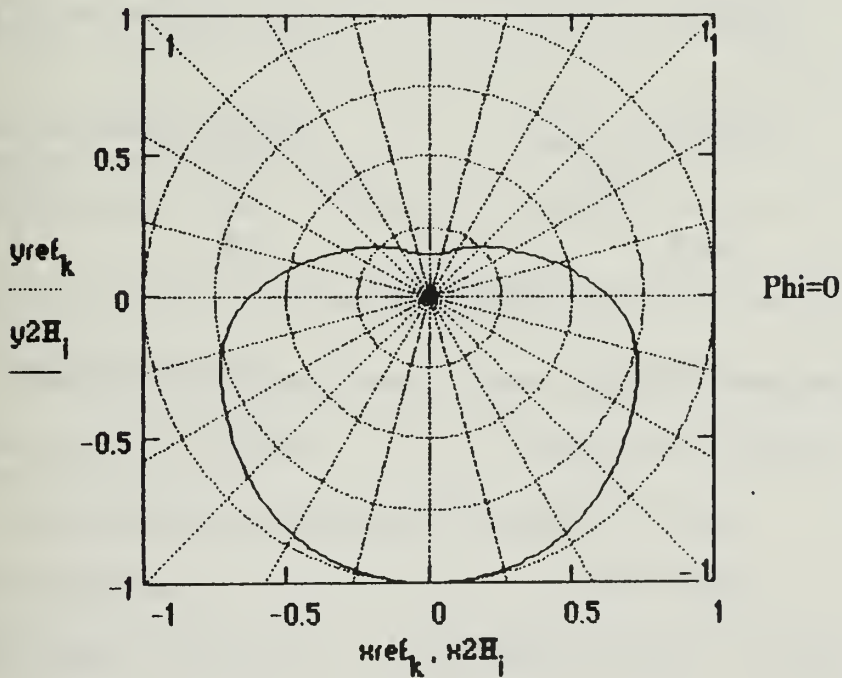
**Radiation Patterns in Horizontal Plane
(Parallel to Ground)**

Space Wave Radiation Pattern (Horizontal)



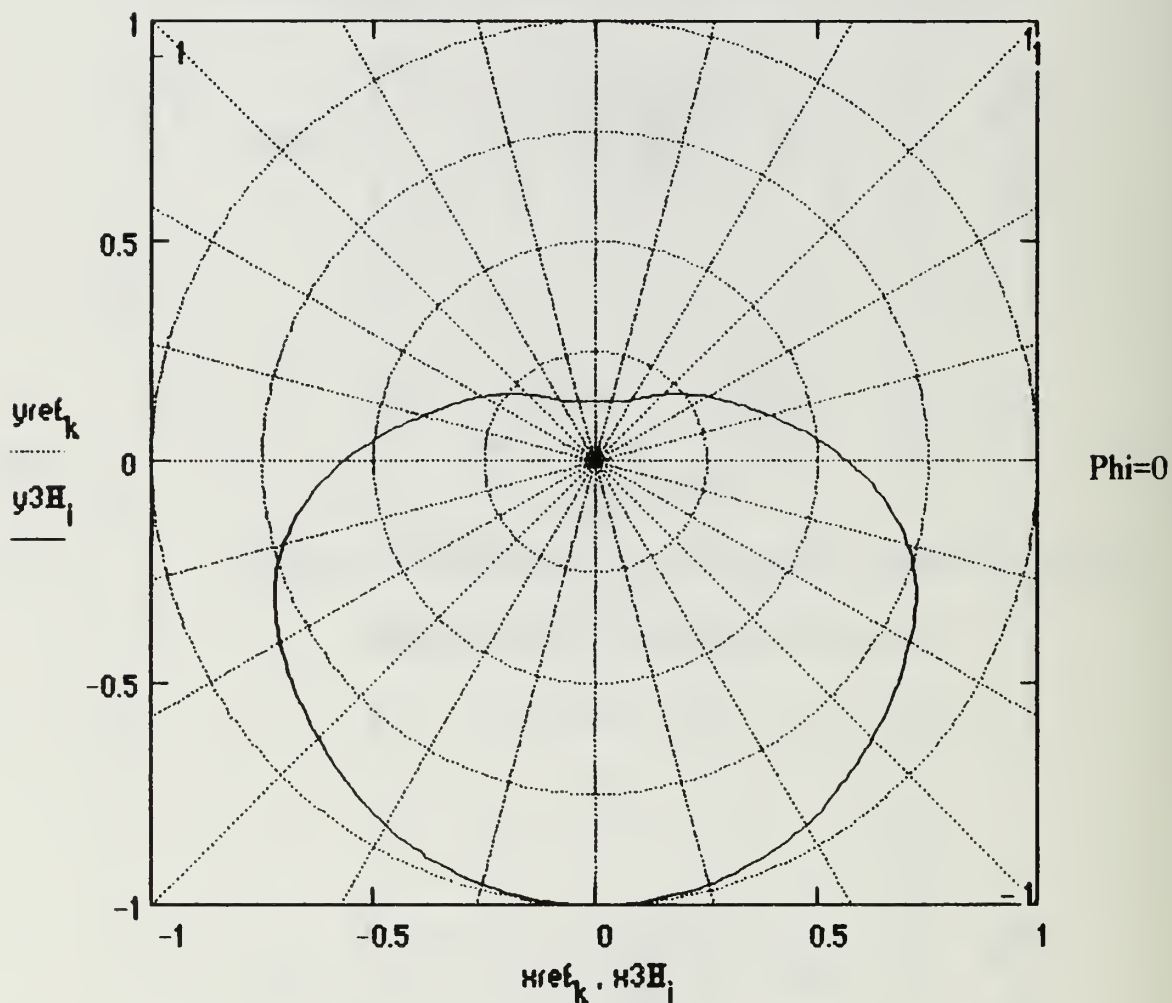
Max E-Field Intensity (Volts per meter) $\max(\text{MagE1H}) = 0.05438$

Surface Wave Radiation Pattern (Horizontal)



Max E-Field Intensity (Volts per meter) $\max(\text{MagE2H}) = 1.09861 \cdot 10^{-4}$

Combined Space and Surface Wave Radiation Pattern (Horizontal)



Max E-Field Intensity (Volts per meter) $\max(\text{MagE3H}) = 0.05427$

$$\text{power}\theta := \frac{30}{\pi \cdot R^2} \cdot \left[\int_{-\frac{\pi}{2}}^{\frac{\pi}{2}} \int_0^{\frac{\pi}{2}} \left| \sum_{\gamma} I_{\gamma} \cdot e^{j \cdot \beta \cdot Y_{\gamma} \cdot \sec(\alpha_2 + \alpha_3) \cdot (\cos(\zeta) \cdot \sin(\alpha_2 + \alpha_3) + \sin(\zeta))} \right|^2 d\alpha_2 d\alpha_3 \right]$$

$$\text{power} := \text{power}\theta$$

$$\text{Radres} := 2 \cdot \text{power}$$

$$\text{sqE3P}_i := \frac{(|\text{MagE3P}_i|)^2}{2 \cdot (120 \cdot \pi)}$$

$$\text{DirectivityP} := \frac{4 \cdot \pi \cdot R^2 \cdot \max(\text{sqE3P})}{\text{power}}$$

$$\text{sqE30}_i := \frac{(|\text{MagE30}_i|)^2}{2 \cdot (120 \cdot \pi)}$$

$$\text{Directivity0} := \frac{4 \cdot \pi \cdot R^2 \cdot \max(\text{sqE30})}{\text{power}}$$

Total Power Radiated (Watts)

$$\text{power} = 34.29572$$

Radiation Resistance (versus
Maximum Input Current)
(Ohms)

$$\text{Radres} = 68.59144$$

Directivity (or Maximum Power Gain assuming 100% Antenna Efficiency)

Phi = pi/2 Plane

Phi = 0 Plane

$$\text{DirectivityP} = 13.63346$$

$$\text{Directivity0} = 4.50794$$

Effective Isotropic Radiated Power (EIRP) (Watts)

Phi = pi/2 Plane

Phi = 0 Plane

$$\text{DirectivityP} \cdot \text{power} = 467.56917$$

$$\text{Directivity0} \cdot \text{power} = 154.6031$$

**Maximum Effective Area (Along Radial of Directivity)
(square meters)**

Phi = pi/2 Plane

$$\frac{(\lambda_5)^2 \cdot \text{DirectivityP}}{4 \cdot \pi} = 301.36553$$

Phi = 0 Plane

$$\frac{(\lambda_5)^2 \cdot \text{Directivity0}}{4 \cdot \pi} = 99.64739$$

**Maximum Effective Length (Along Radial of Directivity)
(meters)**

Phi = pi/2 Plane

$$2 \cdot \sqrt{\frac{\text{Radres} \cdot (\lambda_5)^2 \cdot \text{DirectivityP}}{480 \cdot \pi^2}} = 14.8097$$

Phi = 0 Plane

$$2 \cdot \sqrt{\frac{\text{Radres} \cdot (\lambda_5)^2 \cdot \text{Directivity0}}{480 \cdot \pi^2}} = 8.51594$$

Numerical Distance for Vertical Polarization

$$|Pe_0| = 50.7$$

**Elevation Angle of Directivity (Maximum Gain)
above the Horizon (Degrees)**

Phi = pi/2 Plane

$$\text{AngleP} = 14.28571$$

Phi = 0 Plane

$$\text{Angle0} = \begin{pmatrix} 13.71429 \\ 13.71429 \end{pmatrix}$$

VERTICAL LOG PERIODIC DIPOLE ARRAY

This application calculates far field radiation patterns and parameters associated with vertical log periodic dipole arrays. The antenna is oriented such that the projection of its center axis lies on the positive y-axis of a rectangular coordinate system. The antenna axis can be oriented with respect to the vertical at any angle between zero and ninety degrees. The feed is at the center of the shortest element directly above the origin. The dipole elements are bisected by the antenna axis and are parallel to the z-axis. Required inputs are the number of dipole elements, shortest and second shortest element lengths, separation between the shortest and second shortest elements, radius of the shortest element, height of the feed above the surface, angle of the antenna axis with the vertical, characteristic admittance of the line feeding the antenna, termination impedance of the antenna, transmitted frequency, distance from the antenna, the conductivity and dielectric constant of the surface below the antenna. The planar earth model is assumed in predicting radiation patterns. A sinusoidal current input with a maximum of unity is assumed. All radiation patterns are normalized with respect to the maximum electric field intensity transmitted by the antenna in the plane of interest. The electric field magnitudes to which the patterns are normalized are displayed below their respective plots. Radiation patterns are plotted for the $\phi=0$ and $\phi=\pi/2$ vertical planes perpendicular and parallel to the y-axis respectively. A horizontal radiation pattern is plotted at an elevation selected by the index from the elevation angle index table. Polarization is vertical for all vertical log-periodic antennas.

Input the number of elements	$N := 12$	Input the shortest element's Radius (meters)	$rad_0 := .00918$
Input the length of the shortest element (meters)	$l_0 := 3.673$	Input the length of the second shortest element (meters)	$l_1 := 4.373$
Input the distance from shortest to second shortest element (meters)	$d_0 := 1.0766$	Input the height of the shortest element above the surface (meters)	$H_0 := 6.87$
Input the operating Frequency (Hertz)	$f_5 := 18 \cdot 10^6$	Input the Distance from the Antenna (meters)	$R := 3000$
Input the ground Conductivity	$\sigma := 4$	Input the ground Dielectric Constant	$\epsilon_r := 72$
Input the Characteristic Admittance of the Line Feeding the Antenna (Ohms)	$ADM := \frac{1}{450}$	Input the Termination Impedance connected to longest element (Ohms)	$TIMP := 450$

Input the angle between
the vertical (z axis) and
the antenna axis (degrees)

$\Psi := 78$

Input the elevation index
for which to calculate the
horizontal radiation pattern
(from angle index table)

$w := 285$

NOTE: The Vertical Log-Periodic Dipole mutual impedance calculations are not valid if there is an antenna element whose length is an exact integer multiple of the wavelength. If this occurs, there will be a singularity error in the mutual impedance calculations. If this problem arises, it will be necessary to vary the operating frequency such that no element is exactly an integer multiple of the wavelength.

If the log-periodic calculations of element length and spacing do not represent the desired antenna configuration, you can enter the values directly by selecting the variables l and d , using the define key (shift, colon), and entering the lengths and spacings by separating each successive entry by a comma.

Calculated length
of elements from
shortest to longest

l γ
3.673
4.373
5.20641
6.19864
7.37998
8.78645
10.46098
12.45463
14.82823
17.65419
21.01873
25.02447

Calculated distance
between successive
elements-shortest
to longest

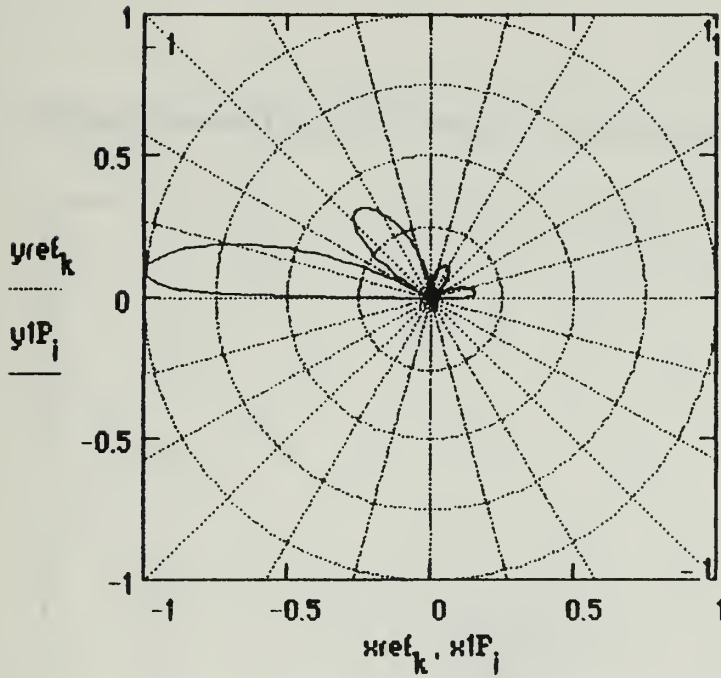
d v
1.0766
1.28178
1.52606
1.8169
2.16316
2.57541
3.06624
3.6506
4.34633
5.17465
6.16084

Calculated radii
of elements from
shortest to longest

rad γ
0.00918
0.01093
0.01301
0.01549
0.01844
0.02196
0.02615
0.03113
0.03706
0.04412
0.05253
0.06254

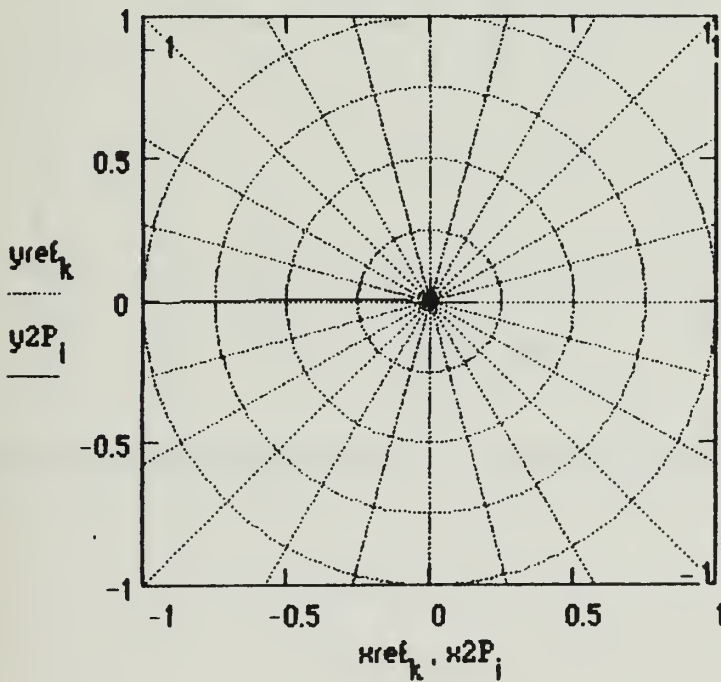
**Radiation Patterns in $\Phi = \pi/2$ Plane
(Perpendicular to X -Axis)**

Space Wave Radiation Pattern ($\Phi = \pi/2$)



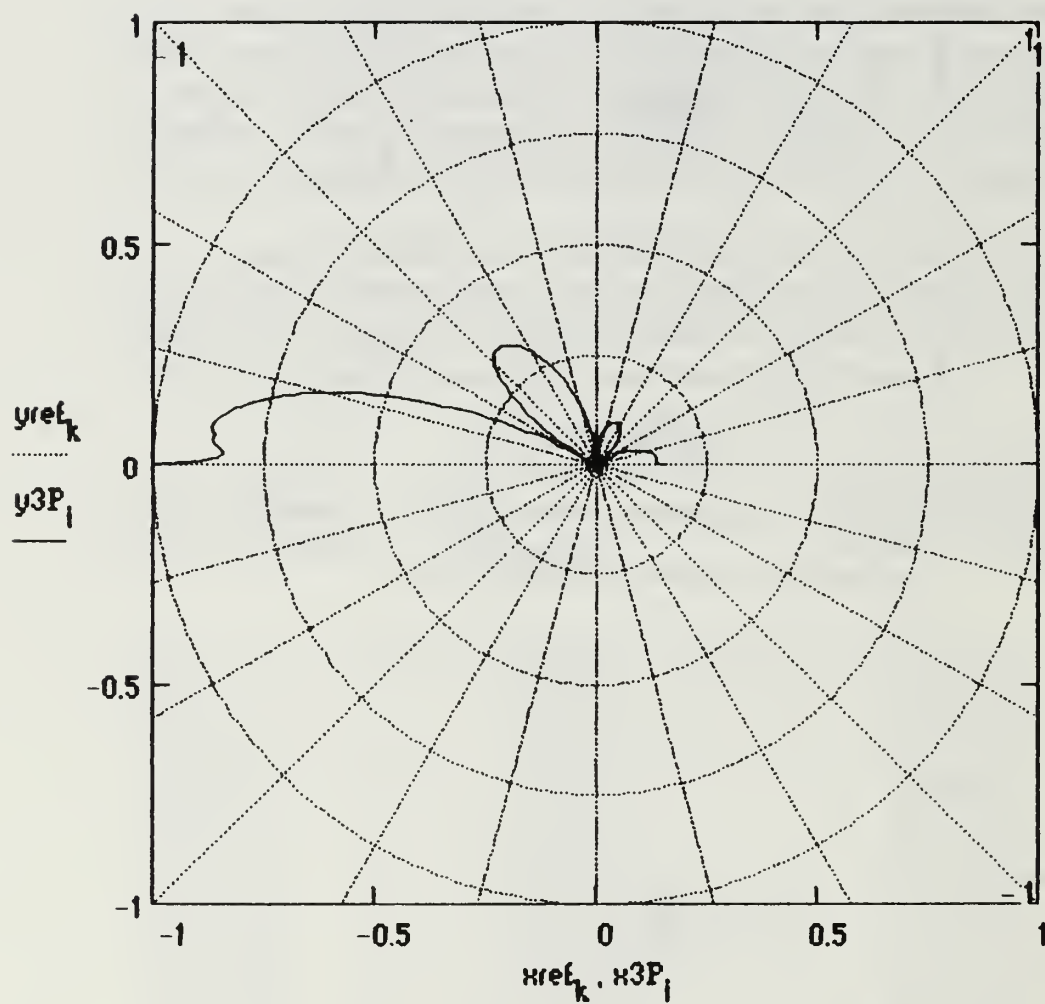
Max E-Field Intensity (Volts per meter) $\max(\text{MagE1P}) = 0.10756$

Surface Wave Radiation Pattern ($\Phi = \pi/2$)



Max E-Field Intensity (Volts per meter) $\max(\text{MagE2P}) = 0.12392$

Combined Space and Surface Wave Radiation Pattern ($\Phi = \pi/2$)

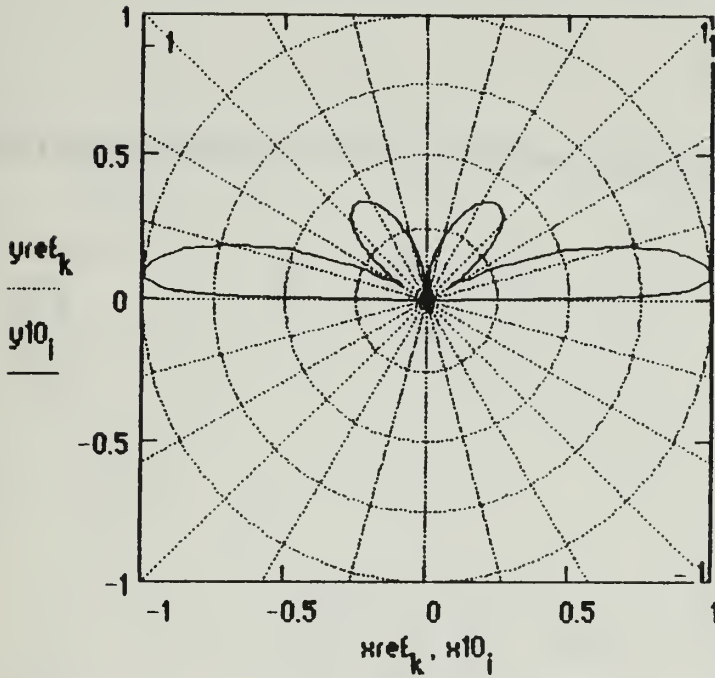


Max E-Field Intensity (Volts per meter)

$$\max(\text{MagE3P}) = 0.12392$$

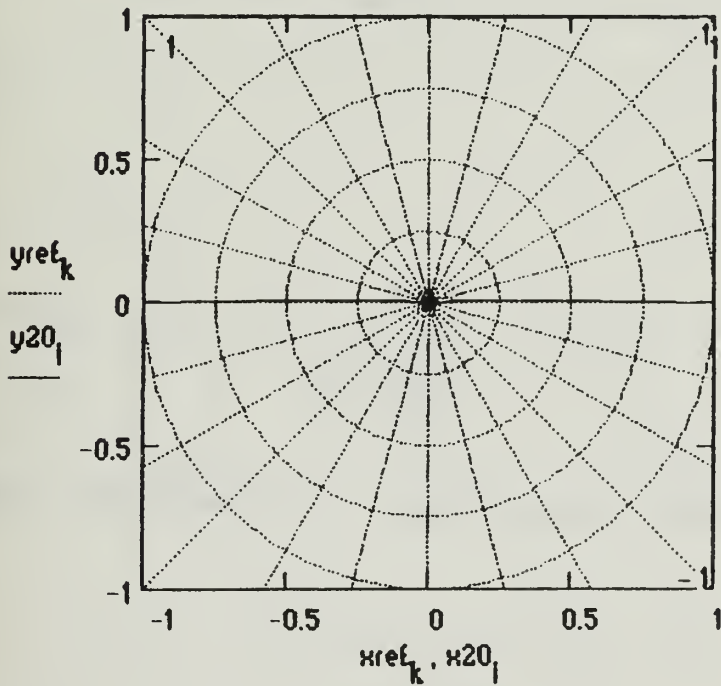
Radiation Patterns in $\Phi=0$ Plane
(Perpendicular to $\Phi=\pi/2$ Plane)

Space Wave Radiation Pattern ($\Phi=0$)



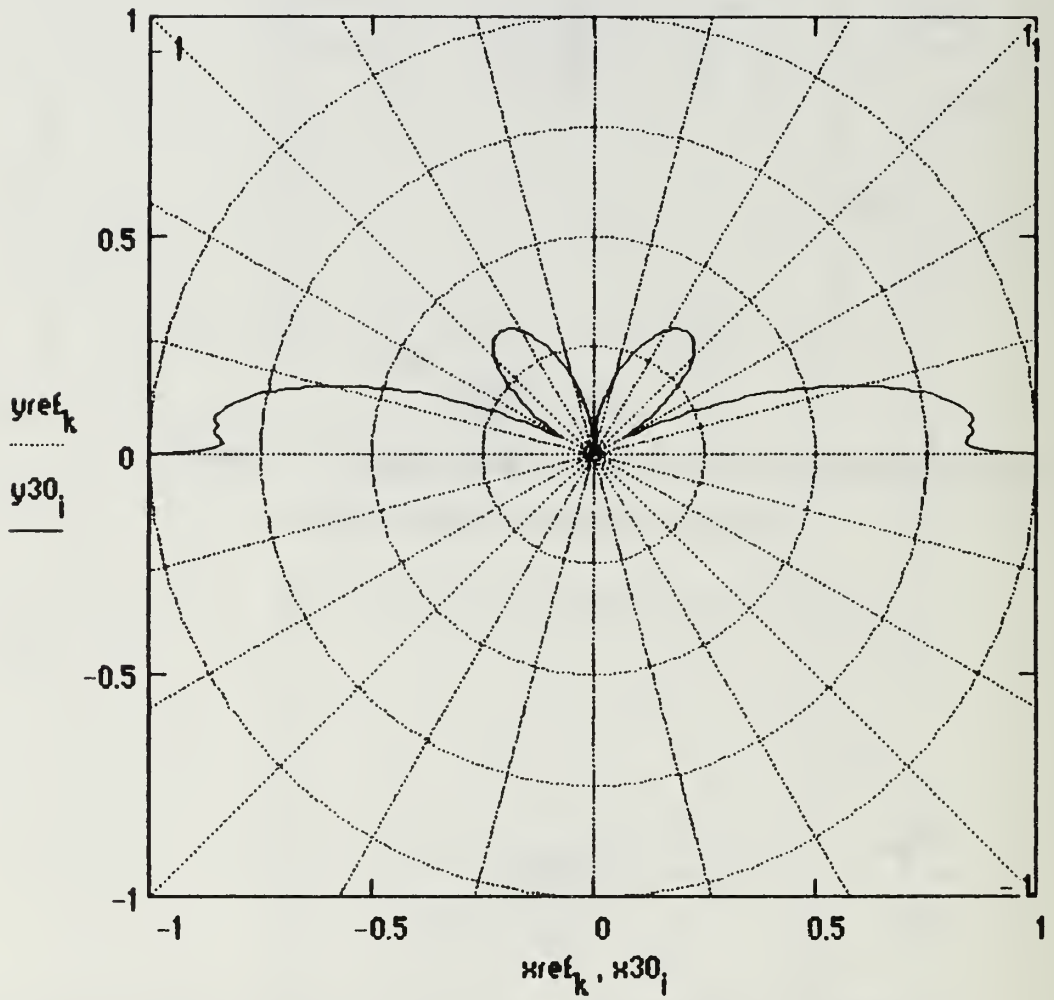
Max E-Field Intensity (Volts per meter) $\max(\text{MagE10}) = 0.06687$

Surface Wave Radiation Pattern ($\Phi=0$)



Max E-Field Intensity (Volts per meter) $\max(\text{MagE20}) = 0.07827$

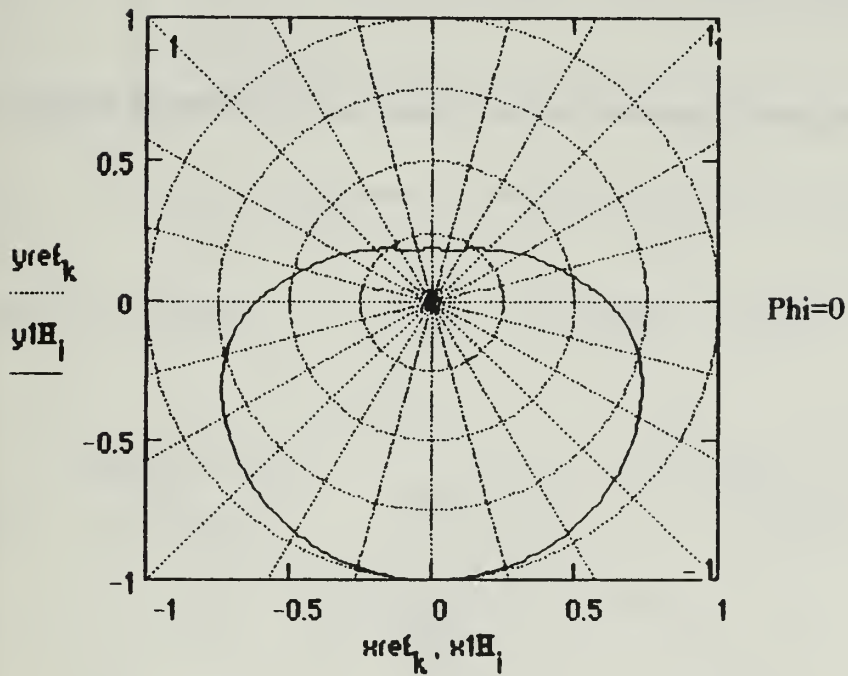
Combined Space and Surface Wave Radiation Pattern ($\Phi=0$)



Max E-Field Intensity (Volts per meter) $\max(\text{MagE30}) = 0.07827$

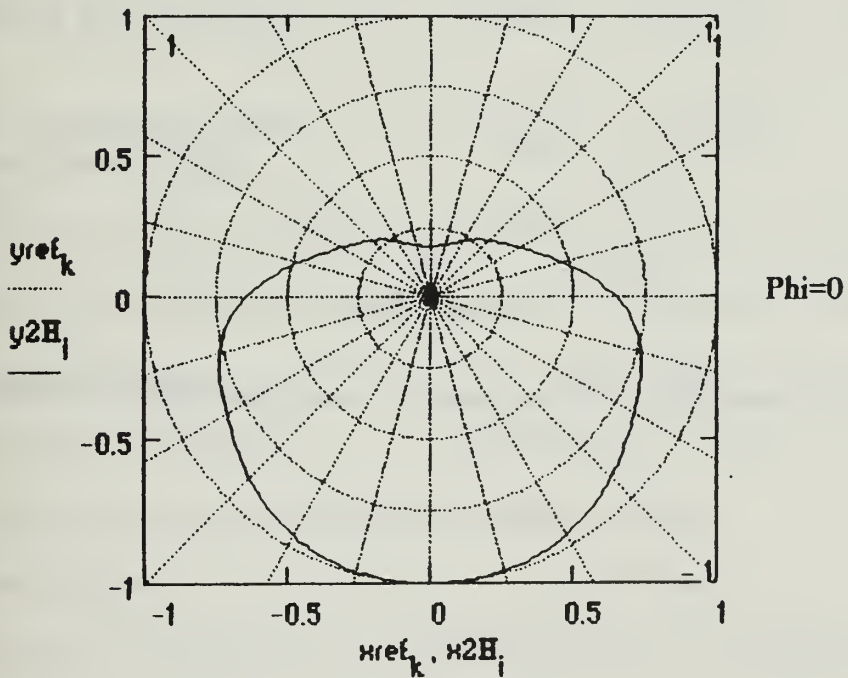
Radiation Patterns in Horizontal Plane (Parallel to Ground)

Space Wave Radiation Pattern (Horizontal)



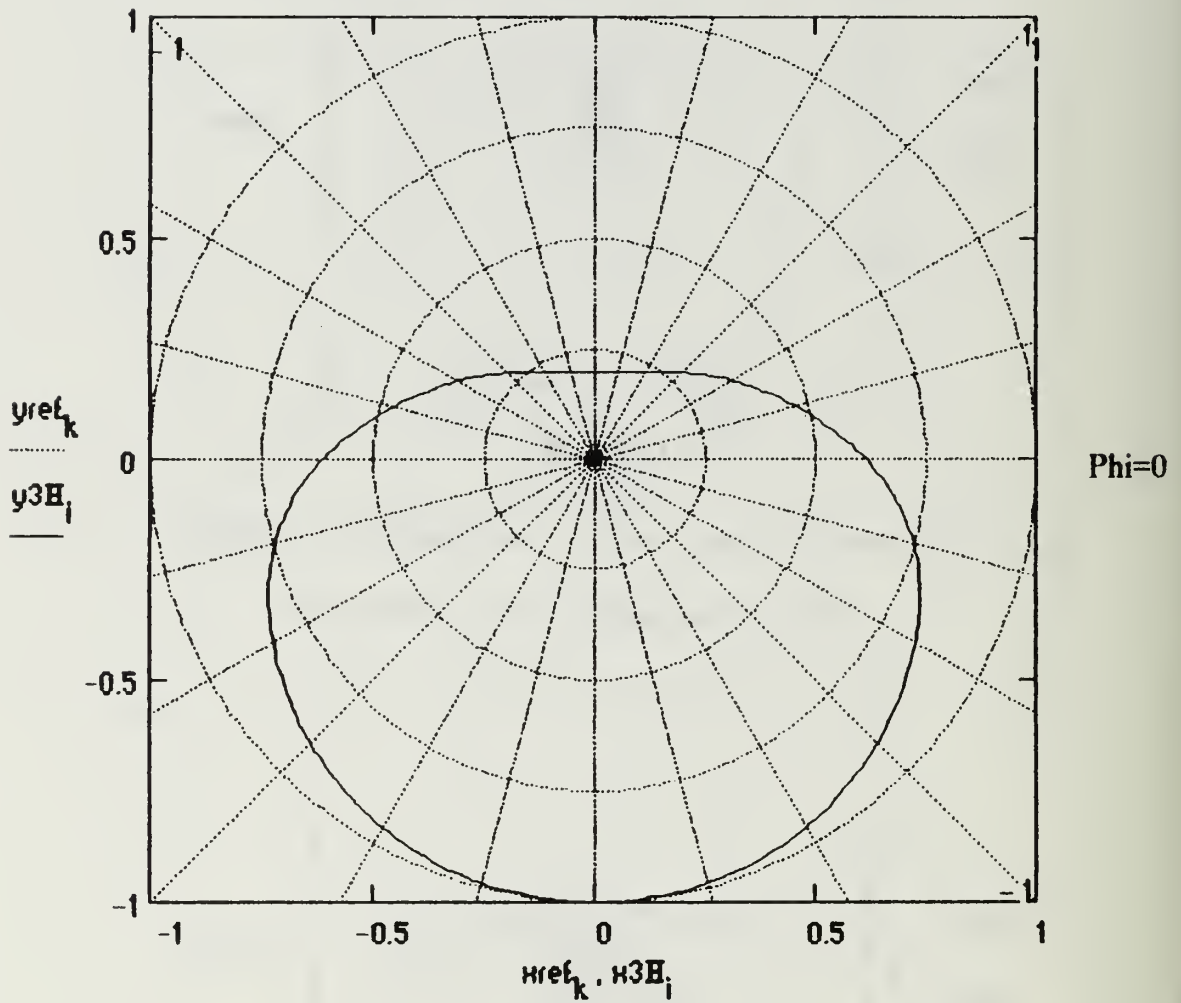
Max E-Field Intensity (Volts per meter) $\max(\text{MagE1H}) = 0.06821$

Surface Wave Radiation Pattern (Horizontal)



Max E-Field Intensity (Volts per meter) $\max(\text{MagE2H}) = 4.93203 \cdot 10^{-5}$

Combined Space and Surface Wave Radiation Pattern (Horizontal)



Max E-Field Intensity (Volts per meter) $\max(\text{MagE3H}) = 0.0682$

$$\text{ver}\theta := \frac{30}{\pi \cdot R^2} \left[\int_{-\frac{\pi}{2}}^{\frac{\pi}{2}} \int_0^{\frac{\pi}{2}} \left| \sum_{\gamma} I_{\gamma} \cdot e^{j \cdot \beta \cdot Y_{\gamma} \cdot \sec(\alpha_2 + \alpha_3) \cdot (\cos(\zeta) \cdot \sin(\alpha_2 + \alpha_3) + \sin(\zeta))} \right| \right]$$

$$\text{power} := \text{power}\theta$$

$$\text{Radres} := 2 \cdot \text{power}$$

$$\text{sqE3P}_i := \frac{(|\text{MagE3P}_i|)^2}{2 \cdot (120 \cdot \pi)}$$

$$\text{DirectivityP} := \frac{4 \cdot \pi \cdot R^2 \cdot \max(\text{sqE3P})}{\text{power}}$$

$$\text{sqE30}_i := \frac{(|\text{MagE30}_i|)^2}{2 \cdot (120 \cdot \pi)}$$

$$\text{Directivity0} := \frac{4 \cdot \pi \cdot R^2 \cdot \max(\text{sqE30})}{\text{power}}$$

Total Power Radiated (Watts)

$$\text{power} = 99.48703$$

Radiation Resistance (versus
Maximum Input Current)
(Ohms)

$$\text{Radres} = 198.97405$$

Directivity (or Maximum Power Gain assuming 100% Antenna Efficiency)

Phi = pi/2 Plane

Phi = 0 Plane

$$\text{DirectivityP} = 23.15454$$

$$\text{Directivity0} = 9.2377$$

Effective Isotropic Radiated Power (EIRP) (Watts)

Phi = pi/2 Plane

Phi = 0 Plane

$$\text{DirectivityP} \cdot \text{power} = 2.30358 \cdot 10^3$$

$$\text{Directivity0} \cdot \text{power} = 919.03096$$

**Maximum Effective Area (Along Radial of Directivity)
(square meters)**

Phi = pi/2 Plane

$$\frac{(\lambda_5)^2 \cdot \text{DirectivityP}}{4 \cdot \pi} = 511.82763$$

Phi = 0 Plane

$$\frac{(\lambda_5)^2 \cdot \text{Directivity0}}{4 \cdot \pi} = 204.19793$$

**Maximum Effective Length (Along Radial of Directivity)
(meters)**

Phi = pi/2 Plane

$$2 \cdot \sqrt{\frac{\text{Radres} \cdot (\lambda_5)^2 \cdot \text{DirectivityP}}{480 \cdot \pi^2}} = 32.87188$$

Phi = 0 Plane

$$2 \cdot \sqrt{\frac{\text{Radres} \cdot (\lambda_5)^2 \cdot \text{Directivity0}}{480 \cdot \pi^2}} = 20.76291$$

Numerical Distance for Vertical Polarization

$$|Pe_0| = 0.14135$$

**Elevation Angle of Directivity (Maximum Gain)
above the Horizon (Degrees)**

Phi = pi/2 Plane

$$\text{AngleP} = 0$$

Phi = 0 Plane

$$\text{Angle0} = \begin{pmatrix} 0 \\ 0 \end{pmatrix}$$

APPENDIX E:
HORIZONTAL LOG-PERIODIC DIPOLE ARRAY COMPUTER OUTPUT

This appendix contains computer hardcopies from the Mathcad horizontal log-periodic dipole array application which show the input values and predicted radiation characteristics for two sample calculations. The configuration is given by the inputs on the first two pages of each printout. The first antenna is mounted above soil ($\epsilon_r=4$ and $\sigma=10^{-3}$) and the second above seawater ($\epsilon_r=72$ and $\sigma=4$). Reference 6 [p. 108] provides the radiation patterns and gain predictions from several sources for the configuration in the first example.

The radiation patterns and maximum directive gain computed by the first Mathcad example are almost identical to the those given in reference 6. The directivity prediction is slightly higher for Mathcad, but the overall similarity among the predicted radiation patterns is remarkably good. The seawater example has results very much like the soil example. For horizontal polarization, the higher conductivity surface below the antenna does not result in a greatly enhanced surface wave and increased directivity as it does for vertical polarization.

HORIZONTAL LOG PERIODIC DIPOLE ARRAY

This application calculates far field radiation patterns and parameters associated with horizontal log periodic dipole arrays. The antenna is oriented such that the projection of its center axis lies on the positive y-axis of a rectangular coordinate system. The antenna axis can be oriented with respect to the vertical at any angle between zero and ninety degrees. The feed is at the center of the shortest element directly above the origin. The dipole elements are bisected by the antenna axis and are parallel to the x-axis. Required inputs are the number of dipole elements, shortest and second shortest element lengths, separation between the shortest and second shortest elements, radius of the shortest element, height of the feed above the surface, angle of the antenna axis with the vertical, characteristic admittance of the line feeding the antenna, termination impedance of the antenna, transmitted frequency, distance from the antenna, the conductivity and dielectric constant of the surface below the antenna. The planar earth model is assumed in predicting radiation patterns. A sinusoidal current input with a maximum of unity is assumed. All radiation patterns are normalized with respect to the maximum electric field intensity transmitted by the antenna in the plane of interest. The electric field magnitudes to which the patterns are normalized are displayed below their respective plots. Radiation patterns are plotted for the $\phi = \pi/2$ and $\phi = 0$ vertical planes parallel and perpendicular to the y-axis respectively. A horizontal radiation pattern is plotted at an elevation selected by the index from the elevation angle index table. Polarization is a varying combination of horizontal and vertical depending on spatial orientation with respect to the antenna.

Input the number of elements	$N := 12$	Input the shortest element's Radius (meters)	$rad_0 := .00144$
Input the length of the shortest element (meters)	$l_0 := 7.219$	Input the length of the second shortest element (meters)	$l_1 := 8.297$
Input the distance from shortest to second shortest element (meters)	$d_0 := 1.659$	Input the height of the shortest element above the surface (meters)	$H_0 := 9.4$
Input the operating Frequency (Hertz)	$f_5 := 12 \cdot 10^6$	Input the Distance from the Antenna (meters)	$R := 3000$
Input the ground Conductivity	$\sigma := 1 \cdot 10^{-3}$	Input the ground Dielectric Constant	$\epsilon_r := 4$
Input the Characteristic Admittance of the Line Feeding the Antenna (Ohms)	$ADM := \frac{1}{300}$	Input the Termination Impedance connected to longest element (Ohms)	$TIMP := 300$

Input the angle between
the vertical (z axis) and
the antenna axis (degrees)

$\Psi := 90$

Elevation index for which
to calculate horizontal pattern
(from angle index table)

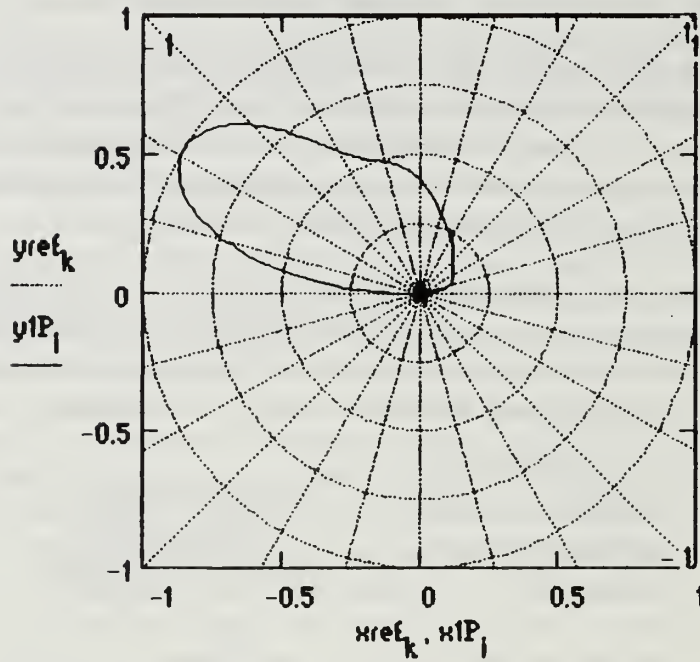
$w := 285$

NOTE: The Horizontal Log-Periodic Dipole mutual impedance calculations are not valid if there is an antenna element whose length is an exact integer multiple of the wavelength. If this occurs, there will be a singularity error in the mutual impedance calculations. If this problem arises, it will be necessary to vary the operating frequency such that no element is exactly an integer multiple of the wavelength.

If the log-periodic calculations of element length and spacing do not represent the desired antenna configuration, you can enter the values directly by selecting the variables l and d, using the define key (shift, colon), and entering the successive lengths and spacings by separating each successive entry by a comma.

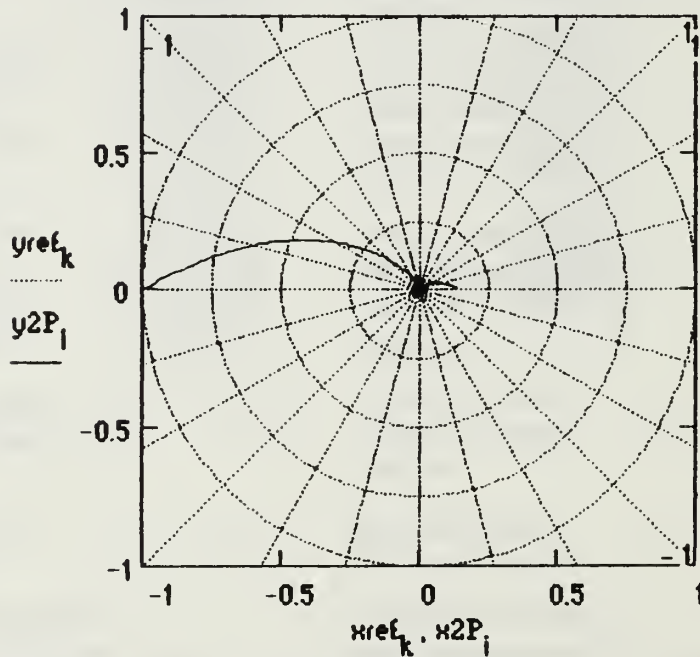
Calculated length of elements from shortest to longest	Calculated distance between successive elements-shortest to longest	Calculated radii of elements from shortest to longest
l	d	rad
γ	v	γ
7.219	1.659	0.00144
8.297	1.90674	0.00166
9.53598	2.19146	0.0019
10.95997	2.51871	0.00219
12.5966	2.89483	0.00251
14.47762	3.32711	0.00289
16.63954	3.82394	0.00332
19.12429	4.39496	0.00381
21.98009	5.05125	0.00438
25.26233	5.80554	0.00504
29.03471	6.67247	0.00579
33.37041		0.00666

Radiation Patterns in $\Phi = \pi/2$ Plane
(Perpendicular to X-Axis and Dipole Elements)
Space Wave Radiation Pattern ($\Phi = \pi/2$)



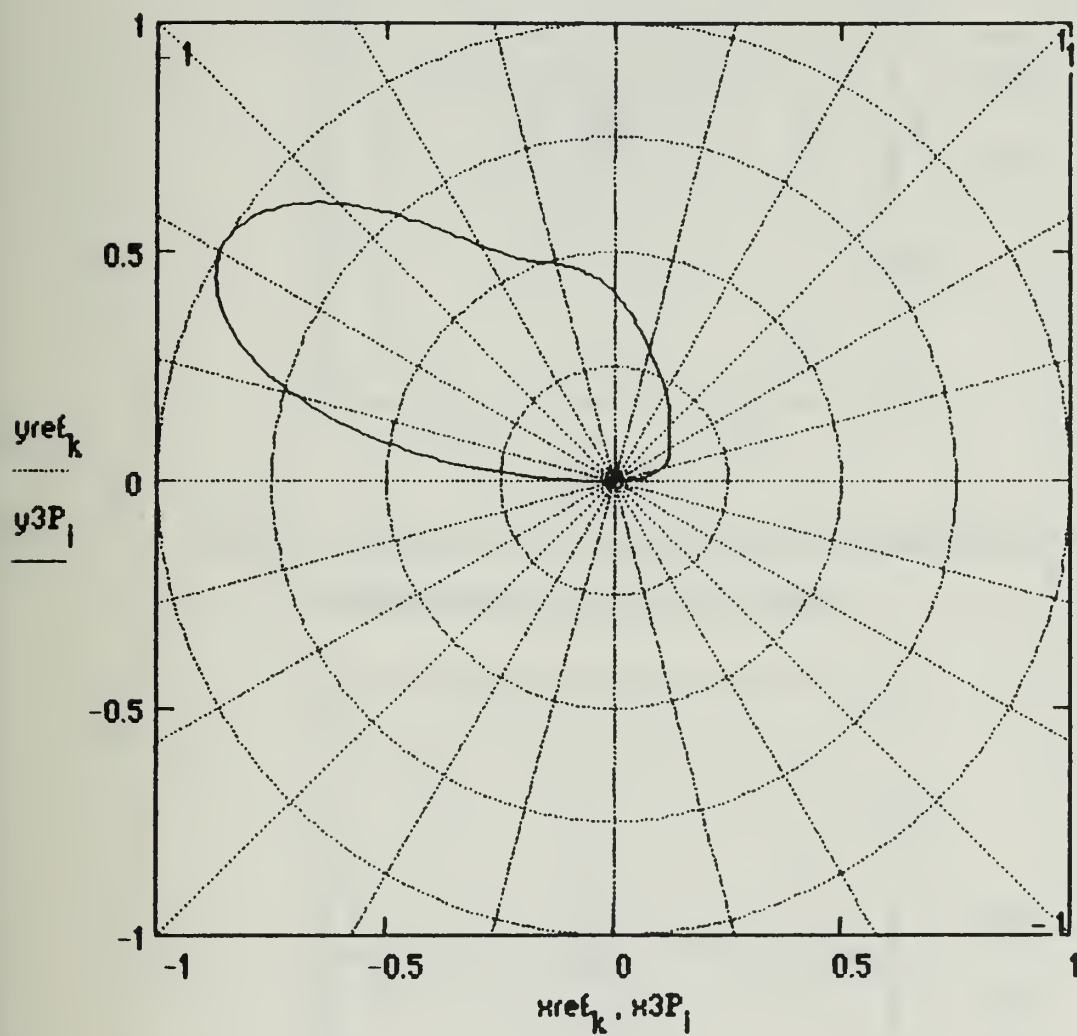
Max E-Field Intensity (Volts per meter) $\max(\text{MagE1P}) = 0.08512$

Surface Wave Radiation Pattern ($\Phi = \pi/2$)



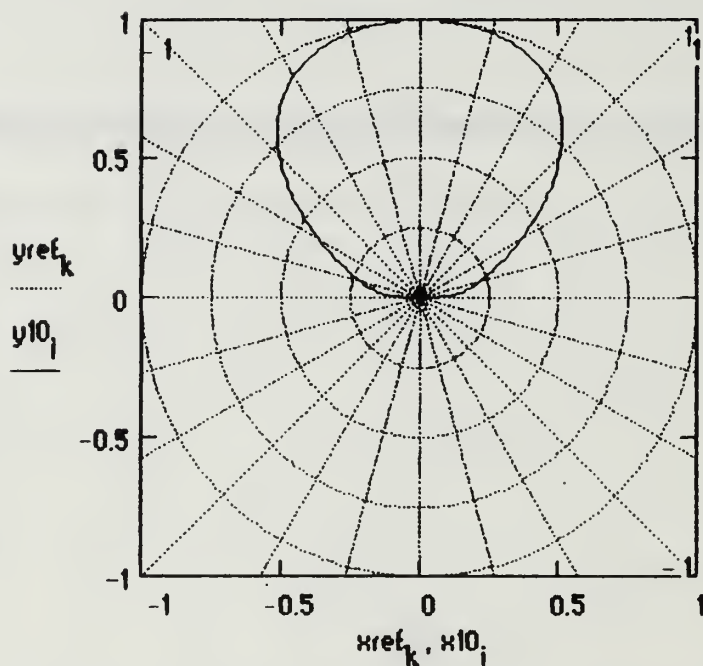
Max E-Field Intensity (Volts per meter) $\max(\text{MagE2P}) = 4.54242 \cdot 10^{-5}$

Combined Space and Surface Wave Radiation Pattern ($\Phi=\pi/2$)



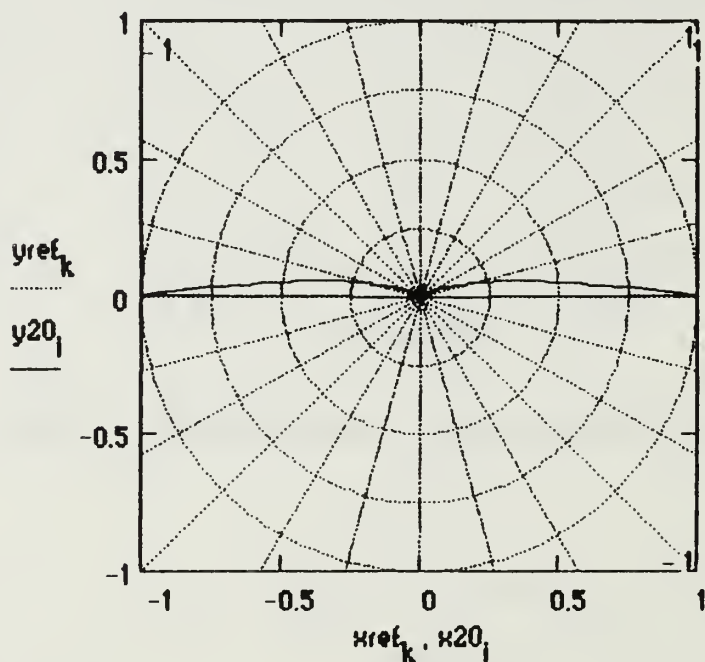
Max E-Field Intensity (Volts per meter) $\max(\text{MagE3P}) = 0.08511$

Radiation Patterns in $\Phi=0$ Plane
(Perpendicular to $\Phi=\pi/2$ Plane)
Space Wave Radiation Pattern ($\Phi=0$)



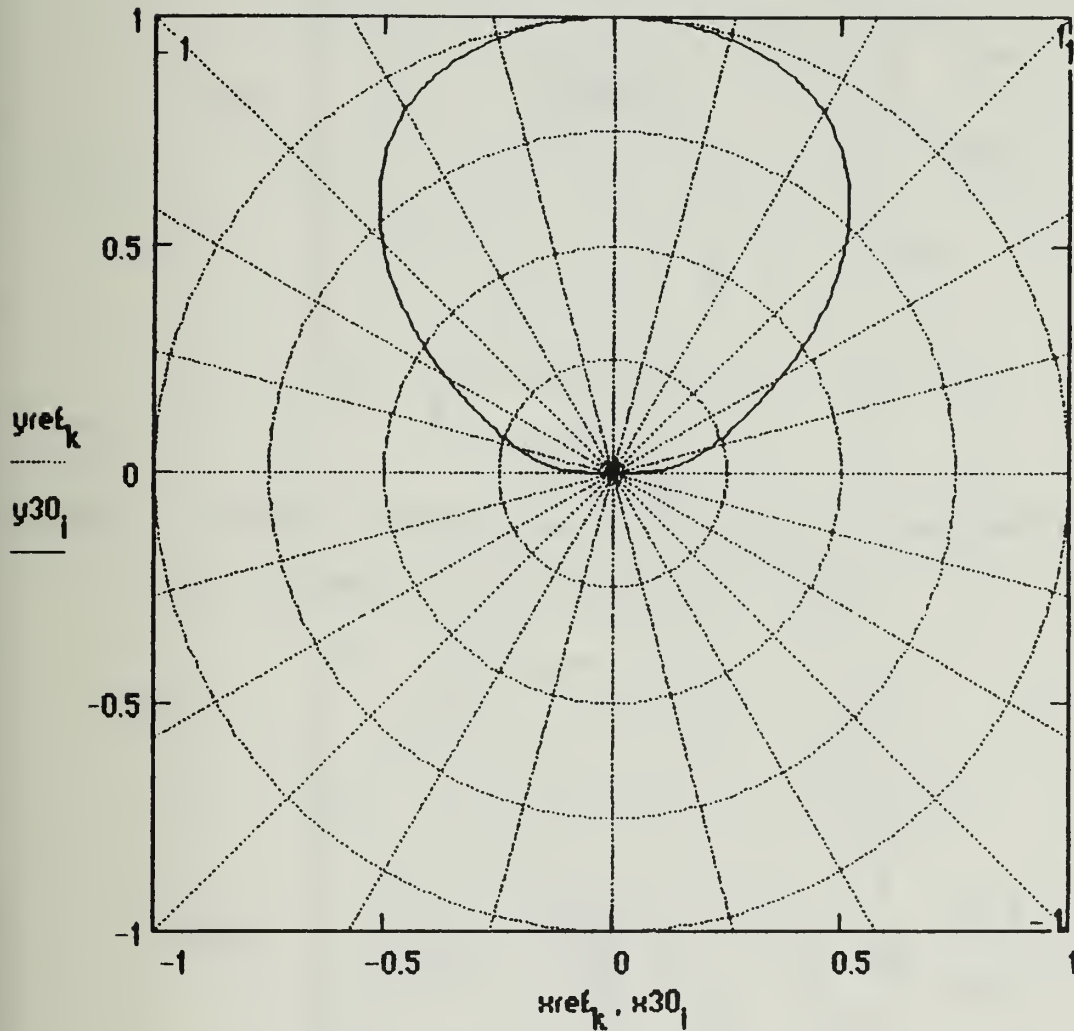
Max E-Field Intensity (Volts per meter) $\max(\text{MagE10}) = 0.03495$

Surface Wave Radiation Pattern ($\Phi=0$)



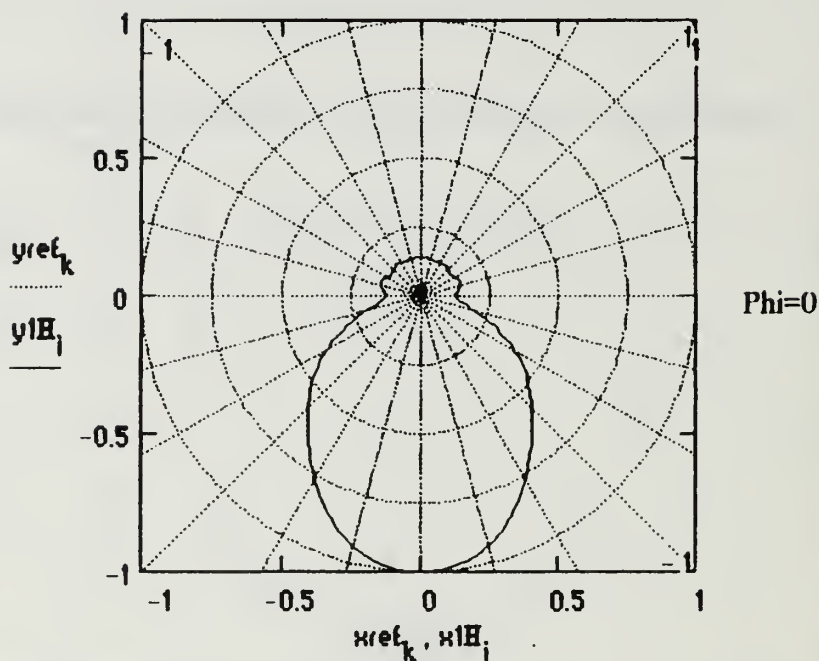
Max E-Field Intensity (Volts per meter) $\max(\text{MagE20}) = 1.45261 \cdot 10^{-4}$

Combined Space and Surface Wave Radiation Pattern ($\Phi=0$)



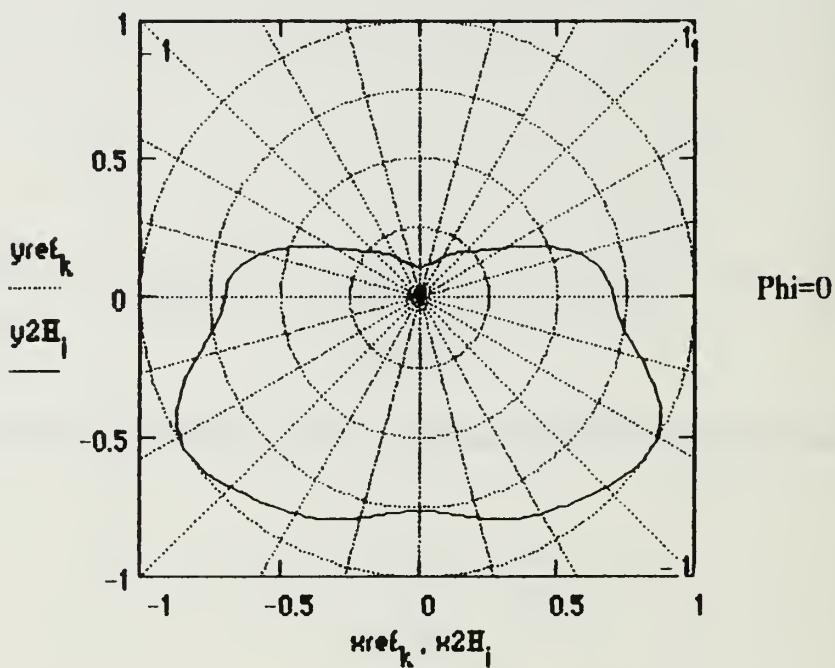
Max E-Field Intensity (Volts per meter) $\max(\text{MagE30}) = 0.03495$

**Radiation Patterns in Horizontal Plane
(Parallel to Ground)**
Space Wave Radiation Pattern (Horizontal)



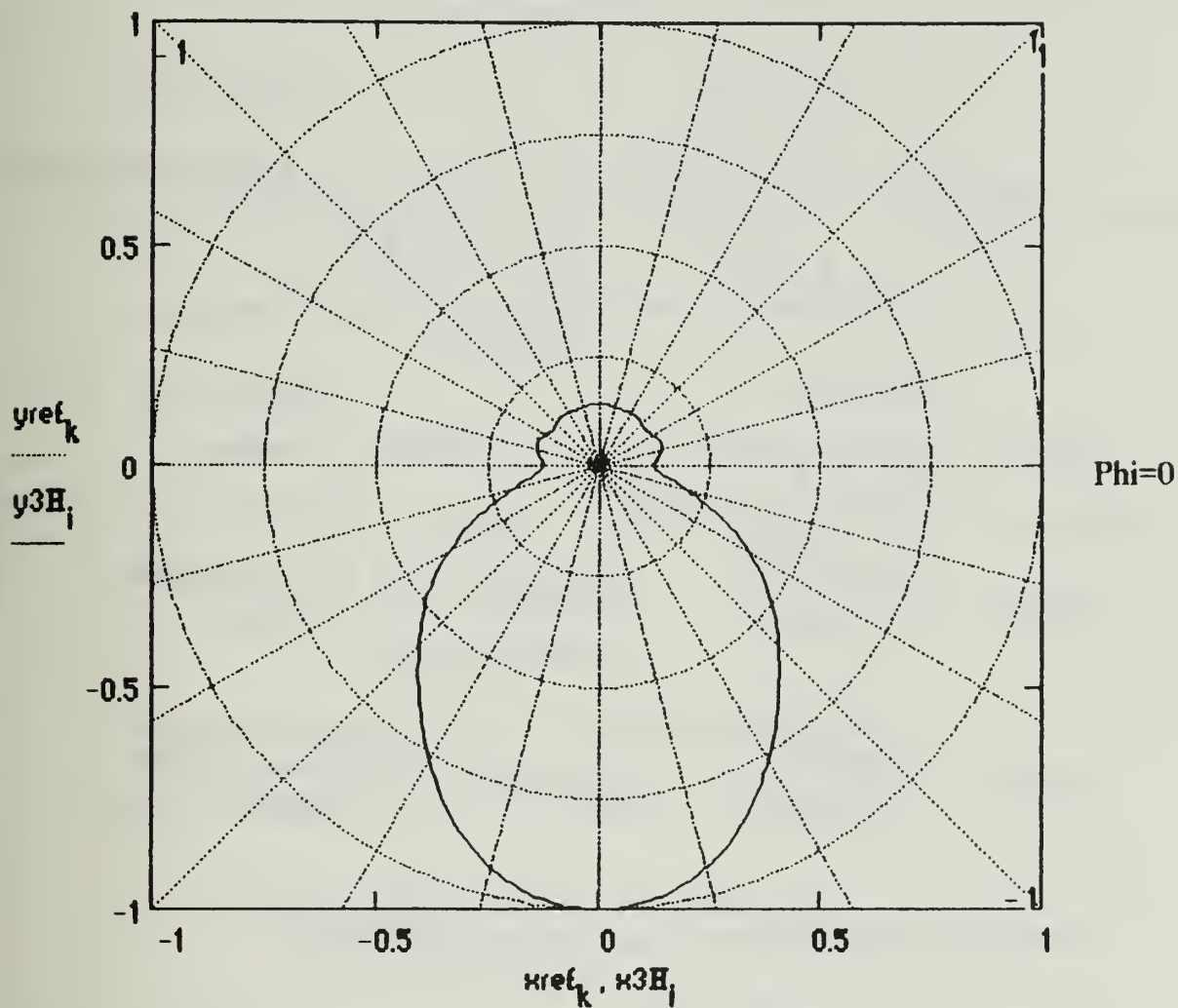
Max E-Field Intensity (Volts per meter) $\max(\text{MagE1H}) = 0.0676$

Surface Wave Radiation Pattern (Horizontal)



Max E-Field Intensity (Volts per meter) $\max(\text{MagE2H}) = 3.44012 \cdot 10^{-5}$

Combined Space and Surface Wave Radiation Pattern (Horizontal)



Max E-Field Intensity (Volts per meter)

$$\max(\text{MagE3H}) = 0.06758$$

$$\text{power}\theta := \frac{30}{\pi \cdot R^2} \cdot \left[\int_{-1.5707963}^{1.5707963} \int_0^{1.5707963} \left| \sum_{\gamma} \left[\frac{\cos(\xi) \cdot \cos(\zeta) \cdot I_{\gamma}}{1 - (\sin(\zeta) \cdot \cos(\xi))^2} \cdot e^{j \cdot \beta \cdot Y_{\gamma} \cdot \csc(\Psi)} \right] \right|^2 d\zeta d\xi \right]$$

$$\text{power}\phi := \frac{30}{\pi \cdot R^2} \cdot \left[\int_{-\frac{\pi}{2}}^{\frac{\pi}{2}} \int_0^{\frac{\pi}{2}} \left| \sum_{\gamma} \left[\frac{\sin(\xi) \cdot I_{\gamma}}{1 - (\sin(\zeta) \cdot \cos(\xi))^2} \cdot e^{j \cdot \beta \cdot Y_{\gamma} \cdot \csc(\Psi)} \cdot \{\cos(\zeta) \cdot \cos(\xi)\} \right] \right|^2 d\zeta d\xi \right]$$

$$\text{power} := \text{power}\theta + \text{power}\phi$$

$$\text{Radres} := 2 \cdot \text{power}$$

$$\text{sqE3P}_i := \frac{(|\text{MagE3P}_i|)^2}{2 \cdot (120 \cdot \pi)}$$

$$\text{DirectivityP} := \frac{4 \cdot \pi \cdot R^2 \cdot \max(\text{sqE3P})}{\text{power}}$$

$$\text{sqE30}_i := \frac{(|\text{MagE30}_i|)^2}{2 \cdot (120 \cdot \pi)}$$

$$\text{Directivity0} := \frac{4 \cdot \pi \cdot R^2 \cdot \max(\text{sqE30})}{\text{power}}$$

Total Power Radiated (Watts)

$$\text{power} = 83.98604$$

Radiation Resistance (versus
Maximum Input Current)
(Ohms)

$$\text{Radres} = 167.97209$$

Directivity (or Maximum Power Gain assuming 100% Antenna Efficiency)

Phi = pi/2 Plane

Phi = 0 Plane

$$\text{DirectivityP} = 12.93749$$

$$\text{Directivity0} = 2.18175$$

Effective Isotropic Radiated Power (EIRP) (Watts)

Phi = pi/2 Plane

Phi = 0 Plane

$$\text{DirectivityP} \cdot \text{power} = 1.08657 \cdot 10^3 \quad \text{Directivity0} \cdot \text{power} = 183.23657$$

Maximum Effective Area (Along Radial of Directivity)
(square meters)

Phi = pi/2 Plane

Phi = 0 Plane

$$\frac{(\lambda_5)^2 \cdot \text{DirectivityP}}{4 \cdot \pi} = 643.45795$$

$$\frac{(\lambda_5)^2 \cdot \text{Directivity0}}{4 \cdot \pi} = 108.51135$$

Maximum Effective Length (Along Radial of Directivity)
(meters)

Phi = pi/2 Plane

Phi = 0 Plane

$$2 \cdot \sqrt{\frac{\text{Radres} \cdot (\lambda_5)^2 \cdot \text{DirectivityP}}{480 \cdot \pi^2}} = 33.86438 \quad 2 \cdot \sqrt{\frac{\text{Radres} \cdot (\lambda_5)^2 \cdot \text{Directivity0}}{480 \cdot \pi^2}} = 13.90659$$

Numerical Distances

Vertical Polarization

Horizontal Polarization

$$|Pe_0| = 69.28584$$

$$|Pm_0| = 1.26447 \cdot 10^3$$

Elevation Angle of Directivity (Maximum Gain)
above the Horizon (Degrees)

Phi = pi/2 Plane

Phi = 0 Plane

$$\text{AngleP} = 31.42857$$

$$\text{Angle0} = \begin{pmatrix} 89.71429 \\ 89.71429 \end{pmatrix}$$

HORIZONTAL LOG PERIODIC DIPOLE ARRAY

This application calculates far field radiation patterns and parameters associated with horizontal log periodic dipole arrays. The antenna is oriented such that the projection of its center axis lies on the positive y-axis of a rectangular coordinate system. The antenna axis can be oriented with respect to the vertical at any angle between zero and ninety degrees. The feed is at the center of the shortest element directly above the origin. The dipole elements are bisected by the antenna axis and are parallel to the x-axis. Required inputs are the number of dipole elements, shortest and second shortest element lengths, separation between the shortest and second shortest elements, radius of the shortest element, height of the feed above the surface, angle of the antenna axis with the vertical, characteristic admittance of the line feeding the antenna, termination impedance of the antenna, transmitted frequency, distance from the antenna, the conductivity and dielectric constant of the surface below the antenna. The planar earth model is assumed in predicting radiation patterns. A sinusoidal current input with a maximum of unity is assumed. All radiation patterns are normalized with respect to the maximum electric field intensity transmitted by the antenna in the plane of interest. The electric field magnitudes to which the patterns are normalized are displayed below their respective plots. Radiation patterns are plotted for the $\phi = \pi/2$ and $\phi = 0$ vertical planes parallel and perpendicular to the y-axis respectively. A horizontal radiation pattern is plotted at an elevation selected by the index from the elevation angle index table. Polarization is a varying combination of horizontal and vertical depending on spatial orientation with respect to the antenna.

Input the number of elements	$N := 12$	Input the shortest element's Radius (meters)	$rad_0 := .00144$
Input the length of the shortest element (meters)	$l_0 := 7.219$	Input the length of the second shortest element (meters)	$l_1 := 8.297$
Input the distance from shortest to second shortest element (meters)	$d_0 := 1.659$	Input the height of the shortest element above the surface (meters)	$H_0 := 9.4$
Input the operating Frequency (Hertz)	$f_5 := 12 \cdot 10^6$	Input the Distance from the Antenna (meters)	$R := 3000$
Input the ground Conductivity	$\sigma := 4$	Input the ground Dielectric Constant	$\epsilon_r := 72$
Input the Characteristic Admittance of the Line Feeding the Antenna (Ohms)	$ADM := \frac{1}{300}$	Input the Termination Impedance connected to longest element (Ohms)	$TIMP := 300$

Input the angle between
the vertical (z axis) and
the antenna axis (degrees)

$\Psi := 90$

Elevation index for which
to calculate horizontal pattern $w := 285$
(from angle index table)

NOTE: The Horizontal Log-Periodic Dipole mutual impedance calculations are not valid if there is an antenna element whose length is an exact integer multiple of the wavelength. If this occurs, there will be a singularity error in the mutual impedance calculations. If this problem arises, it will be necessary to vary the operating frequency such that no element is exactly an integer multiple of the wavelength.

If the log-periodic calculations of element length and spacing do not represent the desired antenna configuration, you can enter the values directly by selecting the variables l and d , using the define key (shift, colon), and entering the successive lengths and spacings by separating each successive entry by a comma.

Calculated length
of elements from
shortest to longest

Calculated distance
between successive
elements-shortest
to longest

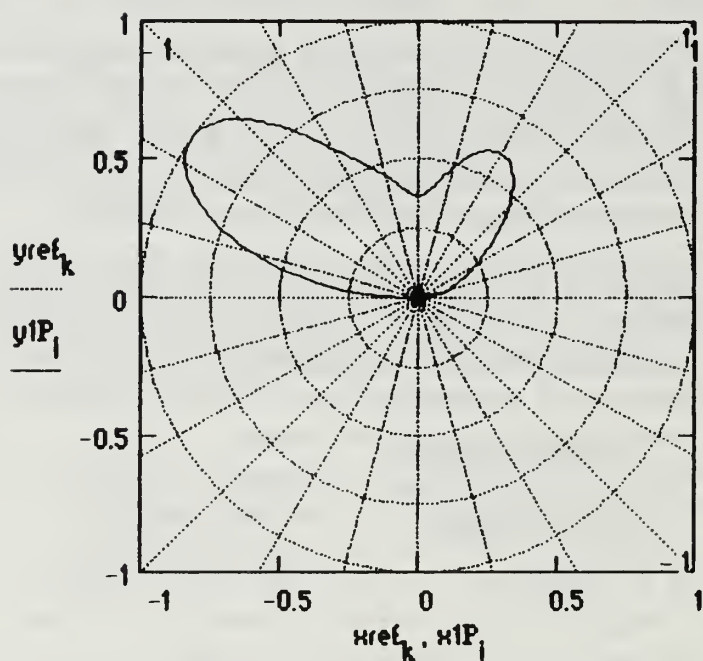
Calculated radii
of elements from
shortest to longest

l γ
7.219
8.297
9.53598
10.95997
12.5966
14.47762
16.63954
19.12429
21.98009
25.26233
29.03471
33.37041

d v
1.659
1.90674
2.19146
2.51871
2.89483
3.32711
3.82394
4.39496
5.05125
5.80554
6.67247

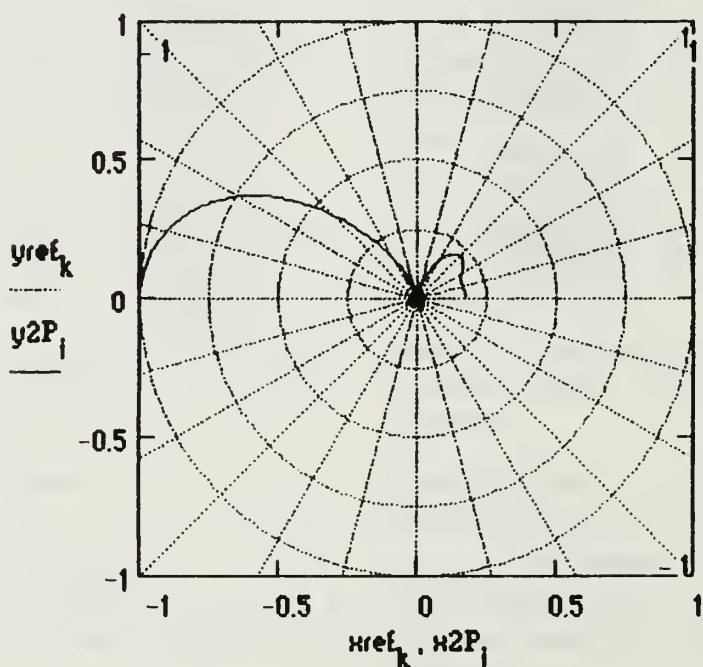
rad γ
0.00144
0.00166
0.0019
0.00219
0.00251
0.00289
0.00332
0.00381
0.00438
0.00504
0.00579
0.00666

Radiation Patterns in $\Phi = \pi/2$ Plane
(Perpendicular to X-Axis and Dipole Elements)
Space Wave Radiation Pattern ($\Phi = \pi/2$)



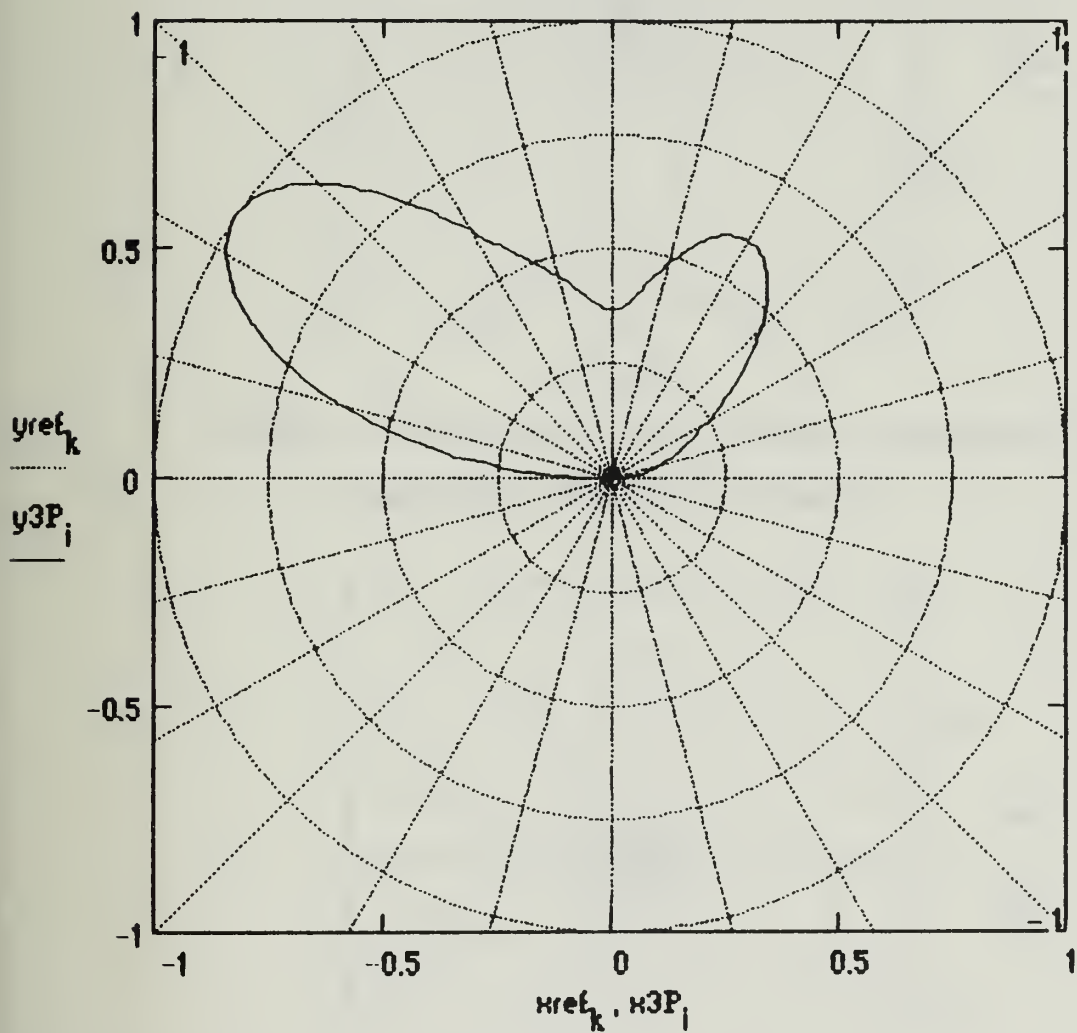
Max E-Field Intensity (Volts per meter) $\max(\text{MagE1P}) = 0.13724$

Surface Wave Radiation Pattern ($\Phi = \pi/2$)



Max E-Field Intensity (Volts per meter) $\max(\text{MagE2P}) = 3.19958 \cdot 10^{-8}$

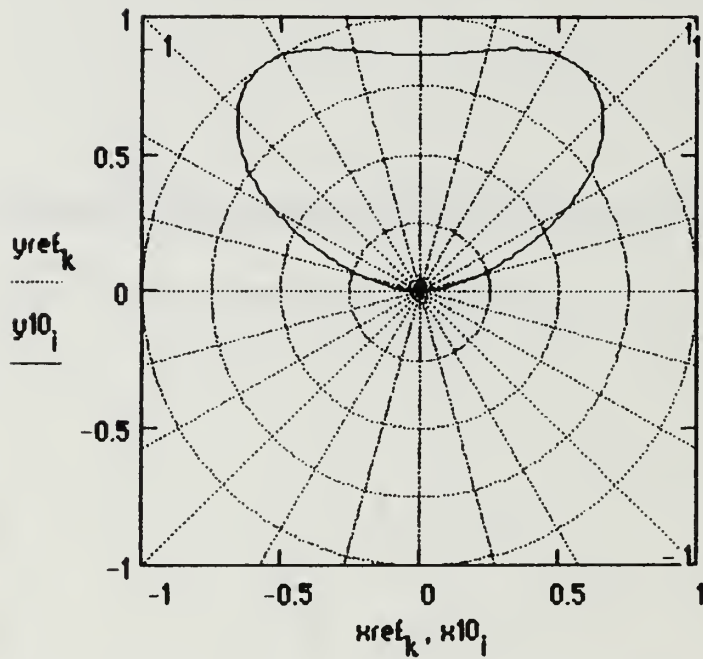
Combined Space and Surface Wave Radiation Pattern ($\Phi = \pi/2$)



Max E-Field Intensity (Volts per meter)

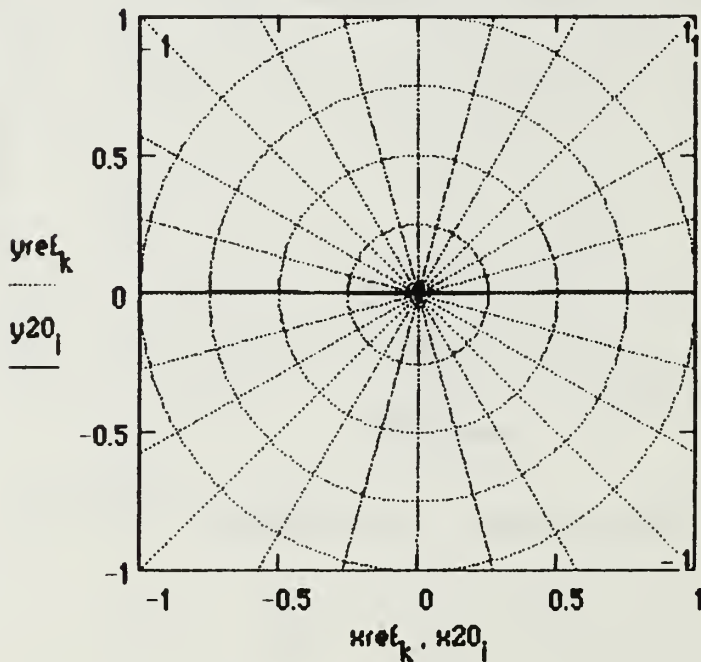
$$\max(\text{MagE3P}) = 0.13724$$

Radiation Patterns in $\Phi=0$ Plane
(Perpendicular to $\Phi=\pi/2$ Plane)
Space Wave Radiation Pattern ($\Phi=0$)



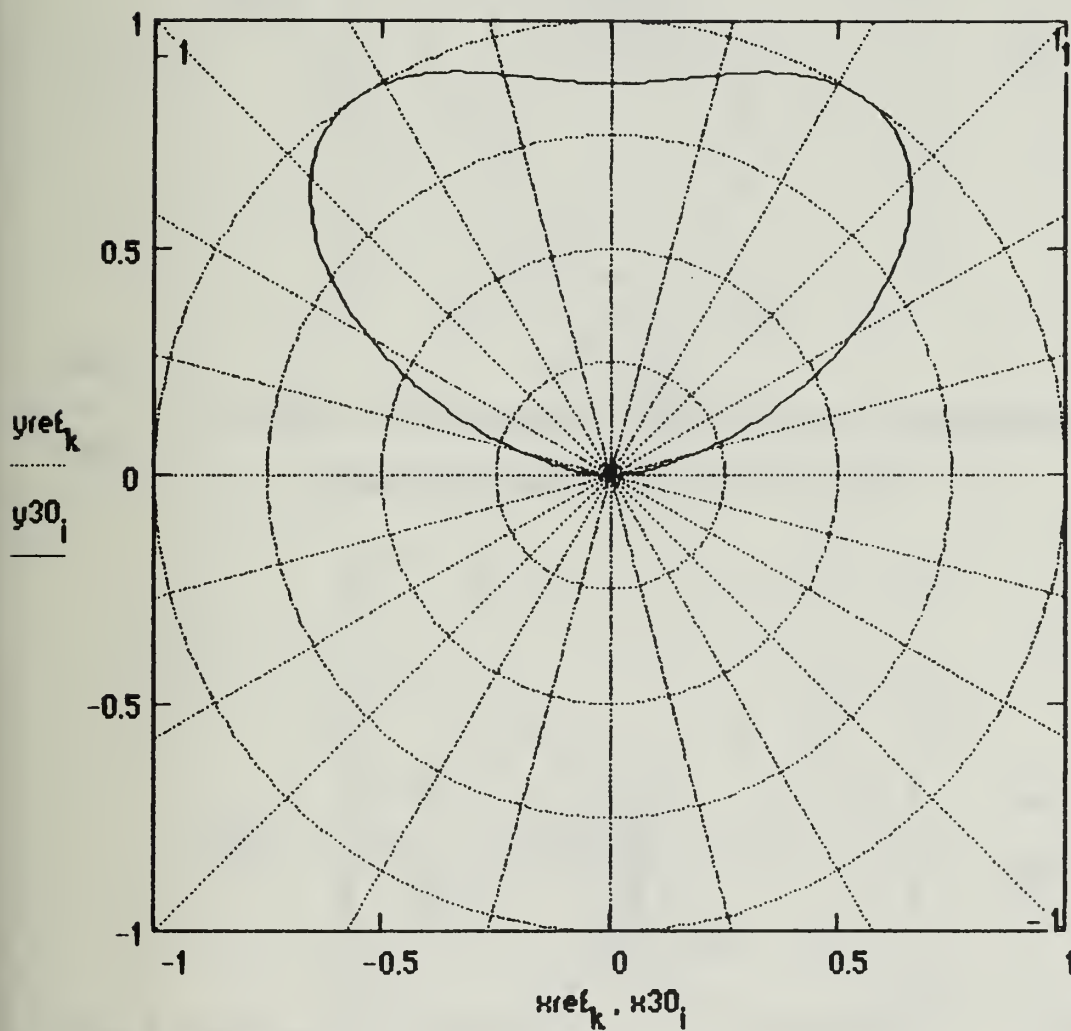
Max E-Field Intensity (Volts per meter) $\max(\text{MagE10}) = 0.05843$

Surface Wave Radiation Pattern ($\Phi=0$)



Max E-Field Intensity (Volts per meter) $\max(\text{MagE20}) = 4.46943 \cdot 10^{-4}$

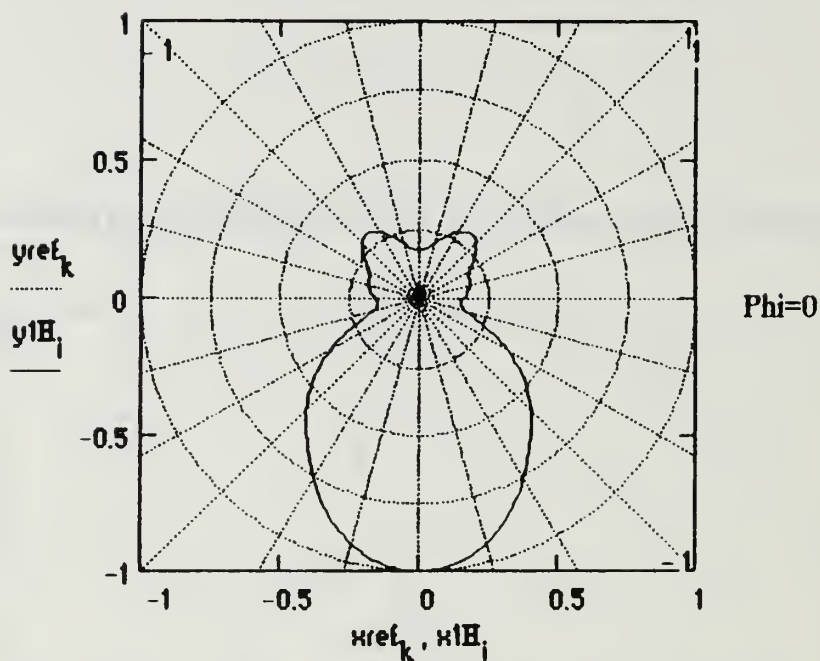
Combined Space and Surface Wave Radiation Pattern ($\Phi=0$)



Max E-Field Intensity (Volts per meter) $\max(\text{MagE30}) = 0.05843$

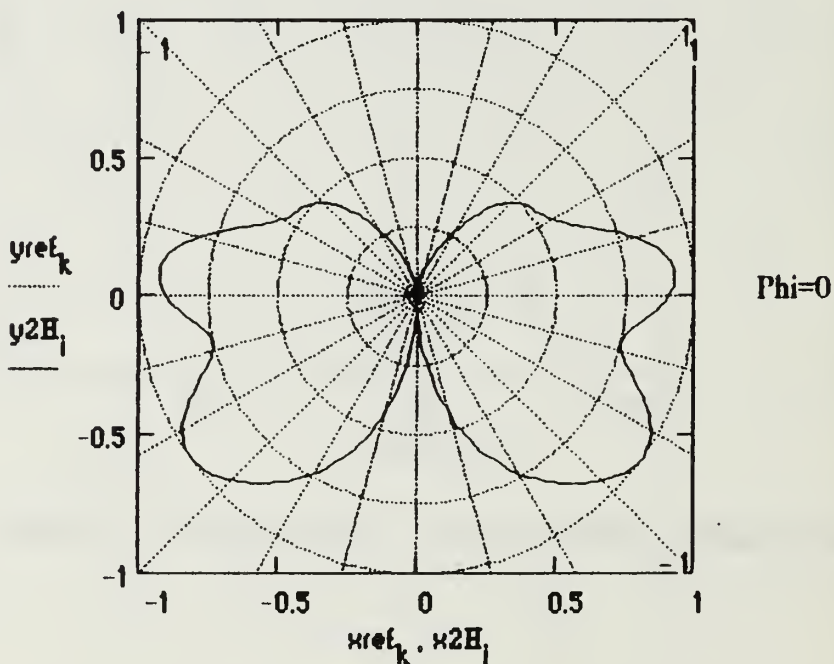
Radiation Patterns in Horizontal Plane (Parallel to Ground)

Space Wave Radiation Pattern (Horizontal)



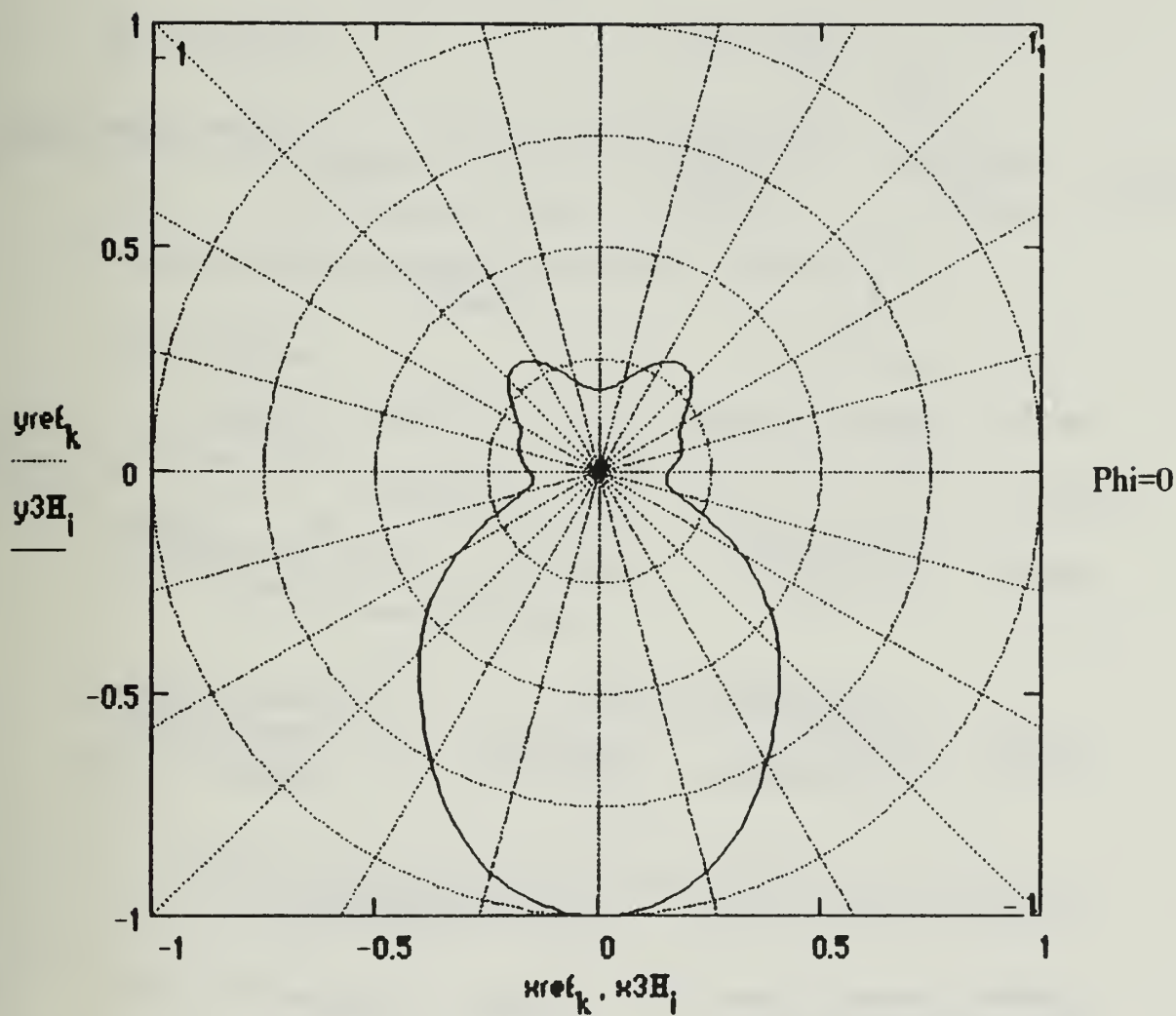
Max E-Field Intensity (Volts per meter) $\max(\text{MagE1H}) = 0.09414$

Surface Wave Radiation Pattern (Horizontal)



Max E-Field Intensity (Volts per meter) $\max(\text{MagE2H}) = 5.57296 \cdot 10^{-7}$

Combined Space and Surface Wave Radiation Pattern (Horizontal)



Max E-Field Intensity (Volts per meter)

$\max(\text{MagE3H}) = 0.09414$

$$\text{power}\theta := \frac{30}{\pi \cdot R^2} \cdot \left[\int_{-1.5707963}^{1.5707963} \int_0^{1.5707963} \left[\left| \sum_{\gamma} \left[\frac{\cos(\xi) \cdot \cos(\zeta) \cdot I_{\gamma}}{1 - (\sin(\zeta) \cdot \cos(\xi))^2} \cdot e^{j \cdot \beta \cdot Y_{\gamma} \cdot \csc(\Psi)} \right] \right| \right] d\zeta d\xi \right]$$

$$\text{power}\phi := \frac{30}{\pi \cdot R^2} \cdot \left[\int_{-\frac{\pi}{2}}^{\frac{\pi}{2}} \int_0^{\frac{\pi}{2}} \left[\left| \sum_{\gamma} \left[\frac{\sin(\xi) \cdot I_{\gamma}}{1 - (\sin(\zeta) \cdot \cos(\xi))^2} \cdot e^{j \cdot \beta \cdot Y_{\gamma} \cdot \csc(\Psi)} \cdot (\cos(\zeta) \cdot \cos(\Psi)) \right] \right| \right] d\zeta d\xi \right]$$

$$\text{power} := \text{power}\theta + \text{power}\phi$$

$$\text{Radres} := 2 \cdot \text{power}$$

$$\text{sqE3P}_i := \frac{(|\text{MagE3P}_i|)^2}{2 \cdot (120 \cdot \pi)}$$

$$\text{DirectivityP} := \frac{4 \cdot \pi \cdot R^2 \cdot \max(\text{sqE3P})}{\text{power}}$$

$$\text{sqE30}_i := \frac{(|\text{MagE30}_i|)^2}{2 \cdot (120 \cdot \pi)}$$

$$\text{Directivity0} := \frac{4 \cdot \pi \cdot R^2 \cdot \max(\text{sqE30})}{\text{power}}$$

Total Power Radiated (Watts)

$$\text{power} = 261.928$$

Radiation Resistance (versus
Maximum Input Current)
(Ohms)

$$\text{Radres} = 523.856$$

Directivity (or Maximum Power Gain assuming 100% Antenna Efficiency)

Phi = pi/2 Plane

Phi = 0 Plane

$$\text{DirectivityP} = 10.78579$$

$$\text{Directivity0} = 1.95488$$

Effective Isotropic Radiated Power (EIRP) (Watts)

Phi = pi/2 Plane

Phi = 0 Plane

$$\text{DirectivityP} \cdot \text{power} = 2.8251 \cdot 10^3 \quad \text{Directivity0} \cdot \text{power} = 512.03765$$

Maximum Effective Area (Along Radial of Directivity)
(square meters)

Phi = pi/2 Plane

Phi = 0 Plane

$$\frac{(\lambda_5)^2 \cdot \text{DirectivityP}}{4 \cdot \pi} = 536.4412$$

$$\frac{(\lambda_5)^2 \cdot \text{Directivity0}}{4 \cdot \pi} = 97.22772$$

Maximum Effective Length (Along Radial of Directivity)
(meters)

Phi = pi/2 Plane

Phi = 0 Plane

$$\sqrt{\frac{\text{Radres} \cdot (\lambda_5)^2 \cdot \text{DirectivityP}}{480 \cdot \pi^2}} = 54.60488 \quad 2 \cdot \sqrt{\frac{\text{Radres} \cdot (\lambda_5)^2 \cdot \text{Directivity0}}{480 \cdot \pi^2}} = 23.24692$$

Numerical Distances

Vertical Polarization

Horizontal Polarization

$$|P_{e0}| = 0.06283$$

$$|P_{m0}| = 2.26211 \cdot 10^6$$

Elevation Angle of Directivity (Maximum Gain)
above the Horizon (Degrees)

Phi = pi/2 Plane

Phi = 0 Plane

$$\text{AngleP} = 34.85714$$

$$\text{Angle0} = \begin{pmatrix} 56.57143 \\ 56.57143 \end{pmatrix}$$

APPENDIX F:
HORIZONTAL YAGI-UDA ARRAY COMPUTER OUTPUT

This appendix contains computer hardcopies from the Mathcad horizontal Yagi-Uda array application which show the input values and predicted radiation characteristics for two sample calculations. The configuration is as given by the inputs on the first three pages of each printout. The first antenna is mounted above soil ($\epsilon_r=4$ and $\sigma=10^{-3}$) and the second above seawater ($\epsilon_r=72$ and $\sigma=4$). Reference 6 [p. 107] provides the radiation patterns and gain predictions from several sources for the configuration in the first example.

The radiation patterns and maximum directive gain computed by the first Mathcad example are almost identical to the those given in reference 6. The directivity prediction is slightly higher for Mathcad, but the overall similarity among the predicted radiation patterns is very good. The seawater example has results very much like the soil example. For horizontal polarization, the higher conductivity surface below the antenna does not result in a greatly enhanced surface wave and increased directivity as it does for vertical polarization.

HORIZONTAL YAGI-UDA ARRAY

This application calculates far field radiation patterns and parameters associated with horizontal Yagi-Uda arrays. The antenna is oriented such that the projection of its center axis lies on the positive y-axis of a rectangular coordinate system. The feed is at the center of a single driven element between a set number of longer parasitic reflector elements and shorter parasitic director elements. Antenna elements are bisected by the antenna axis and are parallel to the x-axis. The center of the first reflector is directly above the origin at a set height on the z-axis. Required inputs are the number of reflector and director elements, individual element lengths, individual element radii, separation between adjacent elements, height of the feed above the surface, transmitted frequency, distance from the antenna, conductivity and dielectric constant of the surface below the antenna. The planar earth model is assumed in predicting radiation patterns. A sinusoidal voltage with a one volt maximum across the input terminals is assumed. All radiation patterns are normalized with respect to the maximum electric field intensity transmitted by the antenna in the plane of interest. The electric field magnitudes to which the patterns are normalized are displayed below their respective plots. Radiation patterns are plotted for the $\phi = \pi/2$ and $\phi = 0$ vertical planes parallel and perpendicular to the y-axis respectively. A horizontal radiation pattern is plotted at an elevation selected by the index from the elevation angle index table. Polarization is a varying combination of horizontal and vertical depending on spatial orientation with respect to the antenna.

NOTE: The Yagi-Uda mutual impedance calculations are not valid if there is an antenna element whose length is an exact integer multiple of the wavelength. If this occurs, there will be a singularity error in the mutual impedance calculations. This should not be a problem since Yagi-Uda Antennas are designed to operate at frequencies such that the driven element is approximately one-half-wavelength long, the reflectors are slightly longer, and the directors are slightly shorter. If the problem does arise, it will be necessary to vary the operating frequency such that no element is exactly an integer multiple of the wavelength.

Input the number of
reflector elements $NR := 1$

Input the number of
director elements $ND := 1$

$$\gamma := 0 .. (NR + ND)$$

$$\delta := 0 .. (NR + ND - 1)$$

This entire page is allotted for these entries to allow for as many elements as necessary.

Input the lengths and radii of the Yagi elements, starting with the outermost reflector and proceeding inward to the driven element. After entering the driven element length and radius, enter those of the director elements, starting with the director next to the driven element and proceeding outward to the final element.

$l_{\gamma} =$

15.6
15
14

$rad_{\gamma} =$

.001
.001
.001

$d_{\delta} =$

7.5
6.0

Input the distances between successive elements in the same order as the length and radius inputs. There should be one less entry in the separation distance array than there is in the length and radius array.

Input the operating Frequency (Hertz) $f_5 := 10 \cdot 10^6$

Input the height of the array above the surface (meters) $H_0 := 7.5$

Input the ground Conductivity $\sigma := 1 \cdot 10^{-3}$

Input the ground Dielectric Constant $\epsilon_r := 4$

Input the Distance from the Antenna (meters) $R := 3000$

Index of Refraction

Input the index of the elevation angle for which to calculate the horizontal radiation pattern (from the angle index table) $w := 285$

$$n := \sqrt{\epsilon_r - j \cdot \frac{18000 \cdot \sigma}{(f_5 \cdot 10^{-6})}}$$

Complex Numerical Distance for Vertical Polarization

$$Pe_i := \frac{-j \cdot \beta \cdot (R + H_0 \cdot \cos(\theta_i))}{2 \cdot \sin(\theta_i)^2} \cdot \left(\cos(\theta_i) + \frac{\sqrt{n^2 - \sin(\theta_i)^2}}{n^2} \right)^2$$

Complex Numerical Distance for Horizontal Polarization

$$Pm_i := \frac{-j \cdot \beta \cdot (R + H_0 \cdot \cos(\theta_i))}{2 \cdot (\sin(\theta_i)^2)} \cdot \left[\cos(\theta_i) + \frac{\sqrt{n^2 - (\sin(\theta_i)^2)}}{n^2} \right]^2$$

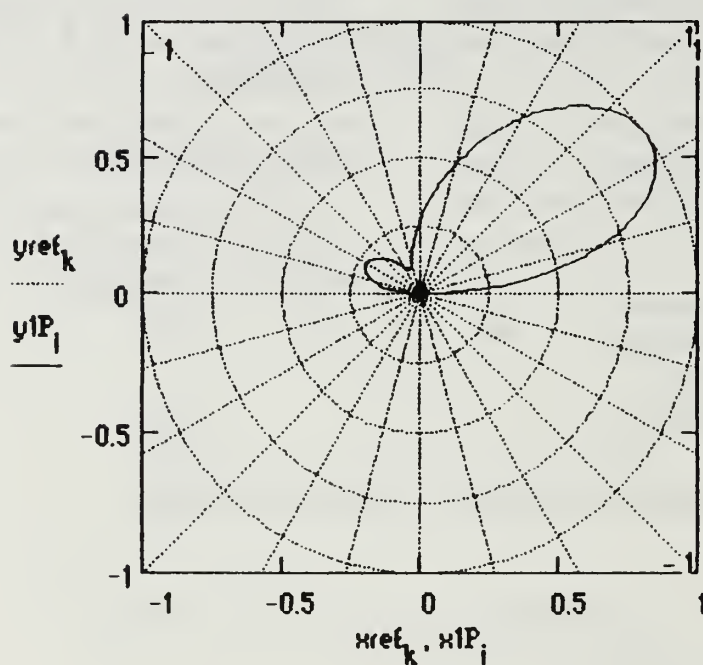
Vertical Reflection Coefficient

$$\Gamma_{v_i} := \frac{\left(\frac{n^2 \cdot \cos(\theta_i)}{n^2} \right) - \left(\frac{\sqrt{n^2 - \sin(\theta_i)^2}}{n^2} \right)}{\left(\frac{n^2 \cdot \cos(\theta_i)}{n^2} \right) + \left(\frac{\sqrt{n^2 - \sin(\theta_i)^2}}{n^2} \right)}$$

Horizontal Reflection Coefficient

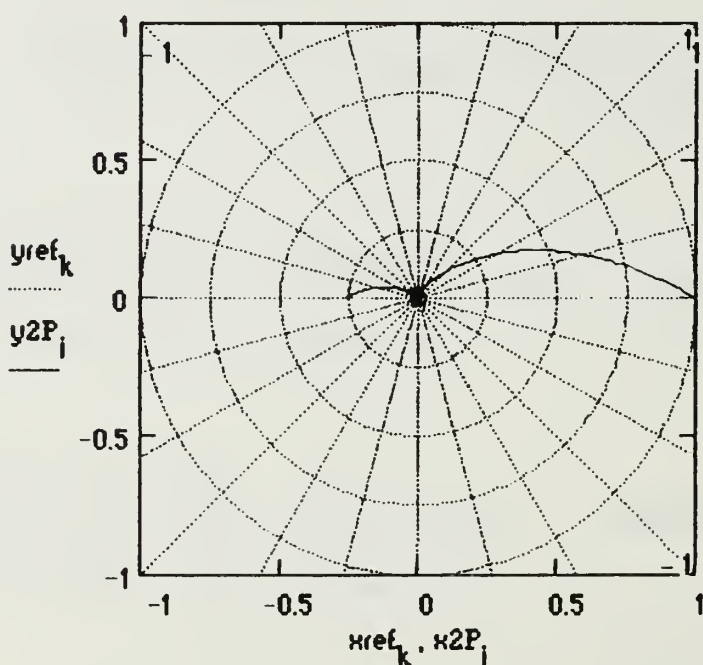
$$\Gamma_{h_i} := \frac{\cos(\theta_i) - \left(\frac{\sqrt{n^2 - \sin(\theta_i)^2}}{n^2} \right)}{\cos(\theta_i) + \left(\frac{\sqrt{n^2 - \sin(\theta_i)^2}}{n^2} \right)}$$

Radiation Patterns in $\Phi = \pi/2$ Plane
(Perpendicular to X-Axis and Dipole Elements)
Space Wave Radiation Pattern ($\Phi = \pi/2$)



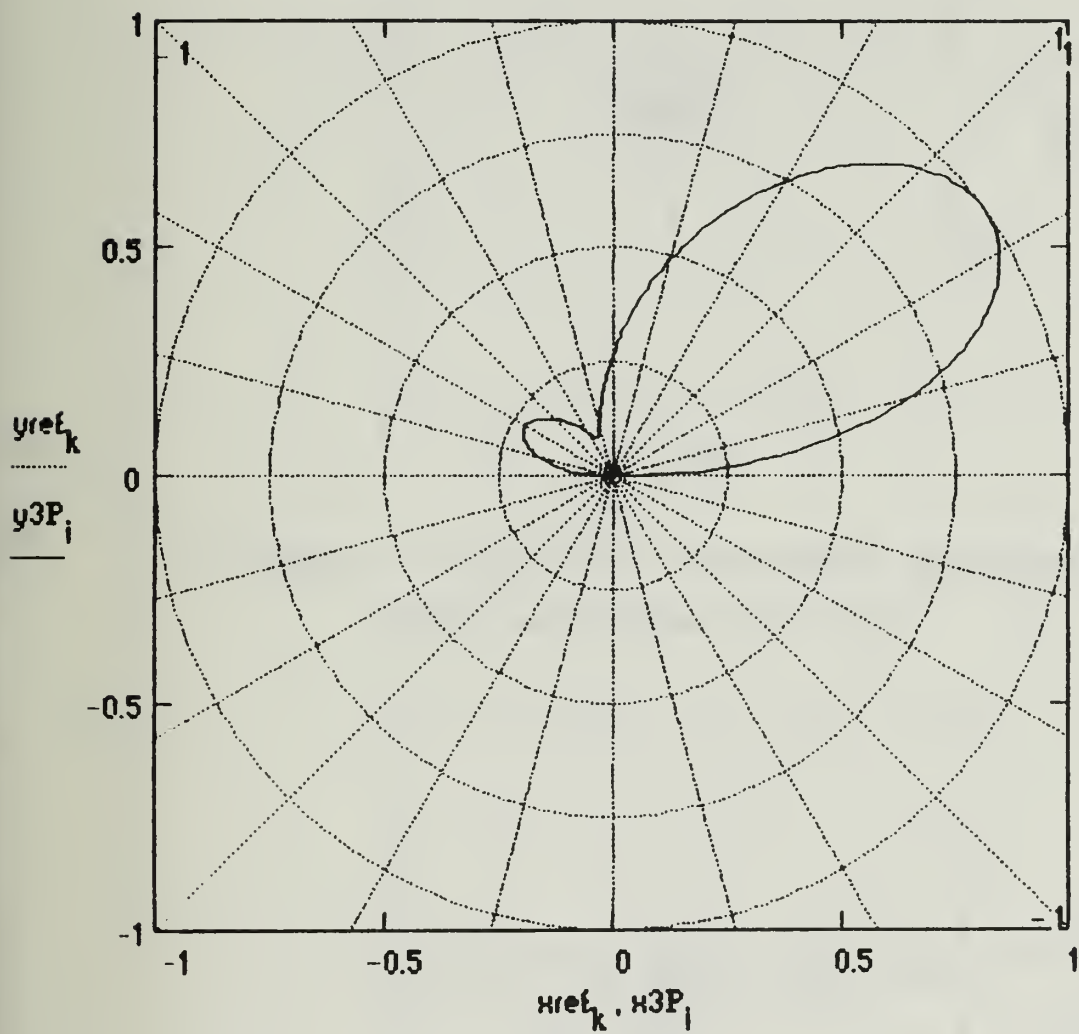
Max E-Field Intensity (Volts per meter) $\max(\text{MagE1P}) = 5.13224 \cdot 10^{-4}$

Surface Wave Radiation Pattern ($\Phi = \pi/2$)



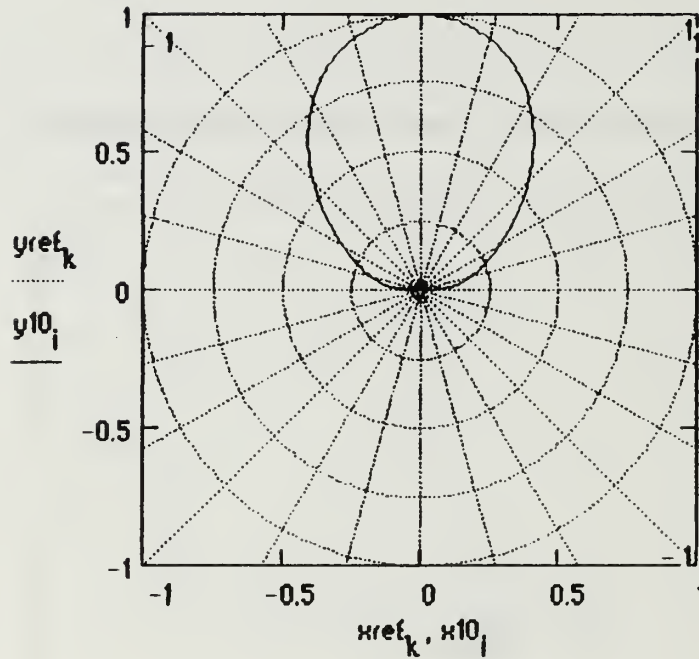
Max E-Field Intensity (Volts per meter) $\max(\text{MagE2P}) = 4.08957 \cdot 10^{-7}$

Combined Space and Surface Wave Radiation Pattern ($\Phi = \pi/2$)



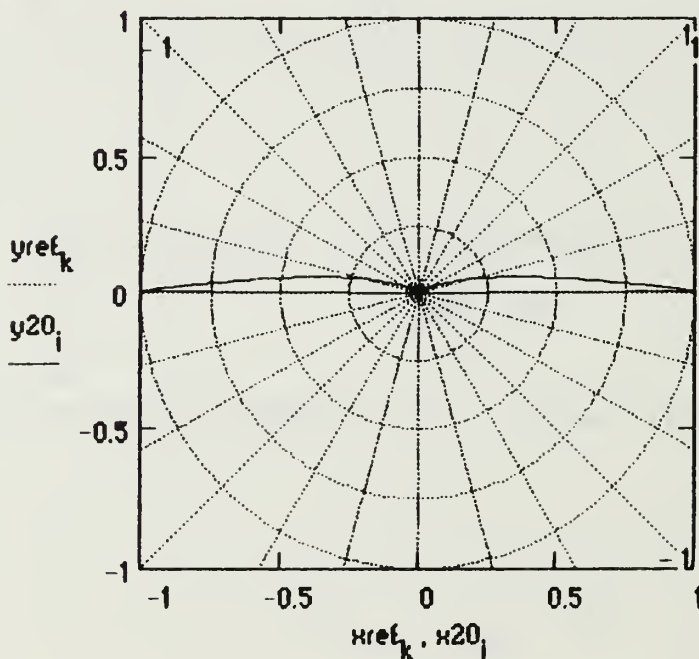
Max E-Field Intensity (Volts per meter) $\max(\text{MagE3P}) = 5.13132 \cdot 10^{-4}$

Radiation Patterns in $\Phi=0$ Plane
(Perpendicular to $\Phi=\pi/2$ Plane)
Space Wave Radiation Pattern ($\Phi=0$)



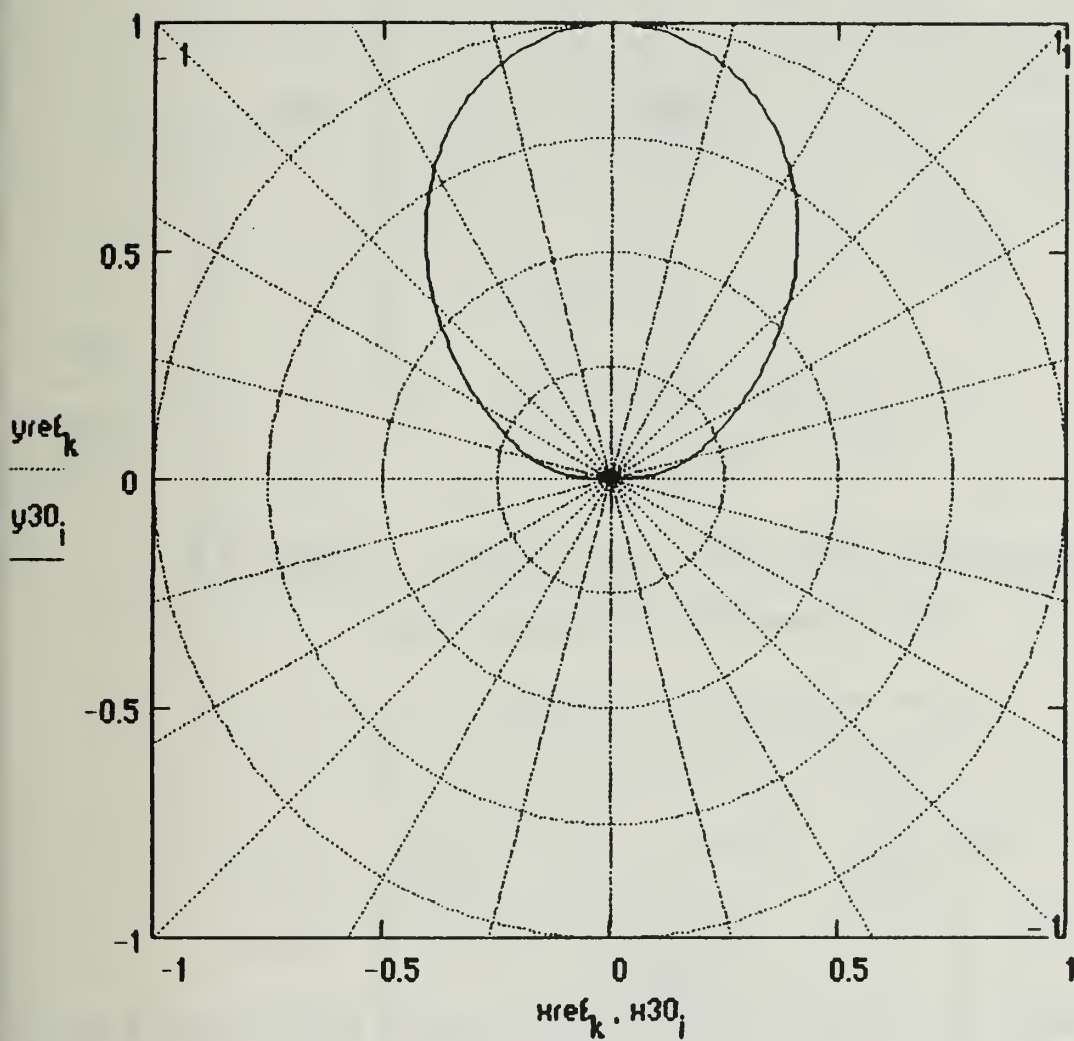
Max E-Field Intensity (Volts per meter) $\max(\text{MagE10}) = 1.35264 \cdot 10^{-4}$

Surface Wave Radiation Pattern ($\Phi=0$)



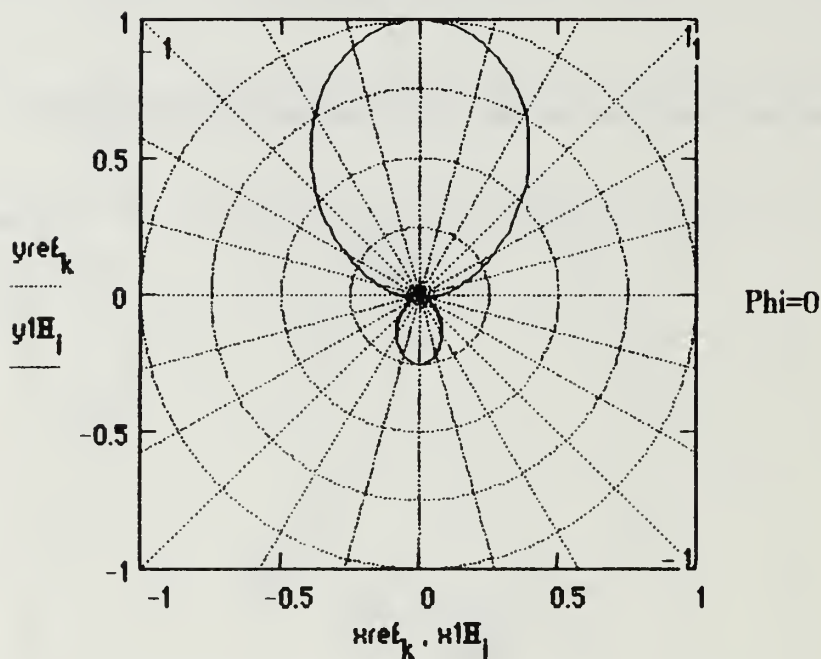
Max E-Field Intensity (Volts per meter) $\max(\text{MagE20}) = 5.32341 \cdot 10^{-7}$

Combined Space and Surface Wave Radiation Pattern (Phi=0)



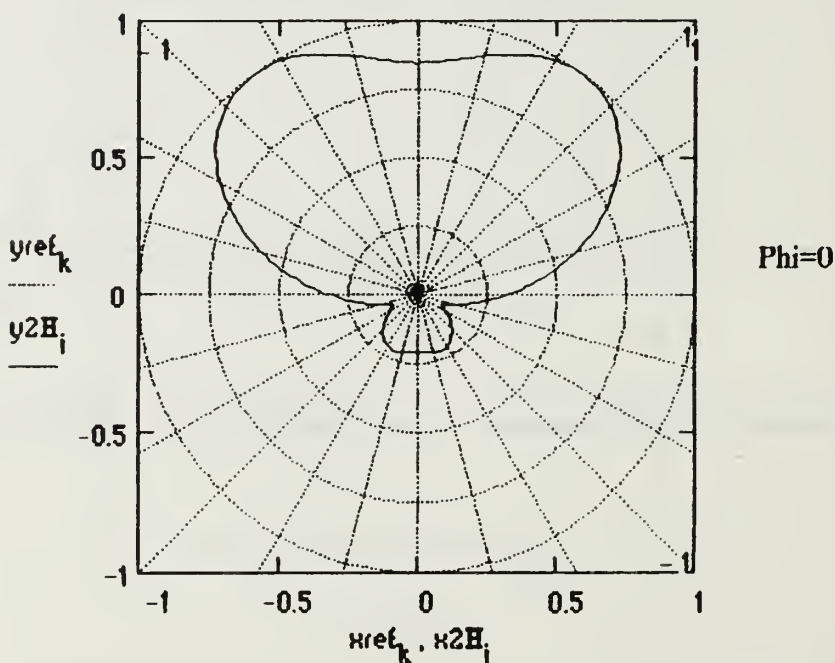
Max E-Field Intensity (Volts per meter) $\max(\text{MagE30}) = 1.35264 \cdot 10^{-4}$

**Radiation Patterns in Horizontal Plane
(Parallel to Ground)**
Space Wave Radiation Pattern (Horizontal)



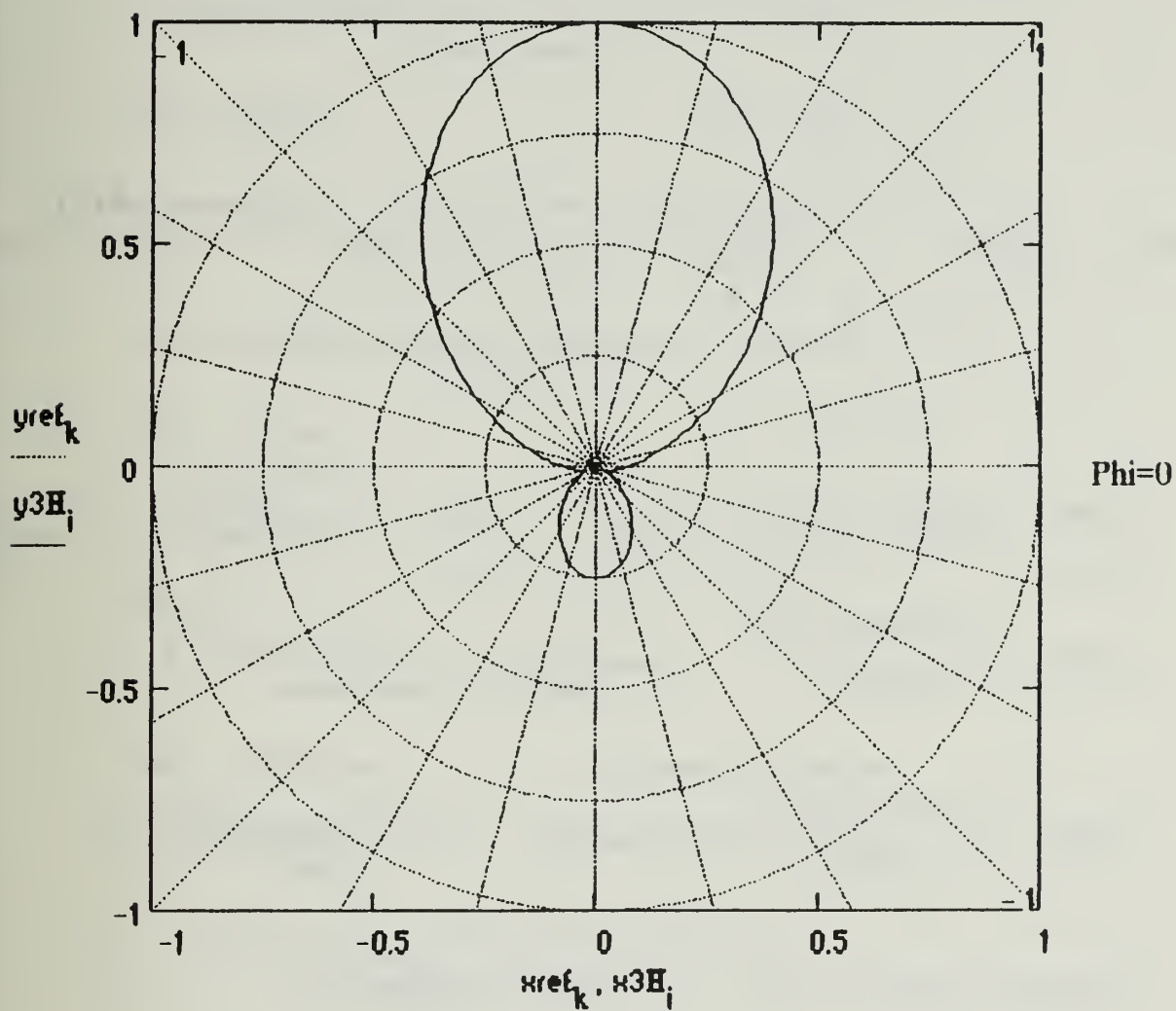
Max E-Field Intensity (Volts per meter) $\max(\text{MagE1H}) = 3.79643 \cdot 10^{-4}$

Surface Wave Radiation Pattern (Horizontal)



Max E-Field Intensity (Volts per meter) $\max(\text{MagE2H}) = 2.73697 \cdot 10^{-7}$

Combined Space and Surface Wave Radiation Pattern (Horizontal)



Max E-Field Intensity (Volts per meter) $\max(\text{MagE3H}) = 3.7942 \cdot 10^{-4}$

$$\text{power}\theta := \frac{30}{\pi \cdot R^2} \left[\int_{-1.5707963}^{1.5707963} \int_0^{1.5707963} \left| \sum_{\gamma} \left[\frac{\cos(\xi) \cdot \cos(\zeta) \cdot I_{\gamma}}{1 - (\sin(\zeta) \cdot \cos(\xi))^2} \cdot e^{j \cdot \beta \cdot D_{\gamma} \cdot \sin(\zeta)} \right] \right|^2 d\zeta d\xi \right]$$

$$\text{power}\phi := \frac{30}{\pi \cdot R^2} \left[\int_{-\frac{\pi}{2}}^{\frac{\pi}{2}} \int_0^{\frac{\pi}{2}} \left| \sum_{\gamma} \left[\frac{\sin(\xi) \cdot I_{\gamma}}{1 - (\sin(\zeta) \cdot \cos(\xi))^2} \cdot e^{j \cdot \beta \cdot D_{\gamma} \cdot \sin(\zeta) \cdot \sin(\xi)} \right] \right|^2 d\zeta d\xi \right] \cdot (\cos(\beta))$$

$$\text{power} := \text{power}\theta + \text{power}\phi$$

$$\text{Radres} := \frac{(\text{VREF}_{\text{NR}})^2}{2 \cdot \text{power}}$$

$$\text{sqE3P}_i := \frac{(|\text{MagE3P}_i|)^2}{2 \cdot (120 \cdot \pi)}$$

$$\text{DirectivityP} := \frac{4 \cdot \pi \cdot R^2 \cdot \max(\text{sqE3P})}{\text{power}}$$

$$\text{sqE30}_i := \frac{(|\text{MagE30}_i|)^2}{2 \cdot (120 \cdot \pi)}$$

$$\text{Directivity0} := \frac{4 \cdot \pi \cdot R^2 \cdot \max(\text{sqE30})}{\text{power}}$$

Total Power Radiated (Watts)

$$\text{power} = 0.00266$$

Radiation Resistance (versus
Maximum Input Current)
(Ohms)

$$\text{Radres} = 187.94973$$

Directivity (or Maximum Power Gain assuming 100% Antenna Efficiency)

Phi = pi/2 Plane

Phi = 0 Plane

$$\text{DirectivityP} = 14.84639$$

$$\text{Directivity0} = 1.03163$$

Effective Isotropic Radiated Power (EIRP) (Watts)

Phi = pi/2 Plane

Phi = 0 Plane

$$\text{DirectivityP} \cdot \text{power} = 0.0395$$

$$\text{Directivity0} \cdot \text{power} = 0.00274$$

Maximum Effective Area (Along Radial of Directivity)
(square meters)

Phi = pi/2 Plane

Phi = 0 Plane

$$\frac{(\lambda_5)^2 \cdot \text{DirectivityP}}{4 \cdot \pi} = 1.06329 \cdot 10^3$$

$$\frac{(\lambda_5)^2 \cdot \text{Directivity0}}{4 \cdot \pi} = 73.88536$$

Maximum Effective Length (Along Radial of Directivity)
(meters)

Phi = pi/2 Plane

Phi = 0 Plane

$$\sqrt{\frac{\text{Radres} \cdot (\lambda_5)^2 \cdot \text{DirectivityP}}{480 \cdot \pi^2}} = 46.04814 \quad 2 \cdot \sqrt{\frac{\text{Radres} \cdot (\lambda_5)^2 \cdot \text{Directivity0}}{480 \cdot \pi^2}} = 12.13848$$

Numerical Distances

Vertical Polarization

Horizontal Polarization

$$|P_{e0}| = 57.12622$$

$$|P_{m0}| = 1.09911 \cdot 10^3$$

Elevation Angle of Directivity (Maximum Gain)
above the Horizon (Degrees)

Phi = pi/2 Plane

Phi = 0 Plane

$$\text{AngleP} = 36$$

$$\text{Angle0} = \begin{pmatrix} 89.71429 \\ 89.71429 \end{pmatrix}$$

HORIZONTAL YAGI-UDA ARRAY

This application calculates far field radiation patterns and parameters associated with horizontal Yagi-Uda arrays. The antenna is oriented such that the projection of its center axis lies on the positive y-axis of a rectangular coordinate system. The feed is at the center of a single driven element between a set number of longer parasitic reflector elements and shorter parasitic director elements. Antenna elements are bisected by the antenna axis and are parallel to the x-axis. The center of the first reflector is directly above the origin at a set height on the z-axis. Required inputs are the number of reflector and director elements, individual element lengths, individual element radii, separation between adjacent elements, height of the feed above the surface, transmitted frequency, distance from the antenna, conductivity and dielectric constant of the surface below the antenna. The planar earth model is assumed in predicting radiation patterns. A sinusoidal voltage with a one volt maximum across the input terminals is assumed. All radiation patterns are normalized with respect to the maximum electric field intensity transmitted by the antenna in the plane of interest. The electric field magnitudes to which the patterns are normalized are displayed below their respective plots. Radiation patterns are plotted for the $\phi = \pi/2$ and $\phi = 0$ vertical planes parallel and perpendicular to the y-axis respectively. A horizontal radiation pattern is plotted at an elevation selected by the index from the elevation angle index table. Polarization is a varying combination of horizontal and vertical depending on spatial orientation with respect to the antenna.

NOTE: The Yagi-Uda mutual impedance calculations are not valid if there is an antenna element whose length is an exact integer multiple of the wavelength. If this occurs, there will be a singularity error in the mutual impedance calculations. This should not be a problem since Yagi-Uda Antennas are designed to operate at frequencies such that the driven element is approximately one-half-wavelength long, the reflectors are slightly longer, and the directors are slightly shorter. If the problem does arise, it will be necessary to vary the operating frequency such that no element is exactly an integer multiple of the wavelength.

Input the number of
reflector elements NR := 1

Input the number of
director elements ND := 1

$$\gamma := 0 .. (NR + ND)$$

$$\delta := 0 .. (NR + ND - 1)$$

This entire page is allotted for these entries to allow for as many elements as necessary.

Input the lengths and radii of the Yagi elements, starting with the outermost reflector and proceeding inward to the driven element. After entering the driven element length and radius, enter those of the director elements, starting with the director next to the driven element and proceeding outward to the final element.

Input the distances between successive elements in the same order as the length and radius inputs. There should be one less entry in the separation distance array than there is in the length and radius array.

$l_{\gamma} :=$

15.6
15
14

$rad_{\gamma} :=$

.001
.001
.001

$d_{\delta} :=$

7.5
6.0

Input the operating Frequency (Hertz) $f_5 := 10 \cdot 10^6$

Input the height of the array above the surface (meters) $H_0 := 7.5$

Input the ground Conductivity $\sigma := 4$

Input the ground Dielectric Constant $\epsilon_r := 72$

Input the Distance from the Antenna (meters) $R := 3000$

Index of Refraction

Input the index of the elevation angle for which to calculate the horizontal radiation pattern (from the angle index table) $w := 285$

$$n := \sqrt{\epsilon_r - j \cdot \frac{18000 \cdot \sigma}{(f_5 \cdot 10^{-6})}}$$

Complex Numerical Distance for Vertical Polarization

$$Pe_i := \frac{-j \cdot \beta \cdot (R + H_0 \cdot \cos(\theta_i))}{2 \cdot \sin(\theta_i)^2} \cdot \left(\cos(\theta_i) + \frac{\sqrt{n^2 - \sin(\theta_i)^2}}{n^2} \right)^2$$

Complex Numerical Distance for Horizontal Polarization

$$Pm_i := \frac{-j \cdot \beta \cdot (R + H_0 \cdot \cos(\theta_i))}{2 \cdot (\sin(\theta_i)^2)} \cdot \left[\cos(\theta_i) + \sqrt{n^2 - (\sin(\theta_i)^2)} \right]^2$$

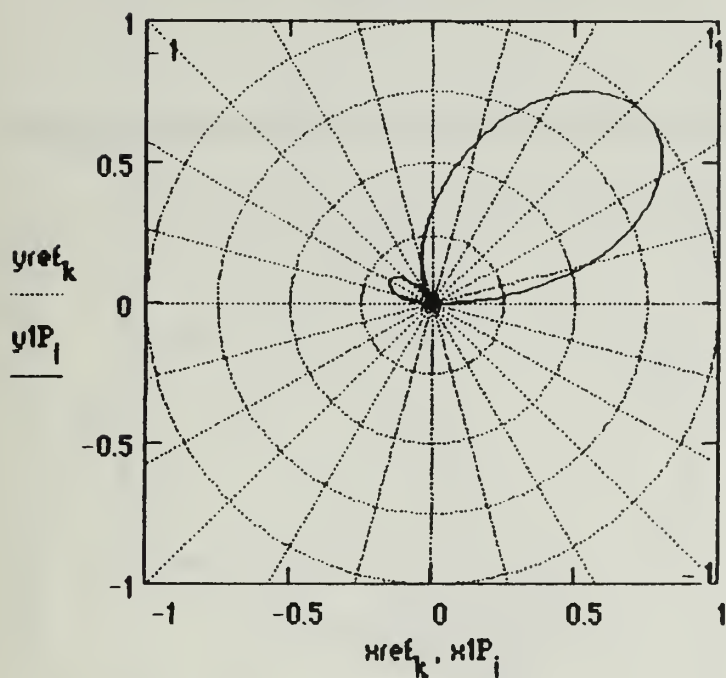
Vertical Reflection Coefficient

$$\Gamma_{V_i} := \frac{(n^2 \cdot \cos(\theta_i)) - \left(\sqrt{n^2 - \sin(\theta_i)^2} \right)}{(n^2 \cdot \cos(\theta_i)) + \left(\sqrt{n^2 - \sin(\theta_i)^2} \right)}$$

Horizontal Reflection Coefficient

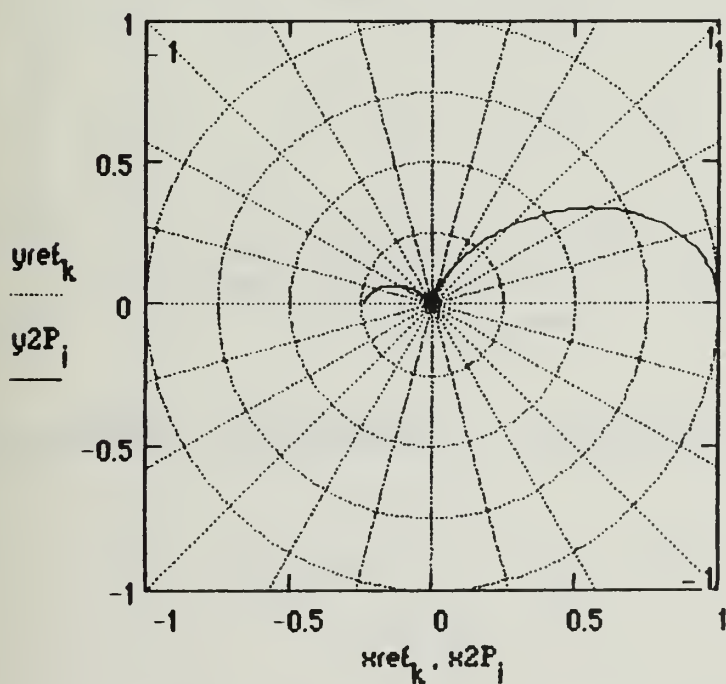
$$\Gamma_{H_i} := \frac{\cos(\theta_i) - \left(\sqrt{n^2 - \sin(\theta_i)^2} \right)}{\cos(\theta_i) + \left(\sqrt{n^2 - \sin(\theta_i)^2} \right)}$$

Radiation Patterns in $\Phi = \pi/2$ Plane
(Perpendicular to X-Axis and Dipole Elements)
Space Wave Radiation Pattern ($\Phi = \pi/2$)



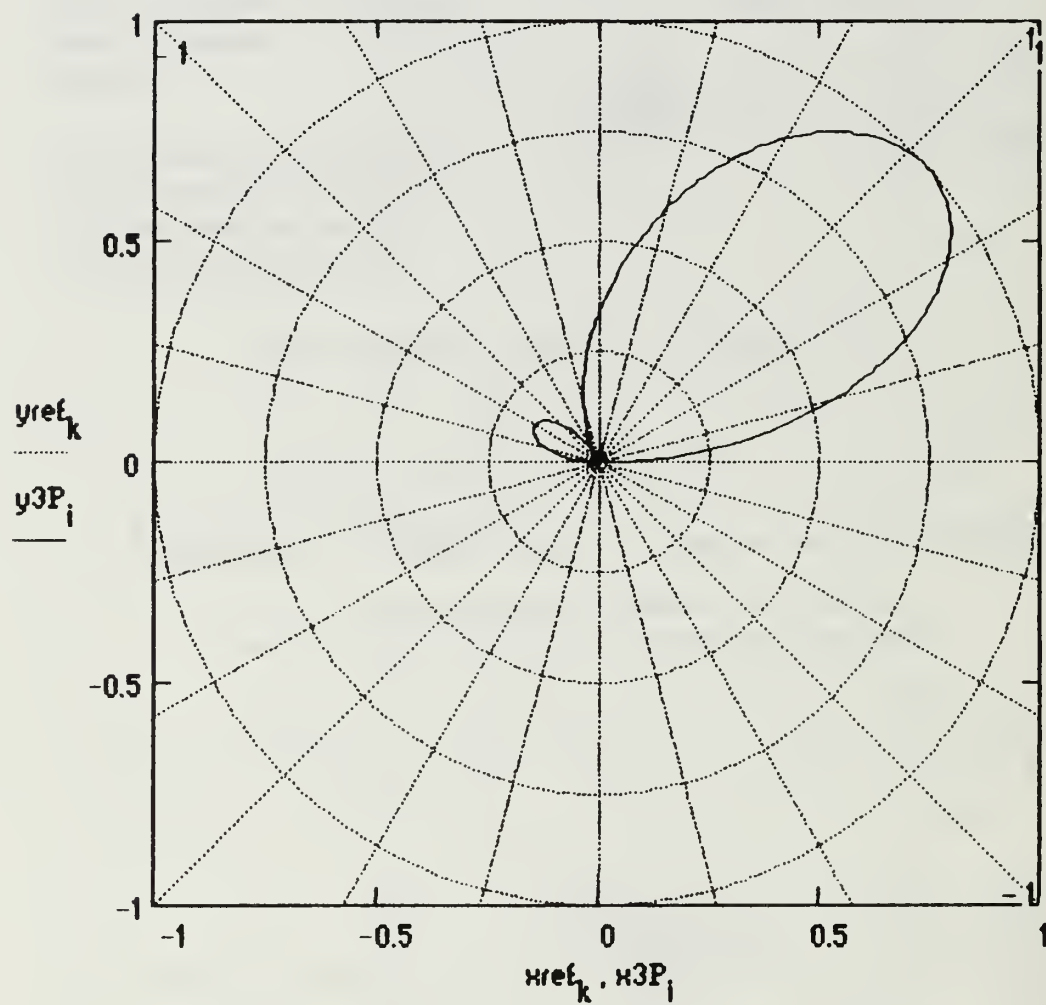
Max E-Field Intensity (Volts per meter) $\max(\text{MagE1P}) = 6.85595 \cdot 10^{-4}$

Surface Wave Radiation Pattern ($\Phi = \pi/2$)



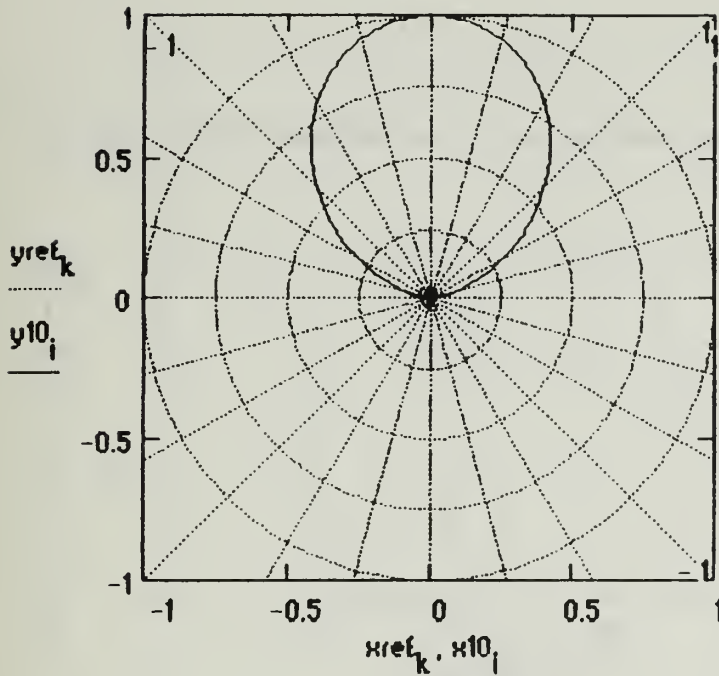
Max E-Field Intensity (Volts per meter) $\max(\text{MagE2P}) = 2.16533 \cdot 10^{-10}$

Combined Space and Surface Wave Radiation Pattern ($\Phi=\pi/2$)



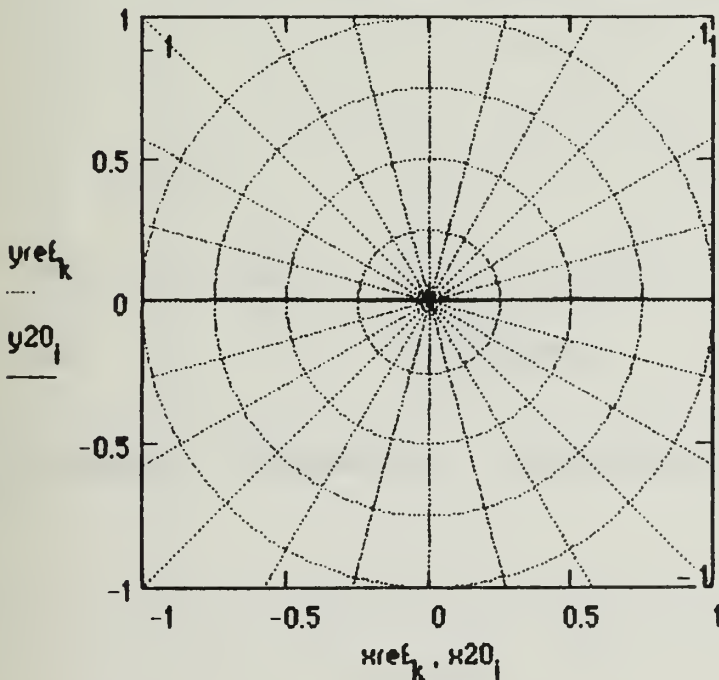
Max E-Field Intensity (Volts per meter) $\max(\text{MagE3P}) = 6.85595 \cdot 10^{-4}$

Radiation Patterns in $\Phi=0$ Plane
(Perpendicular to $\Phi=\pi/2$ Plane)
Space Wave Radiation Pattern ($\Phi=0$)



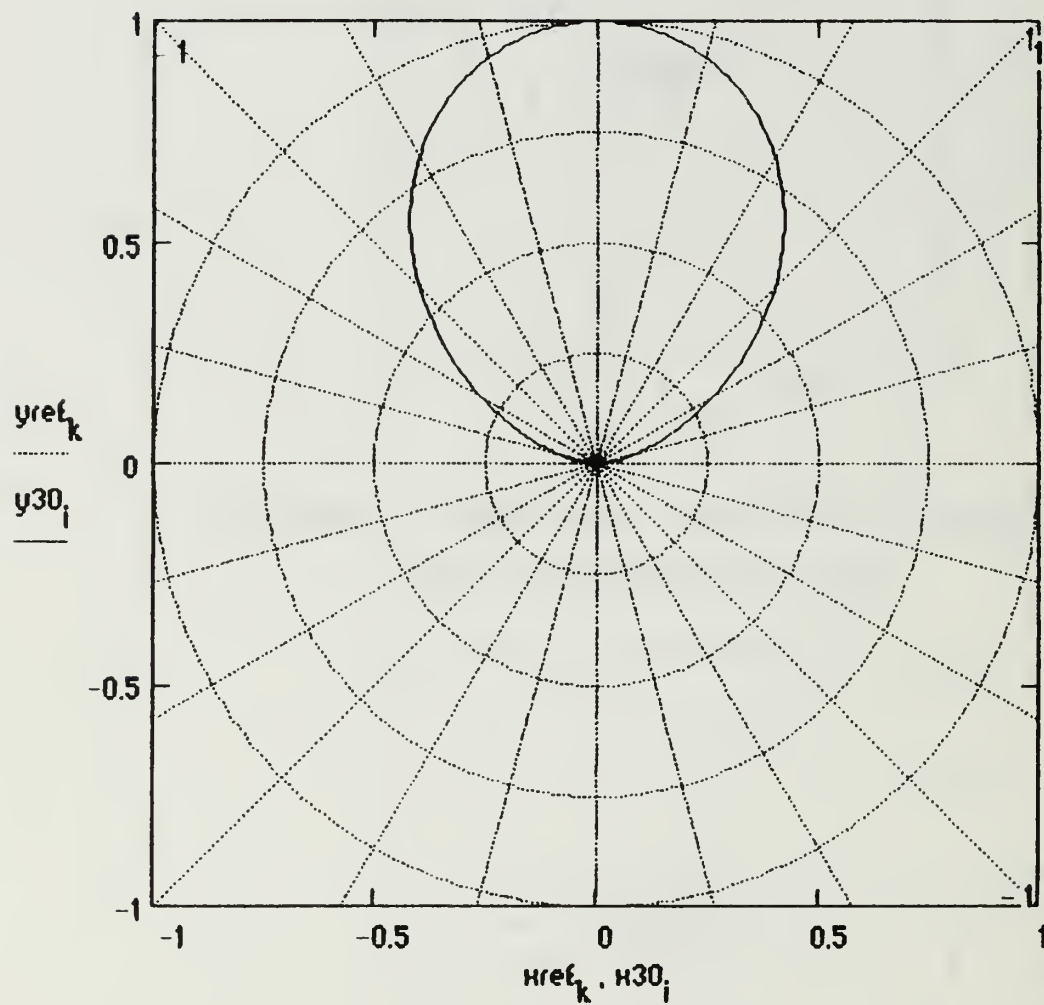
Max E-Field Intensity (Volts per meter) $\max(\text{MagE10}) = 2.32256 \cdot 10^{-4}$

Surface Wave Radiation Pattern ($\Phi=0$)



Max E-Field Intensity (Volts per meter) $\max(\text{MagE20}) = 9.86965 \cdot 10^{-7}$

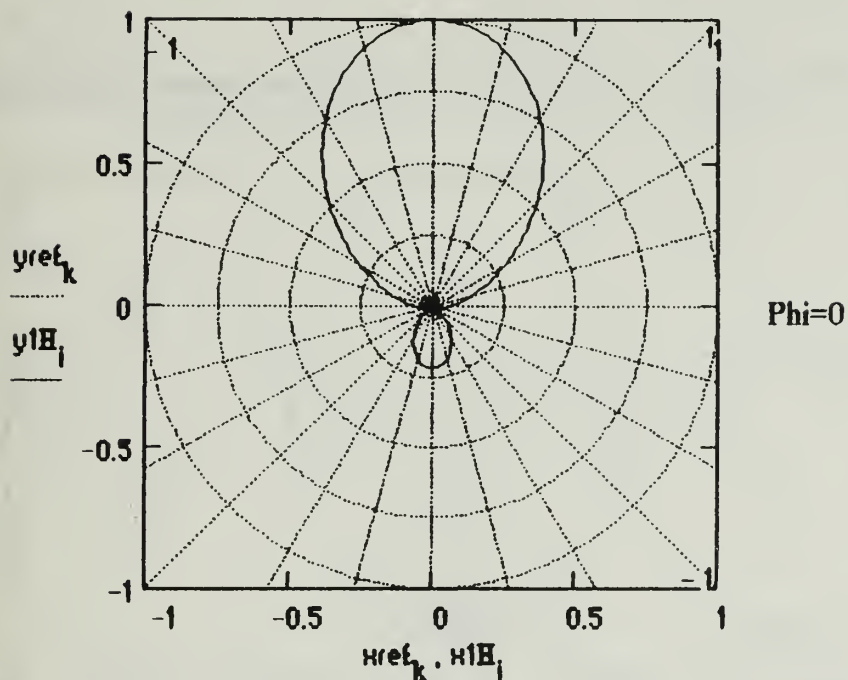
Combined Space and Surface Wave Radiation Pattern (Phi=0)



Max E-Field Intensity (Volts per meter) $\max(\text{MagE30}) = 2.32256 \cdot 10^{-4}$

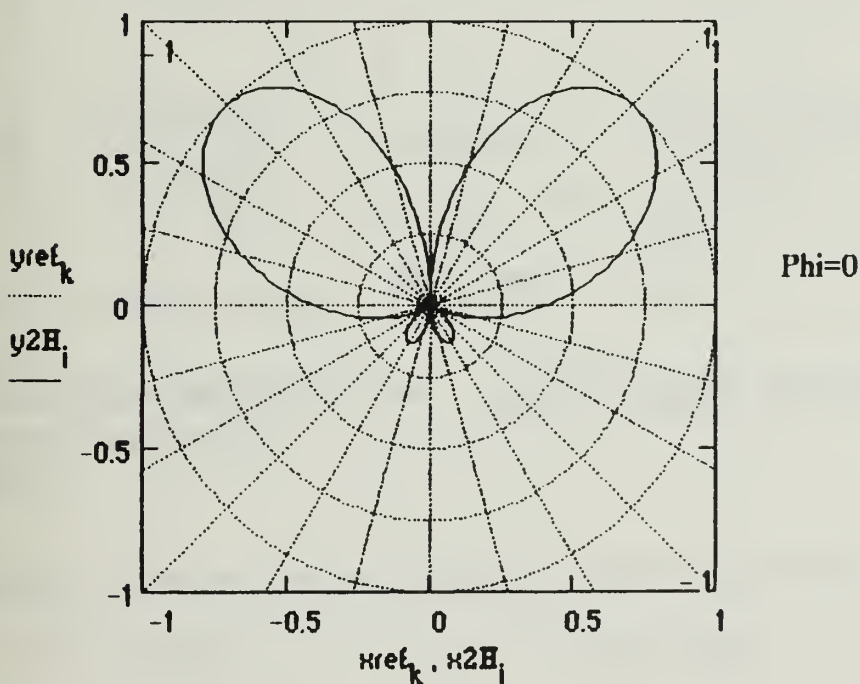
Radiation Patterns in Horizontal Plane (Parallel to Ground)

Space Wave Radiation Pattern (Horizontal)



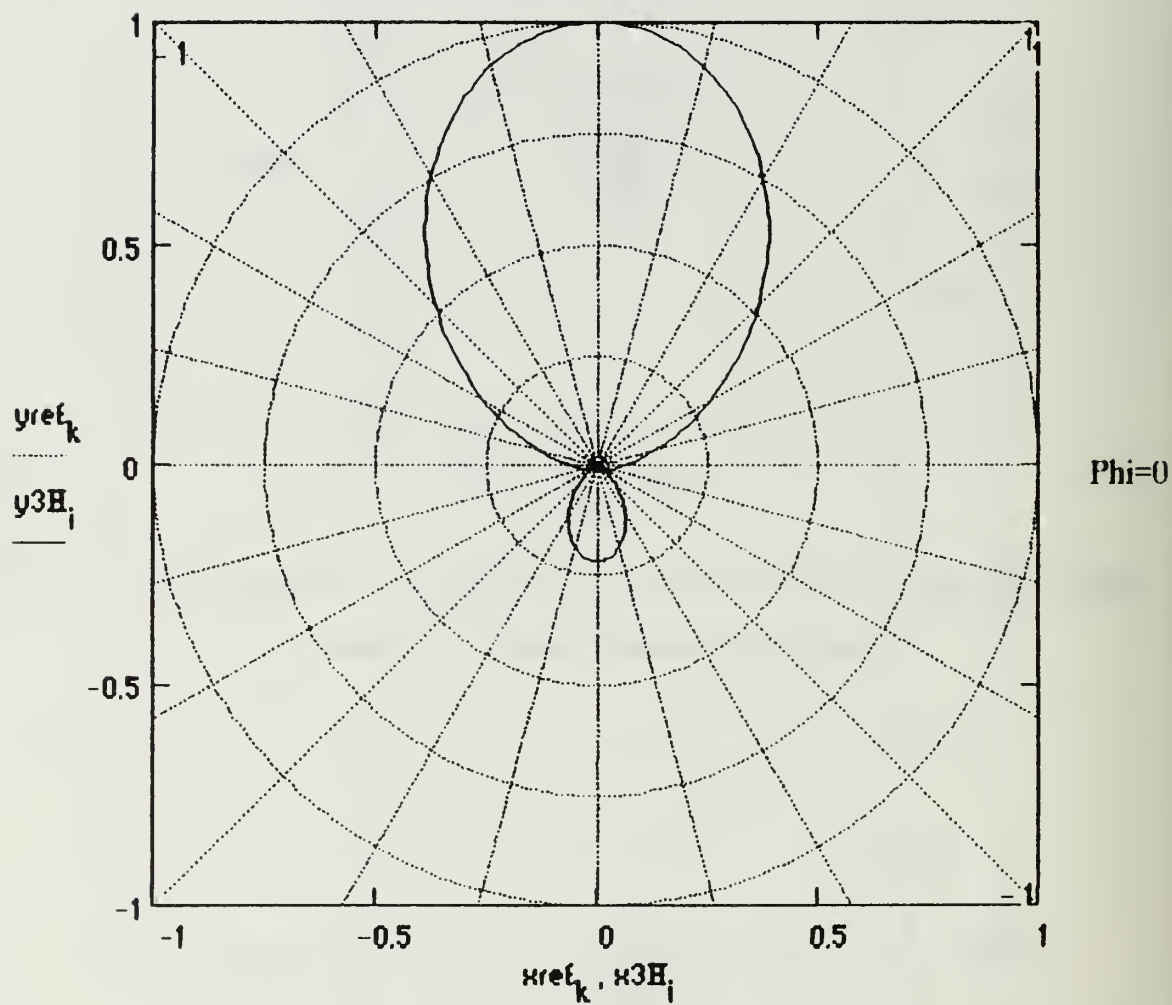
Max E-Field Intensity (Volts per meter) $\max(\text{MagE1H}) = 4.25018 \cdot 10^{-4}$

Surface Wave Radiation Pattern (Horizontal)



Max E-Field Intensity (Volts per meter) $\max(\text{MagE2H}) = 3.10467 \cdot 10^{-9}$

Combined Space and Surface Wave Radiation Pattern (Horizontal)



Max E-Field Intensity (Volts per meter) $\max(\text{MagE3H}) = 4.25018 \cdot 10^{-4}$

$$\text{power}\theta := \frac{30}{\pi \cdot R^2} \cdot \left[\int_{-1.5707963}^{1.5707963} \int_0^{1.5707963} \left| \sum_{\gamma} \left[\frac{\cos(\xi) \cdot \cos(\zeta) \cdot I_{\gamma}}{1 - (\sin(\zeta) \cdot \cos(\xi))^2} \cdot e^{j \cdot \beta \cdot D_{\gamma} \cdot \sin(\zeta)} \right] \right|^2 d\zeta d\xi \right]$$

$$\text{power}\phi := \frac{30}{\pi \cdot R^2} \cdot \left[\int_{-\frac{\pi}{2}}^{\frac{\pi}{2}} \int_0^{\frac{\pi}{2}} \left| \sum_{\gamma} \left[\frac{\sin(\xi) \cdot I_{\gamma}}{1 - (\sin(\zeta) \cdot \cos(\xi))^2} \cdot e^{j \cdot \beta \cdot D_{\gamma} \cdot \sin(\zeta) \cdot \sin(\xi)} \cdot \cos(\beta \cdot \dots) \right] \right|^2 d\zeta d\xi \right]$$

$$\text{power} := \text{power}\theta + \text{power}\phi \quad \text{Radres} := \frac{(\text{VREF}_{NR})^2}{2 \cdot \text{power}}$$

$$\text{sqE3P}_i := \frac{(|\text{MagE3P}_i|)^2}{2 \cdot (120 \cdot \pi)} \quad \text{DirectivityP} := \frac{4 \cdot \pi \cdot R^2 \cdot \max(\text{sqE3P})}{\text{power}}$$

$$\text{sqE30}_i := \frac{(|\text{MagE30}_i|)^2}{2 \cdot (120 \cdot \pi)} \quad \text{Directivity0} := \frac{4 \cdot \pi \cdot R^2 \cdot \max(\text{sqE30})}{\text{power}}$$

Total Power Radiated (Watts) power = 0.00482

Radiation Resistance (versus
Maximum Input Current)
(Ohms) Radres = 103.76004

Directivity (or Maximum Power Gain assuming 100% Antenna Efficiency)

Phi = pi/2 Plane

Phi = 0 Plane

DirectivityP = 14.63143

Directivity0 = 1.67913

Effective Isotropic Radiated Power (EIRP) (Watts)

Phi = pi/2 Plane

Phi = 0 Plane

$$\text{DirectivityP} \cdot \text{power} = 0.07051$$

$$\text{Directivity0} \cdot \text{power} = 0.00809$$

Maximum Effective Area (Along Radial of Directivity) (square meters)

Phi = pi/2 Plane

Phi = 0 Plane

$$\frac{(\lambda_5)^2 \cdot \text{DirectivityP}}{4 \cdot \pi} = 1.0479 \cdot 10^3$$

$$\frac{(\lambda_5)^2 \cdot \text{Directivity0}}{4 \cdot \pi} = 120.25911$$

Maximum Effective Length (Along Radial of Directivity) (meters)

Phi = pi/2 Plane

Phi = 0 Plane

$$2 \cdot \sqrt{\frac{\text{Radres} \cdot (\lambda_5)^2 \cdot \text{DirectivityP}}{480 \cdot \pi^2}} = 33.96559$$

$$2 \cdot \sqrt{\frac{\text{Radres} \cdot (\lambda_5)^2 \cdot \text{Directivity0}}{480 \cdot \pi^2}} = 11.50637$$

Numerical Distances

Vertical Polarization

Horizontal Polarization

$$|P_{e0}| = 0.04363$$

$$|P_{m0}| = 2.26206 \cdot 10^6$$

Elevation Angle of Directivity (Maximum Gain) above the Horizon (Degrees)

Phi = pi/2 Plane

Phi = 0 Plane

$$\text{AngleP} = 41.71429$$

$$\text{Angle0} = \begin{pmatrix} 89.71429 \\ 89.71429 \end{pmatrix}$$

References

1. Cheng, David k., *Field and Wave Electromagnetics*, Addison-Wesley Publishing Company, 1989.
2. Balanis, Constantine A., *Antenna Theory Analysis and Design*, John Wiley & Sons, Inc., 1982.
3. Stutzman, Warren L. and Thiele, Gary A., *Antenna Theory and Design*, John Wiley & Sons, Inc., 1981.
4. Kraus, John D., *Antennas*, McGraw-Hill Book Company, 1988.
5. Jordan, Edward C. and Balmain, Keith G., *Electromagnetic Waves and Radiating Systems*, Prentice-Hall, Inc., 1968.
6. Cheng, Sooyoung and Maddocks, Hugh C., *The Accessible Antenna Package Combined Antenna and Propagation Model*, ITT Research Institute, Technical Report ESD-TR-80-102, July 1981.
7. Sommerfeld, A., *The Propagation of Radio Waves in Wireless Telegraphy*, p. 665, Ann. Physik, Volume 28, 1909.
8. Norton, K. A., *The Propagation of Radio Waves over the Surface of the Earth and in the Upper Atmosphere*, p. 1367, Proc. IRE, Volume 24, 1936; p. 1203, Proc. IRE, Volume 25, 1937; p. 1192, Proc. IRE, Volume 25, 1937.
9. Abramowitz, M. and Stegun, I. A., *Handbook of Mathematical Functions*, National Bureau of Standards Applied Mathematics Series, Volume 55, December 1972.
10. Ma, M. T., *Theory and Application of Antenna Arrays*, John Wiley & Sons, Inc., 1974.
11. Cox, C. R., *Mutual Impedance Between Vertical Antennas of Unequal Heights*, p. 1367, Proc IRE, Volume 35, November 1947.
12. King, H. E., *Mutual Impedance of Unequal Length Antennas in Echelon*, p. 306, IRE Trans. Antennas and Propagation, Volume AP-5, No. 3, 1957.

Initial Distribution List

1. Defense Technical Information Center 2
Cameron Station
Alexandria, VA 22304-6145
2. Library, Code 52 2
Naval Postgraduate School
Monterey, CA 93943-5000
3. Chairman, Code AE 1
Department of Aeronautical and Astronautical Engineering
Naval Postgraduate School
Monterey, CA 93943-5000
4. Chairman, Code EC 1
Department of Electrical and Computer Engineering
Naval Postgraduate School
Monterey, CA 93943-5000
5. Professor R. C. Robertson, Code EC/Rc 3
Department of Electrical and Computer Engineering
Naval Postgraduate School
Monterey, CA 93943-5000
6. Professor Richard W. Adler, Code EC/Ab 1
Department of Electrical and Computer Engineering
Naval Postgraduate School
Monterey, CA 93943-5000
7. LT Daniel S. Dietrich 1
4387 Atwater Arch
Virginia Beach, VA 23456
8. NAVMARINTCEN 4
ATTN: Mr. Ron Ullom
DI433
4301 Suitland
Washington, DC 20395-5020

DUDLEY KNOX LIBRARY



3 2768 00330047 6